

PRECAMBRIAN GEOLOGY OF THE CENTRAL MAZATZAL MOUNTAINS, ARIZONA

(Part I)

and

LEAD ISOTOPE HETEROGENEITY IN PRECAMBRIAN IGNEOUS FELDSPARS

(Part II)

Thesis by

Kenneth Raymond Ludwig

In Partial Fulfillment of the Requirements

for the Degree of

Doctor of Philosophy

California Institute of Technology

Pasadena, California

1974

(Submitted July 31, 1973)

ACKNOWLEDGMENTS

This work has been made possible by the assistance and support of many people, among whom my thesis advisor, Dr. Leon Silver, is foremost. His knowledge, enthusiasm, and support have been invaluable. Mrs. G. Baenteli was of continuing assistance in the laboratory, and Mr. J. Alvarez performed the bulk of the laboratory maintenance. C. Conway and T. Anderson provided much stimulating discussion, as well as assistance in the field. Mr. D. Robbins generously provided lodging, knowledge of the Mazatzal Mountains geography, and companionship during the weeks in the field. My wife, Vera, has been a continuing source of support throughout the days in the field and nights in the laboratory. Mrs. E. Bell is responsible for the excellent typing of the manuscript.

The field-work and petrographic investigations were supported primarily by the National Science Foundation grant GA-15989, and also by the Harvey S. Mudd Endowment Fund. The laboratory work was supported by the Atomic Energy Commission, contract AT(04-3)-767.

ABSTRACT

Part I

The Mazatzal Mountains are located in Gila, Yavapai, and Maricopa counties in central Arizona. The rocks in the central part of this range are dominantly Precambrian, and the only younger stratified rocks are of Tertiary or younger age. The Precambrian rocks have undergone a Precambrian regional metamorphism to lower greenschist grade.

Two main mappable units of stratified rocks are present: the Alder series and the Red Rock rhyolite. Previous work (Wilson, 1939) had indicated that the Alder series is a clastic sedimentary pile, and that it lies in fault contact with an older Red Rock rhyolite. This work shows that the Alder series consists of about one-third directly accumulated volcanic material, another third of slightly reworked volcanic material, and the remaining third of argillites, quartzose sandstones, and limestones. The total thickness of the section is unknown, but is at least 14000' (4200 meters). The overall character of the Alder series is eugeosynclinal, in view of its great thickness, the abundance of volcanics, the thick sections of volcanic sandstones and wackes, and an overall trend towards more shallow-water deposited rocks towards the top of the section. The volcanics of the Alder series, however, are predominantly felsic (dacites to rhyolites), and basalts and pillow lavas, though present, are not abundant.

The Red Rock rhyolite is a thick (at least 1000 meters) pile of extrusive rhyolitic volcanics including abundant ash-flow tuffs. There

is no evidence of a fault between the Red Rock rhyolite and the Alder series. The Red Rock rhyolite lies with depositional contact and without apparent unconformity on the uppermost Alder series beds. In the lower Gold Creek area, a feeder dike to the Red Rock rhyolite penetrates the uppermost Alder series, and broke the surface at the time of accumulation of the Red Rock rhyolite.

The lithologies of the Alder series show a fairly continuous evolution from sediments and volcanics accumulated in relatively deep water to sediments and volcanics accumulated in progressively more shallow water, and finally to sediments and volcanics accumulated under intermittently subaerial conditions. The basin of accumulation of the Alder series became progressively more shallow, at least partly because of the large volumes of volcanic material which accumulated there, until the eruption of the tremendous amounts of volcanics of the Red Rock rhyolite obliterated the remaining vestiges.

The Red Rock rhyolite is petrographically and chemically indistinguishable from some of the volcanics in the uppermost Alder series. It evidently accumulated from sources which were active in latest Alder series time and which contributed to the uppermost Alder series section. Thus at least locally, the Alder series - Red Rock rhyolite contact intertongues. The thickness of the Red Rock rhyolite and the abundance of associated intrusives increases to the northeast, suggesting a probable direction of the source area, perhaps the Precambrian alkali rhyolite complex of Tonto Basin described by Conway (1973).

Several generations of shallow intrusive rocks penetrate the Alder

series and the Red Rock rhyolite. Two types of felsic porphyries were emplaced before folding, while one type of felsic porphyry was emplaced after folding. Mafic volcanic sheets and dikes which intruded in and near the Red Rock mass of the Red Rock rhyolite may have been emplaced during ~~the~~ folding.

Chemical analyses were obtained for nine samples of the Precambrian rocks of the central Mazatzal Mountains. These analyses suggest that the volcanic rocks of the lower Alder series are dominantly dacitic, while the upper Alder series volcanics are dominantly rhyolitic. The chemical composition of the upper Alder series volcanics and the Red Rock rhyolite are generally quite similar to modern, unaltered alkalic rhyolites.

The structural framework of the area is dominated by tight, north-eastward-trending folds. The Red Rock rhyolite is exposed at the cores of synclines, while a faulted anticlinal structure cuts off the oldest Alder series beds to the southeast of Mt. Peeley. These large-scale structures are of Precambrian age.

Isotopic age determinations using the U-Pb method on cogenetic zircon fractions were performed on upper Alder series volcanics. The apparent age indicated by the analyses is 1730 ± 20 m.y. The upper Alder series volcanics are not distinguishable in apparent age from the Red Rock rhyolite as determined by Silver (1964). This apparent age is distinctly younger than the ages obtained for previously-correlated rocks in the Prescott-Jerome area, and confirms the suspicions of Anderson et al (1971) that the Yavapai schist of the Prescott-Jerome

area is not correlable with the type Alder series.

Part II

The lead of high-purity, acid-washed K-feldspar concentrates from five Precambrian granites was removed in a stepwise fashion by two different techniques. Both the technique of stepwise volatilization under vacuum and the technique of stepwise partial attack by hydrofluoric acid yielded leads from the same K-feldspar concentrate which varied significantly in their isotopic composition.

The patterns of lead isotopic variation from the feldspar concentrates show that the lead isotopic heterogeneity is due to a variable component of radiogenic lead which was generated since the crystallization of the rock. Two classes of lead isotopic variation were observed:

(I) Parallel and colinear variation in the 206/204, 207/204, and 208/204 ratios, suggesting that the feldspar incorporated lead derived from long-term uranium and thorium decay from a source with constant Th/U, and

(II) Variation in the 206/204 ratio independent of any 207/204 and 208/204 variation. This suggests that the feldspar contains lead derived from the continuing separation and concentration of a U^{238} intermediate-daughter, probably Rn^{222} .

The amount and type of radiogenic lead incorporated by the five feldspar concentrates correlates with the concentrations of uranium and thorium in the rocks and with the geologic age and history of the

rocks. Thus the rock with the highest uranium content (the Lawler Peak granite) has the K-feldspar with the greatest amount of uranium-derived radiogenic lead, and the rock with the highest thorium content (the Marble Mts. granite) has the K-feldspar with the greatest amount of thorium-derived radiogenic lead. The calculated Th/U values for the sources of the radiogenic leads ranges from two to eleven. Th/U values in this range are reasonable for several common granitic accessory minerals of appreciable U and Th content, but are higher than the Th/U values of the zircons in the rock.

For two of the rocks, the Payson granite of Arizona and the Giants' Range granite of Minnesota, the composition of the radiogenic lead of the K-feldspar concentrates suggests that the rocks were disturbed by nearby Precambrian intrusives. The apparent time of incorporation of the radiogenic lead of the K-feldspar of the Giants' Range granite is 1010 ± 150 m.y., which correlates well with the time of intrusion of the Duluth gabbro complex at 1120-1140 m.y. (Silver and Green, 1972).

Although the least radiogenic lead fractions derived from the K-feldspar concentrates were significantly closer to the composition of the original feldspar lead, in no case was the original feldspar lead isolated. Moreover, because the least volatile lead fractions of some of the feldspar concentrates were more radiogenic in character than fractions of lesser volatility, it appears that the technique of stepwise volatilization is not promising for the routine isolation of original feldspar leads. The technique of stepwise hydrofluoric acid

attack, however, yielded a greater isolation of original feldspar leads in fewer and simpler steps. This technique may be useful for the routine removal of the greatest part of the radiogenic lead component of Precambrian feldspars, and with further development may lead to the complete isolation of the original leads of such feldspars.

The isotopic compositions of the least radiogenic fractions of the three 1450 ± 20 m.y. southwestern granites have almost no variation in $207/204$ ($15.39 \pm .02$) and less than 1% variation in $206/204$ ($16.32 \pm .08$). Calculations using the patterns of lead isotopic heterogeneity of these feldspars suggest that the original $206/204$ values of these rocks were close to 16.16. The observed least radiogenic $208/204$ value of the high-thorium (142 ppm) Marble Mts. granite is distinctly higher than those of the other two 1450 ± 20 m.y. granites. These patterns suggest that these rocks were derived from a common, long-lived source, which source underwent a differentiation so as to cause a change in Th/U and Th/Pb a few hundreds of millions of years before the emplacement of the granites.

TABLE OF CONTENTS

	<u>Page</u>
ACKNOWLEDGMENTS	ii
ABSTRACT	
Part I	iii
Part II	vi
LIST OF FIGURES, TABLES, AND PLATES	xv
<u>PART I: PRECAMBRIAN GEOLOGY OF THE CENTRAL MAZATZAL MOUNTAINS, ARIZONA</u>	
INTRODUCTION	1
Previous Work and Regional Setting	1
Scope and Purpose of Present Work	5
GEOGRAPHY	7
Location and Accessibility	7
Physical Features, Climate, and Vegetation	7
GEOLOGIC UNITS	11
Alder Series	11
General Characteristics	11
Environment of Accumulation	11
Evolution of the Alder Series Basin	13
Mapping Style	15
Mapped Units	21
Crystal-Lithic tuffs	21
lithologies	21
structures	22
distribution	25
environment of accumulation	25
Ord member	26
lithologies	26
distribution	27

	<u>Page</u>
West Fork member	30
lithologies	31
sedimentary structures	32
metamorphic and deformational effects	32
distribution	32
thickness	33
environment of accumulation	33
Horse Camp member	33
lithologies	34
sedimentary structures	38
metamorphic and deformational effects	39
distribution	40
environment of accumulation	40
Cornucopia member	42
lithologies	43
lapilli-crystal tuffs	43
vitric tuffs	49
basaltic flows, pillow lavas, and bedded cherts	49
volcanic breccias	58
metamorphic and deformational effects	61
lapilli-crystal tuffs	61
basaltic flows, pillow lavas, and bedded cherts	64
volcanic breccias	64
chemistry	65
environment of accumulation	66
lapilli-crystal tuffs	66
basaltic flows, pillow lavas, and bedded cherts	67
volcanic breccias	70
distribution	70
East Fork member	72
lithologies	73
northwest of Red Rock syncline	73
Mt. Peeley lithologies	76
vitric tuff sub-unit	77
Mt. Ord lithologies	81
sedimentary structures	81
metamorphic and deformational effects	82
distribution	83
environment of accumulation	83

	<u>Page</u>
Oneida member	84
lithologies	84
northwest limb of Red Rock syncline	84
southeast limb of Red Rock syncline	91
sedimentary and volcanic structures	92
chemistry	93
distribution	94
environment of accumulation	95
Telephone Canyon member	96
lithologies	99
sedimentary structures and textures	110
metamorphic and deformational effects	110
chemistry of volcanics	111
distribution	114
environment of accumulation	115
Red Rock Rhyolite	116
Time Interval between Red Rock Rhyolite and Alder Series	117
Sources of the Red Rock Rhyolite	119
Lithologies	120
outcrop appearance	120
microscopic textures	129
Metamorphic and Deformational Effects	141
Chemistry	142
Distribution	143
Environment and Mechanism of Accumulation	144
Intrusive Rocks	146
Gold Creek Intrusives	146
chemistry	148
Pine Mountain Porphyry Intrusives	149
Unfoliated Rhyodacitic Intrusives	155
Andesitic-Dacitic Intrusive Sheets	156
Andesitic Stock: Mt. Ord Andesite	157
Diorite Dikes	161
CHEMISTRY OF THE PRECAMBRIAN ROCKS OF THE CENTRAL MAZATZAL MOUNTAINS: SUMMARY	163
METAMORPHISM	164
Alder Series Rocks	164
Red Rock Rhyolite	166
Intrusive Rocks	166
STRUCTURE	168

	<u>Page</u>
SEQUENCE OF EVENTS	171
AGE DETERMINATIONS	179
Samples	179
grbrc	179
tfbrc	180
Analytical Techniques	181
Results	181
APPENDIX I: CHEMICAL ANALYSES	185
APPENDIX II: THIN-SECTION DESCRIPTIONS OF SELECTED ROCKS	191
BIBLIOGRAPHY - PART I	214
<u>PART II: LEAD ISOTOPE HETEROGENEITY IN PRECAMBRIAN IGNEOUS FELDSPARS</u>	
INTRODUCTION	220
Purpose and Scope of Work	220
Rock and Mineral Leads: Background	220
Feldspar Leads: Previous Works	224
SAMPLES: INTRODUCTION	226
Lawler Peak Granite	226
Ruin Granite	227
Marble Mts. Granite	228
Payson Granite	229
Giants' Range Granite	229
EXPERIMENTAL TECHNIQUES AND ANALYTICAL PROCEDURES	231
Sample Preparation	231
Volatilization Procedure	232
Stepwise HF-Dissolution Procedure	234
Total Feldspar and Whole Rock Analyses	234
Concentration Determinations	235
Blanks	235
Mass Spectrometry	235
EXPERIMENTAL RESULTS - INTRODUCTION	239
Whole Feldspars, Whole Rocks, and Acid Leaches	239
Lawler Peak Granite	239
Whole Feldspar	239
Feldspar Acid Leach	239
Whole Rock	242

	<u>Page</u>
EXPERIMENTAL RESULTS - INTRODUCTION (Cont'd)	
Whole Feldspars, Whose Rocks, and Acid Leaches	
Ruin Granite	245
Whole Feldspar	245
Whole Rock	245
Marble Mts. Granite	246
Whole Feldspar	246
Whole Rock	247
Payson Granite	248
Whole Feldspar	248
Whole Rock	248
Giants' Range Granite	248
Whole Feldspar	248
Whole Rock	248
VOLATILIZATION EXPERIMENTS	250
Lawler Peak Granite	250
K-feldspar Concentrate	250
Quartz-Plagioclase Concentrate	254
Ruin Granite K-Feldspar	256
Marble Mts. Granite K-Feldspar	265
STEPWISE HF ATTACK EXPERIMENTS	275
Payson Granite K-Feldspar	275
Lawler Peak Granite K-Feldspar	278
DISCUSSION OF EXPERIMENTAL RESULTS	281
Lawler Peak Granite - Major Patterns	281
Volatilized Leads	281
K-Feldspar	281
Quartz-Plagioclase Concentrate	285
Detailed Analysis of the Lawler Peak Granite	
Feldspar Lead Systematics	286
Reversals in Trend of Volatilized Leads	286
Implications of the Lead Obtained by Stepwise	
HF Attack of the Lawler Peak Granite K-Feldspar	
Concentrate	289
Ruin Granite K-Feldspar Volatilized Leads - Major	
Patterns	291
Anomalous Lead Fractions	293
Detailed Analysis of Ruin Granite K-Feldspar Lead Data	295
Marble Mts. Granite K-Feldspar Volatilized Leads -	
Major Patterns	298
Giants' Range K-Feldspar Lead - Major Patterns	302
Payson Granite K-Feldspar Lead Data - Major Patterns	305

	<u>Page</u>
CONCLUSIONS AND IMPLICATIONS	308
Isolation of Original Feldspar Leads	308
Origin of the Radiogenic Feldspar Lead Components	310
Original Lead of the 1450 ± 20 m.y. Granites	315
Estimates of Original Leads	316
Results of Calculations	322
Comments on Precambrian Feldspar Lead Analyses	324
General Summary	326
APPENDIX I: RADIOACTIVE DECAY SYSTEMATICS AND LEAD EVOLUTION EQUATIONS	329
APPENDIX II: RADIOGENIC-COMMON LEAD MIXING EQUATIONS	332
APPENDIX III: MASS-SPECTROMETRIC DATA COLLECTION MODES	335
APPENDIX IV: FITTING OF STRAIGHT LINES TO THE LEAD ISOTOPE DATA	337
APPENDIX V: ROCK THIN-SECTION DESCRIPTIONS	339
PHOTOMICROGRAPHS OF ROCKS AND FELDSPAR CONCENTRATES	344
BIBLIOGRAPHY - PART II	359

LIST OF FIGURES, TABLES, AND PLATES

Part I

Figure	Page
1	8
2	10
3	12
4	184
5	189
6	190

Table	Page
I	183
II	186
III	187
IV	188

Plate	Page
1	18
2	20
3	24
4	24
5	29
6	29
7	36
8	36
9	46
10	46

LIST OF FIGURES, TABLES, AND PLATES

Part I (Continued)

Plate	Page
11	48
12	48
13	52
14	52
15	55
16	55
17	57
18	57
19	60
20	61
21	63
22	63
23	75
24	75
25	80
26	80
27	87
28	88
29	88
30	98
31	101
32	107
33	109
34	113
35	122
36	122
37	125
38	125
39	127

LIST OF FIGURES, TABLES, AND PLATES

Part I (Continued)

Plate	Page
40	127
41	132
42	132
43	134
44	134
45	136
46	136
47	138
48	138
49	140
50	140
51	151
52	151
53	154
54	154
55	159
56	173
57	175

Map: Geology of the Central Mazatzal Mtns.	In pocket
---	-----------

LIST OF FIGURES, TABLES, AND PLATES

Part II

Figure	Page
1	244
2	252
3	253
4	255
5	258
6	261
7	262
8	263
9	267
10	268
11	269
12	271
13	272
14	273
15	277
16	279
17	288
18	300

Table

1	236
2	238
3	240
4	243
5	251
6	257

LIST OF FIGURES, TABLES, AND PLATES

Part II (Continued)

Table	Page
7	259
8	260
9	266
10	270
11	276
12	320
13	321

Plate	
1	345
2	345
3	346
4	346
5	347
6	347
7	348
8	348
9	349
10	349
11	350
12	350
13	351
14	351
15	352
16	352
17	353
18	353

LIST OF FIGURES, TABLES, AND PLATES

Part II (Continued)

Plate	Page
19	354
20	354
21	355
22	355
23	356
24	356
25	357
26	357
27	358
28	358

INTRODUCTION

PREVIOUS WORK AND REGIONAL SETTING

The Precambrian rocks of the central Mazatzal range were first described by Ransome (1915, 1916), who inspected the quicksilver deposits of the area, and constructed a schematic geologic sketch-map. Lausen (1926) briefly studied the quicksilver deposits. Wilson (1939) mapped the area now covered by the northern half of the Reno Pass quadrangle to a scale of about 1:60,000, and focused his attention to the Precambrian geology. In this classic paper, the Alder series and the Red Rock rhyolite were first defined.

Wilson regarded most of the contrasting lithologies of the Alder series as being in fault contact. These lithologies were described as shales, metashales, argillaceous grit (locally schistose), conglomerate, and quartzite. He considered the Red Rock rhyolite as being in fault contact with the Alder series, and, because of clasts similar to the Red Rock rhyolite in conglomerates of the Alder series, regarded the Red Rock rhyolite as older than the Alder series.

By the time of publication of Wilson's 1939 paper, the work of geologists over the preceding forty years had allowed a degree of understanding of the regional stratigraphy and geologic history of the Precambrian rocks of Arizona to be reached (Wilson, 1922; Darton, 1925; Hinds, 1936, and also Ransome, 1903; Jaggar and Palache, 1905; Lindgren, 1926), and the rocks of the central Mazatzal range assumed a regional

significance to the Precambrian geology of Arizona. At this time, the Precambrian chronology of central Arizona was believed to be essentially the following (in chronological order):

Deposition of a thick sequence of volcanic and sedimentary rocks whose basement is not exposed,

- These rocks were termed the Yavapai Schist (Jaggard and Palache, 1905; Lindgren, 1926) or Yavapai Group (Wilson, 1939), and were recognized in the Jerome-Prescott region, the Mazatzal range, eastern Tonto Basin, Pine Creek, and the Del Rio area. The type Alder series and Red Rock rhyolite were considered by Wilson to be part of the Yavapai Group —

followed by,

Regional uplift and erosion,

followed by,

Deposition of the Mazatzal quartzite and related rocks,

- In the Mazatzal range and in Pine Creek, an unconformity was recognized between the Deadman quartzite (Mazatzal range) or Mazatzal quartzite (Pine Creek) and the underlying Red Rock rhyolite. The Mazatzal quartzite and the Deadman quartzite are typically massive, reddish, cross-bedded quartzites. The Mazatzal quartzite was recognized in the northern Mazatzal range, in Pine Creek, in eastern Tonto Basin, on Four Peaks, and in the Del Rio area near Prescott —

followed by,

Uplift, faulting, metamorphism, and intrusion of granites,

- This event was termed the Mazatzal Revolution by Wilson,

followed by,

Long erosional interval, then deposition of the younger Precambrian Apache series.

However, Anderson (1951) later cautioned against correlation of such units as the type Alder series and the type Yavapai schist in the absence of direct physical relationships such as superposition of beds. He also warned against correlation of the structural events recorded by the older Precambrian rocks of Arizona in the absence of firm lithologic correlations, but did regard the "Mazatzal Revolution" as being a possible and singular older Precambrian orogeny.

Cooper and Silver (1954) noted a possible correlation between the Pinal schist of the Johnny Lyon Hills of southeast Arizona and the Yavapai schist. They suggested that they may have originated in a major geosynclinal trough of unknown extent, and which was the orogenic site of the Mazatzal Revolution.

Gastil (1958) correlated rocks in the Diamond Butte quadrangle, about thirty miles east of the central Mazatzal range, with the type Alder series, Red Rock rhyolite, and Mazatzal quartzite. Unlike Wilson, however, Gastil regarded the (correlated) Red Rock rhyolite as younger than the (correlated) Alder series. Silver (1964) obtained an apparent age of 1715 ± 15 m.y. for the Red Rock rhyolite, for the correlated unit (Flying W formation) in the Diamond Butte quadrangle, and for a thin rhyolite interbedded in the Mazatzal quartzite at Pine Creek. He also obtained an apparent age of 1660 ± 15 m.y. for a post-deformational granite located about ten miles south of the type Red Rock rhyolite and Alder series, and suggested that the type Mazatzal orogeny must have

occurred within the 1660 m.y. - 1715 m.y. interval. The coincidence of this interval with the time limits established by Silver on older Precambrian deformation in southern Arizona and California were regarded by him as indicative of a widespread orogenic event equivalent to the Mazatzal revolution. This term, however, has been recently abandoned both by Silver (personal communication) and Livingston and Damon (1968) in view of disagreement on its proper usage and possible inclusion within the term of more than one orogenic event.

Later work by Silver (1967) and Blacet et al. (1971) yielded apparent ages of 1760 m.y. to 1820 m.y. for the volcanics in the type Yavapai schist, which implies that the Red Rock rhyolite cannot be contemporaneous with the Yavapai schist of the Jerome-Prescott region. Anderson et al. (1971) have recently abandoned the correlation of the type Alder series with the type Yavapai.

Livingston and Damon (1968) obtained an apparent age of 1600 ± 100 m.y. on a rhyodacitic ignimbrite which they correlate with the Red Rock rhyolite, and apparent ages of 1400-1425 m.y. on plutons intrusive into Mazatzal quartzite-correlated rocks. They suggest that the Mazatzal revolution occurred at about 1400-1425 m.y.

Silver (1967) has suggested that the pre-Apache stratified rocks of Arizona fall into two age groups: the older with ages of 1760-1820 m.y. (north of 33° N latitude), and the younger with ages of 1710-1725 m.y. (south of 34° N latitude), east of 112° W longitude). The boundary between these two age provinces was not directly observed, and may cross the Mazatzal range near the area mapped in the present study.

SCOPE AND PURPOSE OF PRESENT WORK

This study was undertaken with three main aims;

- 1) to determine the relation of the Red Rock rhyolite to the Alder series,
- 2) to determine the internal stratigraphy of the Alder series (and Red Rock rhyolite, if possible) and the actual petrologic nature of the rocks, and
- 3) to determine the nature and timing of the deformation, intrusive, and metamorphic history of the Alder series and Red Rock rhyolite.

The first aim is important for several reasons. The relative ages of the Red Rock rhyolite and the Alder series as interpreted by Wilson (1939) have been disputed by Gastil (1958, and above, p. 3), and in any case Wilson's assignment does not seem to be based on conclusive evidence. But if Wilson is correct, and the Red Rock rhyolite is older than the Alder series, then Silver's radiometric date of 1715 ± 15 m.y. for the Red Rock rhyolite requires that the Alder series cannot be correlable with the type Yavapai schist.

If the Alder series is older than the Red Rock rhyolite, the contact between the two would become of some importance. The boundary of the two older Precambrian age provinces proposed by Silver (1967, and above, p. 4) must pass within about fifteen miles of the northern Reno Pass quadrangle area. Thus the Red Rock rhyolite-Alder series contact might represent a major time break and province boundary.

The uncertainty in correlation among the type Alder series,

Yavapai schist, Pinal schist, and the Alder series-correlated rocks in the Diamond Butte area required the determination of a stratigraphy within the Alder series and Red Rock rhyolite. Also necessary to reduce the uncertainties in these correlations is an understanding of the environment of accumulation of the type Alder series rocks, and a good petrologic characterization of the various lithologies in the formation.

The third aim was, of course, necessary for the determination of the stratigraphy of the Red Rock rhyolite and Alder series. The deformational, intrusive, and metamorphic history of the rocks also was studied for the purpose of possible correlations with orogenic events which deformed other older Precambrian rocks in Arizona.

GEOGRAPHY

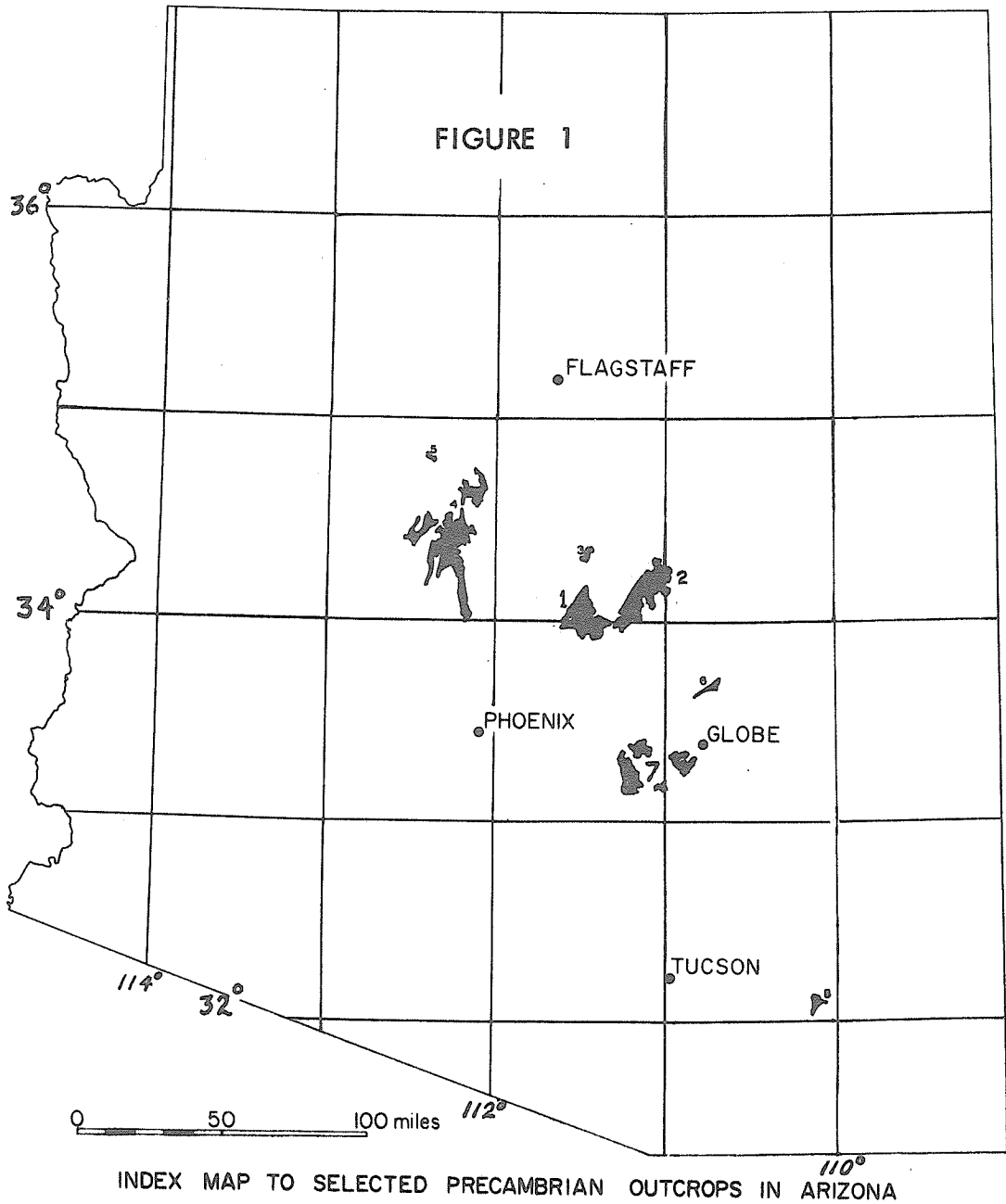
LOCATION AND ACCESSIBILITY

The area mapped comprises approximately the northern half of the Reno Pass $7\frac{1}{2}'$ quadrangle, central Arizona, as is roughly bounded by the meridians $110^{\circ}30'$, $111^{\circ}22'30''W$, and the parallels $34^{\circ}00'$, $33^{\circ}56'15''$ (fig. 1). The area lies in the central part of the Mazatzal range, in Maricopa and Gila counties. A good paved highway, Arizona State Highway 87, crosses the area and permits rapid access from either the town of Payson, about 30 miles to the north, or Phoenix, about 50 miles to the south. Access north of Arizona 87 is provided by a dirt road which skirts Pine Butte, turns west at the northern boundary of the Reno Pass quadrangle, and ends at Thicket Springs on the southeast flank of Mt. Peeley. Truck and jeep roads provide access to the various mercury mines in the area. The only good road on Mt. Ord is the access road to the microwave and fire lookout installations on its summit. North of the Reno Pass quadrangle, in the $15'$ Payson quadrangle, most of the adjoining area is in the Mazatzal Wilderness area, where access is restricted to a few foot trails.

PHYSICAL FEATURES, CLIMATE, AND VEGETATION

Most of the mapped area north of Slate Creek can be regarded as a south-facing slope of the Mazatzal Mountains. The highest elevations in the mapped area are the slopes of Mt. Peeley, about 6600', and the lowest elevations in the Slate Creek drainage, about 3500'. The main

- 1: Mazatzal Mountains
- 2: Tonto Basin (including Diamond Butte Quadrangle)
- 3: Pine Creek (Natural Bridge)
- 4: Prescott - Jerome region
- 5: Del Rio
- 6: White Ledges
- 7: Pinal Mountains region - Pinal Schist
- 8: Johnny Lyon Hills - Little Dragoon Mountains



drainages are the East and West forks of Sycamore Creek (referred to as Alder Creek in the work of Wilson, 1939). These creeks are almost dry in the summers, but may flow several feet deep during the early spring months. The main drainages, mountains, springs, and roads of the area are shown in figure 2.

The topography is one of prominent stream valleys, steep slopes and rounded ridges. Plant cover varies from grasses and cactus on the lower elevations to manzanita, 'scrub' oak, locust and juniper between about 4500' and 5500', to forests of pine, oak, cedar and juniper on the highest north-facing slopes.

The climate is characterized by cool winters, with daytime temperatures seldom falling below 35°F, and hot summers, with daytime temperatures in the 85°-100°F range. Rainfall is modest, probably about 15" per year.

There is generally less than about ten permanent occupants of the area, with those people located at the various mining camps. The land is used as cattle range, and there is sporadic activity at some of the mines.

GEOGRAPHIC INDEX MAP
of the
CENTRAL MAZATZAL MTS.

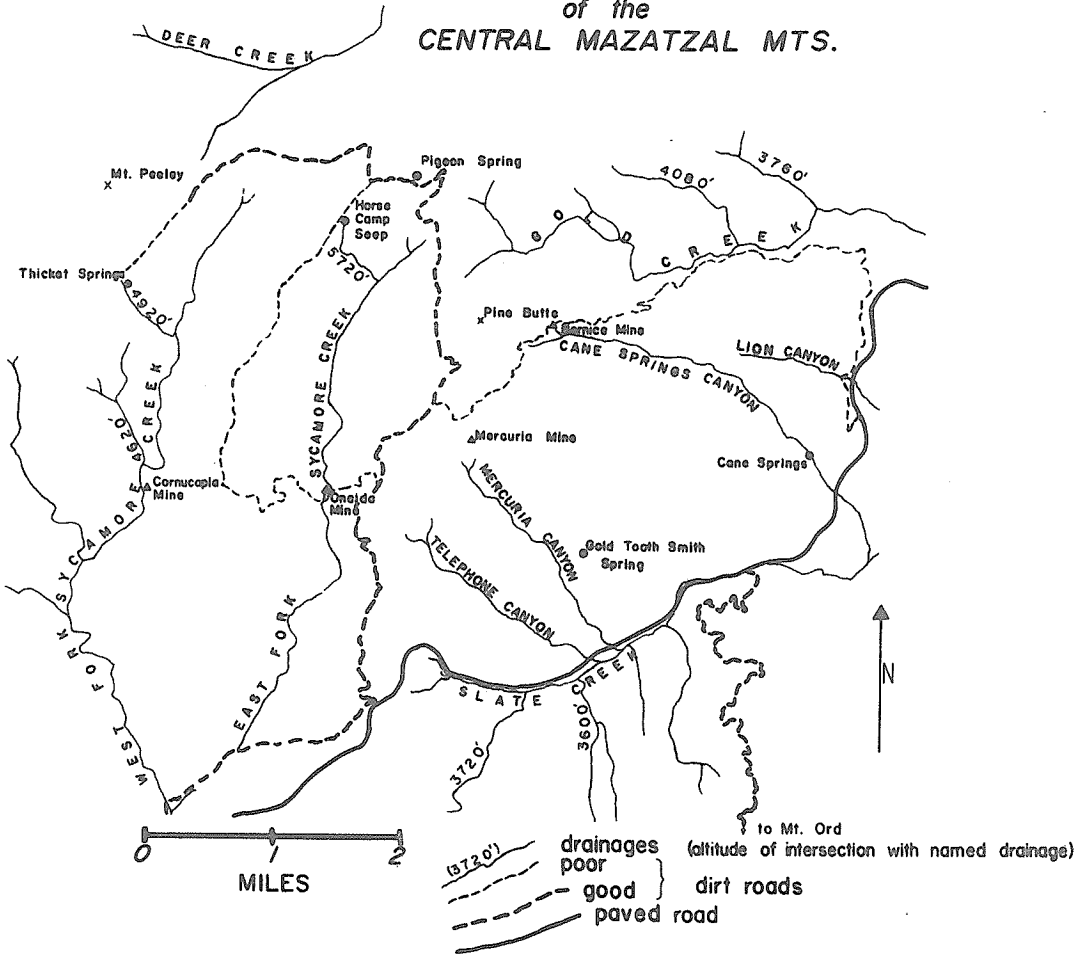


Figure 2

GEOLOGIC UNITS

ALDER SERIES

General Characteristics

The Alder series (defined by Wilson, 1939) is a thick section (more than 14,000') of metavolcanic and metasedimentary rocks intruded by several generations of sheets and dikes (fig. 3). Although the rocks of the Alder series have been sheared and foliated to varying degrees, and undergone greenschist facies metamorphism, the original lithologic character of much of the section can still be ascertained. In most cases, therefore, lithologic terms describing the Alder series rocks are not referred to as, for instance, meta-sandstones, meta-tuffs, or meta-conglomerates, but rather as sandstones, tuffs, or conglomerates.

An important characteristic of the Alder series is its volcanic content. About one-third of the section is directly accumulated volcanic rock -- mostly felsic pyroclastics -- while another third is sedimentary rock rapidly derived from a volcanic source-terrain (volcanic sandstones and graywackes). Of the remainder of the section, about one-half is argillaceous rock, and half quartz wackes and quartzites.

Environment of Accumulation

The overall character of the Alder series is eugeosynclinal, in view of such eugeosynclinal characteristics (Pettijohn, 1957; Kay, 1951) as its

- a) relatively great thickness

GENERALIZED STRATIGRAPHIC COLUMN OF ALDER SERIES
Northwest limb of Red Rock Syncline

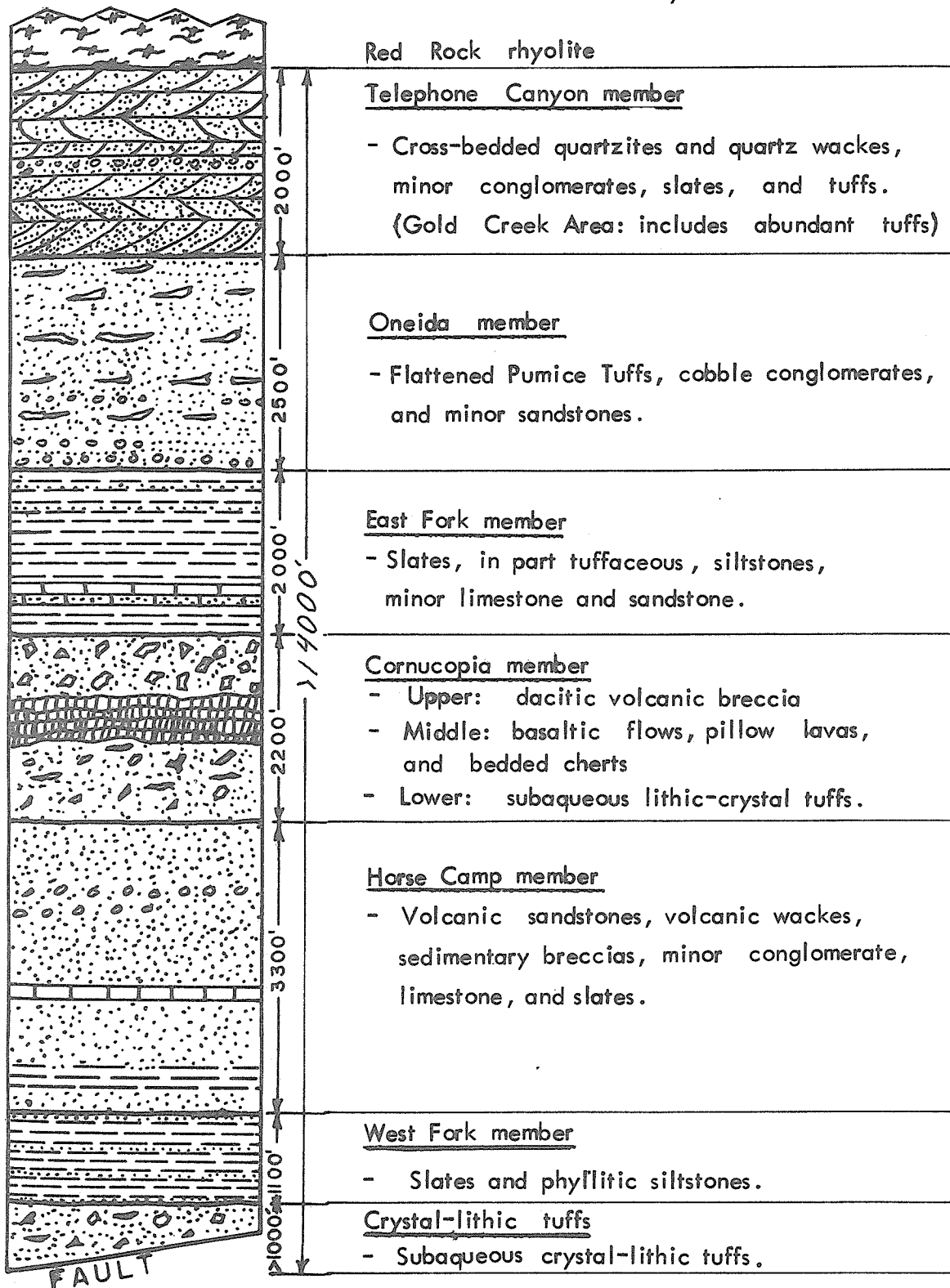


Figure 3

- b) abundance of extrusive volcanics, including some pillow lavas
- c) thick sections of volcanic sandstones and graywackes
- d) overall trend towards more mature and more shallow-water deposited rocks at the top of the Alder series section (quartzites, quartz wackes, conglomerates).

However, the Alder series deviates in character from classical eugeo-synclinal sections in that the mafic volcanics (pillow-lavas and other basaltic flows) are distinctly less abundant than dacitic to rhyolitic volcanics. Also, the argillaceous rocks of the Alder series are less abundant than the volcanic sandstones and graywackes.

The relatively minor amount of basaltic rocks present in the exposed Alder series section, however, may not be representative of the complete section. The general trend of lithologic variation with position in the section, in fact, suggests that the Alder series rocks below the lowest exposed horizons could contain abundant additional basaltic flows.

Evolution of the Alder Series Depositional Basin

The lower half of the exposed Alder series is composed mostly of slates, poorly bedded and sorted volcanic sandstones, subaqueous dacitic tuffs, pillow lavas, and bedded cherts. In this part of the section, such sedimentary structures and cross-bedding, ripple-marks, and scouring are very rare. These rocks were accumulated under exclusively subaqueous conditions, and in water deep enough so that they were deposited below the wave and current base. The presence of cherts interbedded with pillow lavas is also suggestive of relatively deep water, since a

high water pressure greatly favors a high degree of concentration and supersaturation of dissolved silica (Bailey *et al.*, 1964, p. 65).

The first true conglomerates, with abundant rounded cobbles, appear at the base of the Oneida member of the Alder series, about 4000' below the base of the Red Rock rhyolite. Above this horizon, the first sediments giving evidence of significant reworking and of current effects are present. The abundance of such rocks increases with relative position in the section. In the uppermost member of the Alder series (the Telephone Canyon member), the dominant lithologies are cross-bedded true quartzites and quartz wackes. In this part of the section, subaerial felsic volcanic material first occurs, with progressively greater abundance towards the northeast. The chemical similarity of these volcanics to the overlying Red Rock rhyolite and the spatial coincidence of pronounced increase in abundance of these volcanics, the Red Rock rhyolite, and petrologically similar shallow intrusives, all argue that these subaerial Alder series rhyolites are related to the Red Rock rhyolite.

Thus the trend of lithologies with position in the section suggests that the basin of accumulation of the Alder series became progressively shallower starting at Oneida member time, until near-shore sedimentary facies such as cross-bedded quartzites were common. At the same time that the near-shore facies rocks were being abundantly laid down, rhyolitic vulcanism with sources to the northeast were emphasizing the effects of the uplift of the basin by pouring in large volumes of felsic volcanic material. The result was the attainment of intermittent subaerial conditions towards the northeast in latest

Alder series time, while a continuous section of shallow-water sediments was accumulating elsewhere.

The eruption of the large volumes of rhyolite of the Red Rock rhyolite occurred either during the accumulation of the latest quartzites or after a short period of final uplift. The appearance of the Red Rock rhyolite -- massive, exclusively subaerial, and at least 4000' thick -- marked the end of the Alder series depositional basin. Moreover, no later deep basin was evidently developed in the same area. Overlying the Red Rock rhyolite, just north of the mapped area, is a thick section of cross-bedded quartzites and shales (the Mazatzal and Deadman quartzites and the Maverick shale), while in the Tonto Basin area, the Alder series-correlated rocks are overlain by rocks similar to these cross-bedded quartzites (Clay Conway, personal communication).

The area of the crust which was involved in the downwarping which resulted in the basin of Alder series accumulation was at least 25 miles in length (the distance to the correlable rocks in Tonto Basin to the northeast). The area might well span more than 150 miles, however, as the eugeosynclinal rocks of the Pinal schist in the Dragoon quadrangle, described and dated by Silver (1955, 1961, 1967) are similar in age (1715 ± 15 m.y.) and character to the rocks of the Alder series.

Mapping Style

Detailed stratigraphic control within the Alder series was difficult to obtain, because the conditions of accumulation which controlled the lithologies of the Alder series were evidently quite

variable, both in time and space. Only relatively thick and laterally persistent lithologic types proved to be generally mappable, and even these commonly showed significant variations along strike.

The boundaries of many of these mappable units are gradational over distances of 100 to 1000 feet; thus relatively small-scale structures which slightly offset such contacts might have well remained undetected. Also, variations in the degree of foliation and recrystallization of these weakly metamorphosed rocks obscure correlations of lithologies over distances of miles.

The area north of Arizona State Highway 87 was mapped in some detail. On the north slopes of Mt. Ord, south of this highway, much poorer exposures and access allowed only what must be called reconnaissance mapping to be done in this area. Much of the information on these rocks stems from observations (hand-specimen and thin-section) on samples taken at about 800' intervals along the Mt. Ord access road. Some of the contacts along this road are located only to the accuracy of the sample spacing, since the degree of alteration of the rocks in the roadcuts in many cases precludes accurate field identification of their genetic type.

In this report, unnamed drainages will be named according to the elevation, from the appropriate topographic base, at which they join a named drainage. Thus the tributary of Gold Creek which intersects Gold Creek near 4080', according to the Reno Pass quadrangle topography, is referred to as the 4080' fork of Gold Creek. The drainages referred to in this report are identified in figure 2.

Plate 1: View looking northwest from the divide between the east and west forks of Sycamore Creek. The West Fork of Sycamore Creek is the drainage in the right foreground. The Red Rock rhyolite makes up the far ridge, whose high points to the southwest and northeast, respectively, are Sheep Mt. and Mt. Peeley. The Red Rock rhyolite-Alder series contact is exposed on the near flank of the ridge. The light-colored, resistant rocks cropping out on the ridges of the middle distances are unfoliated rhyodacitic intrusive sheets.



Plate 1

Plate 2: View looking south towards Mt. Ord (high peak in distance) across Slate Creek. Resistant quartzite beds in the Alder series crop out along the north flank of Mt. Ord. The change in vegetation from brush to pine and juniper high on the mountain approximately marks the Alder series-Mt. Ord andesite contact.



Plate 2

Mapped Units

CRYSTAL-LITHIC TUFFS

The oldest exposed rocks of the Alder series on the northwest side of the Red Rock syncline are massive, typically blue-green, crystal-lithic tuffs. They comprise a typically non-resistant unit which crops out poorly, except in creek beds. The lower contact is a fault which juxtaposes breccias of the Cornucopia member against the crystal-lithic tuffs. The unit grades upward into the maroon slates of the West Fork member of the Alder series. The latter transition is marked by interbedding of crystal-lithic tuffs with slates or foliated mudstones, and occurs in a stratigraphic thickness of about 150'.

Lithologies

The crystal-lithic tuffs are composed exclusively of massive, coarsely foliated, coarse-grained tuffs composed of altered volcanic fragments and crystals of plagioclase and quartz. Typical rocks of the unit are a pale blue-green color on fresh surfaces, and weather to various shades of tan. Angular, $\frac{1}{2}$ mm to 2 mm pink plagioclase grains are visible in hand-specimen, and appear to be set in a fine-grained matrix.

Thin-section examination of the crystal-lithic tuffs shows that they are composed of from 5% to 40% quartz and plagioclase grains of greater than 0.1 mm size (the ratio of quartz to plagioclase varies from about 0.1 to 1.5 in four thin-sections examined), from 60% to 90% volcanic lithic clasts, and less than about 5% of fine-grained matrix

material (plates 3, 4).

The larger grains of quartz and plagioclase (unzoned albite or possibly sodic oligoclase) are subhedral and 0.1-2 mm in size. Many of the quartz grains show rounding and embayment. The lithic fragments are moderately elongate in the direction of foliation (length:width in cross-section of two to four), and average about 2 mm in length. They are fine-grained, leucocratic, and are partially altered to sericite and chlorite. Some of the lithic clasts contain quartz or plagioclase phenocrysts. Because of the difficulty in distinguishing between highly altered, fine-grained lithic fragments and any altered, fine-grained matrix around the larger lithic and crystal clasts, the estimate of less than 5% matrix material in the rock is somewhat crude.

Most of the lithic clasts apparently deformed during the metamorphism and not accumulation, because neither extreme flattening (length/width ratios greater than 5) nor deformation of lithic clasts around angular crystals are common, except in samples from the uppermost part of the unit.

Braids and elongate aggregates of sericite and chlorite are abundant. Epidote is present in only trace amounts, although the chlorite mode averages about 15%.

Structures

The unit as a whole is devoid of small-scale depositional structures. Examination of thin-sections of four samples from the lowest-exposed to the uppermost horizons suggests an increase of more highly deformed (hence, possibly pumiceous) lithic clasts towards the

Plate 3: Photomicrograph of crystal-lithic tuff member of the Alder series (2 × 3 mm field, plane polarized light). The larger, lighter grains are plagioclase. The 'matrix' consists mostly of plagioclase, sericite, and some chlorite, and is actually mostly altered lithic clasts.

Plate 4: Same as plate 3, but crossed nicols.

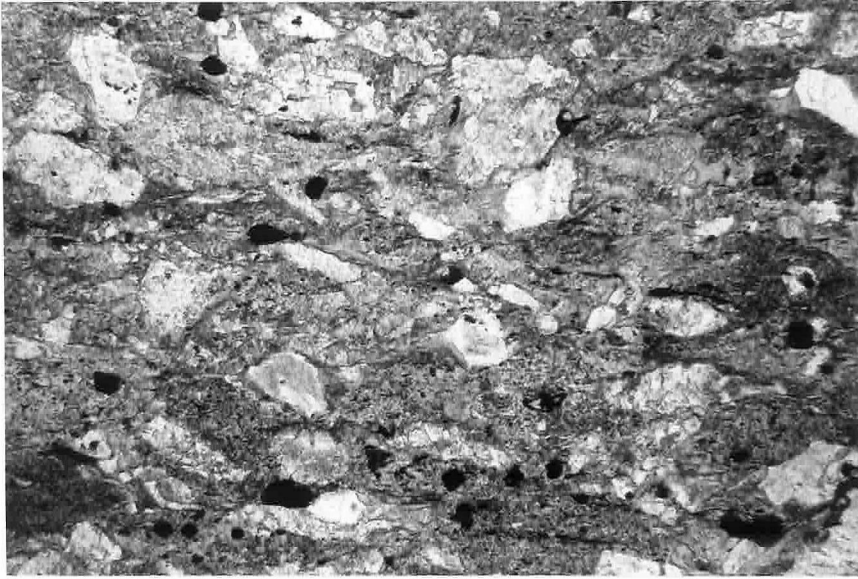


Plate 3

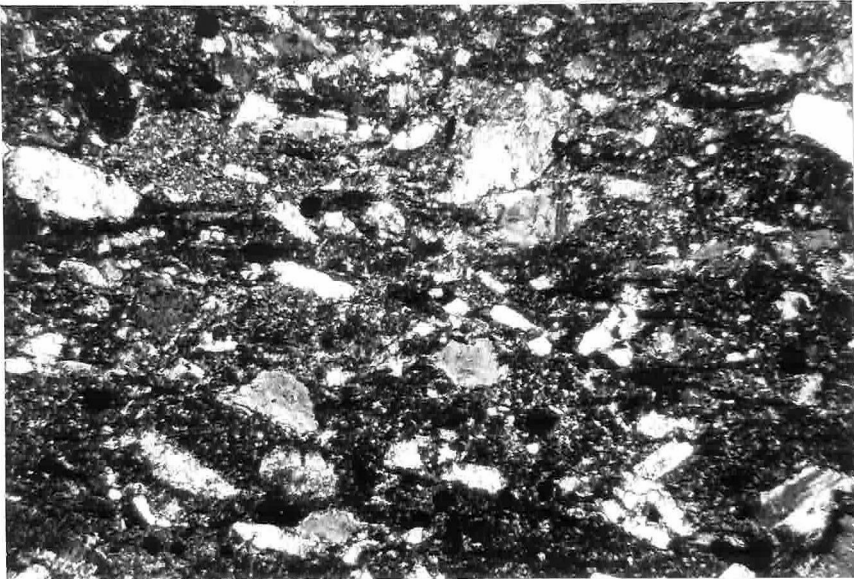


Plate 4

top of the unit, possibly reflecting a gross grading.

Mechanical deformation of the unit near the fault which forms its northwesterly limit is not readily apparent, except for the presence of numerous small (5-10 mm widths), discordant quartz grains. The breccias of the Cornucopia member near this fault are, in contrast, intensely veined and brecciated.

Distribution

The unit is exposed in a northeast-trending belt which passes within 2000' southeast of Thicket Springs. Best exposures are obtained in the drainage which intersects the West Fork of Sycamore Creek at 4920' elevation. The exposed thickness of the crystal-lithic tuffs varies from about 1000' at the western boundary of the Reno Pass quadrangle to no exposure at the northern boundary of the quadrangle, due to progressive truncation by faulting.

No confidently correlable rocks were observed on the southeast limb of the Red Rock syncline. The Ord member sandstones and tuffs, however, may be related (p. 26).

Environment of Accumulation

The abundance and preservation of the igneous forms of the quartz and plagioclase grains require that the materials have been very rapidly incorporated from the volcanic source. However, the absence of both large (over 4 mm) clasts and significant fine-grained matrix material is evidence of an efficient sorting process. These characteristics are best obtained by the mechanisms described by Fiske and Matsuda (1964)

in connection with submarine ash-flow deposits. The relatively fine grain size of these tuffs may reflect a relatively distant source. An air-fall origin for these tuffs cannot be ruled out; however, the degree of winnowing of fine ash which is required seems unlikely.

ORD MEMBER

The oldest exposed rocks of the Alder series on the southeast side of the Red Rock syncline are fine-grained, chlorite-rich meta-sandstones and interbedded dacitic tuffs. These rocks, mapped only in reconnaissance, conformably underlie the coarse, bedded sandstones of the Horse Camp member, and are intruded by Pine Mt. Porphyry-type rhyodacitic rocks.

The contact of the Ord member with the overlying Horse Camp member is gradational over about 100' of section, and is marked by the disappearance (going down-section) of bedding, decrease of grain size from coarse to fine sand, and appearance of persistent blue-green (when fresh) color. The unit is not resistant, and is poorly exposed except in the larger drainages.

Lithologies

In outcrop, the rocks are typically massive, well-foliated, fine to medium-grained, and blue to blue-green in color. No sedimentary structures were observed.

Thin section examination shows that they consist predominantly of .05 mm - .5 mm angular to subrounded quartz. The original matrix material has recrystallized to chlorite, sericite, and opaques, present

as parallel stringers and elongate aggregates. The quartz grains are subequant to slightly elongate (parallel to foliation), with a mosaic structure present in some of the larger grains. The abundance of quartz grains in the sandstones varies from about 40% to 70% (plates 5 and 6). No feldspar grains are visible in thin section.

The abundance of chlorite and opaque minerals in the sandstones of the Ord member is in contrast with the low content of ferric minerals in most of the sandstones of the rest of the Alder series. This evidently reflects an original matrix rich in Fe and Mg. Possibly this matrix consisted, in part, of fine ash of dacitic composition from the dacitic tuffs(?) intercalated in the unit.

These tuffs(?) are dark blue, massive, foliated, fine-grained rocks exposed in the middle of the unit. In thin section, chlorite, epidote, and fine-grained opaques are seen to comprise up to 90% of the rock, with very fine-grained quartz and feldspar(?) making up the remainder. Trace amounts of subhedral, corroded, 0.1 mm - 0.5 mm quartz and plagioclase phenocrysts are present. The rock is identified as a possible tuff because of strong textural suggestions of abundant, compressed relict shards.

Distribution

The Ord member of the Alder series is exposed on the Mt. Ord road near the 5000' level, and again between the elevations of about 5600' and 5780'. The precise distribution of the Ord member and intrusives into it along the Mt. Ord road may be more complex than as mapped because, without outcrops of fresh rock, the two lithologies are not

Plate 5: Photomicrograph of Ord member sandstone (2 × 3 mm field, plane polarized light). Lighter grains are quartz, medium-gray, highly elongate patches are chlorite. Note elongation and alignment of quartz grains parallel to foliation.

Plate 6: Same as plate 5, but crossed nicols.

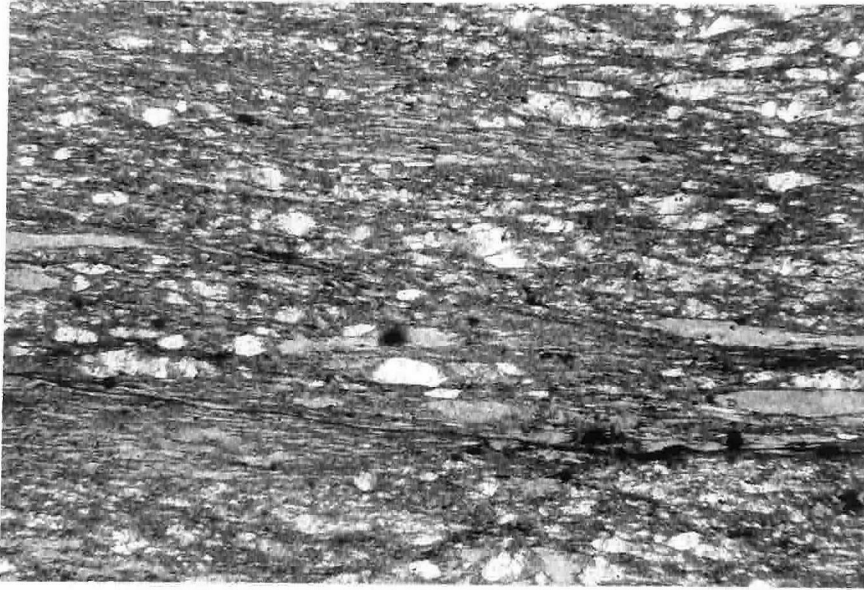


Plate 5

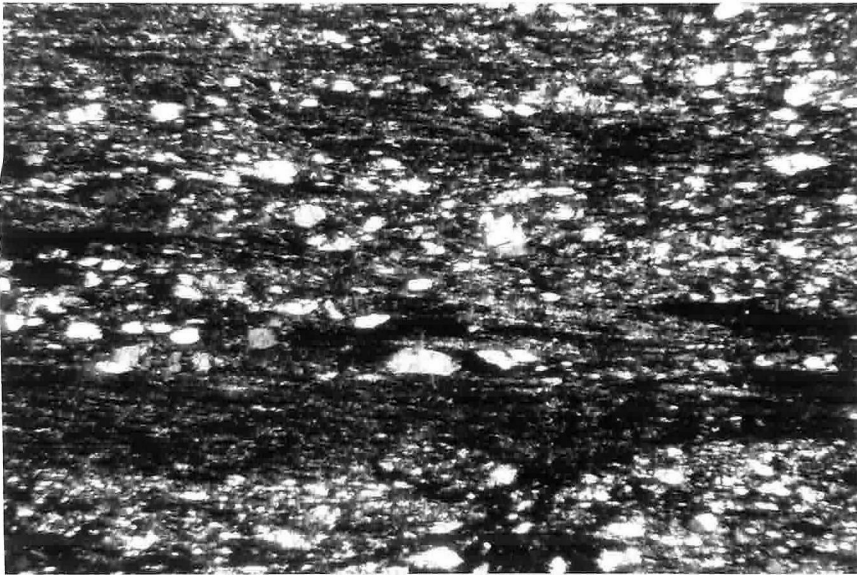


Plate 6

easily distinguishable. In the north-flowing fork which joins Slate Creek at 3600' elevation, the unit crops out from as low as about 4620', to at least as high as 4800'.

No strictly comparable rocks to the Ord member lithologies crop out on the northwest limb of the Red Rock syncline. However, the slates, siltstones, and fine-grained sandstones of the West Fork member occupy a similar stratigraphic horizon and may be equivalent to the Ord member, but slightly more reworked and with oxidized instead of reduced iron. An alternate correlation is that, in the absence of West Fork member lithologies on Mt. Ord, the Ord member impure sandstones and dacitic tuffs represent a finer-grained facies of the crystal-lithic tuffs. This correlation implies that the Ord member was accumulated further from the volcanic source of the crystal-lithic tuffs, so that the volcanic material of the Ord member was introduced by air-fall rather than submarine debris flow.

WEST FORK MEMBER

The West Fork member of the Alder series (new name, for exposures in the upper West Fork of Sycamore Creek) is a predominantly fine-grained sequence of slightly metamorphosed shales, siltstones, and volcanic sandstones. The most common lithology is a maroon phyllite with intermittent laminations of lighter colored rock.

The West Fork member conformably overlies the crystal-lithic tuffs of the Alder series, except where the tuffs are cut out by the Thicket Springs fault. The unit conformably underlies the volcanic wackes and sandstones of the Horse Camp member. This contact is

gradational, and was defined in the field by the first appearance, going up-section, of persistent sandy lithologies. In the northeast part of the mapped area, the contact is intruded by a relatively thick (800') felsite sheet.

The unit is non-resistant, and crops out poorly even in creek bottoms.

Lithologies

Within the boundaries of the Reno Pass quadrangle, the West Fork member consists predominantly of maroon slates and phyllites, and contains only minor interbeds of sandstone. Just north of the northern boundary of the Reno Pass quadrangle, however, abundant, medium-grained sandstones and wackes crop out in roadcuts on the Thicket Springs road. Near the western boundary of the quadrangle, the unit contains intercalated, pale blue, fine-grained tuffs, but these rocks do not persist to the northeast.

Microscopic inspection of the slates shows that they consist of very fine-grained (less than .01 mm) reddish-brown opaques and equally fine-grained quartz and feldspar(?), in about equal abundance. The slightly coarser-grained phyllites contain abundant (40%) sericite as oriented, highly elongate patches and finely disseminated flakes. The coarsest-grained sample examined (collected in the north fork of McFarland Canyon) contains about 30% poorly sorted, angular, 0.1 mm - 0.4 mm quartz and plagioclase (plagioclase the more abundant), some of which are subhedral. Euhedral, 1 mm pyrite crystals are present in trace amounts. The matrix in this coarsest-grained sample is more

abundant than the clasts, and contributes about 25% chlorite, 35% sericite, and 10% quartz + feldspar to the modal composition of the rock.

Sedimentary Structures

Graded bedding, cross-bedding, and channeling are absent from most outcrops of the West Fork member. The outcrops of sandy beds near the Gila-Maricopa county line (in the Payson quadrangle) do contain such structures, however, and give consistent southeast directions for the tops of the beds.

Metamorphic and Deformational Effects

The West Fork member is consistently and pervasively foliated, so that the finer-grained rocks have a slaty cleavage, and some a micaceous sheen on parting surfaces. Although the slates are not competent, foliation and bedding are generally concordant.

Distribution

The West Fork member is exposed in a northeast-trending belt which intersects the West Fork of Sycamore Creek at the 5000' level. The best exposures of the unit crop out in the main tributaries to the West Fork of Sycamore Creek.

The lithologies of the West Fork member were not recognized on the southeast limb of the Red Rock syncline (on Mt. Ord). The chlorite-rich sandstones and siltstones of the Ord member (see p. 30), however, may be correlable.

Thickness

The West Fork member attains a maximum apparent exposed thickness of about 2000' at the southwest limit of the mapped area. To the northeast, near the northern boundary of the Reno Pass quadrangle, the thickness is as low as about 1000'. The apparent variation in thickness of the unit may in part be due to a degree of duplication of section by folding to the southeast.

Environment of Accumulation

The general fine-grained character and lack of abundant sedimentary structures reflecting current action suggests that the depositional environment was reasonably placid. The textural immaturity of the larger clasts in the coarser lithologies, however, may indicate that a slow input of relatively fresh material, rather than extensive reworking of older material, was responsible for the character of the unit. A very modest gradient between the source region and the sites of deposition, therefore, is indicated. This is consistent with the lack of significant volcanic material in the sediments, and implies that a period of volcanic quiescence obtained during deposition.

HORSE CAMP MEMBER

The Horse Camp member of the Alder series (new name, for typical exposures near Horse Camp Seep) is characterized by:

- 1) the abundance of volcanic lithic clasts in its beds,
- 2) a predominantly moderate ($\frac{1}{2}$ - 4 mm) grain size, and
- 3) its sedimentary nature.

The unit lies conformably above the West Fork member on the northwest side of the Red Rock syncline, and conformably above the Ord member on the southeast side of the syncline. It lies conformably below the Cornucopia member.

The rocks of the Horse Camp member crop out moderately well, although continuous exposures are found only in the larger drainages. Silicified and quartz-veined zones within the unit, however, are resistant, and form northeast-trending ridges which crop out continuously for more than a mile.

The stratigraphic upper limit of the Horse Camp member was defined in the field by the disappearance of sedimentary structures and textures (but not necessarily all stratification), and microscopically by the appearance of abundant volcanic textures that would normally be destroyed during sedimentation (see the discussion of such textures in the description of the Cornucopia member).

Lithologies

The most common lithology in the Horse Camp member is a medium to coarse-grained, poorly sorted, faintly bedded volcanic sandstone (plates 7 and 8). Phyllites, gravelly volcanic wackes, sedimentary breccias, and cobble conglomerates are present in the unit to a subsidiary degree. Limestone, dolomite, and bedded chert beds are locally present, but do not form persistent horizons.

The volcanic sandstones and wackes are typically gray to blue-green in stream-polished outcrops. On ridges and in roadcuts, the rocks are commonly tan, maroon, and pale purple. Foliation within the

Plate 7: Photomicrograph of volcanic sandstone of Horse Camp member (Alder series). Light-colored clasts are plagioclase and quartz, gray grains are both sericitized plagioclase and altered felsic volcanic clasts. The dark clasts are evidently altered mafic volcanics, some displaying relict plagioclase lathes. 2 × 3 mm field, plane polarized light.

Plate 8: Same as plate 7, but crossed nicols.

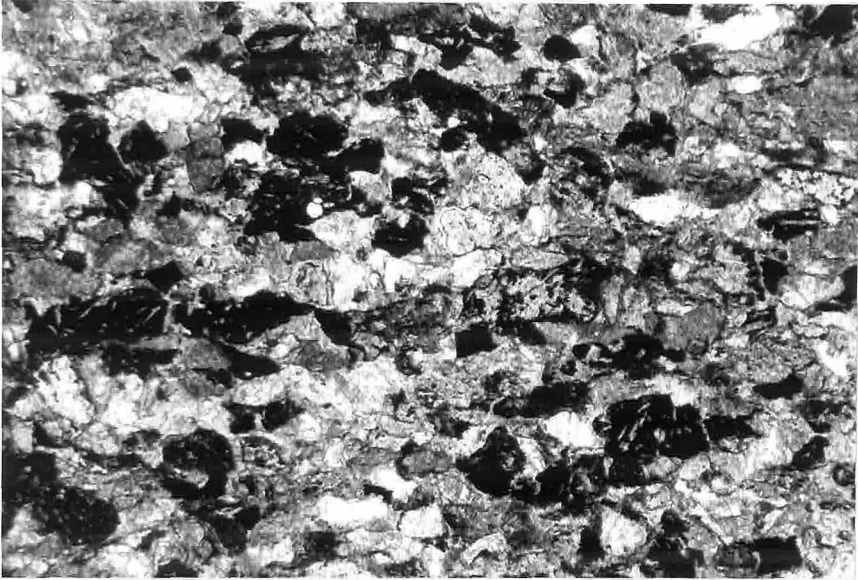


Plate 7

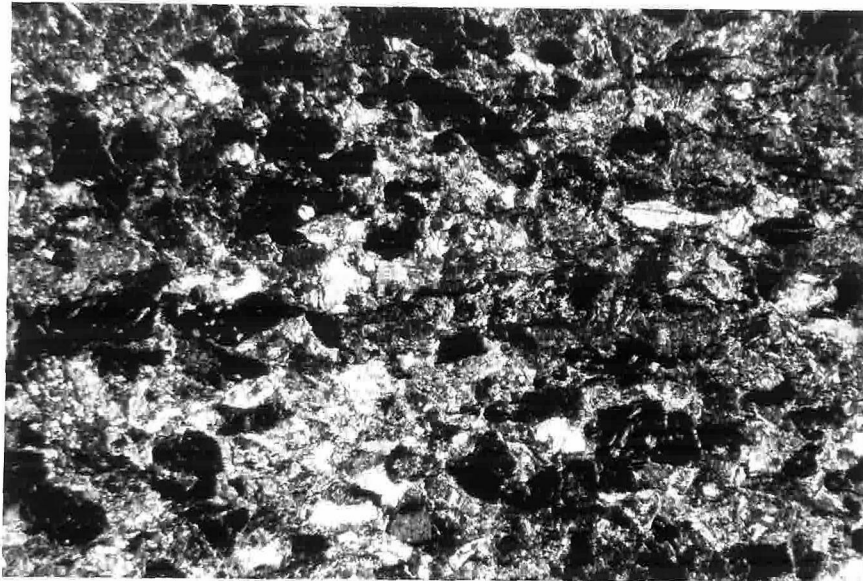


Plate 8

volcanic sandstones and wackes is generally faint, although in highly weathered outcrops it may be quite evident.

The identifiable clasts of hand-specimens of these rocks are fine-grained lithic fragments (generally volcanic if identifiable, occasionally shale), plagioclase, quartz, and jasper. Microscopic examination of the volcanic sandstones and wackes reveals the plagioclase to be unzoned, partially sericitized albite (possibly also some sodic oligoclase). The lithic fragments are of two main types:

1) felsic volcanics -- composed either of fine-grained, interlocking quartz and feldspar (less than .05 mm in grain size), or of ultrafine-grained (less than .01 mm) material, similar in texture to the lapilli in the lithic-crystal tuffs of the overlying Cornucopia member; or,

2) mafic volcanics -- partially or wholly altered to opaque minerals. Some clasts display abundant, small plagioclase laths in the opaque matrix (possibly relict hyalopilitic texture).

A minor clast type is composed wholly of chlorite. These probably also are altered mafic volcanics.

The matrix material of the volcanic sandstones does not generally exceed 5% of the rock, and has been recrystallized to sericite, chlorite, opaque minerals, and clays(?). No detrital heavy minerals were observed, possibly due to small grain-size and the obscuring effects of the matrix. The volcanic sandstones are generally moderately to poorly sorted, although a few very poorly sorted beds are present (notably exposed in roadcuts on the Thicket Springs road), and also some more texturally mature, phyllite-transitional types near the base of the unit.

The sedimentary breccias contain poorly sorted, $\frac{1}{2}$ " - 18" clasts of felsic volcanics, shale, sandstone, and jasper in a poorly sorted, sandy matrix. Conglomerate beds in the Horse Camp member are composed of pebbles and cobbles of felsic volcanics and jasper.

Carbonate beds within the Horse Camp member are typically thin (1" - 20") and dolomitic. Interbeds of massive volcanic wacke, and chert and jasper bands (1" - 3" thick) are common. Rare beds of massive, pink limestone up to 50' thick also occur. Bands of bedded chert or jasper are present in some outcrops of the volcanic sandstones and wackes.

On the southeast limb of the Red Rock syncline, on Mt. Ord, the Horse Camp member lithologies are somewhat different than the above described types in that,

- 1) they are richer in quartz and much poorer in mafic volcanic lithic clasts,
- 2) the unit includes beds of massive, highly resistant, moderately sorted quartzites,
- 3) sedimentary breccias and conglomerates are less common, and,
- 4) the rocks are more foliated, so that lithic clasts are distinctly stretched, and even quartz clasts somewhat deformed.

Sedimentary Structures

Original bedding is well-preserved in the outcrops of the Horse Camp member on the northwest limb of the Red Rock syncline. Bedding thicknesses are thinnest (as thin as a few inches) in the lower horizons of the unit, whereas the upper horizons tend to be massive.

Crossbedding, graded bedding, and channeling were rarely observed in outcrops (such outcrops were found at only four localities, all on the northwest limb of the syncline).

Metamorphic and Deformational Effects

On the northwest limb of the Red Rock syncline, the medium and coarse-grained lithologies are relatively free from metamorphic and deformational effects. Microscopic examination of the rocks reveals the presence of oriented sericite and elongate aggregates of opaque minerals, probably resulting from alteration of matrix material. The clasts have also been affected, but in a more subtle manner. The quartz grains are, in general, fresh-looking (sharp rims, clear, angular), but in the more foliated rocks have been slightly stretched, concordant with foliation, and have developed ragged edges. The plagioclase grains are fresh looking in some of the rocks, but more commonly are partially or completely altered to sericite and/or epidote. Authigenic or metamorphic overgrowths on the quartz and plagioclase grains are uncommon.

Euhedral carbonate rhombs which crosscut the sedimentary textures are scattered through some of the rocks, as well as 1 mm - 3 mm pods of carbonate aggregates. These rhombs (ankerite?) alter to a brownish, amorphous material.

The rocks of the Horse Camp member exposed on Mt. Ord, as mentioned above, are more sheared. Even the lithic clasts in these rocks are stretched and partially altered to sericite, and the quartz clasts are markedly stretched and even sericitized at their leading and trailing edges.

Distribution

The Horse Camp member is exposed in two northeast-trending belts flanking the Red Rock syncline. On the northwest side, the unit crosses the West Fork of Sycamore Creek between the elevations of about 4700' and 4900'. It is best exposed in the West Fork of Sycamore Creek, and in the Horse Camp Seep area. Southeast of the syncline, the unit crosses the Mt. Ord road between about 4600' and 5000', with best exposures in the northward flowing fork which joins Slate Creek at 3600'.

Thickness

On the northwest limb of the Red Rock syncline, the Horse Camp member varies in thickness from 2000' to 3500', thickening to the northeast. On Mt. Ord, the unit varies from about 700' to 1800' in thickness, also thickening to the northeast. Coarser-grained lithologies (coarse volcanic wackes and breccias) seem to be more abundant to the northwest, and may be responsible, at least in part, for the trend of thickening.

Environment of Accumulation

The heterogeneous character of the sediments of the Horse Camp member, and the abundance of volcanic debris as clast material, suggest an environment in which sedimentation was the result of erosion of a volcanic topography of significant complexity. The source regions may have harbored active volcanic centers, which centers either increased in activity with time, or migrated closer to the observed site of deposition. Such a conclusion is reasonable from the trend of the unit to contain more unreworkeed volcanic material towards the uppermost beds,

so that a complete gradation, up-section, into the subaqueous ash or debris flows of the Cornucopia member occurs.

Periods of active vulcanism of either great intensity or of close proximity would have increased the relief of the source areas of the sediments of the Horse Camp member, resulting in an increased clastic input, and thus in deposition of the coarsest and most immature sediments (breccias, conglomerates, and grits) of the unit. Periods of either volcanic quiescence or relatively great distance of active volcanic centers would have allowed reworking of a much reduced clastic input, resulting in deposition of the moderately sorted sandstones, argillites, and limestones of the unit.

The absence of common current-indicating structures in the sandstones of the Horse Camp member implies relatively deep-water deposition. Evidence of deposition by large-scale gravity slides or turbidity currents was not recognized, however. This suggests that although the gradient between the source region and the depositional region was steep enough to permit accumulation of coarse, immature material, it was shallow enough to prevent large-scale subaqueous transport and deposition.

Some information as to the source-regions of the Horse Camp member is given by an apparent, but subtle, increase in coarser sandstone and breccia lithologies to the northeast, combined with the generally finer-grained character of the unit on Mt. Ord. The implied direction of the source-region is thus roughly northeast.

CORNUCOPIA MEMBER

The Cornucopia member of the Alder series (new name, for exposures near the Cornucopia Mine) consists of coarse lithic tuffs, fine vitric tuffs, basaltic flows, bedded cherts, and felsic volcanic breccias. The unit conformably overlies the volcanic sandstones of the Horse Camp member, and underlies the slates and limestones of the East Fork member. Most of the lithologies of the Cornucopia member are poorly exposed. In some localities, however, the volcanic breccias and brecciated chert and jasper are resistant.

The contact of the Cornucopia member with the East Fork member is not exposed, or is intruded by sheets of the Pine Mt. porphyry. The contact with the underlying Horse Camp member (examined in detail only on the northwest side of the Red Rock syncline) is gradational over a thickness of section of about 500'. It was defined in the field by the disappearance of sedimentary structures and textures, going up-section, and microscopically by the appearance of volcanic textures that would normally be destroyed during sedimentation. Such textures include the presence of abundant euhedral and subhedral quartz grains (many being intricately corroded and embayed), delicate relict shard forms, and pumice fragments which show evidence of deformation during or shortly after accumulation. Transitional lithologies between the upper Horse Camp and lower Cornucopia members may be seen, in thin section, to be essentially texturally immature volcanic debris, but without preservation of the most delicate volcanic textures. They are difficult to classify in outcrop.

Lithologies

In the East Fork of Sycamore Creek, a gross internal stratigraphy of the Cornucopia member may be applied which appears valid for most of the exposures on the northwest side of the Red Rock syncline.

<u>Thickness</u>		<u>Predominant Lithologic Type</u>
	top	
500'±	↑	Dacitic-rhyodacitic volcanic cobble breccias
1000'±		Basaltic flows, pillow lavas, intercalated bedded chert
100'±		Fine-grained vitric tuffs
400'±		Lapilli-crystal tuffs
	bottom	

Except for the zone of the bedded cherts, these lithologic types were not mapped as separate horizons due to the difficulty of identifying weathered samples and to generally poor exposures of this unit.

Lapilli-Crystal Tuffs:

These rocks, present at the base of the unit, appear massive and medium-grained in outcrop, with colors of blue-green to gray (when fresh). Some coarse-grained types show elongate, fine-grained lithic fragments up to 5 mm in size. The average size of the lithic clasts is 1 mm to 2 mm. Angular, pink and white feldspar is present in 5% - 20% abundance. In some exposures, a faint stratification is discernible, but in general these tuffs appear structureless on a scale of a few feet, displaying neither bedding nor clast size

grading. Towards the top of the zone of occurrence of the lapilli-crystal tuffs, coarse breccias are intercalated. These breccias contain angular clasts of fine-grained, felsic volcanics from less than one-half inch to about two feet in size. The clasts vary in color and texture, and were evidently derived from a heterogeneous source. The wide size range, lack of sorting, and presence of a significant (more than 15%) finer-grained matrix to the clasts suggests a subaqueous debris flow origin for these coarse breccias.

Microscopic examination of the lapilli-crystal tuffs (plates 9, 10, 11, 12) shows that they consist typically of abundant (20% - 70%) very fine-grained felsic lapilli. These lapilli occur both as flattened or otherwise deformed shapes, and also as angular, crudely equant types. The deformed lapilli tend to be crudely spindle-shaped, and to be dented by angular feldspar or quartz crystals. Some lithic fragments exhibit vague, delicate, close-spaced parallel linear elements which R. S. Fiske (personal communication) suggests may be relict long-tube pumice textures. All of the lithic fragments are very fine-grained (less than .05 mm, generally less than .01 mm). They are all more or less altered to sericite and/or chlorite, and possibly ultrafine-grained epidote.

Quartz and plagioclase (albite or possibly sodic oligoclase) crystals are present, with abundances ranging from 5% to 30%, and plagioclase/quartz ratios from one to twenty. Most grains are anhedral to subhedral, with a few euhedral grains of both quartz and feldspar, and appear typically igneous. Many of the quartz crystals are rounded

Plate 9: Photomicrograph of lapilli-crystal tuff from Cornucopia member (Alder series). All of the lighter grains are sodic plagioclase. The grain in the top center of the field is an altered, fine-grained felsic volcanic clast, as is the large grain in the center of the field. Note the texture of fine, parallel lineaments in the large lithic clast (relict long-tube pumice texture?). 2 × 3 mm field, plane polarized light.

Plate 10: Same as plate 9, but crossed nicols.

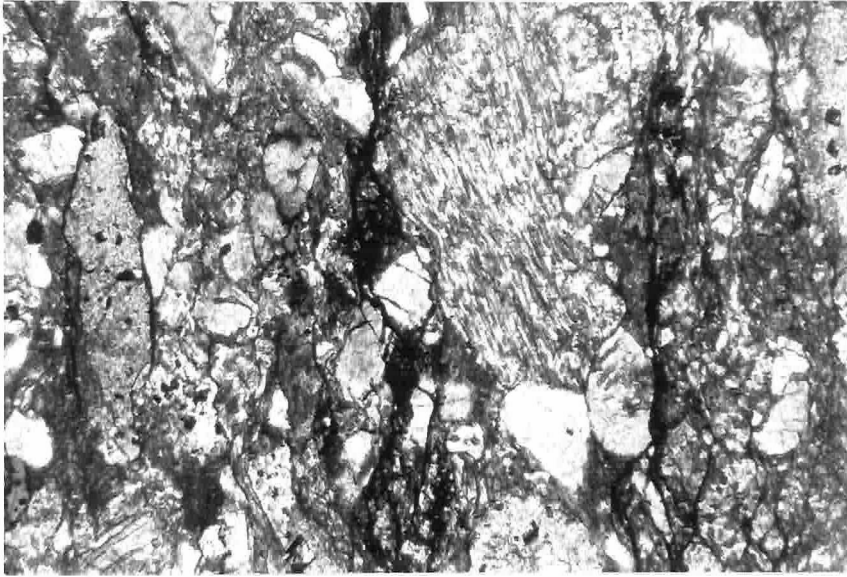


Plate 9

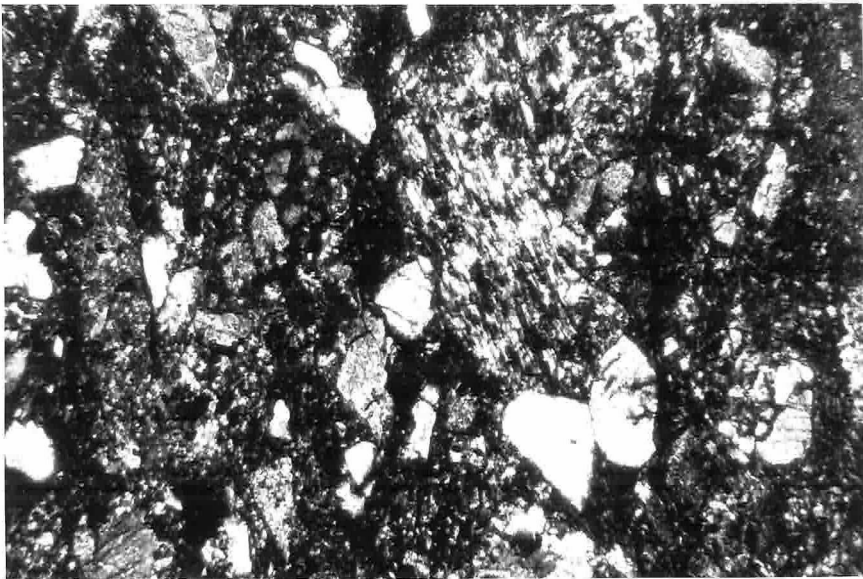


Plate 10

Plate 11: Photomicrograph of lapilli-crystal tuff from Cornucopia member (Alder series). Lighter grains are both quartz and sodic plagioclase. The lithic clasts are fine-grained, felsic volcanics, partially altered to sericite and chlorite. Note faint, relict long-tube pumice textures (?) in some of the lithic clasts, deformation of one lithic clast by another in the lower center. 6 × 9 mm field, plane polarized light.

Plate 12: Same as plate 11, but crossed nicols.

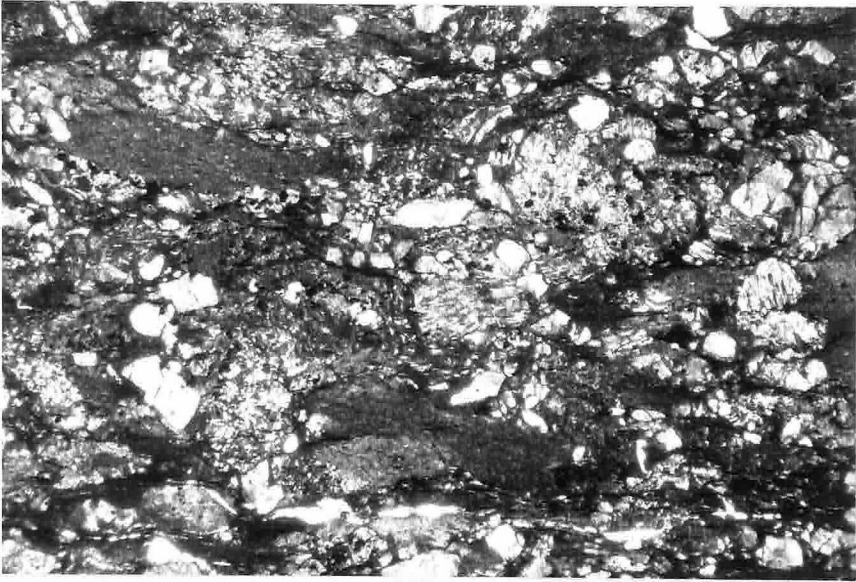


Plate 11

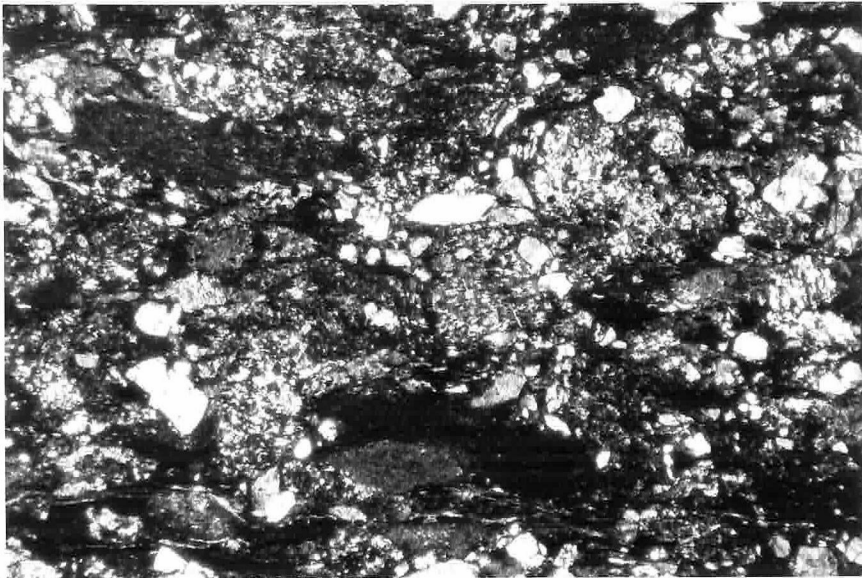


Plate 12

and embayed. The plagioclase is moderately fresh looking, with a slight sericitic alteration, and is unzoned. The size range of most of the quartz and plagioclase grains is 0.2 mm - 1 mm.

Possible relict shard forms are visible in the matrix material, and are now composed of fine-grained quartz, sericite, and feldspar. Many delicate arcuate and forked shapes, from 0.1 mm - 1 mm, are present.

The amount of matrix material in these rocks is difficult to estimate, as the boundaries of fine-grained, partially sericitized or chloritized lithic fragments are somewhat obscure, but appears to be less than 10%, and possibly less than 5% (see plates 7-10).

Vitric Tuffs:

In the East Fork of Sycamore Creek, between the zones of lapilli-crystal tuff and bedded chert-pillow lavas, about 100' of bedded, dense, fine-grained, blue to white rock is exposed. In thin-section, these rocks display abundant relict outlines of .05 mm to 0.1 mm shards. No phenocrysts were observed, and most of the original textural elements are obscured by sericitization and by recrystallization to fine-grained, interlocking quartz and feldspar. These rocks were recognized only in the above locality.

Basaltic Flows, Pillow Lavas, and Bedded Cherts:

Basaltic flows and pillow lavas crop out in several localities. They tend to be poorly exposed, so that their character is evident only in major drainages where fresh exposures are common. They are restricted to the stratigraphic zone indicated on page 43, but are not always present within this zone. Northwest of the Red Rock

syncline, they are intimately associated with thin units of bedded cherts.

The basaltic flows and pillow lavas are typically dark gray to dark blue, coarsely foliated, and fine-grained except for abundant $\frac{1}{2}$ mm - 2 mm amygdules of calcite, or of subsequently weathered-out minerals. The amygdules are commonly elongate and aligned. Best exposures of pillow structures are in the East Fork of Sycamore Creek (plate 13), where small (about 6" \times 12"), flattened, aligned pillows rest in a matrix of fine-grained, tan, dolomitic material. On the southeast limb of the Red Rock syncline, the pillow lavas are not associated with bedded cherts, and tend to have much larger pillows (about 18" \times 36") and no dolomitic matrix. Northwest of the Thicket Springs fault, no pillow lavas occur within the mapped area; however, reconnaissance in the Cornucopia member in Deer Creek, about one mile north of the northern limit of the mapped area, shows that they are not completely missing in this part of the structure. These exposures are of 6" - 36" pillows, some of which are broken, in a dense, fine-grained matrix which is in part dolomitic. The pillows are amygdaloidal, with the elongate amygdules aligned roughly parallel with the rims of the pillows.

Thin-section examination of the basaltic rocks shows that albite phenocrysts up to 1 mm are preserved and abundant in some types, but absent in others. In samples with well-preserved groundmass textures, plagioclase or relict plagioclase is present as randomly oriented lathes (.05 mm - 0.1 mm). Some of these rocks, however, retain no trace of original groundmass texture. Other minerals in the groundmass are

Plate 13: Pillow lava in Cornucopia member (Alder series) exposed in the East Fork of Sycamore Creek. For microscopic appearance of the rock, see plate 16.

Plate 14: Photomicrograph of basaltic flow in Cornucopia member, containing pseudomorphs of chlorite and carbonate after olivine(?) and pyroxene. Amygdules of chlorite and carbonate are also present. 6 × 9 mm field, plane polarized light.



Plate 13

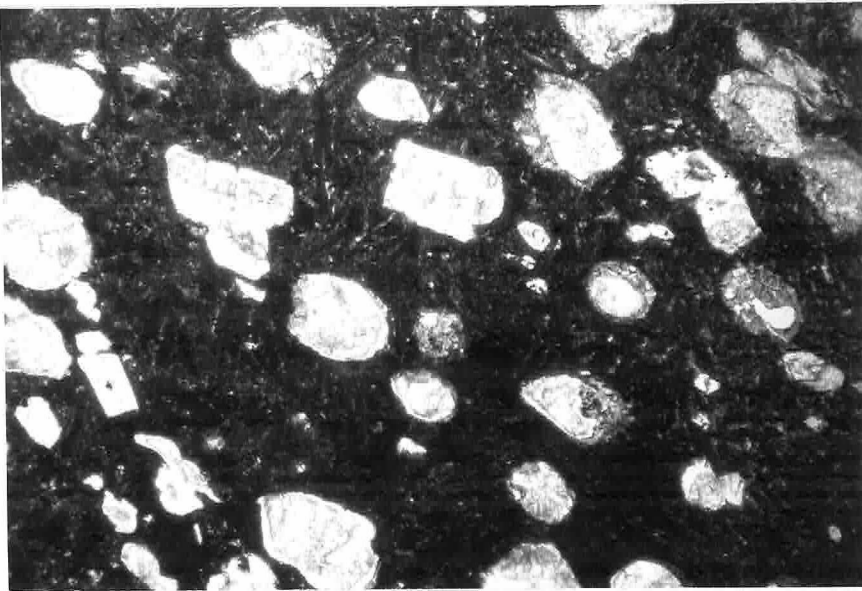


Plate 14

chlorite, carbonate, and opaque minerals. Only one sample examined showed relict mafic phenocrysts. This rock (plates 14, 15, 16) contains abundant chlorite and carbonate-filled forms which suggest the shapes of phenocrysts of pyroxene and olivine. It is the only Alder series rock examined which retains definite petrographic indication (besides abundance of opaque minerals and chlorite) of an original mafic composition. The abundant amygdules of the rock consist either of fibrous chlorite, carbonate, or both (plate 16).

On the northwest side of the Red Rock syncline, the zone of basaltic flows and pillow lavas contains several thin (15' - 50') units of bedded chert and jasper. The beds are thin (at most 6"), with colors of blue, black, white, and red. At several localities -- notably Gold Creek and the West Fork of Sycamore Creek -- the chert and jasper are brecciated and are embedded in a matrix of fine-grained, dense, blue rock (plate 17), or in tan dolomite (plate 18).

Microscopic examination of the bedded cherts shows that they consist of very fine-grained, interlocking, quartz + feldspar(?) (less than .005 mm), reddish amorphous opaque minerals, and disseminated, fine (.05 mm - .1 mm) rhombs of carbonate (ankerite?). The opaque minerals and the carbonate define a faint stratification of the rock. The matrix of the bedded cherts was examined in one sample, and proved to be of very fine-grained (less than .005 mm) material, evidently chlorite, sericite, and amorphous opaques. The matrix displays a gross structure, defined by concentrations of the opaque minerals, which is strongly suggestive of slightly deformed crossbedding on a 1 mm scale.

Plate 15: Photomicrograph of matrix of rock shown in plate 14, showing relict texture of randomly oriented plagioclase lathes. 2 × 3 mm field, plane polarized light.

Plate 16: Photomicrograph of a pillow from the outcrop shown in plate 13, displaying abundant, aligned amygdules of chlorite (predominantly), quartz, and carbonate. 6 × 9 mm field, plane polarized light.

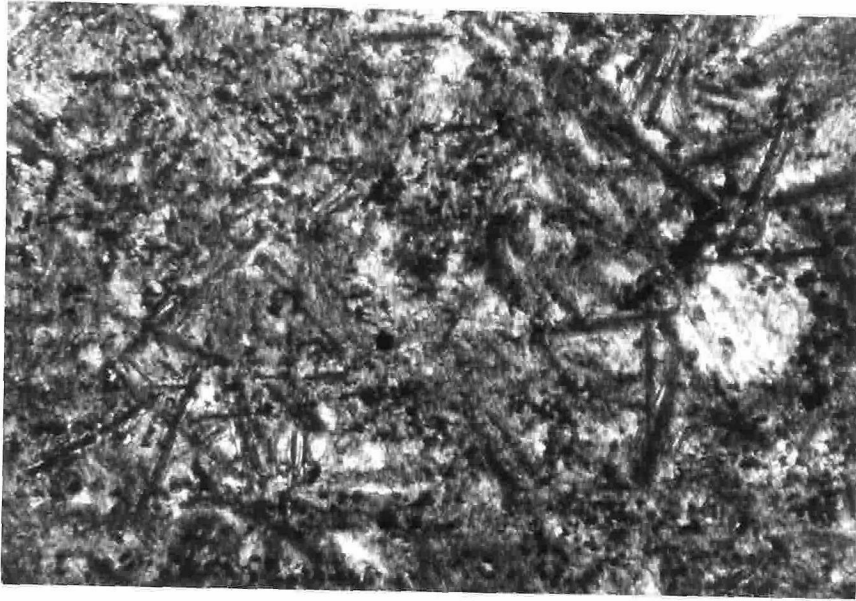


Plate 15

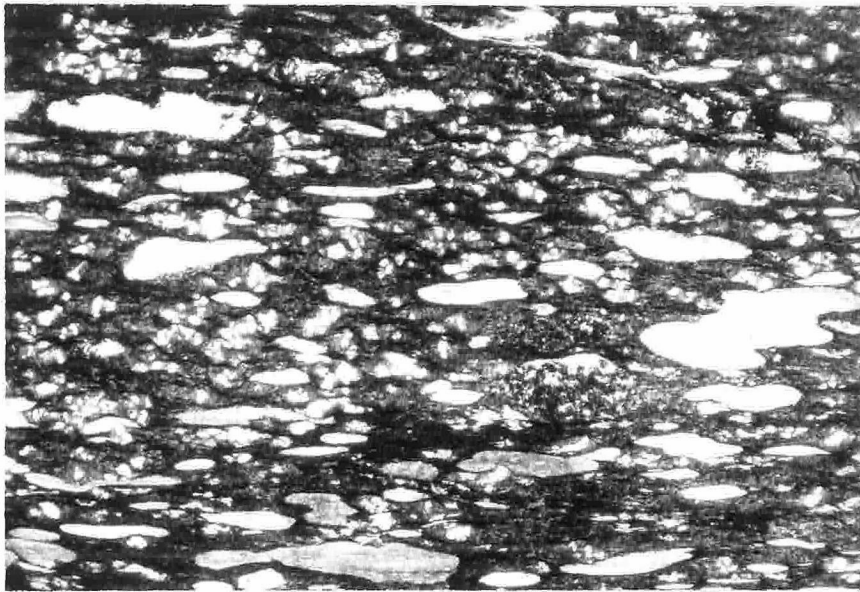


Plate 16

Plate 17: Jasper breccia in Cornucopia member (Alder series) exposed in upper Gold Creek. The clasts are fragments of bedded jasper and chert. The matrix (dark blue in color) is very fine-grained, tough material, possibly altered and silicified volcanic ash. Undisturbed bedded chert and jasper crop out, with continuous exposure, about ten feet from the site of the photograph.

Plate 18: Jasper breccia in Cornucopia member (Alder series), exposed in the West Fork of Sycamore Creek. The dark clasts are fragments of bedded jasper and chert, and the white, irregular patches and veins are quartz. The matrix is dolomite.



Plate 17



Plate 18

Volcanic Breccias:

The uppermost lithologic type of the Cornucopia member generally consists of coarse, felsic volcanic breccias (plates 19, 20) containing angular to subrounded clasts from less than an inch to more than two feet in size. The breccias occur as massive beds, at least 30' thick, in a zone 500' to 1000' thick on both sides of the Red Rock syncline and Thicket Springs fault.

The breccias crop out poorly, except on the south flank of Mt. Peeley, near the McFarland Canyon pack trail, where five to 10-foot reefs of the rock stand in relief. The clasts range in color from dark gray to dark blue to white, and are generally roughly equant in shape. In most outcrops, however, a few of the clasts are elongate, and in one outcrop on Mt. Ord, a majority of clasts are both elongate and aligned. The clasts contain abundant pink or white 1 - 2 mm feldspar phenocrysts in a fine-grained, dense groundmass. Bleached rims, about $\frac{1}{2}$ " to 1" wide, are present in the clasts of breccias on the south flank of Mt. Peeley, but do not represent a widespread feature.

Because of the similarity in texture and composition of the clasts of the breccia and the matrix of the breccia, it is difficult to distinguish the boundaries of the clasts in the outcrop. Consequently, the clastic nature of the rock is generally obscured except in fairly fresh exposures. The only clasts observed besides the felsic (plagioclase or plagioclase-quartz) porphyries were very sparse jasper pebbles, present in only a few outcrops.

In thin-section, the clasts of the volcanic breccia show $\frac{1}{2}$ mm to 4 mm subhedral to euhedral quartz and plagioclase phenocrysts.

Plate 19: Volcanic breccia in Cornucopia member (Alder series), south of Thicket Springs. The clasts and matrix material are plagioclase-quartz porphyry.

Plate 20: Close-up of volcanic breccia of Cornucopia member (near the location of plate 19).

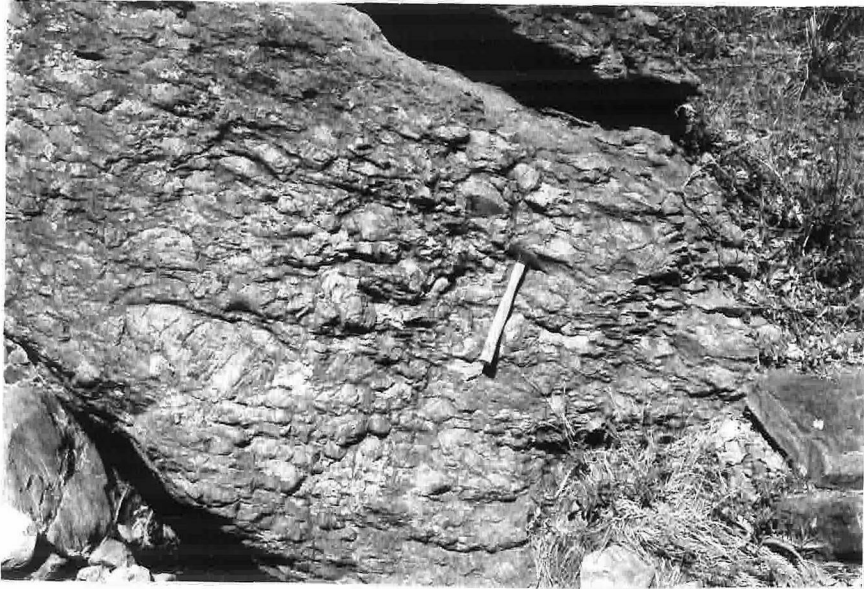


Plate 19



Plate 20

The plagioclase phenocrysts are unzoned, moderately fresh albite, in some cases partially altered to epidote. Aggregates of chlorite and epidote, pseudomorphic after hornblende(?) phenocrysts are present in some of the rocks. The groundmass consists of fine-grained (.01 mm to .05 mm), interlocking quartz and feldspar, and is altered to a variable degree (10% - 30%) to fine-grained sericite, chlorite, and epidote. Thin-sections cut across clast-matrix boundaries show no essential difference in mineralogy between clast and matrix, or between different clasts. The clasts are visually discernible from the matrix by differences in phenocryst size and abundance, and in degree of alteration of the fine-grained groundmass (plate 21).

Metamorphic and Deformational Effects

Lapilli-Crystal Tuffs:

Elongate aggregates of sericite, chlorite, and opaque minerals oriented parallel to the foliation of these rocks are characteristic. Chlorite also occurs as droplet-like forms in the more altered lapilli, and in areas which appear to have been rich in glass shards. Epidote is either absent, or is present only as very fine, disseminated grains. Most samples examined contain anhedral carbonate grains which crosscut the depositional and deformational texture of the rock. These carbonate grains are large (up to 5 mm), and contain dust-like opaque mineral inclusions which are oriented so as to cause the grains to appear pleochroic.

The freshest outcrops of the lapilli-crystal tuffs show only a faint foliation; however, the foliation is generally conspicuous in weathered outcrops.

Plate 21: Photomicrograph of dacitic volcanic breccia from Cornucopia member. At least three textural domains are visible in the photomicrograph. All phenocrysts are albite. 6 × 9 mm field, crossed nicols.

Plate 22: Deformed slates of East Fork member (Alder series) in the East Fork of Sycamore Creek.

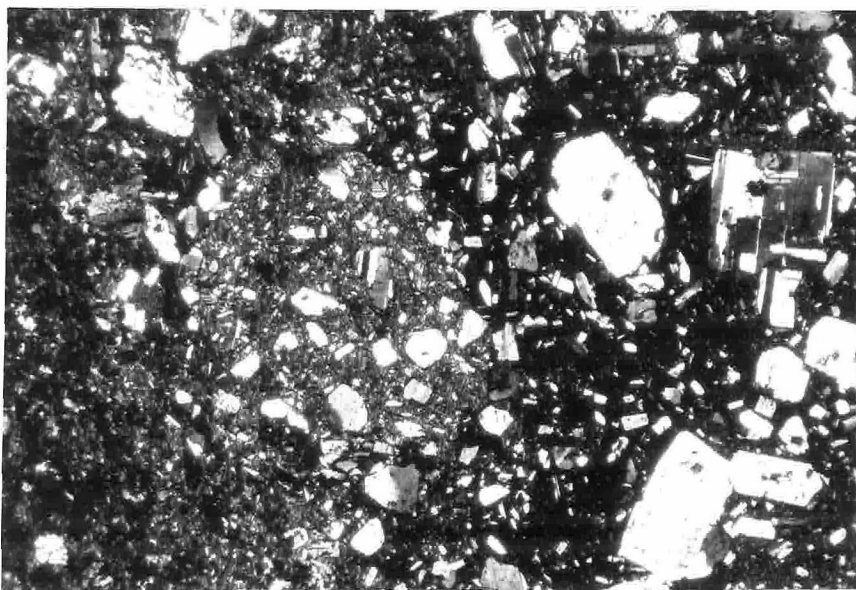


Plate 21



Plate 22

Basaltic Flows, Pillow Lavas, and Bedded Cherts:

Although the degree of recrystallization of the basaltic rocks is such that virtually no original mafic minerals remain, the degree of shearing, and thus of shear-induced recrystallization, seems to have been slight. Equant mafic mineral pseudomorphs and irregular-shaped amygdules have not been stretched; nor have the delicate relict ground-mass textures shown in plate 16 been modified. The absence of identifiable epidote in the basaltic rocks implies either that,

1) metamorphic reaction kinetics played an important part in establishing the present mineral assemblage, since epidote is normally formed from low-grade metamorphic recrystallization of mafic volcanics, or

2) the rocks were essentially spilitic, inhibiting epidote formation by lack of calcium.

The latter possibility is discussed in a later section.

The bedded cherts also show little metamorphic and deformational effects. They are not foliated, nor do they show tight folding. They do, however, display some open folding on a scale of tens of feet. The fine-grain size of the quartzo-feldspathic parts of the cherts, and the dust-like character of the opaque minerals in some of them indicates relatively little metamorphic recrystallization.

Volcanic Breccias:

The volcanic breccias, like the other lithologies of the Cornucopia member, are only slightly foliated. They typically weather into large, roughly equant to slightly tabular boulders. Microscopic effects of deformation are similarly slight. Sericitization of feldspars and of

the groundmass is not pronounced, and takes the form of disseminated flakes and randomly oriented aggregates rather than the elongate, preferentially oriented aggregates of the more strongly foliated rocks of the Alder series.

Epidote is always present in the breccias, and occurs as fine-grained aggregates and disseminated grains after parts of the groundmass and plagioclase phenocrysts. Minor amounts of chlorite are also present, and are generally associated with epidote aggregates. The albitic composition of the unzoned, rather large plagioclase phenocrysts clearly reflects metamorphic albitization of these crystals, in view of the normal CaO content of the rock (table II, Appendix I).

Cornucopia Member: Chemistry

One sample of the volcanic breccia lithology, and two of the lapilli-crystal tuff lithology were analyzed for their major element chemistry (table II, Appendix I). The breccia, except for a rather low K_2O content, is very similar to Nockolds' average dacite + dacite-obsidian (Nockolds, 1954). The two lapilli-crystal tuff samples both have normative corundum (2.8% for I, 0.7% for II), reflected in the presence of sericite, and may have undergone some change in Na, K, and Si concentrations during sericitization. Their present chemical composition, however, is also close to Nockolds' average dacite + dacite-obsidian, except for their CaO and (equivalent) FeO contents. Comparatively, the two lapilli-crystal tuff samples are distinctly low in CaO, and high in equivalent FeO. The three Cornucopia member samples are

plotted on quartz-plagioclase-orthoclase and AFM diagrams in figures 5 and 6, respectively, in Appendix I.

Environment of Accumulation

Lapilli-Crystal Tuffs:

A direct, pyroclastic volcanic origin for the lapilli-crystal tuffs of the Cornucopia is suggested -- but not proved -- by several textural features of the rocks. The abundance and preservation of euhedral and subhedral quartz and feldspars and the presence of delicate relict shard forms is inconsistent with any degree of normal sedimentary transport. Mass transport of large volumes of material such as in a turbidity current or subaqueous debris flow, however, could have preserved these textures.

The abundance of similar-appearing, very fine-grained pumiceous clasts in the rocks suggests either direct pyroclastic derivation from a volcanic source or rapid erosion and deposition from such a source. The scarcity of fine-grained matrix material in the lapilli-crystal tuffs, and the degree of sorting of the clasts, however, favors the interpretation of accumulation by subaqueous ash-flows, as described by Fiske and Matsuda (1964). Such ash-flows are described by them as derived from downslope movements of cold slurries of ash and pumice from the flanks of erupting, submarine volcanoes. Qualities characteristic of such deposits are an abundance of pumiceous clasts, many of which are elongate and contain long, tube-like bubbles (long-tube pumice), scarcity of fine-grained matrix material, a high degree of sorting, and grading of the individual flows and of the overall deposit.

The lapilli-tuffs of the Cornucopia member meet all but the last criterion. Relict long-tube pumice texture may be faintly seen in some of the clasts in plates 9-12 (suggested by Fiske, personal communication), and is not uncommon.* Small and large-scale clast size grading was not recognized in the field, however. The absence of apparent grading, the presence of intercalated, poorly sorted breccias, and the transitional nature of the base of the rocks (from volcanic sandstones to lapilli tuffs), are important differences from the subaqueous ash-flow deposits described by Fiske (1963) and Fiske and Matsuda (1964). A possible explanation is that the lapilli-tuffs of the Cornucopia member were deposited much further from the volcanic sources. If this were the case, then the ash-flows would tend to be slightly reworked towards the limit of their travel, and to be intercalated with debris flows from submarine slopes composed of typical subaqueous ash-flow material. The upper Horse Camp member-lower Cornucopia member transition might then mark the time of volcanic input that was either sufficiently nearby or sufficiently large that epiclastic reworking would no longer be operative.

Basaltic Flows and Bedded Cherts:

The stratigraphic assemblage of pillow-lavas and bedded cherts is rather common in eugeosynclinal assemblages (Turner and Verhoogen, 1960, p. 261; Bailey et al., 1964, p. 65). It is now widely believed (Turner

* According to Fiske and Matsuda (1964), pumice with equant, non-communicating vesicles float and are dispersed, whereas the long-tube variety quickly becomes waterlogged by capillary action, and sinks.

and Verhoogen, *ibid.*, Bailey *et al.*, *ibid.*) that the bedded cherts associated with the pillow lavas were formed by either chemical or organic precipitation of silica from greatly supersaturated seawater, the reaction of the molten or very hot and glassy basaltic pillow lavas with sea water supplying the necessary silica. The pillow lavas are, in many cases, spilitic. As mentioned above (p. 64), the Cornucopia member pillow lavas, being low or lacking in epidote, may also be essentially spilitic. The main difference between the Cornucopia member pillow lava-bedded chert association and typical eugeosynclinal assemblages is the relative insignificance of the thicknesses of both the basalts and the bedded cherts in the Alder series section.

The bedded cherts -- especially those zones which are brecciated -- were remarked on by previous geologists. Ransome (1915, 1916) and Lausen (1926) evidently regarded the bedded cherts and jasper as being within the stratified section, while Wilson (1939) concluded that they are Tertiary hydrothermal deposits that rested on an erosion surface of the Alder series.* This study shows that the bedded chert and jasper are clearly within the Alder series. They show no discordance, even when brecciated, at their contacts with the basaltic rocks of the Cornucopia member, and they occur in a conformable stratigraphic zone which persists for at least four miles. Outcrops in Gold Creek which display both bedded and brecciated jasper in a single exposure (plate 17 shows

* An apparently conformable, northeast-striking body of massive jasper of apparent replacement origin is present within the Horse Camp member about 1000' southwest of Pigeon Spring. This body should not be confused with the cherts and jasper within the Cornucopia member.

the brecciated jasper in this outcrop) prove that the bedded and brecciated chert and jasper are of the same origin.

The mechanism of brecciation and of formation, locally, of the carbonate matrix is not clear. Pertinent observations are that,

1) breccias with carbonate matrix are themselves veined by nets or boxworks of $\frac{1}{2}$ " - 3" quartz veins (plate 18),

2) breccia zones may be thin -- down to a foot thick -- and are conformable with the bedding of the unbrecciated chert and jasper,

3) conformable, inch-thick dolomitic veins or beds occur within the Alder series rocks for hundreds of feet on either side of the zones of jasper breccia with a carbonate matrix, and

4) the sole clast lithology of the breccias is chert and jasper.

It is possible that the zone of brecciation is due to bedding-plane shearing (during the regional deformation of the area) restricted to the zone of thin-bedded and relatively incompetent cherts and jasper. The appearance of the breccias in Gold Creek, however, (plate 17) is more suggestive of a sedimentary, intraformational breccia, because the matrix is very similar in appearance to the fine-grained, dark-colored tuffs which crop out on either side of the breccia zone. Also, no quartz veining is present in this locality.

A reasonable explanation for these jasper and chert breccias is that they were formed contemporaneously with the accumulation of the volcanics and bedded cherts by small-scale gravity sliding or by current breakup of possibly still soft bedded silica-rich material, during a period of volcanic quiescence.

Volcanic Breccias:

The identification of the breccias of the Cornucopia member as volcanic, rather than sedimentary, is made because of the textural immaturity and lithologic similarity of the clasts, the identity of composition of the clasts and their matrix, and the absence of any sedimentary textures within the zone of the breccias. It is also noteworthy that intercalated lithologies which occur in the Thicket Springs area and are not coarsely clastic are coarse crystal tuffs of similar composition to the breccia.

The absence or scarcity of clasts deformed during accumulation is consistent with the accumulation of relatively cool material. The absence of pumiceous clasts suggests that the breccias are not the result of a simple (little or no sorting) pyroclastic event. Submarine debris flows, triggered by volcanic activity and from a uniform volcanic source region, are a reasonable mechanism for the formation of these breccias. A direct pyroclastic origin is also possible, since pumiceous clasts would likely be sorted from the denser, solid fragments in an aqueous environment. The great areal extent of the Cornucopia member breccias suggests that volcanic event was a major one, and that there existed a significant gradient between the source regions and the depositional regions now exposed.

Cornucopia Member: Distribution

The Cornucopia member is exposed in three northeast-trending belts. On the lower flanks of Mt. Peeley, the volcanic breccia lithology of the unit is exposed in a continuous band which extends for several

miles both to the northeast and west of the Reno Pass quadrangle. Only this uppermost Cornucopia member lithology is exposed here, as the lower parts of the unit are faulted out against the Thicket Springs fault.

The second belt crosses both forks of Sycamore Creek, intersecting the locality of the Cornucopia mine, and is continuous for at least five miles. All of the described lithologies are present within this belt; however, they do not uniformly persist for the mapped length. The fine-grained vitric tuffs were recognized only in the region near the East Fork of Sycamore Creek. The basaltic flows and pillow lavas do not persist as far northeastward as upper Gold Creek, although a few bedded cherts are still present there.

The third belt, on the north flank of Mt. Ord, crosses the Mt. Ord road between the elevations of about 4600' and 4400'. The breccias persist across the mapped part of Mt. Ord, and basaltic flows and pillow lavas crop out in at least one drainage. Bedded cherts apparently are missing from the Mt. Ord section. The lapilli tuffs are probably present, but were not identified microscopically in the samples taken from this area.

The trends defined by the distribution of the Cornucopia member lithologies are,

- 1) disappearance of the uppermost lithologies -- volcanic breccias, flows, and pillow lavas -- to the northeast,
- 2) thickening of the lapilli-crystal tuffs to the northeast (northwest of the Red Rock syncline axis), but
- 3) apparent thinning or disappearance of the lapilli-crystal tuffs to the southeast (southeast of the Red Rock syncline axis), and

4) thinning of the entire Cornucopia member across the Red Rock syncline axis to the southeast.

The first two trends suggest a volcanic source-region distinct from the source-regions of later Alder series and Red Rock rhyolite volcanic material.

EAST FORK MEMBER

The East Fork member of the Alder series (new name, for exposures in the East Fork of Sycamore Creek) consists of typically maroon slates and phyllites, with subsidiary limestone, limey sandstone, and local coarse lithic wackes. The unit crops out poorly except in creek beds. The East Fork member overlies the volcanic breccias of the Cornucopia member, and underlies the jasper-bearing conglomerate or grits of the Oneida member (northwest of the Red Rock syncline), the quartzites and tuff-breccias of the Oneida member (southeast side of syncline, Mt. Ord), or the Red Rock rhyolite (Mt. Peeley).

The contact relations with the Oneida member are conformable and gradational over a few tens of feet. The contact with the Red Rock rhyolite on Mt. Peeley appears conformable within a stratigraphic thickness of about one hundred feet for the mile length along which the vitric tuff sub-unit is exposed, and within one thousand feet for the three miles of observed contact. The contact itself is not exposed, but appears to be depositional, as no evidence of unusual shearing was detected in the regions giving best exposure near the contact (within

ten to one hundred feet).

Lithologies

Northwest of Red Rock Syncline (East and West Forks of Sycamore Creek, Gold Creek):

The East Fork member lithologies in this region are maroon-colored slates and phyllites with subsidiary limestones and limey siltstones. The slates commonly show a fine lamination and, in some cases, sandy interbeds. The uppermost horizons of the unit are relatively coarse-grained, and contain small pebbles of jasper. The grain size and abundance of jasper pebbles increases with proximity to the conglomerate of the Oneida member.

Near the base, a persistent thick limestone bed, about 50' thick, is present. The limestone is a reddish-maroon, massive, and contains a variable (1%-30%) degree of clastic (coarse sand, quartz and jasper) material. At Gold Creek, near the northeastward limit of mapped East Fork member, the slates and phyllites (and sandstones, which appear in this region) are limey for a few hundred feet on either side of the limestone exposure.

Microscopic examination of the laminated slates shows that they are in part tuffaceous, with the coarser interbeds (laminae) containing abundant recrystallized (to fine-grained quartz and feldspar) coarse shards (see plate 23). The finer-grained laminae are now composed of reddish opaque minerals, and very fine-grained (less than .01 mm) quartz and feldspar. Sericite stringers are abundant in the finer-grained laminae.

Plate 23: Photomicrograph of phyllite of East Fork member (Alder series). Note abundant, light-colored shard-forms. 2 × 3 mm field, plane polarized light.

Plate 24: Photomicrograph of vitric tuff sub-unit of East Fork member, showing abundant relict shards and angular chips of quartz and feldspar in a fine-grained matrix. 2 × 3 mm field, plane polarized light.

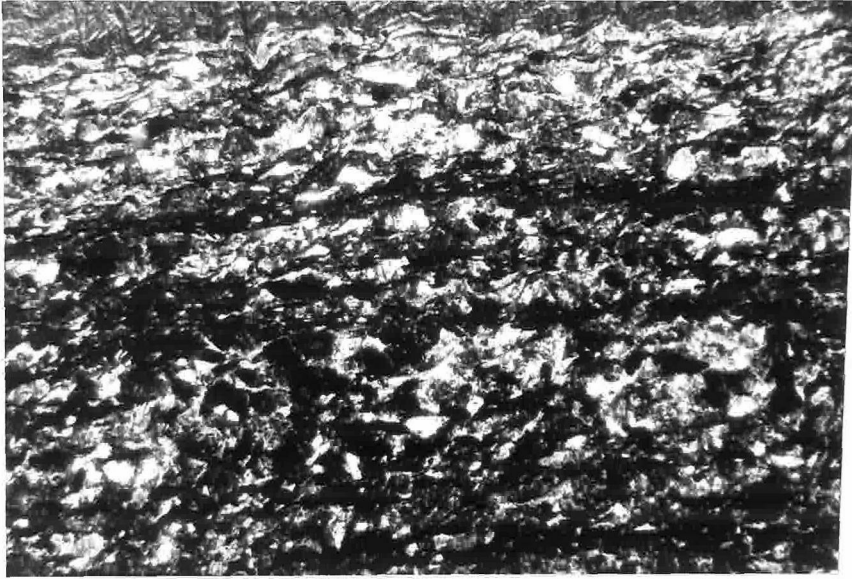


Plate 23

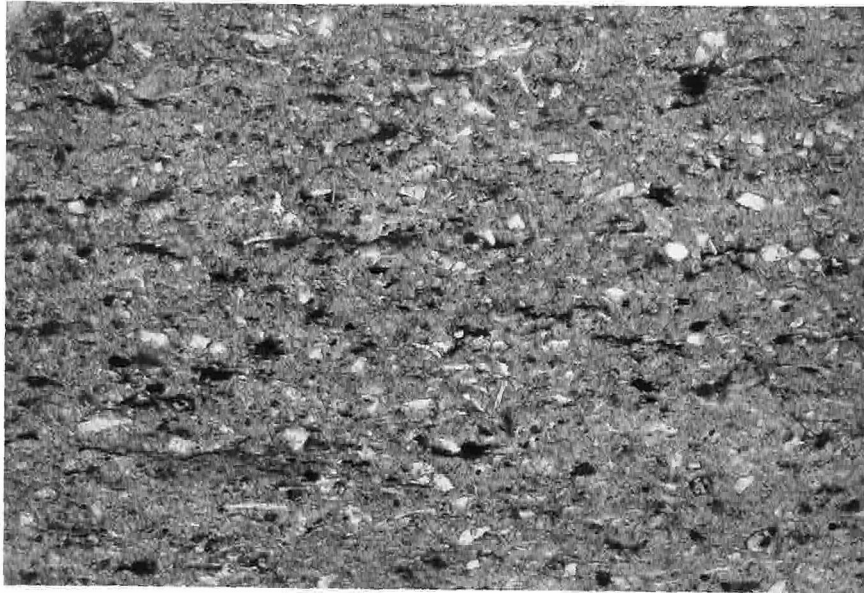


Plate 24

Mt. Peeley Lithologies:

The dominant lithologies here are also maroon slates and phyllites; coarser-grained interbeds, however, are not uncommon in the area between Deer Creek (in the Payson quadrangle) and the Gila-Maricopa County line (also in the Payson quadrangle, near its southern boundary). These coarse-grained rocks are volcanic sandstones with sparse, angular quartz and abundant fine-grained, elongate (oriented) lithic clasts, moderately to poorly sorted.

The basal beds of the Mt. Peeley exposures of the East Fork member are fine to medium-grained, pale blue-green, well-foliated rocks which grade into the maroon phyllites. The clasts appear in hand-specimen to be angular, $\frac{1}{2}$ mm - 1 mm feldspar and fine-grained lithic fragments.

In thin-section, the laminated slates appear very similar to the tuffaceous slates exposed in the East Fork of Sycamore Creek. They contain abundant, coarse shards in coarse-grained laminae, and fine-grained opaques, quartz and feldspar in the fine-grained and deeply colored (maroon) laminae. The coarse volcanic sandstone interbeds exposed near Deer Creek show, in thin-section, abundant fine-grained lithic clasts of varying composition (based on degree of chloritization or on opaque mineral abundance), most of which are pronouncedly elongate in the plane of bedding. The most common lithic clast type consists of fine-grained (.01 mm - .05 mm) interlocking quartz and feldspar, with a variable amount of sericite. Many of the clasts, however, consist mostly of black opaque minerals or of opaque minerals and chlorite.

Quartz is not abundant (about 3% mode), and occurs in forms which strongly suggest that they were broken subhedral phenocrysts.

The proportion of matrix material is difficult to estimate in the presence of the metamorphic effects on the volcanic clasts (so that fine-grained epidote, chlorite and sericite obscure clast boundaries), but is probably less than 10%.

The basal blue-green, medium-grained beds of the unit on Mt. Peeley appear, in thin-section, to be tuffaceous, with a high crystal content. Quartz and plagioclase (in equal abundance) form about 30% of the rock, and occur as subhedral to anhedral 0.1 mm to 3 mm grains. A few fine-grained, leucocratic lithic fragments of 1 mm - 3 mm size are resolvable, but the degree of alteration of the rock (about 35% sericitized) and the abundance (15%) of disseminated, fine-grained opaques prohibit identification of the original character of the rock. Both leucocratic lithic fragments or coarse shards might have been abundant.

East Fork member - vitric tuff sub-unit:

A massive, fine-grained tuff occurs within the uppermost horizons of the East Fork member on Mt. Peeley, near Thicket Springs. This lithology forms a mappable sub-unit within the East Fork member, and is valuable as the only such horizon close to the overlying Red Rock rhyolite. It crops out for about 3/4 mile only, and has an average thickness of about 250'. The tuff is overlain and underlain by siltstones and mudstones, with the lower contact not exposed. The upper contact is sharp to within a few feet, and is distinguished primarily by a color change from pale green (the color of the unweathered tuff) to

light maroon.

The rocks of this sub-unit crop out poorly, but are exposed in road and trail cuts. In outcrop and hand-specimen, little or no foliation is visible. The rock weathers to a light brown color, and is weathered to this color along pervasive, irregular fractures. Millimeter-sized crystals of quartz and feldspar are distinguishable in hand samples from the lower horizons of the unit, although not abundant, but are not visible in samples from the middle and uppermost horizons. The rock is generally fine-grained, and shows no bedding either on a small or large scale.

Microscopic examination of samples from this tuff unit reveals, in the higher horizons, the presence of abundant relict shards from .01 mm to .05 mm (plates 24, 25). The shard-bearing type also contains about 10% opaque minerals, which occur in elongate forms defining a planar texture. About 5% of angular chips of .01 mm - .05 mm quartz and feldspar are present throughout the rock. Fine-grained quartz, feldspar, and sericite make up the remainder of the shard-bearing types.

Some samples of the sub-unit near the shard-bearing horizons do not show any relict shards, although the other textures and the mineralogy of the rocks are very similar. Samples from the lower parts of the sub-unit contain about 3% sodic plagioclase phenocrysts (1 mm - 3 mm, subhedral to anhedral) and trace amounts of $\frac{1}{2}$ mm - 1 mm, subhedral to anhedral quartz in a fine-grained, dense, interlocking groundmass of quartz, feldspar, and sericite. The sericite is abundant (about 25%) and oriented so that the rock has microscopically visible foliation.

Plate 25: Photomicrograph showing detail of thin-section of vitric tuff sub-unit of East Fork member. Note characteristic shapes of relict shards. 0.5×0.7 mm field, plane polarized light.

Plate 26: Flattened pumice fragment with flame structure in tuff of Oneida member (Alder series) in the East Fork of Sycamore Creek.

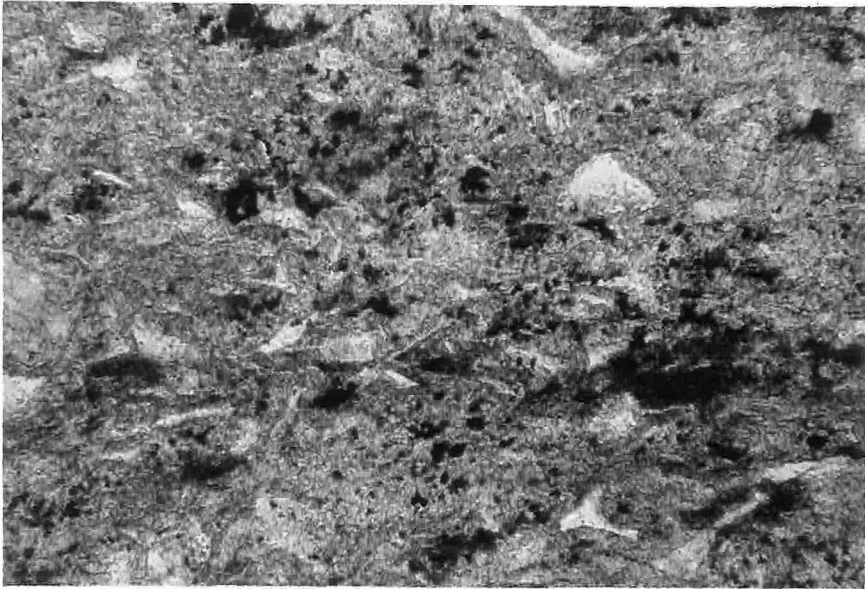


Plate 25



Plate 26

Mt. Ord Lithologies:

In the northward-flowing creek which joins Slate Creek at 3600' elevation, the rocks of the East Fork member are thin-bedded (1/16" to 6"), fine to medium-grained, moderately foliated types with colors from purple and blue to white. They are interbedded with 10' to 20' thick beds of massive, white to pink, coarse-grained quartzite. The clasts of the thin-bedded clastics were not examined microscopically. The quartzite clasts are poorly sorted, angular, and are stretched parallel to foliation. About 15% of the rock consists of a partially sericitized matrix of fine-grained quartz + feldspar. The quartz clasts are strained, and the smaller ones are ragged edged and partially sericitized.

Sedimentary Structures

Structures such as graded or cross-bedding and channeling are rare within most of the East Fork member. However, a few exposures which contain interbeds of sandstone do show multiple cycle graded bedding, and the coarse interbeds in outcrops between the Gila-Maricopa county line and Deer Creek show numerous examples of all three structures. In this area, the direction of bedding tops is consistently to the northwest.

In the outcrops in the East and West forks of Sycamore Creek, and in upper Gold Creek, only one exposure giving direction of bedding tops was found. This outcrop, which has multiple graded bedding of thin sandstone beds, gives southeastward tops. No original bedding orientation information was obtained from the Mt. Ord exposures of the unit.

Outcrops which display deformation which may be contemporaneous with deposition were observed in the East Fork of Sycamore Creek (plate 22). Crumpled, folded, and rotated regions of slate occur within otherwise well-bedded rock, and are possibly due to penecontemporaneous, soft-sediment deformation.

Metamorphic and Deformational Effects

The coarser-grained rocks of the East Fork member have undergone the greatest degree of recrystallization, probably due to the greater content of Ca, Mg, and K (in the feldspars and lithic fragments). Sericite is most abundant in the coarser-grained rocks, as is epidote. Chlorite, though not abundant in any of the samples of the East Fork member examined in thin-section, is generally present with 1% - 5% mode in both fine and coarser-grained types.

The preservation of the very fine-grained textures of the slates and phyllites shows that both the grade of metamorphism and the approach to equilibrium of the metamorphic mineral assemblage was not great. This is all the more significant when the degree of foliation and other deformation which the slates and phyllites record is considered.

Although the upper and lower contacts of the East Fork member are conformable with the foliation, the rocks within the unit are, in many cases, folded and distorted so that foliation is oblique to bedding, small-scale (tens of feet) and larger-scale (hundreds of feet) folding is observed and inferred, and several planes of foliation are displayed. In most of the section, however, a single plane of foliation is concordant, or nearly concordant, with bedding planes.

Distribution

The East Fork member is exposed in three northeast-trending belts. The belt which crosses the southeast flank of Mt. Peeley varies in thickness from about 500' to over 1800'. No general trend of thickening can be established (reconnaissance to the west of the mapped area in the Mt. Peeley region indicates that the apparent trend of westward thinning does not persist).

On the northwest side of the Red Rock syncline, the apparent thickness of the East Fork member varies from 1500' to 2500'. This apparent thickness may include some duplication due to folding, as the slates are strongly deformed in some localities. Best exposures are in the East Fork of Sycamore Creek between about 4560' and 4800'.

On the southeast side of the syncline, on Mt. Ord, the apparent thickness varies from 200' to 800', thickening to the southwest. The unit here is best exposed in the northward-flowing creek which joins Slate Creek at 3600'.

Environment of Accumulation

The East Fork member was evidently deposited under conditions of slow clastic input, hence limited local relief, and whereby only the finest-grained and most easily transported volcanic debris could be incorporated. The presence of limestone within the unit confirms the relative quiescence of the depositional environment.

The basal lithology of the vitric tuff sub-unit has a dense, fine-grained groundmass and evidently conformably underlies the upper, clastic-appearing and shard-rich lithologies. Thus the vitric tuff

sub-unit may represent an air-fall tuff with an intensely welded base. If this is so, then this part of the East Fork member was accumulated subaerially. The limited extent of outcrop of the vitric tuff sub-unit probably reflects a limited region of shallow water or above water rather than a localized pyroclastic input, because such fine ash would probably have been rapidly and widely disseminated by a deep-water environment.

The source regions of the East Fork member appear to be similar to those of the underlying Cornucopia member, in that apparent thinning to the northeast, southeast, and northwest suggest a generally south-westerly direction for the source region.

ALDER SERIES - ONEIDA MEMBER

The Oneida member of the Alder series (new name, for exposures near the Oneida mine in the East Fork of Sycamore Creek) consists of tuffs and tuff-breccias alternated with conglomerates, conglomeratic quartzites, and wackes. The unit conformably overlies the East Fork member, and conformably and gradationally underlies the quartzites of the Telephone Canyon member. The latter contact was defined by the first appearance, going up-section, of abundant and persistent sandstones and quartzites.

Lithologies

Northwest Limb of Red Rock Syncline:

The dominant lithologies of the Oneida member are felsic tuffs and tuff-breccias. In outcrop, these rocks are dark gray, blue, or

purple in color, fine-grained but with sparse, 1 mm subhedral quartz and feldspar, and in some cases contain barely distinguishable flattened felsic volcanic lithic clasts. These lithic clasts range from a few inches to a foot in length, and in some outcrops show flame-like terminations. Some of the smaller clasts are highly flattened, with wispy outlines (plates 26, 27). Such textures strongly imply that these features are flattened pumice fragments, and the rocks coarse tuffs. Some outcrops of these rocks contain felsic volcanic clasts and (very rare) jasper clasts which are only slightly deformed (length:width ratios in cross-section less than two). The matrix of these clasts is similar to those of rocks containing only highly flattened clasts -- very fine-grained, dense, and usually sparsely dotted with crystals.

Microscopic examination of the tuffs shows that the matrix is similar to the clasts, with both containing 5% - 20% phenocrysts of subhedral to anhedral quartz and/or sodic plagioclase from $\frac{1}{2}$ mm to 5 mm in size, in a matrix of partially sericitized, fine-grained interlocking quartz and feldspar. Many of the phenocrysts are elongate and show evidence of tensional fracturing. Opaque minerals make up 5% to 10% of the rocks, and occur both as small (.01 mm - 0.1 mm) disseminated, anhedral grains and as embayed, subhedral, $\frac{1}{2}$ mm - 2 mm grains. The sericite distribution (generally about 35% modal abundance), together with trains and fine elongate traces of opaque minerals, define a pronounced foliation. The quartz and plagioclase phenocrysts are also affected by the sericite, so that the leading and trailing edges of elongate and aligned quartz grains are ragged, and the plagioclase is partially sericitized (plates 28, 29).

Plate 27: Tuff of Oneida member in the West Fork of Sycamore Creek. The rock contains abundant, very highly flattened (and stretched?) pumice fragments. The field of view of the photograph is about 2' x 3'.



Plate 27

Plate 28: Photomicrograph of flattened pumice tuff of Oneida member (Alder series). Foliation is defined by sericite, and by alignment of elongate opaque minerals and quartz. All of the phenocrysts in this field are quartz. The high degree of sericitization and foliation prohibits distinction of primary lapilli boundaries. 6×9 mm field, plane polarized light.

Plate 29: Same as plate 28, but crossed nicols.



Plate 28

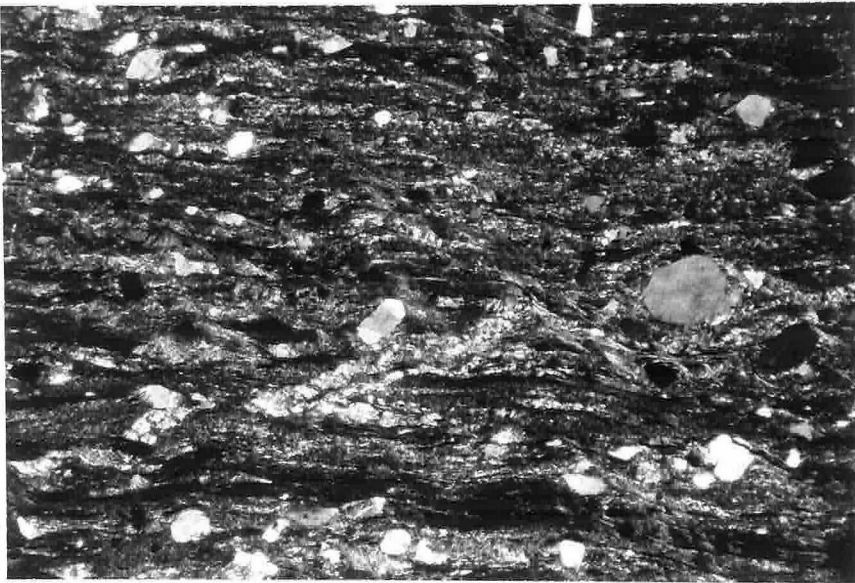


Plate 29

The textures of these tuffs suggest that they were welded tuffs; however, the degree of recrystallization of these rocks does not permit identification of such diagnostic features as deformed shards. It cannot be ruled out that the pumiceous clasts were flattened during accumulation in an aqueous environment by load deformation of the soft, altered, glassy pumice.

A pebble to cobble conglomerate (about 200' thickness) is the basal lithology of the Oneida member northwest of the Red Rock syncline. Its clasts are jasper and felsic volcanics, neither of which are much deformed. The matrix is predominantly sand-sized, and in some horizons grades into coarse sandy interbeds. The stratigraphic position of this conglomerate is extensively intruded by the Pine Mt. porphyry. The coarsest facies are thus exposed intermittently, in the East Fork of Sycamore Creek, and about two miles northeast of Pine Butte. A conglomerate facies gradational with the underlying East Fork member slates, with mostly pebble-sized jasper and rhyolite clasts, is exposed against the northern and northwestern Pine Mt. porphyry contact on Pine Butte. This lithology contains more and finer-grained matrix and interbedded phyllite than the conglomerate in the East Fork of Sycamore Creek.

A cobble conglomerate with highly stretched felsic volcanic clasts (and some much rarer, slightly deformed jasper clasts), about 300' thick, overlies the basal conglomerate in the East Fork of Sycamore Creek. The felsic volcanic clasts vary in color from white to tan to purple, and have dimensions from $\frac{1}{4}$ " \times 6" to 1" \times 12" (cross-sections perpendicular to cleavage) for the more elongate to about 2" \times 5" for the least elongate. The matrix of the clasts constitutes about 25% of

the rock, and is fine-grained. Rocks of this type are also present as interbeds throughout the Oneida member.

Higher in the section, the matrix material of the conglomerate is coarser (sand and granule size) and contains abundant quartz and lithic granules. Sandstone interbeds are more common up-section. In the East Fork of Sycamore Creek, by about 1750' stratigraphically above the base of the Oneida member, the rocks are fine-grained and dense, with no sedimentary structures or textures. The tuffs described above are common in the upper two-thirds of the unit, and are interbedded with a few stretched cobble conglomerate beds and sandstones.

Southeast Limb of Red Rock Syncline:

The jasper-bearing conglomerate which marks the base of the Oneida member northwest of the Red Rock syncline axis is not present in the southeast limb of that structure. Here, the unit chosen to mark the base of the Oneida member is a 50' thick, resistant, poorly sorted coarse-grained quartzite. Stratigraphically below this unit are several hundred feet of thin-bedded sediments which locally grade into quartzites. Agglomeratic(?) rocks are exposed for about 1000' above the basal unit. These agglomerates (?) appear, on first impression, to be fine-grained, purple and blue slates and phyllites without coarse clastic texture. Closer examination, however, reveals the presence of highly elongate (about 1" x 15" in cross-section) clasts. In thin-section, these rocks may be seen to contain abundant millimeter-sized, elongate amygdules(?) of carbonate in a matrix of disseminated, anhedral opaque minerals (predominant), very fine-grained carbonate, and sericite(?).

Epidote, albite, and chlorite are not present. These clasts were possibly originally vesicular mafic volcanics which have been altered (either before or during metamorphism) from their original chemical composition, so that the usual low-grade metamorphic mineral assemblage for a mafic volcanic was not produced.

The agglomerates(?) are intruded in several horizons by dark green, massive, unfoliated or faintly foliated mafic intrusives. These rocks have been recrystallized to an assemblage of chlorite-opaques-epidote-plagioclase. They have poorly defined contacts with the country rock.

The upper layers of the Oneida member on the southeast limb of the Red Rock syncline exposed in Slate Creek and Telephone Canyon are predominantly maroon, white, and pale blue slates. Thin-section examination of these slates suggests the presence of abundant, 0.1 mm - 0.5 mm relict shards disseminated throughout some of them; much of this slaty section, therefore, is probably tuffaceous.

The uppermost layers of this part of the Oneida member contain some sandstone and quartzite beds interbedded with the slates. The uppermost extent of the unit was chosen to be the first appearance, going up-section, of persistent quartzites and sandstones.

Sedimentary and Volcanic Structures

Only one bedding top determination was made in the Oneida member, although several sedimentary zones are present in the unit. This determination was made from channeled sandstone interbeds in the basal conglomerate in the East Fork of Sycamore Creek, and indicated southeast tops.

Original volcanic structures within the pyroclastic rocks of the unit are commonly obscured by the intense deformation which they have undergone. A difficult question is thus raised by those outcrops which display both highly elongate felsic volcanic clasts, and near-equant jasper and felsic volcanic clasts (always less abundant than the highly elongate type) in the same outcrop. In these cases, it is not clear whether the elongate clasts were tectonically stretched, or whether much of the elongation is due to deformation during accumulation (as hot pumice fragments or soft, hydrated and altered pumice fragments). The coexistence of apparently deformation-resistant (near-equant) clasts and highly deformed clasts suggests that the near-equant felsic volcanic clasts were either intrusive or massive extrusive types, whereas the highly flattened clasts were pumice fragments which would have been easily deformed either tectonically or during accumulation.

Outcrops which have extreme (length:width ratios in cross-section of greater than ten, with flame-like terminations) elongation of clasts and with few or no jasper or near-equant felsic volcanic clasts are probably purely tuffaceous in composition. The matrix of these rocks is both macroscopically and microscopically nearly identical to the clasts. These coarsely clastic tuffs, in some exposures, grade into rocks with only the faintest clastic textures, such as in plates 26 and 27.

Metamorphic and Deformational Structures

The rocks of the Oneida member are pervasively foliated. Except for the basal conglomerate in the East Fork of Sycamore Creek, nearly

all lithologies are quite schistose, with the dominant northeasterly-striking cleavage characteristic of the region. The foliation is locally discordant with bedding, and there is a second foliation (similar in strike to the dominant foliation, but slightly shallower dip) in some outcrops, but no persistent structural pattern was recognized.

Oneida Member: Chemistry

One sample from the flattened pumice tuff lithology of the Oneida member was analyzed for its major element composition (table II, Appendix I). The rock has 4.6% normative corundum, reflected by an abundance of sericite in its mode. The main effect of the alteration which presumably accompanied the sericitization was evidently a loss of K. Otherwise, the composition of the rock (except for its high equivalent FeO content) is similar to that of other felsic volcanic rocks with similar silica contents. If the calcium and sodium contents of the sample have not been greatly altered, the original rock appears to have been an (iron-rich?) alkali rhyolite.

The chemical composition of the sample is plotted on quartz-plagioclase-orthoclase and AFM diagrams in figures 5 and 6, respectively, Appendix I.

Distribution

On the northwest side of the Red Rock syncline, the best exposures of the Oneida member are in the East and West Forks of Sycamore Creek. The only complete section of the unit is found in the East Fork of Sycamore Creek, where its apparent thickness is about 2500'. The

unit is extensively intruded by the Pine Mt. porphyry on the northwest side of the Red Rock syncline.

On the southeast side of the syncline, the apparent exposed thickness is about 2800', and does not appear to vary significantly. Best exposures are in the northward-flowing fork of Slate Creek which joins Slate Creek at 3600', and in lower Telephone Canyon.

Environment of Accumulation

The rocks of the Oneida member on the northwest side of the Red Rock syncline form a suite apparently accumulated under subaerial(?) to shallow subaqueous conditions. If the lithic tuffs with highly flattened clasts were welded ash-flow tuffs, then they accumulated under subaerial conditions (Rankin, 1960), and the sandstones and quartzites probably represent near-shore depositional facies. The cobble conglomerates (except for the basal conglomerates), in view of their poor sorting and lack of sedimentary structures or sandstone interbeds, may be debris-flow derived. If the lithic tuffs accumulated in a subaqueous environment, they may also have resulted from debris flows. Thus the source terrane of the coarsely clastic material of the Oneida member was evidently dominantly or exclusively volcanic, and composed of massive and pumiceous felsic volcanics. The lithic tuffs reflect a significant volume of volcanic activity contemporaneous with deposition.

The basal conglomerate of the Oneida member (on the northwest side of the syncline) probably records the resumption of Alder series vulcanism. This vulcanism may have created the necessary felsic volcanic material and relief required for transport of the clasts of the

conglomerates, debris flows, and stretched pumice tuffs. The period of greatest volcanic activity was evidently early in Oneida member time, because the unit as a whole is grossly graded. A gradual diminution of volcanic activity, coupled with erosion of the source regions, resulted in the deposition of less of the coarsely clastic and less volcanic-rich lithologies towards the top of the unit.

On the southeast side of the Red Rock syncline, the Oneida member is much poorer in conglomeratic rocks, and much richer in fine-grained (now slaty) tuffs. This trend indicates that the source regions of the Oneida member volcanics and conglomerates lay in a northerly or northwesterly direction.

TELEPHONE CANYON MEMBER

The Telephone Canyon member (new name, for exposures in Telephone Canyon) is a series of sandstones (quartzites, quartz-wackes, and lithic-feldspathic wackes), granule conglomerates, with subordinate conglomerates, slates, tuffs, and mafic flows in most of the mapped area. In the northwest part of the mapped area, the unit also contains abundant massive and bedded tuffs and felsic volcanic breccias. A distinctive characteristic of the sandstones of the Telephone Canyon member is their abundant crossbedding (plate 30).

The Telephone Canyon member conformably overlies the tuffs of the Oneida member, and conformably (or disconformably?) underlies the Red Rock rhyolite. The latter contact is intruded in most localities by mafic sheets, and is discussed in the section on the Red Rock rhyolite.

Plate 30: Cross-bedding in conglomeratic sandstone of the Telephone Canyon member (Alder series). Lower Gold Creek.



Plate 30

The sediments of the unit typically are moderately resistant, with fair outcrop even on slopes and ridges. The quartzites of the unit are quite resistant, and were mapped explicitly to give a degree of internal stratigraphic control.

Lithologies

The most common lithologic types within the unit (except in the area north of Cane Springs Canyon) are medium to coarse grained, moderately to poorly sorted sandstones. Those sandstones and granule conglomerates with clasts large enough to be identifiable in outcrop display clasts of quartz (most abundant), feldspar, jasper, and fine-grained lithic fragments. The sandstones are commonly white, tan, or blue-purple in color and weather to a rusty brown.

Granule and pebble conglomerates are intercalated within the sandstones. These conglomerates contain some jasper fragments, but in all cases, the most common clasts are massive felsic volcanics. The coarse clastics are more common in a northeasterly direction. Thin-section examination of the sandstones shows that they are mostly quartz wackes and quartzites, with moderately to poorly sorted, angular clasts. The matrix material is fine-grained quartz, feldspar, and sericite. Detrital heavy minerals are not abundant, but a few small zircon and tourmaline grains are present in some of the sandstones. Opaque minerals are also present in the matrix to a variable degree (generally less than 10% of the matrix), and occur as elongate patches and braids parallel to foliation (see plate 31).

The lithic and feldspathic wackes contain abundant angular and

Plate 31: Photomicrograph of quartz wacke from lower Telephone Canyon member of Alder series. The foliation of the rock is defined both by elongation and alignment of the quartz clasts and by preferred orientation of the quartz, feldspar, and sericite of the matrix. Note the ragged appearance of the leading and trailing edges of the quartz clasts, due to incipient reaction.

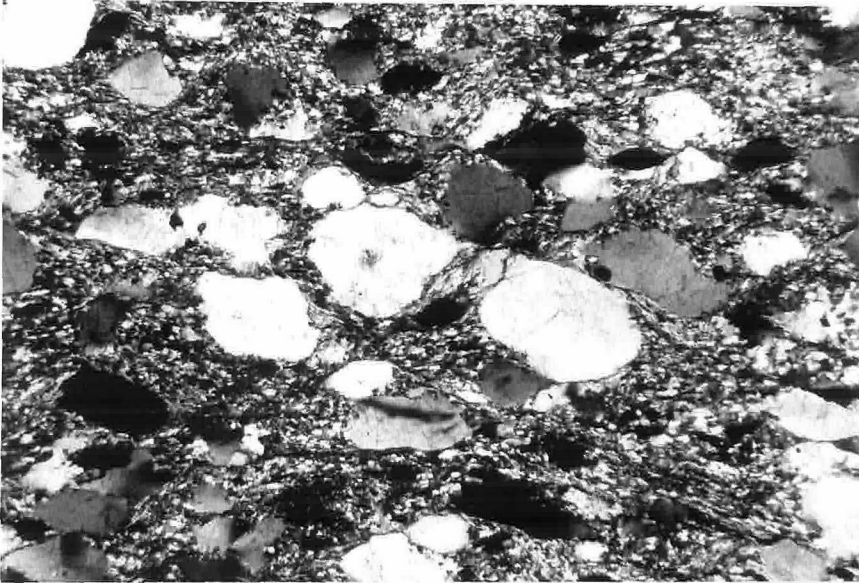


Plate 31

subhedral sodic plagioclase (n_D less than 1.54), and at least two types of volcanic lithic clasts. The more common lithic clast type is a fine-grained, felsic volcanic which in some cases contains small (less than $\frac{1}{2}$ mm) quartz or feldspar phenocrysts. The less common type has been altered to amorphous opaque minerals or to chlorite. These clasts were evidently originally mafic volcanics. The lithic and feldspathic wackes are most abundant in the uppermost Telephone Canyon member.

A few mafic volcanic flows occur as 20' - 50' thick beds in the Telephone Canyon member in the Gold Creek area. Here, they persist for over a thousand feet along strike. Only the presence of vesiculated tops and persistence over a significant distance in a well-defined stratigraphic horizon permits these flows to be distinguished from the andesitic-dacitic intrusive sheets. In some cases, it is possible that such flows were mapped as the intrusive sheets.

North of Cane Springs Canyon, on the north of the Red Rock syncline, the Telephone Canyon member is markedly different in overall lithologic character. The difference is enough that the characterization of the unit as a series of sandstones, wackes, and conglomerates is not valid in this area. Two trends distinguish the northeastern exposures of the Telephone Canyon member; the greater and progressive thickness of the unit north of Cane Springs Canyon, and the much greater (or dominant) quantity of rhyolitic volcanic material, both directly accumulated and reworked. The change in character is evidently gradational, and can be traced in specific beds in a few instances.

The layers which are conglomeratic, with intercalated sandstones, on the Bernice Mine - Gold Creek road (R9E., T7N., Section 34) do not

apparently extend southwestward into Cane Springs Canyon as conglomerates. In Gold Creek (a distance of about ~~one~~ half mile), the same bed is much thicker (increasing from less than fifteen feet to more than fifty feet), contains larger and more abundant felsic volcanic clasts, and does not have intercalated sandstones. Further to the northeast, in the fork of Gold Creek which joins Gold Creek at 4080', a rhyolite breccia appears at about the same stratigraphic horizon. This breccia has no sedimentary textures or structures, and contains blocks of rhyolite up to three feet in size.

Pyroclastic beds are rare in the Telephone Canyon member to the southwest of Cane Springs Canyon. In Gold Creek, pyroclastics and rhyolite breccias are present, and a mile to the northeast (in the 4080' fork of Gold Creek), such lithologies, including welded vitric tuffs, are common. Still further to the northeast (in the 3760' fork of Gold Creek), all but the uppermost 1500' of the Telephone Canyon member are predominantly rhyolitic tuffs and breccias. In the Gold Creek area, even the uppermost layers of the Telephone Canyon member contain interbedded sedimentary breccias, felsic tuffs, and lithic wackes.

The tuffs of the Telephone Canyon member north of Cane Springs Canyon are of several types. Pale green welded vitric tuffs with a dense, interlocking texture and sparse, millimeter-sized quartz and plagioclase phenocrysts occur in several 10' - 100' thick beds in the 3760' and 4080' forks of Gold Creek. These rocks have compressed shards of about 1 mm size, and are now about 50% sericite. In some cases, they have gradational contacts with underlying or overlying conglomerates, sandstones, or siltstones.

Lithic tuffs of different clast types, composition, and origin are abundant in the Telephone Canyon member in the Gold Creek region. Some of these contain exclusively felsic volcanic clasts, whereas others (less common) contain some clasts which are now composed mostly of opaque minerals and which are in part amygdaloidal. The degree of deformation of the clasts is variable. Some types contain abundant angular clasts, while even the clasts with rounded boundaries are only moderately elongate. Others contain mostly highly deformed, evidently pumiceous clasts with flame-like terminations and pronounced deformation about large crystals or angular clasts. All types have $\frac{1}{2}\%$ - 2% quartz and plagioclase phenocrysts, or broken fragments of subhedral crystals. The size of the lithic fragments in these tuffs ranges from about 2 mm to several centimeters.

Densely welded ash-flow tuffs are common in the Telephone Canyon member in the northeasternmost part of the mapped area, north of Gold Creek and east of the Reynolds Mine. Such rocks, together with rhyolite breccias, make up a tongue of thick, massive, resistant rhyolite which forms the prominent northeasterly trending ridge north of Gold Creek at the eastern edge of the Reno Pass quadrangle. This reddish, massive rhyolite is distinguishable from the Red Rock rhyolite only by its stratigraphic location.

This massive rhyolite in the Telephone Canyon member (shown explicitly on the map) conformably overlies bedded, foliated tuffs and breccias (contact exposed in the 3760' fork of Gold Creek). At its southeastern margins, the body is faulted against felsic volcanic intrusives and foliated felsic tuffs. Its maximum exposed thickness is

about 2500'. In the 3760' fork of Gold Creek, where the apparent exposed thickness is only about 1700', the massive rhyolite is predominantly flowbanded rhyolite (plates 32, 33). Abundant flattened pumice clasts are present in some types, and range in length from about one-half foot to more than one foot. The lowermost two hundred feet of the massive rhyolite shows no flowbanding in outcrop, and only very faintly in thin-section.

Rhyolite cobble breccias are common to the northeast of the 3760' fork of Gold Creek in the massive rhyolite, but are not a dominant lithology. Like the Red Rock rhyolite, the massive rhyolite of the Telephone Canyon member shows little or no metamorphic foliation in outcrop.

In thin-section, the welded tuffs of the massive rhyolite show abundant flattened pumice fragments of various sizes. The abundance of phenocrysts ($\frac{1}{2}$ mm - 5 mm varies from about 2% to 8%. Quartz greatly predominates as the phenocryst in some of the rocks, with subsidiary orthoclase or plagioclase phenocrysts. In others, orthoclase is as abundant as the quartz. The orthoclase generally is perthitic, and in one sample (from the basal, unbanded lithology) is faintly zoned and has a thin albite rim. The rocks contain from one to twenty percent sericite. In the flowbanded types, the sericite is generally aligned with the banding, but in the unbanded lithologies it occurs as disseminated flakes. Primary devitrification textures are preserved in most of the rocks. Such textures include very fine-grained rims surrounding (and in optical continuity with) some phenocrysts, axiolitic texture in the cores of some pumice fragments, and randomly oriented cracks in

Plate 32: Welded tuff (massive rhyolite sub-unit) in the Telephone Canyon member (Alder series), showing abundant flattened pumice fragments. The plane of the photograph is nearly vertical. 3760' fork of Gold Creek.

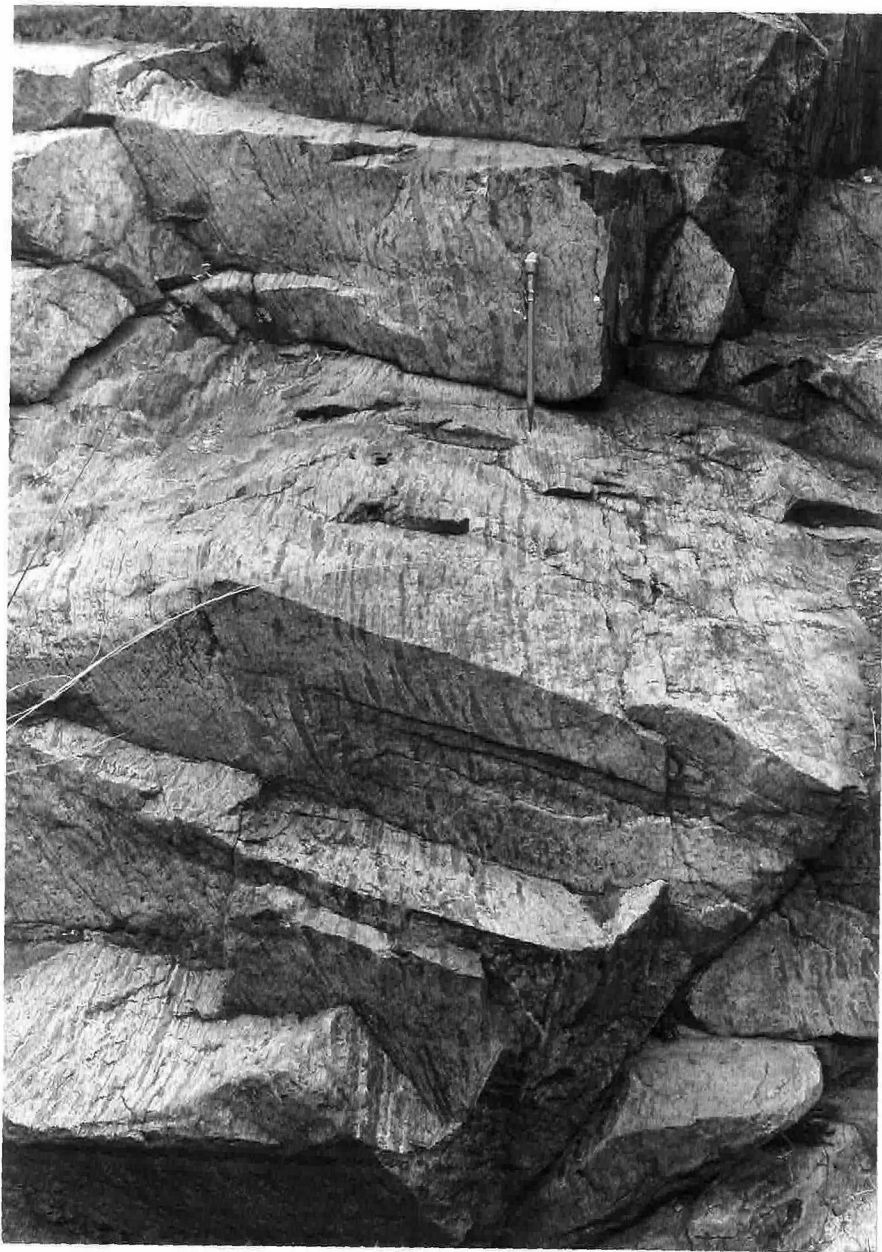


Plate 32

Plate 33: Detail of flowbanding in the massive rhyolite sub-unit of the Telephone Canyon member. 3760' fork of Gold Creek.



Plate 33

unbanded areas of groundmass.

It is of interest that K-feldspar phenocrysts were observed only in the Red Rock rhyolite and some of the volcanics of the Telephone Canyon member north of Cane Springs Canyon. These volcanics are the massive rhyolite sub-unit and the rhyolite breccia described on page 179.

Sedimentary Structures and Textures

The crossbedding which is common in the sandstones of the upper part of the Telephone Canyon member permits good control of the possibility of isoclinal folding within that part of the unit (plate 30). No evidence for such folding was found. Bedding tops are everywhere towards the Red Rock rhyolite. Graded bedding in conglomeratic beds permitted extension of this control to the middle layers of the unit.

Metamorphic and Deformational Effects

Most of the Telephone Canyon member shares the pervasive northeasterly-striking foliation of the rest of the Alder series. The finer-grained lithologies, such as the slates and mudstones, are the most strongly foliated, whereas the coarser sandstones are generally only faintly foliated, except where the foliation is discordant with bedding. The quartz grains of the sandstones tend to be elongate and aligned parallel to the foliation, and have frayed edges characteristic of the more sheared rocks of the rest of the Alder series. Some of the pebble and cobble conglomerates are strongly sheared. They have highly stretched felsic volcanic clasts with length to perpendicular diameter ratios up to 10:1.

Most of the tuffs in the Telephone Canyon member are foliated.

However, the massive rhyolite sub-unit of the lower Gold Creek region shows almost no metamorphic foliation, even at its base. Within a hundred feet or so of the fault at its southeastern contact, however, it does show brecciation, silicification, and slickensides.

Small-scale structures within the Telephone Canyon member are generally confined to the slaty interbeds, which in a few outcrops are tightly folded on a scale of a few feet. In the northeastern part of the mapped area, however, many of the fine-grained beds and some of the coarser sandstones are folded (both open and tight forms) with amplitudes of up to 20 feet, and have one or two secondary planes of foliation. One larger structure, an S-shaped fold with a radius of curvature of over one hundred feet, has caused pronounced bedding-foliation discordance in the upper Cane Springs Canyon drainage (plate 34).

Telephone Canyon Member Volcanics: Chemistry

Two rhyolites from the volcanics which inflate the Telephone Canyon member in the Gold Creek region were analyzed for their major element chemistry (table III, Appendix I). Sample I is a monolithologic rhyolite breccia (mapped explicitly in this locality) which at the collection locality (the 4080' fork of Gold Creek) appears to be exclusively volcanic. The sample was used for an absolute age determination, and is described more fully on page 179. Sample II is a welded lapilli tuff from the massive rhyolite sub-unit of the Telephone Canyon member, collected in the 3760' fork of Gold Creek.

The composition of the rhyolite breccia is similar to Nockolds'

Plate 34: Sandstone and cobble conglomerate in Telephone Canyon member of Alder series, just north of upper Cane Springs Canyon. Bedding planes are parallel to the plane of the photograph (and the conglomerate face above the hammer), while the plane of foliation is nearly perpendicular (cleavage planes of upper right of field).



Plate 34

average alkalic rhyolite + rhyolite-obsidian. The compositions of these samples are plotted on quartz-plagioclase-orthoclase and AFM diagrams (figs. 5 and 6, Appendix I, respectively). The welded lapilli tuff sample, on the quartz-plagioclase-orthoclase diagram, falls in the middle of the field of young rhyolite obsidians as compiled by Anderson (1968). The rock thus has probably not undergone significant alteration of its original alkali contents.

The similarity in the compositions of the welded lapilli tuff and the Red Rock rhyolite samples are striking. In view of the association of the position of the two rock types and their strong physical similarity, the near-coincidence of the chemical compositions of the massive rhyolite sub-unit of the Telephone Canyon member and the Red Rock rhyolite probably reflect a genetic association.

Distribution

The Telephone Canyon member is exposed in two northeast-trending belts, on either side of the type Red Rock rhyolite. On the northwest side of the Red Rock syncline, the thickness of the unit is quite variable. Where the Pine Butte road crosses the unit, for example, it is less than 1500' thick, whereas in the East Fork of Sycamore Creek, the thickness approaches 3000', and in Gold Creek it is more than 3000' thick. The best exposures of the unit on the north side of the syncline are in the East Fork of Sycamore Creek, in Cane Springs Canyon, and in the fork joining Gold Creek at 4080'.

On the southeast side of the Red Rock syncline, the unit has an exposed thickness of about 3000'. The consistency of this thickness is

uncertain, because the complete section is exposed for only about a mile along strike. Best exposures are in Telephone and Mercurio canyons.

Environment of Accumulation

The sandstones and conglomerates of the Telephone Canyon member were evidently deposited in a shallow subaqueous environment, which permitted the formation of crossbedding by bottom currents. It was also near enough to shore that large angular cobbles could be incorporated in the conglomeratic beds. The relatively minor role played by volcanic rock in most of the mapped Telephone Canyon member section (except in the northeast part of the mapped area) implies that, following the vulcanism which deposited the lithic tuffs of the upper Oneida member, a time of relative volcanic quiescence occurred.

The abundance of rhyolite breccias and welded tuffs in the Telephone Canyon member northeast of Cane Springs Canyon shows that there were intervals of subaerial accumulation. The striking increase of volume of these felsic volcanics towards the northeast in this region suggests that a significant subaerial volcanic center was developed in this direction. This volcanic center was very likely the same center that shortly afterwards produced the volcanics of the Red Rock rhyolite.

RED ROCK RHYOLITE

The Red Rock rhyolite is a massive pile of welded vitric (formerly) and lithic tuffs, volcanic breccias, flows, and possibly intrusives, of rhyolitic and rhyodacitic composition. The unit is resistant, and crops out well in creek beds, on ridges, and on some slopes. Slight variations in the weathering characteristics of individual lithologies permit the perception of stratigraphic trends within the unit for distances up to a mile along the steepest slopes.

The Red Rock rhyolite overlies the Telephone Canyon member at both limbs of the Red Rock syncline, and rests upon the East Fork member on the southern and southeast flank of Mt. Peeley. The latter contact has been described on page 72. The Red Rock rhyolite-Telephone Canyon member contact is intruded by mafic sheets everywhere in the mapped area except in the extreme southwestern corner, in the 3840' fork of the West Fork of Sycamore Creek.

At this location, the Red Rock rhyolite rests directly upon quartzites of the Telephone Canyon member. There is some reason to suspect that this contact may be a fault here. The quartzites within five feet of the Red Rock rhyolite are friable, have a deep red color (although the common color for these uppermost quartzites in this area is white to purplish blue), and show microscopic evidence of strong shearing (extreme elongation, crushing, and strain of the quartz grains). It is possible, though, that this shearing is the result of bedding-plane slippage due to accommodation of the stresses induced by the formation of the Red Rock syncline. The Red Rock rhyolite shows no evidence of anomalous shearing

or foliation at or near the contact.

Time Interval between Red Rock Rhyolite and Alder Series

There does not appear to be a major unconformity between the Alder series and the base of the Red Rock rhyolite. No major mappable units are crosscut. Wherever stratigraphic control of the Alder series within a few hundred feet of the Red Rock rhyolite exists, the contact is conformable within less than a hundred feet. In addition, layering attitudes within the lower Red Rock rhyolite are generally fairly consistent with those of the uppermost Alder series, with the exception of the area near lower Gold Creek.

However, the absence of the upper two members of the Alder series (the Oneida member and Telephone Canyon member) on the flanks of Mt. Peeley, in the northwest part of the mapped area, requires that either,

1) the Oneida member and Telephone Canyon member were not laid down in the Mt. Peeley area, or they were thin enough so that a relatively brief erosional interval was sufficient for their removal, or that,

2) sources of the Red Rock rhyolite broke the surface earlier in the Mt. Peeley region than to the southeast, so that the lower beds of the Red Rock rhyolite on Mt. Peeley are not time-equivalent to the lowest beds of the type Red Rock rhyolite.

The first hypothesis is, in fact, consistent with the apparent trend of thinning of the combined Oneida and Telephone Canyon members from southeast to northwest, across the Red Rock syncline. This would

perhaps also require a gentle uplift in the northwest part of the mapped area during latest Alder series time, to account for the presence of conditions of very low depositional rates, or even net erosion.

In the region between Gold Creek and Cane Springs Canyon, the stratigraphic control established within the upper Telephone Canyon member does not indicate significant discordance between the uppermost Alder series beds and the contact with the Red Rock rhyolite. This control was provided by two beds in the Telephone Canyon member:

- 1) the massive, resistant quartzite bed, mapped explicitly, which extends from the 4080' fork of Gold Creek to within 1000' of Cane Springs Canyon, and

- 2) the uppermost exposed Telephone Canyon member beds, exposed for about one-half mile to the east of the Red Rock rhyolite feeder dike to about three-quarters of a mile to the west of that dike.

These uppermost-exposed beds are very coarse-grained, green-colored lithic-quartz wackes. They have a thickness of about fifty feet. The lithic clasts are fine-grained, and have altered to an assemblage of chlorite-opaque minerals - (quartz + feldspar). The abundance of chlorite and opaque minerals suggests that the lithic fragments were of dacitic, rather than a more felsic, composition. The Red Rock rhyolite, therefore, apparently was deposited on a surface with no more than about fifty feet relief in this area.

Between the intrusive rhyolite feeder to the Red Rock rhyolite (exposed between 3890' and 4000' in Gold Creek) and the faults which juxtapose the younger gravels to the west, however, discordance between

base of the Red Rock rhyolite and the attitudes of the underlying Alder series beds indicates an apparent angular unconformity. In view of the evidence which suggests that the sources of the Red Rock rhyolite began their activity in latest Alder series time (see the discussion on the Telephone Canyon member rhyolites in the Gold Creek area, pp. 114-115) this deformation must have occurred in a short time interval compatible with the life of a rhyolitic volcanic center. In fact, swelling and deformation of the upper Telephone Canyon member may have been caused by the intrusion of the rhyolitic stock mentioned above, and thus be almost contemporaneous with the first eruptions of the Red Rock rhyolite.

Sources of the Red Rock Rhyolite

A feeder to the Red Rock rhyolite is exposed in the lower Gold Creek area. This feeder directly relates the Red Rock rhyolite to the oldest generation of intrusives into the Alder series. It extended from the plagioclase-quartz porphyry which crosses Gold Creek at about 4000', and apparently fed directly into the main mass of the Red Rock rhyolite. A continuous transition from rock with abundant, $\frac{1}{2}$ mm - 5 mm quartz and plagioclase phenocrysts, to brecciated, fine-grained, phenocryst-free felsic volcanic rock identical to the basal lithologies of the Red Rock rhyolite in this area, can be traced in this dike. Its thickness -- about 800' in exposed cross-section -- is sufficient that it could have supplied a significant volume of the now-exposed Red Rock rhyolite. Very likely, though, other feeders and vents located in a roughly northeasterly direction also supplied large volumes of rhyolite to the unit.

Lithologies

The Red Rock rhyolite appears to consist of only a limited compositional range of felsic volcanic rock (rhyolite to rhyodacite), most (possibly all) of which is extrusive. Several textural and structural types of rock resulted from various mechanisms of extrusion and accumulation. Because the two large bodies of the Red Rock rhyolite (henceforth referred to as the Mt. Peeley mass and the Red Rock mass) were sampled for microscopic examination to a limited degree compared to the possible diversity of lithologies within those large masses, and because most outcrops were not fresh enough for detailed identification of lithologic type, the following descriptions may be somewhat biased towards the more distinctive and persistent lithologic types.

Outcrop Appearance:

Five main lithologies have been distinguished in outcrop (but not mapped separately:

- 1) flowbanded types
- 2) welded lithic tuffs
- 3) massive, structureless types
- 4) breccias
- 5) spherulitic or lithophysal types

The flowbanded rocks are laminated in colors of red, black, and white, with surface bandwidths of about 2mm - 4 mm. The bands generally persist unbroken for tens of feet, and in many outcrops are markedly contorted, some even showing closed loops (plates 35, 36). Partially hollow lithophysae are sparsely distributed in some of these rocks. The flowbanded

Plate 35: Flowbanded rhyolite of Red Rock rhyolite with sparse lithophysae. The continuity of the banding suggests a flow-lava origin rather than ash-flow. Cane Springs Canyon.

Plate 36: Intricate flowbanding in Red Rock rhyolite, direction of flow oblique to plane of outcrop. Cane Springs Canyon.



Plate 35



Plate 36

rocks are evidently flow lavas rather than intensely welded ash-flow tuffs, since, according to Ross and Smith (1960, p. 366,

"...if linear elements in unmetamorphosed (flowbanded) rock extend over several feet, the rock is almost surely not a welded tuff."

Welded lithic tuffs (plates 37, 38), found only in the center of the Red Rock mass, show abundant, black, fine-grained, flattened and aligned former pumice fragments in an equally dense, fine-grained, red to pale pink matrix. Cross-sections of the clasts range from less than a sixteenth of an inch in thickness and length to more than a foot in length and an inch in thickness. Their overall shape is tabular, with typical thickness to length ratios of about 1:10. Some of the flattened pumice fragments display flame-like terminations, but they more commonly merely thin to a point (in cross-section) at their extremes. A few small (1 mm) rounded quartz and feldspar phenocrysts are detectable in both matrix and pumice fragments in some cases.

Some rocks are difficult to assign to either an ash-flow or lava-flow origin. These rocks display highly elongate black textural elements (thickness:length in cross-section average about 1:25) and some nearly equant fragments (both in the size range of 1/8" - 4") in lighter-colored fragments. The elongate fragments are stretched and broken to form short trains of small boudin in some cases (plate 39). Whatever the genesis of such rocks, it seems clear that their textures were developed as the result of flow of highly viscous, inhomogeneous material, including fragments which were nearly solid during flow.

Plate 37: Welded tuff in Red Rock rhyolite, showing flattened dark-colored lapilli in a reddish, fine-grained matrix, Mercuria Creek (drainage east of Telephone Canyon).

Plate 38: Detail of welded lapilli tuff of Red Rock rhyolite (polished surface). Scale divisions are in millimeters.



Plate 37

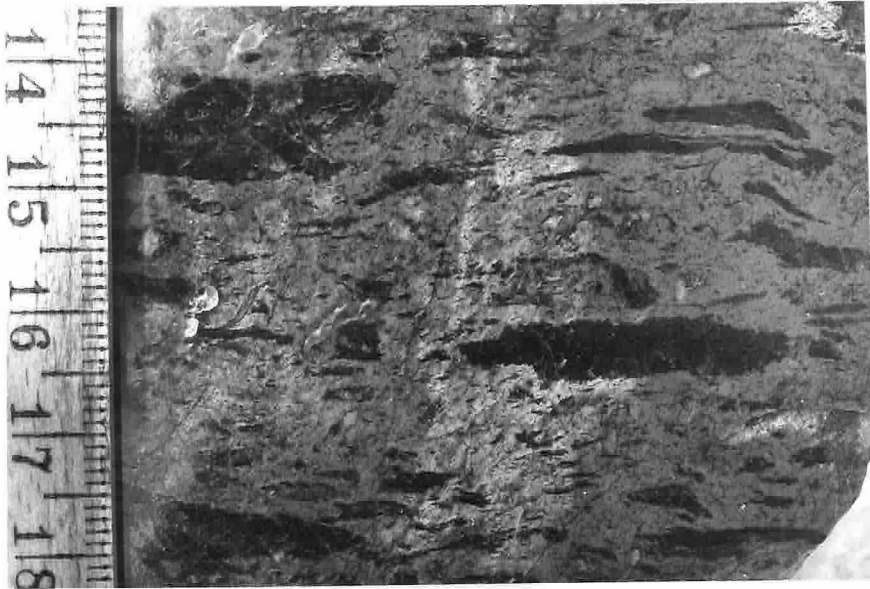


Plate 38

Plate 39: Banded Red Rock rhyolite (polished surface). Whether rocks such as these were flow-lavas or ash-flows is difficult to determine. Small scale divisions are millimeters.

Plate 40: Spherulites in Red Rock rhyolite, with typical hollow-weathered cores. Cane Springs Canyon.

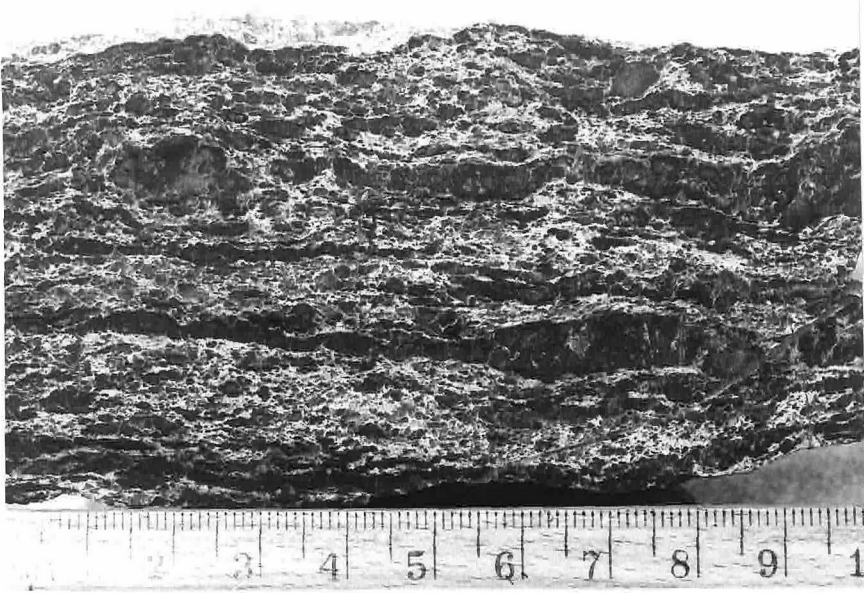


Plate 39



Plate 40

Volcanic breccias and microbreccias occur in the base of the Red Rock mass near the West Fork of Sycamore Creek, and near Gold Creek (the latter are evidently derived from a breccia pipe which fed the Red Rock rhyolite). The brecciated character of these rocks is in some cases visible only on cleavage surfaces, because the clasts and matrix of these rocks are generally very similar in composition and texture. The clasts and matrix are commonly fine-grained, light-colored (gray to pink), and dense. The clasts range from less than a millimeter in size to several centimeters. Near Gold Creek, some clasts with abundant phenocrysts of quartz and feldspar are present. They are similar in appearance to the porphyritic rock of the intrusive which fed the breccia pipe.

Rocks which consist of 30% to 60% spherulites and/or lithophysae are common in both the Red Rock and Mt. Peeley rhyolite masses. The spherulites range from less than a millimeter to about five centimeters in diameter (plate 40). The larger spherulites have both radiating and concentric textural elements. Most of the large spherulites are slightly ovoid. The lithophysae are generally smaller than the spherulites (about 10 mm - 30 mm diameter), and in some outcrops are associated with spherulites. The lithophysae have somewhat irregular outlines (plate 41) and a concentric structure. Some are mostly filled with fine-grained quartz. In the rocks with very abundant (more than half) spherulites or lithophysae, no other structures (flowbanding or flattened pumice fragments) are discernible.

Microscopic Textures:

All of the rocks of the Red Rock rhyolite, except for some breccias, contain phenocrysts of $\frac{1}{2}$ mm - 5 mm size. Quartz is the most common phenocryst (up to 10% mode, generally about 2%), but some rocks contain only plagioclase phenocrysts. The quartz phenocrysts may be euhedral, rounded subhedral, or intricately corroded subhedral in form. The most common feldspar phenocryst (up to 5%) is unzoned, subhedral plagioclase (albite to sodic oligoclase). K-feldspar phenocrysts are present in trace abundance in most of the rocks of the Red Rock rhyolite. In some rocks, they are more abundant than either quartz or plagioclase phenocrysts. The K-feldspar phenocrysts are generally non-perthitic, and may or may not be twinned. Both the K-feldspar and plagioclase phenocrysts are generally somewhat corroded or embayed, and are partially sericitized.

The groundmasses of Red Rock rhyolite lithologies are very fine-grained. The grain size is variable within the dimensions of a thin-section for the banded or clastic rocks. The groundmass consists predominantly of interlocking quartz and feldspar with a variable amount of equally fine-grained black or reddish opaque minerals, unidentified high-index minerals, and (in some rocks) sericite flakes. A patchy structure consisting of equant to slightly elongate polygonal domains of very fine-grained quartz + feldspar in optical continuity is a common groundmass texture in the massive, structureless rocks of the Red Rock rhyolite. Where the patches are elongate, they are aligned, and give the rock a definite preferred orientation fabric when viewed through crossed

polarizers. This texture is in some cases accompanied by areas of fan-like, radiating aggregates of quartz and feldspar, and by delicate, small-scale (less than a few millimeters) boxworks of quartz.

Vitric tuffs were found only in the Mt. Peeley mass, although they may also occur within the Red Rock mass. They could be identified as such only after microscopic inspection. In outcrop, they appear to be massive, fine-grained, and dense, with no apparent structure. In thin-section, abundant relict shards are visible (plates 42 through 46), distinguished from their matrix only by a slightly coarser grain size of the interlocking quartz and feldspar, and by a lesser abundance of fine-grained opaques. The relict shards observed are from 0.1 mm to 2 mm in size, and are generally distorted and compressed in form from typical undeformed shard shapes. Unless compaction during alteration of the glassy shards occurred, the above texture suggests that it was welded during accumulation. The absence of pumice fragments and lack of prominent lineation of textural elements imply an ash-fall mechanism of accumulation rather than ash-flow.

Those rocks which show fine or coarse banding in outcrop display a variety of textures in thin-section. They share a strong alignment of textural elements, which in some rocks (plate 47) swirl and curve in many directions, even within the area of a thin-section. The groundmass of many of these rocks is a brick-red color, due to the presence of abundant, very fine (0.1 mm - .05 mm) hematite(?) grains. This color is not necessarily uniformly distributed, but may be confined to parallel domains, or to irregular patches. Parallel bands of finer and coarse-grained textures, of greater and lesser abundance of black or red opaque

Plate 41: Lithophysal Red Rock rhyolite flow(?). Cane Springs Canyon.

Plate 42: Photomicrograph of vitric tuff of Red Rock rhyolite (Mt. Peeley). Shard structures are well-preserved. Phenocryst in upper left of field is quartz. 6 × 9 mm field, plane polarized light.



Plate 41



Plate 42

Plate 43: Left side of field of plate 42, crossed nicols. The relict shards are composed of interlocking quartz and feldspar, somewhat coarser-grained and freer from fine-grained opaque or high-relief mineral inclusions than matrix.

Plate 44: Photomicrograph of welded vitric tuff from Red Rock rhyolite (Mt. Peeley). Corroded, subhedral quartz phenocrysts rest in a matrix of devitrified shards. 2 × 3 mm, plane polarized light.

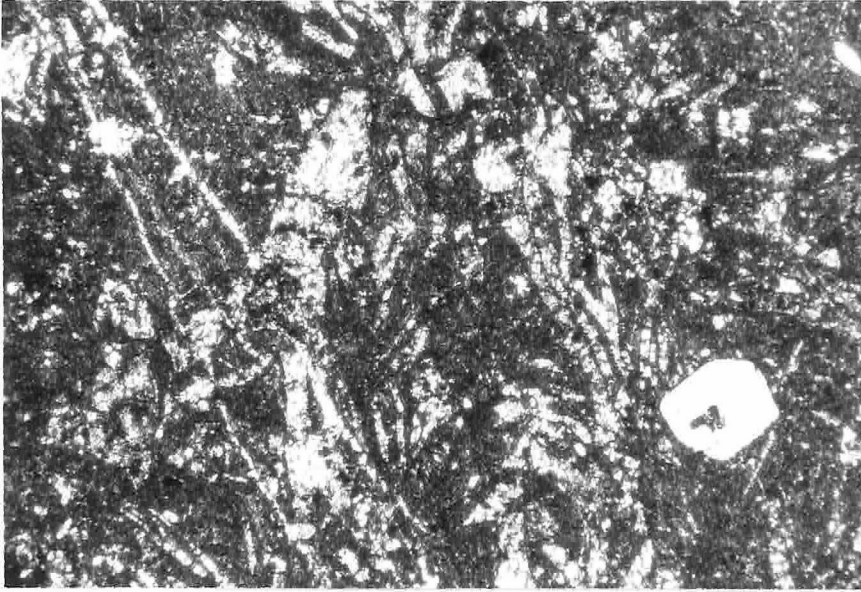


Plate 43

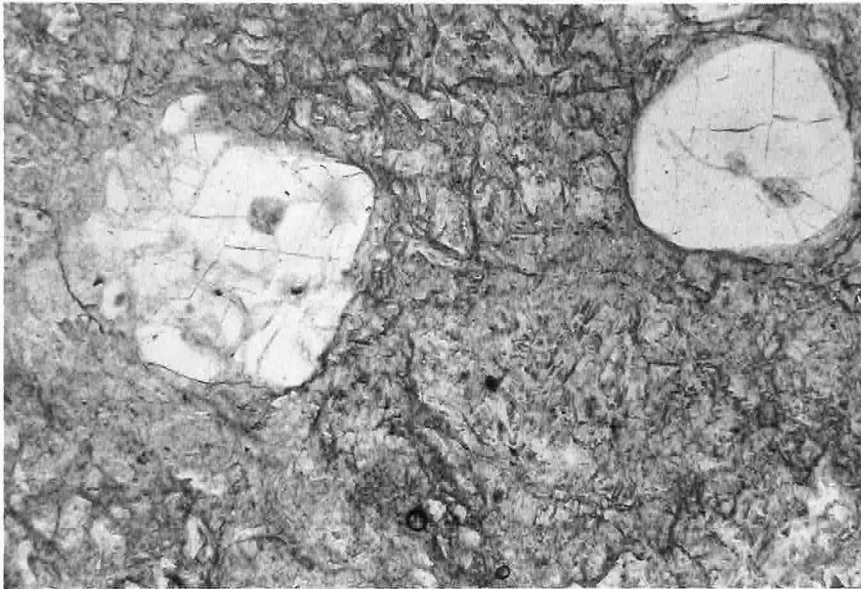


Plate 44

Plate 45: Same as plate 44, but substage diaphragm of microscope reduced to enhance relief (plane polarized light).

Plate 46: Same as plates 44, 45, but crossed nicols. Shards indistinguishable from matrix.

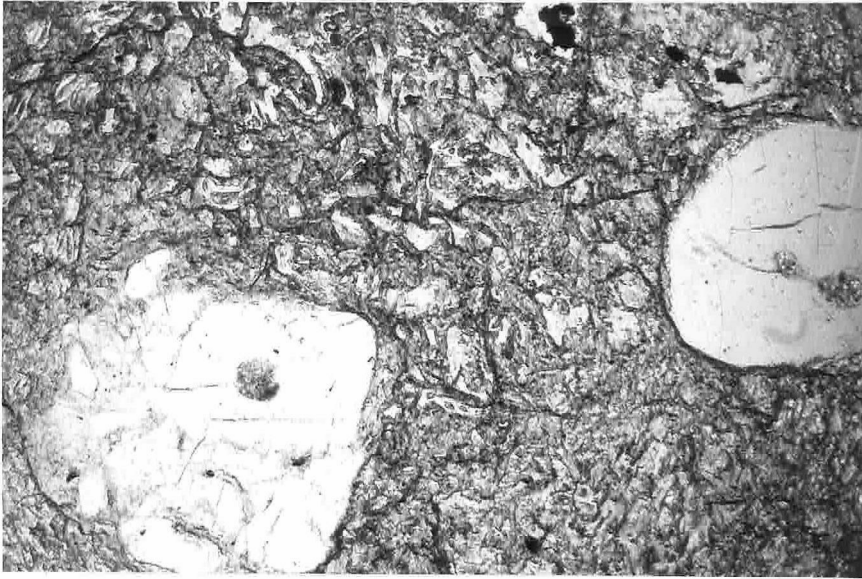


Plate 45

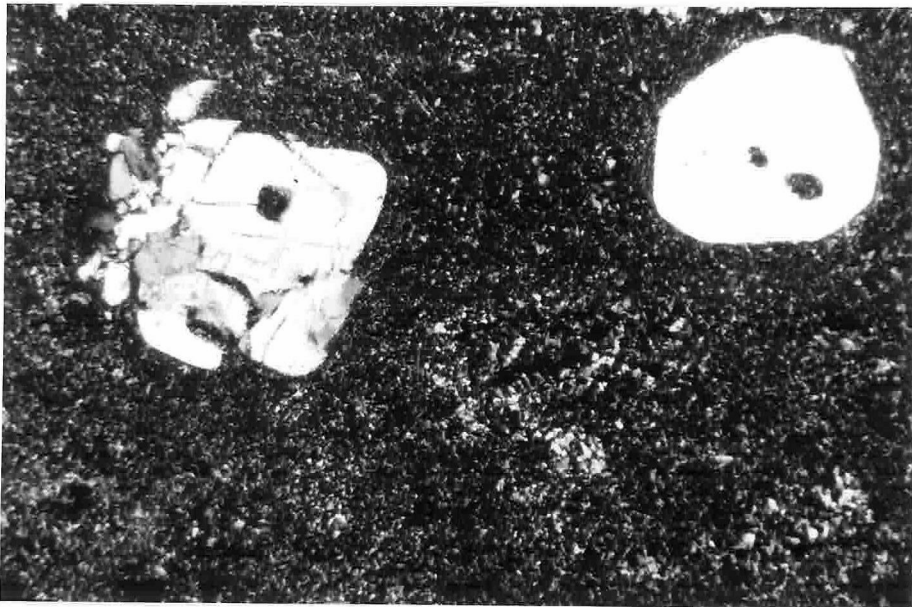


Plate 46

Plate 47: Photomicrograph of flowbanded Red Rock rhyolite showing small-scale flow-structure. The white, angular grains are quartz phenocrysts, and the contorted white patches are fine-grained, interlocking quartz. 6 × 9 mm field, plane polarized light.

Plate 48: Photomicrograph of flowbanded Red Rock rhyolite. The elongate, white area near the center of the field is mostly quartz, and is suggestive of a recrystallized pumice fragment. Some of the aligned, delicately structured areas may be highly compressed piles of fine shards. 6 × 9 mm field, plane polarized light.

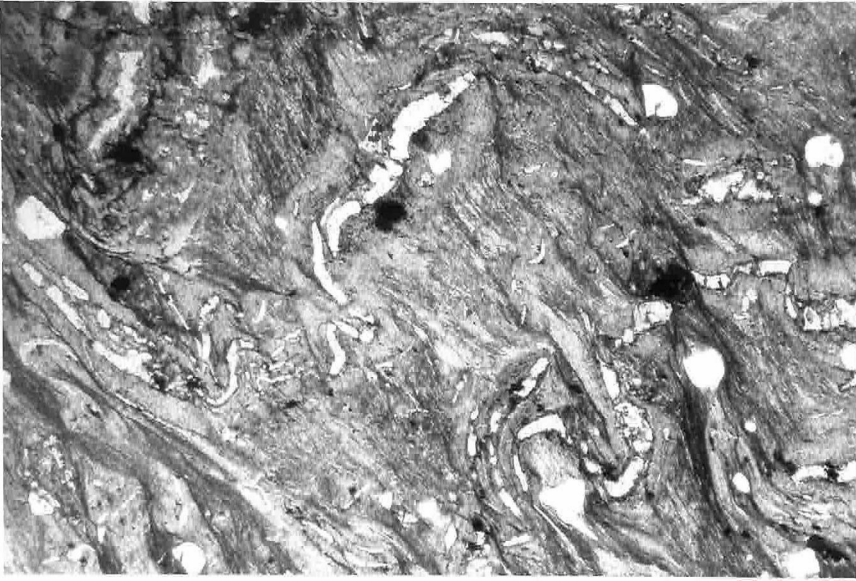


Plate 47



Plate 48

Plate 49: Photomicrograph of rhyolite breccia at the base of the Red Rock rhyolite (near the West Fork of Sycamore Creek). 6 × 9 mm field, plane polarized light, enhanced relief due to reduction of substage diaphragm of microscope.

Plate 50: Same as plate 49, but crossed nicols.

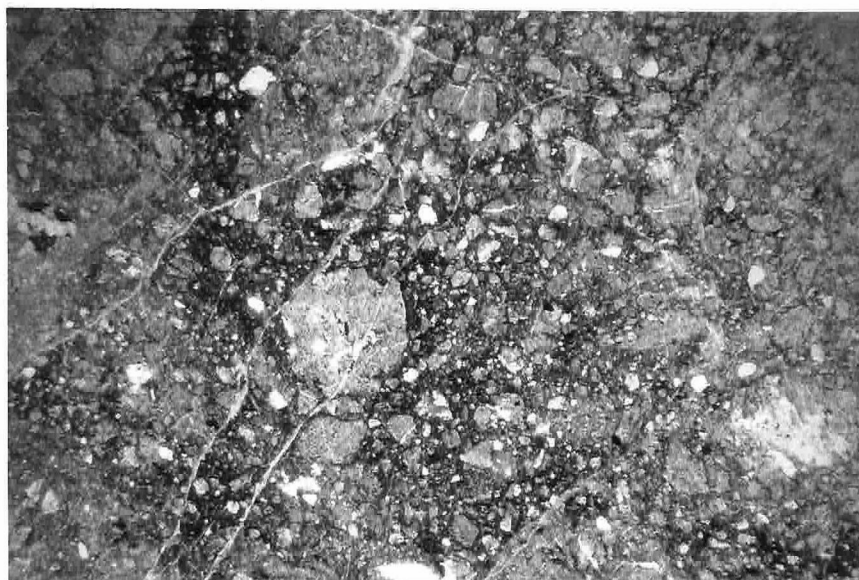


Plate 49

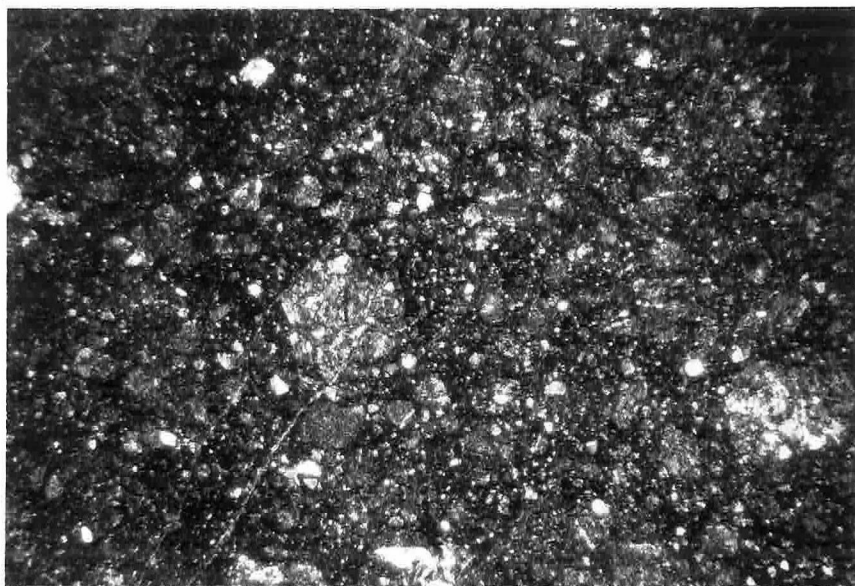


Plate 50

inclusions, and of crudely elongate irregular-shaped, quartz-filled regions give the rock its banded appearance.. The latter textural elements suggest distorted cavity fillings. Regions of crudely fan-shaped radial aggregates of quartz and feldspar, perhaps representing devitrification textures, are present in several of these rocks. Some of the regions showing pronounced alignment of very small-scale features in a fine-grained region of the rock have the appearance of a highly compressed pile of fine shards (plate 48).

Lithic fragments are present in some of the banded rocks, and are generally elongate and aligned. Some are nearly equant, however, and when abundant define brecciated regions within a single thin-section. Most of these lithic fragments are felsic volcanics, consisting mostly of fine-grained quartz, feldspar, and opaques, but some are rich in opaque minerals or chlorite and are clearly more mafic than the rock as a whole. Their origin is not known.

Metamorphic and Deformational Effects

Except for the marginal rocks of the Red Rock mass, most of the Red Rock rhyolite has little or no macroscopic metamorphic foliation. Even in the marginal rocks, the cleavage is developed without conspicuous schistosity. The feldspar phenocrysts, however, have been altered to sericite to a variable degree (in some cases almost completely), and the groundmass of some rocks is partially sericitized. Such groundmass contains aligned braids and flakes of sericite which define a foliation. The banded rocks contain some bands which are preferentially and nearly completely sericitized and always conformable with the igneous banding.

The complete absence of sericite in some of the fine-grained rhyolites of the Red Rock rhyolite must be the result of the extreme resistance to mechanical deformation of the unit, and to its massive character. These qualities would have inhibited the reduction of grain size normally accompanying shearing and also have reduced the permeability of the unit and thus the role of water during metamorphism.

Red Rock Rhyolite: Chemistry

One sample of the Red Rock rhyolite from the Red Rock mass (a welded tuff collected by L. T. Silver in lower Lion Canyon) was analyzed for its major element chemistry (table III, Appendix I). Its composition is very similar to Nockolds' average alkalic rhyolite + rhyolite-obsidian (Nockolds, 1954), and plots in the field of young rhyolite obsidians compiled by Anderson (1968), on the quartz-plagioclase-orthoclase diagram (fig. 5, Appendix I). Thus, the sample of Red Rock rhyolite has not evidently suffered appreciable alteration of its original major-element chemical composition. The only distinctive characteristics of the chemistry of the sample are a low MgO content (0.03%) and rather high Fe_2O_3 content. The abundance of oxidized iron might well reflect oxidation during emplacement and cooling. The strong similarity in chemistry between this Red Rock rhyolite sample and the sample from the massive rhyolite sub-unit of the Telephone Canyon member of the Alder series has already been remarked on (p. 114).

One sample of the Red Rock rhyolite from the Mt. Peeley mass was also analyzed (table III, Appendix I). This rock, a former vitric tuff (see plates 42, 43), is distinctly anomalous in composition

compared to young rhyolites (fig. 5, Appendix I). It has apparently gained silica, and lost sodium (very markedly) and potassium. A similar trend of alteration was noted by Anderson (1968, p. 22, fig. 6) for three rhyolitic rocks from the Prescott-Jerome area. As Anderson points out, such alteration, while possibly metamorphic, could also be due to hydrothermal solutions or hot spring action closely associated with accumulation.

Distribution

The Red Rock rhyolite is exposed in two large masses. The Red Rock mass extends across the center of the mapped area, and intersects Cane Springs Canyon, Telephone Canyon, and the West Fork of Sycamore Creek. The Red Rock mass occupies the core of the Red Rock syncline, and thickens markedly to the northeast (a factor of over four in thickness). The average thickness of each syncline limb at Cane Springs Canyon is about 4000'. Best exposures of the Red Rock mass are in Cane Springs Canyon, while more accessible exposures of less fresh rock are in Telephone and Mercuria canyons.

The Mt. Peeley mass makes up most of Mt. Peeley and Sheep Mt., and extends to the northeast across Deer Creek for over four miles from the summit of Mt. Peeley. The mass extends west of Mt. Peeley for at least two miles. Wilson's mapping (Wilson, 1939) established the general extent of the mass. Total exposed thickness of the Mt. Peeley mass is still unknown because the internal structures have not been defined. Best exposures of the Mt. Peeley mass are found on the steep southeastern slopes of Mt. Peeley.

Correlation of the crude stratigraphy developed in the Cane Springs Canyon exposures in the Red Rock mass was not accomplished, nor was extensive mapping within the Mt. Peeley mass attempted. Examination of float shed from Mt. Peeley indicates that, although spherulitic rhyolites and faintly banded rhyolites are present on Mt. Peeley, the rather thick section of welded lithic tuffs present near the core of the Red Rock syncline is absent. The massive character of the Mt. Peeley mass, its lack of interbedded waterlain rocks, its compositional similarity with the Red Rock mass, and its position on upper Alder series beds support the correlation of the Mt. Peeley mass with the Red Rock mass.

Environment and Mechanism of Accumulation

The presence of welded vitric tuffs on Mt. Peeley and welded lithic tuffs in the Red Rock mass requires that at least part of the Red Rock rhyolite has accumulated subaerially (Rankin, 1960). The similarity of the welded lithic tuffs to known young welded tuffs, and the presence of highly compressed and distorted relict shards in rocks showing microscopic and outcrop evidence of flowage, implies that ash-flow mechanisms played an important part in the deposition of the Red Rock rhyolite. Because such rocks as bedded, fine tuffs or matrix-poor coarse tuffs or tuff-breccias are absent within the unit, subaqueous conditions were either absent during accumulation, or did not persist.

It is likely that the initial surface upon which the Red Rock rhyolite accumulated was elevated in a mild deformational event prior to

the eruption of the first Red Rock rhyolite volcanics, or that the initial volcanic deposition (such as the tuffs and volcanic breccias of the upper Alder series in the Gold Creek area) raised the floor above the water level in the basin, so that all except the lowermost lithologies are terrestrial. The trend of volcanic content of the upper Alder series in the Gold Creek area suggests that the latter process was at least locally the more important.

Two lines of evidence within the mapped area suggest that, if the one feeder dike that has been identified is not the sole source of the Red Rock rhyolite, additional feeder dikes or a single major source may lie roughly to the northeast. The mapped feeder dike stems from intrusives which penetrated the Alder series only slightly more southeast than the 4080' fork of Gold Creek, but which thicken and merge to the northeast. The Red Rock rhyolite appears to thicken to the northeast by about 500' of stratigraphic thickness per thousand feet along strike. Therefore, unless this thickening is only apparent (for example, caused by a gentle plunge of the Red Rock syncline to the northeast), sources for the Red Rock rhyolite are suggested in that direction. A large regional complex of Precambrian intrusive and extrusive rhyolites of similar age to the Alder series can be found about twenty-five miles to the northeast of the mapped area (Gastil, 1958; Conway, 1973), and may be related to the Red Rock rhyolite or its source(s).

INTRUSIVE ROCKS

No plutonic rocks are present in the mapped area. The nearest granites are exposed about three miles to the west of Mt. Peeley, where a large body intrudes the Red Rock rhyolite, and less than a mile south of Mt. Ord, where a large body intrudes the Mt. Ord andesite (Wilson, 1939). All of the rocks intrusive into the Alder series (with the exception of the diorite dikes) are fine-grained porphyritic types, some of which may be related to the extrusive volcanics of the Alder series and Red Rock rhyolite.

Gold Creek Intrusives

The oldest generation of rocks intrusive into the Alder series crop out in lower Gold Creek, and in its northern forks. They are characteristically reddish or purple, resistant, and crop out well in creeks and on slopes. The transition from intrusive porphyry in Gold Creek to extrusive volcanic breccia in the lowermost Red Rock rhyolite has already been described (p. 119). The contacts of the intrusives with the Alder series tend to be sharply discordant, although they become more nearly concordant in a northeasterly direction. In the 4080' fork of Gold Creek, these intrusives are themselves intruded by Pine Mt. porphyry intrusives.

The Gold Creek intrusives can be divided according to their grain-size into two main types. The coarser-grained type crops out in Gold Creek itself and for, at most, a thousand feet further north. In outcrop, the coarser-grained rocks are unfoliated to slightly foliated,

pink to reddish, and have abundant 1 mm - 4 mm subhedral feldspar phenocrysts set in a fine-grained groundmass. Rocks of the fine-grained type crop out further to the west and north. They are exposed in the 4080' and 3760' forks of Gold Creek, and are generally foliated, dark purple rocks. Some outcrops show contorted planar structures evidently produced by deformation during intrusion, while others are coarsely brecciated.

Microscopic examination shows that the coarser-grained types near the feeder dike contain about 60% subhedral, partially sericitized plagioclase in a groundmass of fine-grained quartz + feldspar, sericite, and opaques. No quartz phenocrysts are present. A distinctive textural feature is the abundance of radiating, feathery aggregates of quartz and feldspar which are evidently primary devitrification textures. Further from the feeder dike, both the groundmass and phenocrysts are coarse-grained. The plagioclase occurs as subhedral and euhedral sericitized phenocrysts of about 5 mm length, the groundmass quartz and feldspar as anhedral, interlocking grains up to 1 mm. The plagioclase phenocrysts which are not extensively sericitized are albite. Preferential sericitization of the cores of many plagioclase phenocrysts suggest that they were originally zoned, with more calcic cores. Many have thin rims of alkali feldspar in the groundmass or small phenocrysts. Quartz occurs only in the groundmass. Chlorite, epidote, opaque minerals, apatite, and zircon occur as accessory minerals. Typical modes for the coarser-grained rocks are:

Quartz	10% - 30%
Plagioclase	40% - 60%
Orthoclase	1% - 20%
Chlorite	2% - 10%
Opaques	2% - 4%
Epidote	1% - 3%

The fine-grained type of the Gold Creek intrusives contain either no phenocrysts, or very sparse, anhedral to subhedral quartz phenocrysts. They contain up to 20% black opaque minerals as disseminated and aggregated .05 mm - .5 mm anhedral grains. One sample examined contains abundant small (1 mm - 5 mm), aligned, quartz-filled amygdules. Sericite makes up about 25% of the fine-grained types. The sericite occurs as disseminated flakes and as aligned braids and aggregates.

Gold Creek Intrusives: Chemistry

A sample of the intrusive body which fed the Red Rock rhyolite near Gold Creek, collected about 500' from the breccia zone of the feeder dike itself, was analyzed for its major element chemistry (table III, Appendix I). Its chemical composition is similar to that of the Red Rock rhyolite sample (V in table 6), but slightly less potassic (4.21% K_2O versus 5.11% K_2O), and richer in equivalent iron (4.43% FeO versus 2.43%). Like the Red Rock rhyolite, its composition plots near the middle of the field of young rhyolitic obsidians as compiled by Anderson (1968) on the quartz-plagioclase-orthoclase diagram (fig. 5, Appendix I).

The sample is similar to Nockolds' average alkalic rhyolite + rhyolite-obsidian (Nockolds, 1954), but somewhat higher in iron content.

Pine Mt. Porphyry Intrusives

Rocks mapped as the Pine Mt. porphyry (after Wilson, 1939) are rhyodacitic intrusives which are foliated near their margins, and which were intruded mostly along or near the East Fork member-Oneida member contact on the northwest side of the Red Rock syncline. In outcrop, these rocks range from grey to tan (to pale green on freshly broken surfaces of some types), appear fine-grained (generally with interlocking texture), and may or may not display 1 mm - 5 mm subhedral quartz and feldspar phenocrysts. These intrusives are generally resistant, and crop out well in creeks and on slopes.

Foliation in outcrop can be seen only in the marginal facies (extending from 100' to more than 500' in from the country rock), but can be so pronounced as to give a truly schistose structure. The main part of the Pine Mt. porphyry body averages over 2000' in width, but is accompanied by a multitude of roughly concordant sheets of less than 100' in thickness. The distribution of these thin sheets, as shown on the map, is essentially schematic in localities of poor exposure. In thin-sections of the porphyritic types (plates 51, 52), the phenocrysts are seen to be subhedral, corroded quartz (1 mm - 5 mm, 5% - 10% modal abundance), highly sericitized subhedral plagioclase (1mmmm - 8 mm, about 2% mode, calcic albite or sodic oligoclase), faintly perthitic K-feldspar (untwinned, 1 mm - 5 mm, sericitized, about 1% modal abundance), and 2 mm, subhedral pseudomorphs of muscovite and opaques after biotite(?). The

Plate 51: Photomicrograph of Pine Mt. porphyry intrusive stock. Corroded quartz (clear) and corroded and sericitized plagioclase (gray) phenocrysts in partially sericitized, granular matrix of quartz and feldspar. 6 × 9 mm field, plane polarized light.

Plate 52: Same as plate 51, but crossed nicols.

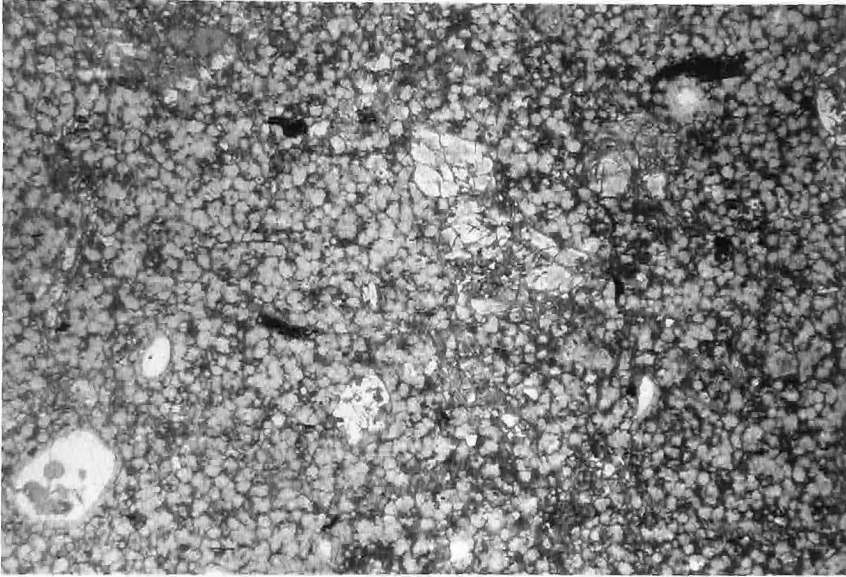


Plate 51

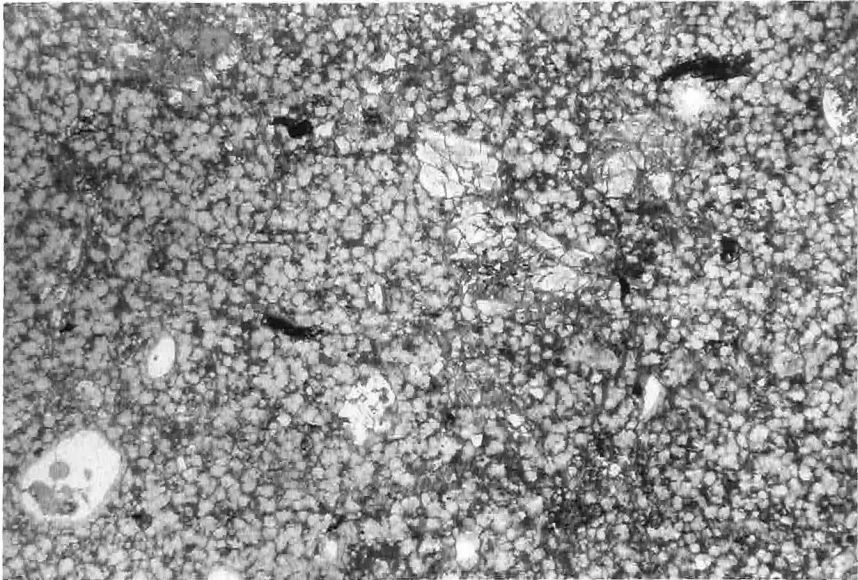


Plate 52

groundmass consists of anhedral, 0.1 mm - 0.3 mm quartz and feldspar, themselves set in a matrix of sericite so that the groundmass contains about 30% sericite. Microscopic examination of the marginal lithologies reveals very sparse or no phenocrysts, and a groundmass similar to the porphyritic types, but with smaller (.05 mm - .1 mm) grain size (plates 53, 54).

The Pine Mt. porphyry crops out in a northeast-trending region which is roughly consistent in its stratigraphic location in the Alder series (never lower in the section than the upper East Fork member, and never higher than the middle Telephone Canyon member). Although Wilson (1939) considered the locus of intrusion to be a fault contact, there is no evidence that such a fault exists in the main region of intrusion; rather, the lithologic changes between the upper East Fork and lower Oneida members are seen to be gradational where exposure permits inspection.

Although a few thin rhyodacitic sheets are exposed on the lower slopes of Mt. Ord on the Mt. Ord access road, they do not extend as far west as the 3600' fork of Slate Creek, and were not mapped. At higher elevations on the north slope of Mt. Ord, on the Mt. Ord access road, an intrusive rhyodacitic body or complex of significant size is present. These rocks are very similar to the Pine Mt. porphyry in that their groundmass and phenocryst texture and composition are closely similar. They tend to be more sheared than the typical Pine Mt. porphyry lithologies, however, and probably because of that do not crop out as well as other intrusives of similar composition in the area.

Plate 53: Photomicrograph of Pine Mt. porphyry marginal facies (sparse to no phenocrysts). A partially corroded and sericitized plagioclase phenocryst is in the center of the field. The matrix appears coarser-grained, due to the sericitization, than is actually the case.

Plate 54: Same as plate 53, but crossed nicols.

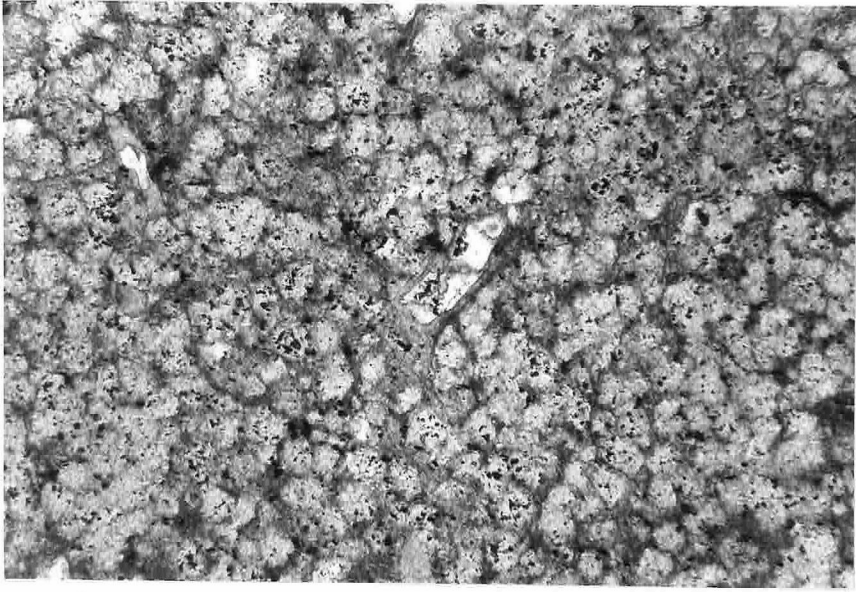


Plate 53

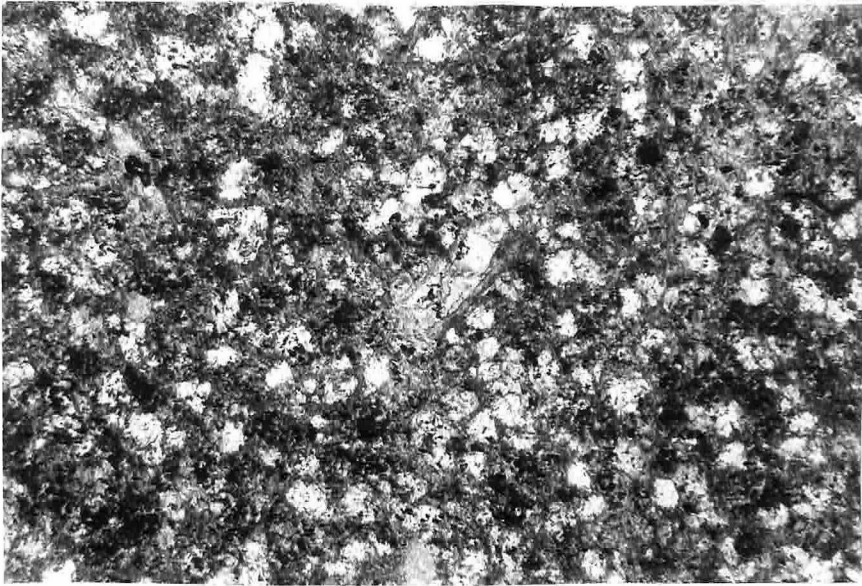


Plate 54

They crop out on the Mt. Ord access road between the elevations of 5100' to 5400' (approximately) and again from 5800' to about 5880', where they are intruded(?) by the Ord andesite. In the absence of mapping away from the Mt. Ord access road below the uppermost horizon of intrusion of these rocks into the Alder series, nothing further can be said about their distribution.

Unfoliated Rhyodacitic Intrusives

Relatively thin sheets of porphyritic rhyodacitic rocks intrude the Alder series in a northeasterly-trending region whose width extends from just below the Red Rock rhyolite-Alder series contact on Mt. Peeley to about a mile to the southeast. The areal distribution of these sheets straddles a major structure of the area. These intrusives have exposed thicknesses from a few feet to over 500 feet, and are roughly concordant with the country rock. An accompanying decrease in size and abundance of phenocrysts close to the country rock suggests that the marginal foliation was produced during emplacement.

The unfoliated rhyodacitic intrusives are tan, white, or deep pink in color, and show 1 mm - 10 mm phenocrysts of quartz and feldspar on fresh surfaces. The groundmass appears fine-grained, dense, and interlocking.

Microscopic examination shows that the rocks contain 10% to 20% quartz phenocrysts (euhedral to subhedral, strained, some corroded), 1% - 5% plagioclase phenocrysts (partially sericitized subhedral-anhedral unzoned albite or oligoclase), and 0% - 1% K-feldspar phenocrysts

(euhedral to subhedral, untwinned). Red-brown opaque mineral aggregates are present in trace amounts, possibly relict after hornblende.

The groundmass is predominantly quartz and feldspar (.05 mm - .1 mm), in the form of anhedral, interlocking, and in some cases, radiating, aggregates. Also in the groundmass are 1% - 10% unoriented sericite flakes and aggregates and 1% - 5% anhedral opaque minerals. No evidence of foliation is present in thin-section.

Andesitic-Dacitic Intrusive Sheets

Dark-colored, roughly concordant intrusive rocks penetrate the Alder series and the Red Rock rhyolite in several horizons within the Red Rock mass and the Telephone Canyon member on both sides of the Red Rock syncline. These rocks are typically dark blue to blue-green where fresh, and weather to a dark brown or black color. Those sheets within the Telephone Canyon member are generally foliated, but those within the Red Rock rhyolite show little or no foliation. The contacts of these sheets with the country rock are in some cases discordant on a small scale (inches to feet) in the few outcrops where their contacts are well-exposed. They are younger than the Pine Mt. porphyry intrusion, as they intrude that body near the Mercuria Mine.

In outcrop, they are generally fine to medium-grained, and in the coarser-grained types, display 1 mm - 3 mm feldspar laths on fresh surfaces. Some of the sheets are amygdaloidal, with $\frac{1}{2}$ cm - 2 cm calcite or carbonate amygdules. The thickest sheets have an exposed width of about 500'. The near ubiquity of these rocks at the contact of the Red

Rock rhyolite and Telephone Canyon member suggests a maximum linear extent of individual sheets of over five miles.

Microscopic examination of these rocks reveals that they are of a variety of types. Most common are fine-grained lithologies containing an assemblage of opaque minerals, epidote (\pm), plagioclase, and chlorite with a grain-size of .05 mm - .1 mm. Slightly coarser-grained types contain subhedral plagioclase laths and, in some cases, interstitial quartz which may be primary. At least one of the sheets contains small ($\frac{1}{2}$ mm), sparse subhedral quartz phenocrysts in a chlorite-rich, partially sericitized groundmass.

Andesitic Stock: Mt. Ord Andesite

A large body of andesitic volcanic rock is exposed on the upper part of Mt. Ord. This body was mapped and described by Wilson (1939) as a pyroxenite. The Mt. Ord andesite (new name) was examined in reconnaissance, and its contact relations investigated only near the Mt. Ord road. In outcrop, the rock is dark gray or black on fresh surfaces, and weathers to a light brown or tan. It is fine-grained, and has a dense, interlocking groundmass texture. Sparse, 2 mm - 10 mm altered pyroxene or olivine phenocrysts can be seen in hand-specimen. No foliation is observable, and spheroidal weathering structures are common. Within 200' of the contact of the body with the Pine Mt. porphyry-type intrusives on the Mt. Ord road, the rock is brecciated (plate 55). It is not known whether the Mt. Ord andesite body was intruded into, or faulted against the Alder series. Wilson (ibid.) judged the body to be

Plate 55: Brecciated Ord andesite near Alder series contact. The matrix and fragments of the breccia are similar in composition.

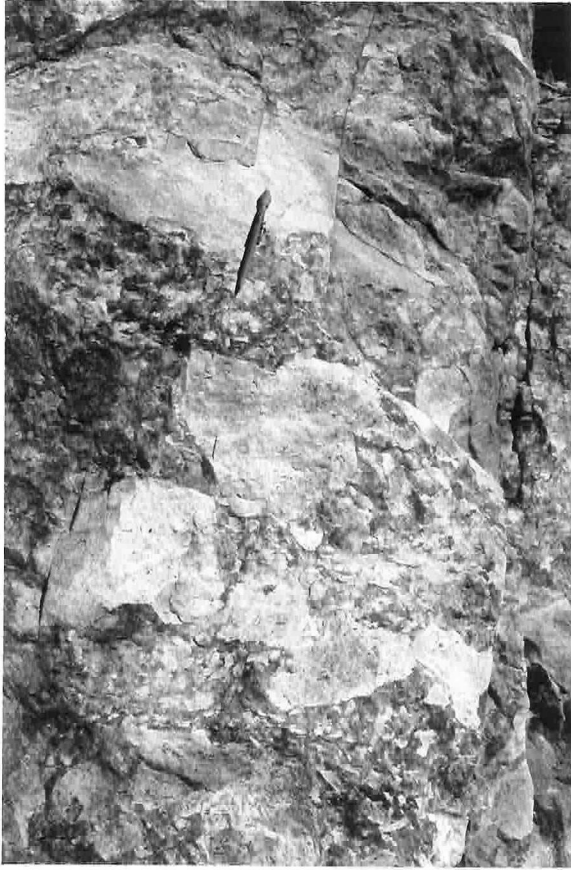


Plate 55

intrusive into the Alder series.

Microscopic examination of the Mt. Ord andesite shows that the common phenocrysts of the rock are plagioclase (1 mm - 3 mm, subhedral, unzoned albite or sodic oligoclase), olivine (1 mm - 3 mm, subhedral-anhedral grains) and clinopyroxene (1 mm - 3 mm subhedral colorless to pale green grains). The olivine phenocrysts are partially reacted to a pale green amphibole and intergrown with clinopyroxene. One sample, more silicic in groundmass character than the others, contained sparse quartz phenocrysts.

The groundmass is fine-grained and consists of .01 mm by .1 mm randomly oriented plagioclase laths (about 20%), fine-grained epidote (about 10%), opaque minerals (about 10%), quartz (about 5%, in vesicles and as radiating aggregates), and very fine-grained minerals of uncertain identification (mostly epidote). Non-porphyrific lithologies of the Mt. Ord andesite consist of fine-grained epidote, chlorite, opaque minerals, feldspar + quartz(?), and sericite. Amygdules of quartz and chlorite are common. These amygdules are irregularly shaped, about two to five millimeters in size, and somewhat elongate and aligned.

Most of the quartz in these rocks appears to be secondary. The unit was probably dacitic to andesitic in original character, and may be related to the andesitic-dacitic intrusive sheets. No geological evidence was found to support this correlation, however.

Diorite Dikes

In the northeastern part of the mapped area, and near Horse Camp Seep, a few medium-grained, dark-colored unfoliated dikes crop out. Some of these dikes trend roughly northwest, in distinct contrast to the other intrusive rocks in the area. They are found both in the Alder series and the Red Rock rhyolite. Because of their tendency to poor and heavily brush-covered exposures, with some spheroidal weathering, they may be more extensive than shown on the map.

The rocks of the diorite dikes are massive, equigranular to slightly porphyritic, and blue-green on freshly broken surfaces. They weather to a gray to brown color. In hand-specimen, one can distinguish about 20% - 30% dark minerals and about 50% pale green and pink feldspar.

Thin-section examination shows that the rock is composed of plagioclase (albite, 50% - 60%), epidote (pistacite and clinozoisite, 5% - 15%), chlorite (5% - 10%), opaque minerals (about 5%), hornblende (2% - 5%), augite (1% - 15%), quartz (1% - 5%), and K-feldspar (trace to 5%, untwinned, non-perthitic, 2V about -50°), and apatite (trace -3%, up to 5 mm). The plagioclase occurs as subhedral laths of 1 mm - 5 mm size, mostly altered to fine-grained epidote. The quartz and K-feldspar are mainly anhedral and interstitial to the other minerals. Micrographic and myrmekitic textures are abundant. The intrusive sheet near Horse Camp Seep is somewhat atypical in mineralogy in that the feldspar is severely chloritized, large epidote grains are absent, and unaltered mafic silicates are present in only some parts of the sheet.

These rocks are not typical diorites, in that the epidote and chlorite appear to be mostly primary minerals, and the plagioclase is unusually sodic. The mineral assemblage may be the result of late-stage reaction with the magmatic fluids at low temperature, or possibly due to emplacement near the end of the thermal metamorphism of the Alder series and Red Rock rhyolite.

It is not clear whether these dikes are Precambrian or younger. Certainly their lack of foliation permits them to be as young as the Tertiary basalts which intrude the Precambrian and Tertiary rocks in and near the mapped area.

CHEMISTRY OF PRECAMBRIAN ROCKSOF THE CENTRAL MAZATZAL MOUNTAINS: SUMMARY

The analyses of two tuffs and one volcanic breccia from the Cornucopia member of the Alder series are all essentially dacitic. The lower Cornucopia member tuffs are petrographically similar to much of the volcanic wackes and sandstones of the underlying, thick, Horse Camp member and also quite like the tuffs of the lowermost-exposed Crystalline tuff member of the Alder series. Thus it appears that the Alder series section below the base of the Oneida member contains large volumes of dacitic volcanic rock. The Oneida member contains the lowest stratigraphic horizons with abundant rhyodacitic or rhyolitic volcanics. If the single analysis of the Oneida member volcanics is typical, their composition occupies an intermediate position between the true rhyolites of the latest Alder series rocks (and Red Rock rhyolite) and the earlier dacitic volcanics of the lower Alder series. The position of the chemical analyses available on the AFM and quartz-plagioclase-orthoclase plots (figs. 5 and 6, Appendix I) are not inconsistent with a single differentiation trend for the suite, although, in view of the small number of analyses and the possibility of alteration during metamorphism, the chemical analyses do not in themselves demonstrate a single differentiation trend.

The similarity in the chemical compositions of the uppermost Telephone Canyon member rhyolites, the Red Rock rhyolite, and the Gold Creek intrusives is reasonably convincing of a genetic relation among

these rocks, which is consistent with strong arguments derived from the geologic and stratigraphic relationships. Conway (1973) has concluded that rocks correlable with the Red Rock rhyolite and upper Alder series in the Tonto Basin area are part of a felsic volcanic and plutonic complex comparable to large modern calderas. Conway's analyses are closely similar to those of the Red Rock rhyolite and related rocks (personal communication), which suggests that the upper Alder series and Red Rock rhyolite may be part of this complex and of the "distinctive alkaline petrographic suite" (Conway, 1973).

METAMORPHISM

Alder Series Rocks

The rocks of the Alder series have undergone a relatively low-grade regional metamorphism, which has resulted in a partial recrystallization to a metamorphic mineral assemblage. The mafic-poor lithologies are now represented by an assemblage of quartz-albite-sericite-chlorite-opaque minerals-(epidote), and the more mafic rocks by the assemblage albite-chlorite-carbonate-opaque minerals-(epidote)-(tremolite)-(sericite). These assemblages belong to the lowest greenschist subfacies of the greenschist facies as defined by Turner and Verhoogen (1960), the quartz-albite-muscovite subfacies. No metamorphic biotite was observed in the Alder series rocks, which indicates that the middle greenschist facies of Turner and Verhoogen (ibid.) was not reached.

The extent to which the observed mineral assemblages have approached equilibrium varies as a function of the chemical composition of the rock, and the degree of mechanical shearing which it has undergone. The mafic-rich rocks, such as the basaltic flows and pillow-lavas of the Cornucopia member, are generally highly recrystallized, though not strongly sheared, and have retained little or none of their original mineralogy. Similarly, although pseudomorphs of pyroxene, olivine, hornblende, or biotite occur in some igneous rocks in many parts of the Alder series, only traces of hornblende or biotite were found preserved. The more leucocratic rocks and minerals, however, are not uncommonly well-preserved (with the exception of plagioclase more calcic than albite).

The leucocratic rocks which have undergone the most recrystallization, such as some of the pyroclastics in the Oneida member, are those which show the greatest degree of alignment of the sericite, and the best cleavage. Those leucocratic rocks which are only faintly foliated, however, such as some of the volcanic wackes of the Horse Camp member or the vitric tuff sub-member within the East Fork member, show only minor development of sericite.

The overall degree of metamorphic recrystallization of the Alder series rocks seems to increase towards the southeast. Northwest of a roughly northeast trending line passing near the Oneida Mine, the Alder series rocks tend to show relatively less effects of recrystallization. The rocks of the upper Oneida member and Telephone Canyon member on the northwest side of the Red Rock syncline appear to be generally more

reacted (mainly to sericite, but also as incipient recrystallization of quartz clasts or phenocrysts), and the Mt. Ord section of the Alder series is also, as a whole, more recrystallized than the lower Alder series section to the northwest of the Oneida mine.

No contact metamorphic effects of any significance were observed associated with the intrusive rocks, although their contacts are exposed in several localities.

Red Rock Rhyolite

The metamorphic effects on the mineralogy of the Red Rock rhyolite are described on page 141. Because the degree of recrystallization of most of the Red Rock rhyolite is generally less than that of the nearest Alder series beds, the possibility that the Red Rock rhyolite underwent only a later, and less intense metamorphism than the Alder series should be mentioned. However, the degree of preservation of textures and mineralogy of the massive rhyolite sub-unit of the Telephone Canyon member of the Alder series is no less than that of most of the Red Rock rhyolite. This fact strongly argues that the less recrystallized nature of the Red Rock rhyolite is due to the same massive, impermeable, shear-resistant character which characterizes the massive rhyolite of the Telephone Canyon member.

Intrusive Rocks

The metamorphic effects on the mineralogy and textures of the intrusives are described in pages 147-161. The Gold Creek intrusives and

the Pine Mt. porphyry evidently record the same metamorphic history as the country rock. The interior of the larger intrusive masses, however, have been less affected by sericitization and shearing than their margins, or than the thinner, sheet-like bodies.

The unfoliated rhyodacitic intrusives have evidently not undergone the same deformational history as the Alder series, because even the thinnest sheets do not contain aligned sericite aggregates. The partial sericitization of the feldspar phenocrysts and the presence of sericite flakes in the groundmass of these rocks, however, suggests that although they were emplaced after the time of major folding and faulting, conditions of low-grade metamorphism had not ended at the time of their intrusion. Or, alternatively, one can call upon a later and unrelated metamorphism to explain the sericitization. Because such an event would not leave a recognizable overprint on the equally low-grade Alder series mineral assemblages, such a hypothesis cannot be substantiated.

The andesitic-dacitic intrusive sheets have undergone metamorphism to a grade indistinguishable from that of the Alder series rocks of similar composition. The Mt. Ord andesite body, unlike the Alder series or the andesitic-dacitic sheets, has retained igneous mafic phenocrysts (clinopyroxene, olivine, hornblende) in its interior. The assemblage albite-epidote, chlorite-quartz that occurs with these minerals, however, suggests that the preservation of the mafic phenocrysts is more the result of an incomplete approach to the equilibrium metamorphic assemblage than an absence of metamorphism. Thus, the Mt. Ord andesite, though possibly younger than the Alder series, evidently

predates the unmetamorphosed, 1660 m.y. Sunflower granite (Silver, 1964) which lies immediately to the south of Mt. Ord.

STRUCTURE

The stratified Precambrian rocks of the northern Reno Pass quadrangle appear to have undergone folding and faulting on a large scale, compared to the dimensions of the area, but in an essentially simple manner. The Red Rock mass of the Red Rock rhyolite occupies the core of a tight syncline, which has resulted in duplication of the Alder series units on either side of the syncline. The thinning of the Red Rock mass towards the southwest may reflect a gentle plunge of the syncline to the northeast. Much of the change in apparent thickness of the Red Rock rhyolite in the Red Rock mass, however, may equally well be attributed to actual thinning of the unit to the southwest. Such a thinning is supported by the abundance of apparently related intrusive and extrusive rhyolites in the uppermost Alder series in the northeast corner of the mapped area. These rhyolites have certainly swelled the uppermost Alder series section, and probably are responsible for the thickening of the Red Rock rhyolite in this area.

An inferred, tight anticline, faulted near its axis, is present in the northwest part of the area. The inferred anticline axis and the fault pass about one mile to the southeast of Mt. Peeley. All of these structures are parallel, and trend to the northeast. Tertiary or younger normal faults are common in the northeast corner of the area, but are not apparent elsewhere.

The Red Rock syncline is defined on the basis of close similarity of lithologies of the Alder series rocks for several thousand feet (perpendicular to the contact) on either side of the Red Rock mass, on the orientation of the tops of their beds, and on the position of the distinctive lithologic pair of the Cornucopia member pillow lavas - volcanic breccias. The limbs of this fold are essentially parallel and nearly vertical. Location of the axis of the syncline, in the absence of a good stratigraphy within the Red Rock rhyolite, is difficult. Drag folds within the Red Rock rhyolite and upper Telephone Canyon member are not common. An exposure of three-cycle graded bedding within a lapilli tuff within the Red Rock rhyolite at about the 4560' level in Cane Springs Canyon indicates northwest tops (thus a syncline axis to the northwest); however, because this observation implies considerable asymmetry of the thickness of the Red Rock rhyolite on the two syncline limbs, the exposure may reflect subordinate folding or be anomalous. A highly contorted and quartz-veined locality in Mercuria Creek at 4300' may reflect the intense deformation at the axis of the fold, especially as this zone occurs close to the axis of symmetry of the Red Rock mass.

The faulted anticline near Mt. Peeley is inferred from the bedding-top reversal across the structure, as well as from correlations of the lithologies on either side. The location of the fault (the Thicket Springs fault) is defined in the field by a narrow zone (20' - 50' thick) of intensely quartz-veined and brecciated rock, best exposed in the 4920' fork of the West Fork of Sycamore Creek.

A steeply-dipping, generally persistently northeast-striking foliation pervades the Alder series rocks, and in some localities, the lowermost Red Rock rhyolite horizons. Within the least competent lithologies, such as the East Fork member slates and the Oneida member schistose welded tuffs, local variations from the dominant northeast-striking foliation may be seen, as well as multiple cleavage planes. The northeast-trending, steeply dipping foliation is evidently axial-plane foliation related to the major folds in the area. The auxiliary cleavage planes observed in some outcrops of the least competent rocks do not appear to be related to any major structure.

Relatively small-scale folding is present in the northeast part of the mapped area, expressed as an (inferred) 'S'-shaped fold with a steeply dipping plane striking roughly east-west. Field evidence of this structure is given by the outcrop pattern of the resistant quartzite which crosses Gold Creek, by extrapolation and interpolation of the distribution of a cobble conglomerate which intersects Gold Creek near 4680', and by the bedding attitudes exposed in the roadcut of the Bernice Mine-Gold Creek road.

This S-fold crosscuts the regional foliation, and is crosscut by the andesitic-dacitic intrusive sheets. It is possible that the bend in the distribution of the Pine Mt. porphyry body at Pine Butte is controlled by this fold, either by intrusion along a folded stratigraphic zone or folding of the body itself.

A steeply dipping, northeast-striking normal fault is present in the northeastern corner of the area. This fault has a prominent, silicified scarp (plates 56, 57) which is easily seen from highway 87

as it crosses Gold Creek. The fault juxtaposes Tertiary gravels (characterized by abundant rounded clasts of coarse granite and Mazatzal quartzite), highly foliated welded tuffs, and felsic intrusive porphyries against massive, unfoliated rhyolite welded tuffs and rhyolite breccias. A Tertiary or younger age is indicated for this fault, because the Tertiary gravels are exposed up to the base of the scarp. The apparent throw of the fault decreases to the southwest. The fault is not evident in and to the southwest of the 4080' fork of Gold Creek. Because the Tertiary gravels were probably only slightly thicker at the time of faulting than now, their presence along the fault suggests a maximum vertical displacement, from ridge-top to scarp base, of about 1000'.

The contact between the Tertiary gravels and the Precambrian rocks in the northwest corner of the mapped area is largely by high-angle faulting. It is possible that much of the contact of the Red Rock rhyolite with the Tertiary gravels to the northeast of Gold Tooth Smith Spring is by similar faulting.

SEQUENCE OF EVENTS

The oldest intrusive rocks are those bodies in the lower Gold Creek drainage. Because one of these bodies broke the surface at the end of Alder series time, they clearly were emplaced before the time of major folding which involved the Alder series and Red Rock rhyolite. The Pine Mt. porphyry intrusives also were intruded before the time of folding. These rocks intrude one of the oldest generation intrusive

Plate 56: Looking north towards silicified fault scarp (post-gravels) at the base of a ridge north of lower Gold Creek. Roadcuts of Arizona state highway 87 are visible in the middle foreground. The ridge behind the scarp consists of massive rhyolite of the Telephone Canyon member of the Alder series, while in front of the scarp are mostly foliated tuffs of the same unit. The Mogollon Rim is visible in the far distance to the right.



Plate 56

Plate 57: Close-up view of the scarp shown in plate 56, looking southwest. The fault trace passes through the saddle visible in the far distance at the extreme left.

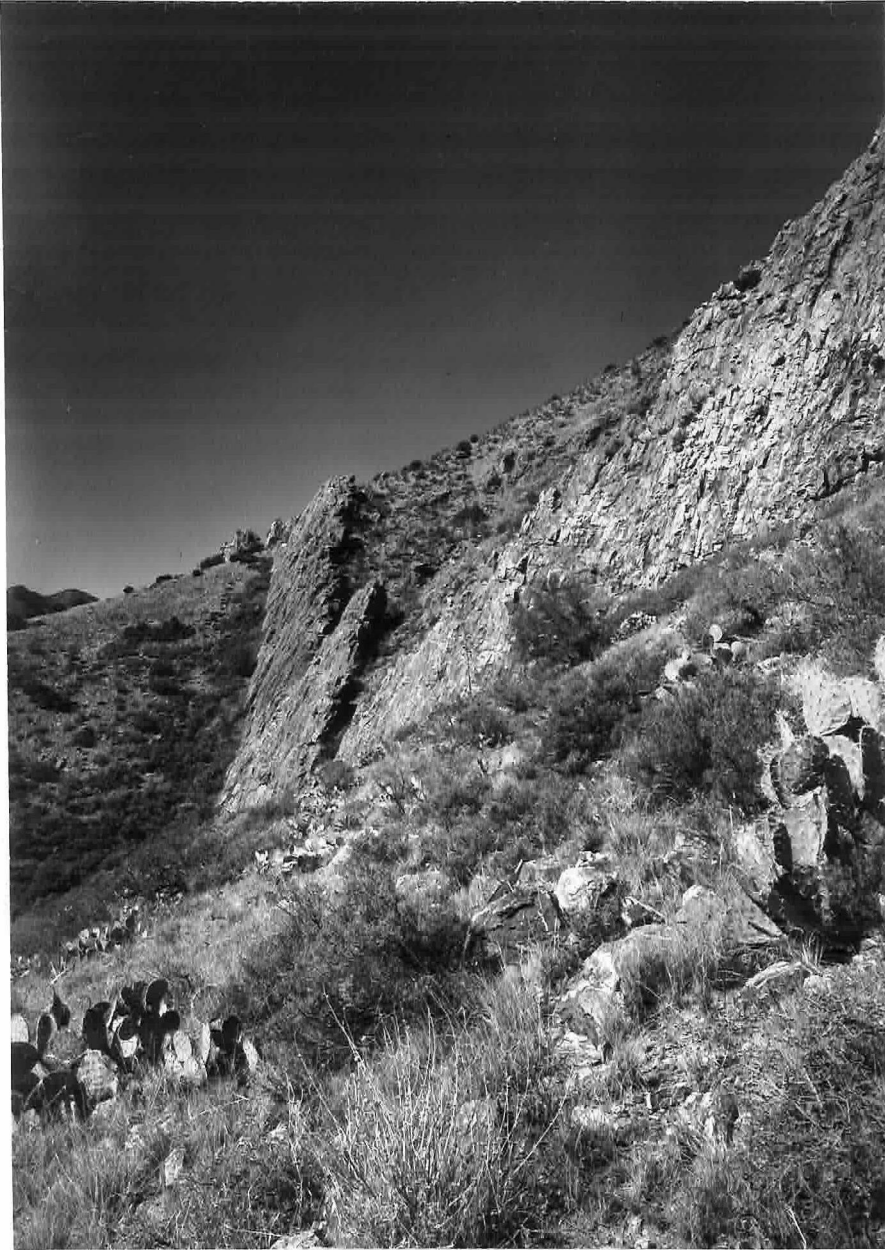


Plate 57

bodies, and are strongly foliated at their margins. If the tentative correlation of these rocks with the intrusives on Mt. Ord is valid, then the rough plane of intrusion of the Pine Mt. porphyry dipped gently to the southeast.

The important characteristics of the andesitic-dacitic sheets, insofar as determining their relative time of intrusion, are,

- 1) they intrude the Pine Mt. porphyry (near the Mercuria Mine),
- 2) they are roughly symmetrically distributed about the axis of the Red Rock syncline, and,
- 3) their foliation varies from slight to marked.

If these sheets were emplaced before the folding, it is difficult to understand why such apparently non-resistant rocks should not have all been strongly sheared. If, conversely, they were emplaced after the folding, one must explain why any foliation is present, and why the sheets should be distributed with rough symmetry about the fold axis. A reasonable explanation is that these sheets were intruded synkinematically, such that earlier-intruded sheets became well-foliated, while the later-intruded ones remained essentially unfoliated. The sheets in the upper Cane Springs Canyon drainage crosscut the 'S'-fold in that area, and thus are clearly later than at least that fold.

The loci of intrusion of these sheets were probably controlled by zones of sheared rock caused by accommodation, along bedding planes, of the stresses of folding. Their persistence along the Red Rock rhyolite-Alder series contact, which in view of the marked contrast of resistance to deformation would be expected to be a plane of slippage during folding, is consistent with this hypothesis.

The Mt. Ord andesite is difficult to place in a sequence of intrusions, because although it is undeformed, its very massiveness may be responsible for an effective shielding against shearing. Because the margins of the body do not display a foliation, and because the primary mafic minerals in some of the samples of the body are preserved, it may be that the Mt. Ord andesite is in fact post-deformational. The general compositional similarity of the rock to the least foliated andesitic-dacitic sheets suggests a common source, although if that is the case it is not clear how the two distinctly separated areas of intrusion arose.

The unfoliated rhyodacitic intrusives in the northwest part of the mapped area were clearly intruded after the time of folding and faulting. Aside from the lack of foliation of these rocks, the distribution of the sheets is in itself strong evidence for a post-deformational time of emplacement -- they are restricted to a relatively narrow band whose location straddles a major fault and an anticline axis. Because it is improbable that similar intrusive sheets would have been emplaced in widely separated stratigraphic horizons, and then fortuitously juxtaposed so as to yield a coherent, more or less continuous distribution, one can conclude that the faulted anticline was formed before emplacement of these rocks. The marked degree of sericitization of the feldspar phenocrysts and groundmass of some of the sheets, however, indicates that metamorphic conditions still prevailed at the time of emplacement.

The sequence of events in the central Mazatzal Mountains is, therefore:

- I. Accumulation of the sediments and volcanics of most of the Alder series, subaqueous deposition.
- II. Gentle uplift, more pronounced to the northeast, intermittent subaerial deposition.
- III. Rhyolitic vulcanism and intrusion in northeastern part of the area, uplift due to intrusions in the lower Gold Creek area.
- IV. Eruption of Red Rock rhyolite from same sources as (III), continuing rhyolite intrusions, disappearance of subaqueous conditions.
- V. Intrusion of Pine Mt. Porphyry.
- VI. Intrusion of andesitic-dacitic sheets.
- VII. Folding, faulting, and metamorphism, possibly overlapping with (VI).
- VIII. Intrusion of rhyodacitic sheets, continuing metamorphism, possibly intrusion of Mt. Ord andesite.

AGE DETERMINATIONS

Preliminary to a more detailed study of the absolute ages of the Precambrian rocks of the central Mazatzal Mountains in the northern Reno Pass quadrangle, two rock samples from the upper part of the Alder series were dated by means of the U-Pb method on cogenetic zircon suites. The results from this work show that the upper Alder series rocks are indistinguishable in age from the Red Rock rhyolite (i.e., within 20 m.y.), with an apparent age of 1730 ± 20 m.y.

SAMPLES

grbrc

This sample is a monolithologic rhyolitic breccia exposed in the 4080' fork of Gold Creek at the 4450' level. The lithology persists as a mappable unit for at least 3000' to the northeast, and about 4000' to the southwest, at which point the lithology displays a few rounded cobbles. A further 3000' to the southwest, the unit is conglomeratic.

At the collection locality, the unit is about 50' thick, overlies volcanic wackes and slates (contact not exposed), and grades up-section into slates. The unit is within the Telephone Canyon member of the Alder series. The breccia consists of about 30% angular, equant rhyolitic cobbles with sizes from 1 cm to 30 cm, but with no well-defined transition from small clasts to coarse matrix material. The larger clasts are massive, and show sparse $\frac{1}{2}$ mm - 2 mm quartz and feldspar phenocrysts, set in a dense, fine-grained groundmass. Thin-section

examination of the rock (Appendix II) shows that the matrix material is similar in texture and composition to the larger clasts. The complete absence of any sorting or variety of clast lithology in this rock suggests that it was emplaced essentially during, or very soon after extrusion, probably as a debris flow.

This sample (grbrc) lies about 2600' stratigraphically below the base of the Red Rock rhyolite.

tfbrc

This sample was collected from the upper part of the Oneida member of the Alder series, at about the 4025' elevation in the West Fork of Sycamore Creek, about 3000' stratigraphically below the base of the Red Rock rhyolite. This part of the Oneida member is a zone of flattened pumice tuffs of at least a several hundred foot thickness. The sampled outcrop contains abundant large (1" × 10" to $\frac{1}{2}$ " × 20") highly elongate and aligned rhyolitic clasts in a dense, fine-grained matrix. Within a few feet of the sampled outcrop, sparsely occurring jasper pebbles are also present.

Thin-section examination (Appendix II) shows a few 1 mm quartz phenocrysts set in a partially sericitized, fine-grained quartz-feldspathic groundmass. No relict shards or flattened pumice fragments were observed, and if originally present would probably have been obscured by the subsequent shearing and recrystallization. The matrix material and the clasts were observed to be similar in both composition and texture.

ANALYTICAL TECHNIQUES

Zircon separates from the crushed rock samples were obtained by density separation in heavy liquids (following preliminary concentration of heavy minerals on the Willfley table), sieving to give separate size distribution populations, and final separation according to magnetic properties on the Frantz. The acid-washed (30 min. warm 50% HNO_3) concentrates were attacked with $\text{Na}_2\text{B}_4\text{O}_7$ and HF, and the lead composition, and lead and uranium concentrations determined by the methods outlined in Silver et al., 1963. Concentrations of U and Pb are reproducible to within 1%, the 206/207 and 206/208 ratios to within 0.2%, and the 206/204 ratios to within 0.5% (usually to within 0.3%).

RESULTS

The results of the analyses (table I) are plotted on the concordia diagram of fig. 4. The points from the Alder series are colinear within analytical error, and fall on a chord with an upper intersection on concordia of 1730 m.y. Because the common lead content of the zircon fractions was rather high, the choice of isotopic composition of the common lead is the main source of uncertainty in the upper intersection of the chord with concordia. The apparent age should, however, be correct within ± 20 m.y.

Data from the Red Rock rhyolite previously obtained by Silver were kindly supplied, and are plotted also on fig. 4. These points, obtained from zircon fractions with only a slight common lead content

(206/204 from about 450 to 925), fall very slightly on the young side of the Alder series chord. Projecting a chord parallel to the Alder series chord but fit to the Red Rock rhyolite data points gives an upper intersection for the Red Rock rhyolite about 5 m.y. younger than the Alder series. This age difference, however, cannot be accurately estimated in view of the relative imprecision of location of the actual Alder series chord, but rather is more realistically said to be within about 20 m.y. of the age of the Alder series.

The apparent age thus obtained for the Alder series is just on the old side of the ages reported by Silver, 1715 ± 15 m.y., for the meta-volcanics which crop out extensively in Arizona to the south and southeast of the type Alder series locality, and distinctly younger than the ages reported by him (1770-1820 m.y.) for meta-volcanics to the north and east, in Arizona, Colorado, and New Mexico, including the Yavapai schist of the Prescott-Jerome region.

The actual age obtained (1730 ± 20 m.y.) for the Alder series suggests the possibility of a boundary province between the 1715 m.y. and 1780 m.y. provinces which is transitional in its rock ages between those two provinces. More precise age determinations on the Alder series and Red Rock rhyolite, as well as geochronological and geological work in the areas to the north and northeast of the Alder series, is needed to confirm this speculation.

Table I

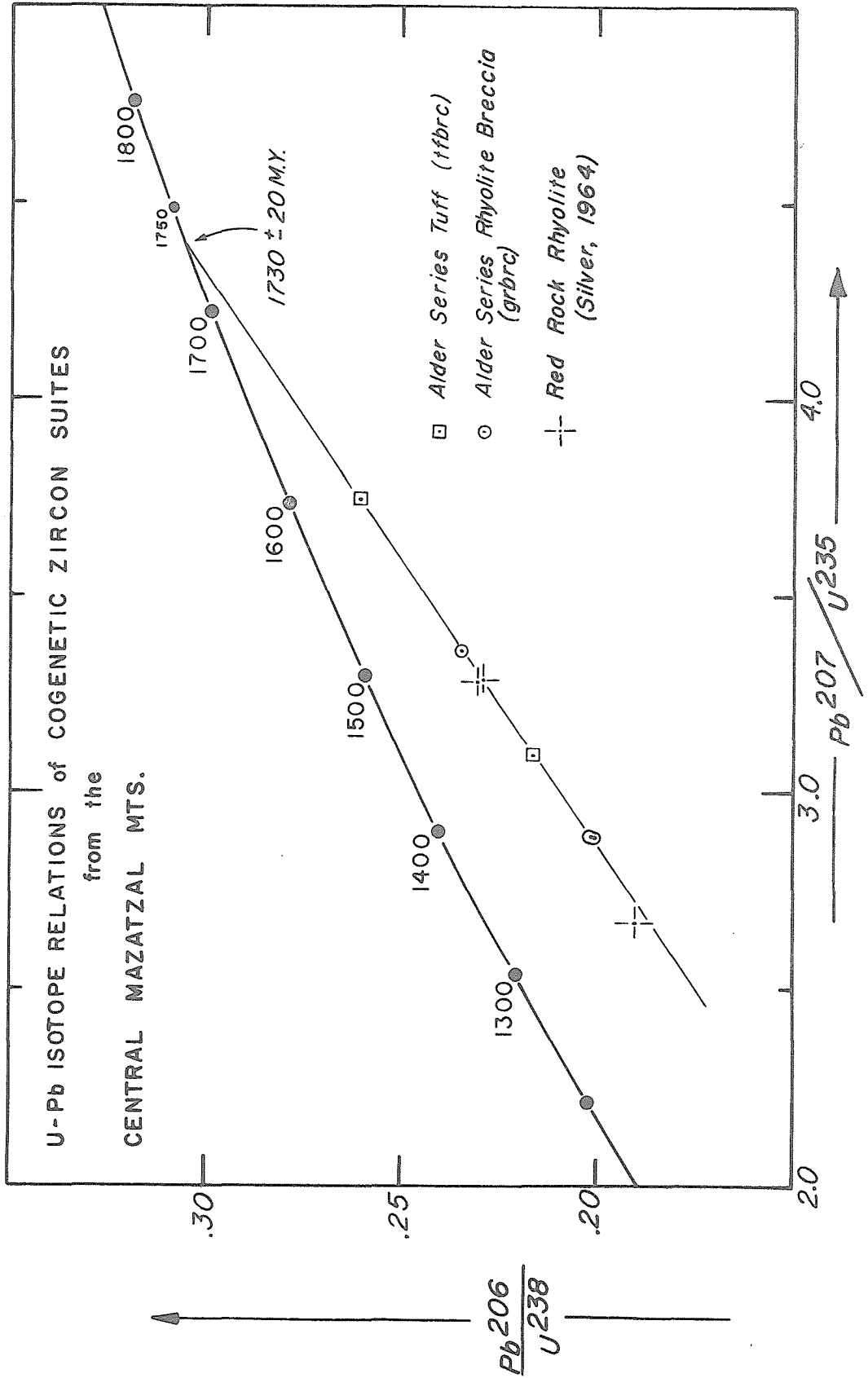
Analyses of Alder Series Zircon Concentrates

ZIRCON FRACTION	Pb Isotope Ratios		U (ppm)	U ²³⁸ μmoles gram	$\frac{207}{206}$ (rad.)	$\frac{206}{238}$ (rad.)	$\frac{207}{235}$ (rad.)
	$\frac{206}{204}$	$\frac{206}{207}$					
<u>gibr</u>							
R200, M0°/20°	325.63	6.8606	4.5381	337	1.4071	.10391	.23485
P200, M2°/25°	382.35	7.1483	4.8930	437	1.8215	.10426	.2010
R200, M3°/20°	304.58	6.7270	4.3580	396	1.6528	.10391	.2018
<u>tfbr</u>							
P200, M2°/25°	301.11	6.7093	4.2107	314	1.3091	.10378	.2167
R+P200, NM2°/20°	276.33	6.5135	-----*	243	1.10117	.10440	.2606

*spiked with Pb²⁰⁸ before attack.

207/206 (radiogenic), Pb²⁰⁶/U²³⁸ (radiogenic), and Pb²⁰⁷/U²³⁵ (radiogenic) calculated using a common lead for correction with 206/204 = 18.50, 207/204 = 15.55, 208/204 = 38.20.

Figure 4



APPENDIX I

Chemical Analyses

Table II

Chemical Analyses of Dacitic and Rhyolitic Rocks
of the Alder Series below the Telephone Canyon Member

	I	II	III	IV
SiO ₂	63.94	67.53	62.47	70.98
TiO ₂	0.56	0.56	0.41	0.49
Al ₂ O ₃	16.19	14.20	15.94	15.92
Fe ₂ O ₃	*	*	3.90	*
FeO	7.71*	6.89*	2.18	4.22
CaO	2.60	3.14	5.54	0.86
MgO	2.22	1.98	2.43	0.19
MnO	n.d.	n.d.	0.05	n.d.
Na ₂ O	5.00	3.99	3.92	4.42
K ₂ O	1.57	1.52	0.74	2.72
H ₂ O(+)	n.d.	n.d.	0.37	n.d.
H ₂ O(-)	n.d.	n.d.	0.37	n.d.
P ₂ O ₅	0.21	0.19	0.17	0.19
CO ₂	n.d.	n.d.	0.06	n.d.
F	n.d.	n.d.	0.02	n.d.
SO ₃	n.d.	n.d.	0.00	n.d.
	100.00	100.00	100.56	99.99

I: Subaqueous lithic-crystal tuff in Cornucopia member, West Fork, Sycamore Creek. (ctf-1)

II: Same as I, but collected about 10' stratigraphically above I. (ctf-2)

III: Volcanic breccia, Cornucopia member, midway between East and West Forks of Sycamore Creek. (23)

IV. Flattened pumice tuff in Oneida member, West Fork Sycamore Creek. (onwtf)

Samples I, II, and IV analyzed by electron microprobe on glasses fused from Li₂B₄O₇-fluxed rock powders, Jay Murray, analyst. Abundances normalized to 100.00.

Sample III analyzed by conventional wet-chemical techniques.

*All Fe calculated as FeO.

n.d.: not determined.

Table III

Chemical Analyses of Red Rock Rhyolite and Related Rocks

	V	VI	VII	VIII	IX
SiO ₂	74.00	85.35	75.95	71.05	74.55
TiO ₂	0.22	0.15	0.23	0.25	0.16
Al ₂ O ₃	12.93	8.24	12.23	14.05	13.84
Fe ₂ O ₃	2.10	0.89	*	4.18	2.37
FeO	0.55	0.44	2.37*	0.67	0.45
CaO	0.64	0.20	0.66	0.39	0.32
MgO	0.03	2.43	0.08	0.09	0.22
MnO	0.03	0.00	n.d.	0.07	0.01
Na ₂ O	3.70	0.31	3.55	4.06	2.48
K ₂ O	5.11	2.92	4.89	4.21	4.36
H ₂ O(+)	0.38	1.21	n.d.	0.99	0.26
H ₂ O(-)	0.28	0.40	n.d.	0.41	0.48
P ₂ O ₅	0.01	0.00	0.03	0.05	0.00
CO ₂	0.14	0.00	n.d.	0.00	0.01
F	0.02	0.04	n.d.	0.12	0.11
SO ₃	0.00	0.00	n.d.	0.00	0.00
	100.14	100.20	99.99	100.59	100.62

V: Red Rock rhyolite welded tuff, Lion Canyon (rr).

VI: Red Rock rhyolite, welded vitric tuff, Mt. Peeley (101).

VII: Massive rhyolite sub-unit, Telephone Canyon member of Alder series, welded tuff, near lower Gold Creek (tcwtf).

VIII: Rhyolite intrusive, feeder to Red Rock rhyolite, Gold Creek (163).

IX: Rhyolite breccia, Telephone Canyon member (dated sample), 4080' fork of Gold Creek (grbrc).

Sample VII analyzed by electron microprobe on glass fused from Li₂B₄O₇-fluxed rock powders, Jay Murray, analyst. Abundances normalized to 100.00

Samples V, VI, VIII, and IX analyzed by conventional wet-chemical techniques.

*All Fe calculated as FeO.

n.d.: not determined.

Table IV

Normative Compositions of Precambrian Rocks of the Central Mazatzal Mountains

	I	II	III	IV	V	VI	VII	VIII	IX
Quartz	20.3	24.0	20.6	30.1	29.9	71.6	32.9	27.3	41.0
Orthoclase	8.6	9.0	4.4	16.1	30.4	17.9	28.6	25.2	26.2
Albite	39.0	33.8	33.2	37.4	31.6	2.7	29.8	34.8	21.3
Anorthite	10.6	14.4	23.7	3.1	3.2	1.0	3.1	1.6	1.6
Diopside	-	-	2.3	-	-	-	-	-	-
Hypersthene	17.3	16.6	14.8	7.4	4.3	2.2	4.1	8.2	5.1
Corundum	2.8	0.7	-	4.6	0.4	4.4	1.1	2.3	0.3
Ilmenite	1.0	1.1	0.8	0.9	0.0	0.1	0.4	0.5	0.0
Apatite	00.5	0.4	0.4	0.4	0.0	0.0	0.1	0.1	0.0

Sample Identification and Location:

- I: (ctf-1) Cornucopia member, subaqueous lithic-crystal tuff. 4630' fork of the West Fork of Sycamore Creek, 4660' elevation.
- II: (ctf-2) Same as I, but about 10' to the south.
- III: (23) Cornucopia member volcanic breccia, near junction of the Horse Camp Seep pack trail and Cornucopia Mine-Oneida Mine pack trail.
- IV: (onwtf) Oneida member flattened pumice tuff. West Fork, Sycamore Creek, 3990' elevation.
- V: (rr) Red Rock rhyolite welded tuff, lower Lion Canyon (collected by L. T. Silver).
- VI: (101) Red Rock rhyolite welded vitric tuff, $\frac{1}{2}$ mile due north from Thicket Springs on Mt. Peeley, 6160' elevation.
- VII: (tcwtf) Massive rhyolite sub-unit of Telephone Canyon member, 3750' fork of Gold Creek, 4150' elevation.
- VIII: (163) Rhyolite intrusive, feeder to Red Rock rhyolite, near fork of Gold Creek at 4080'.
- IX: (grbrc) Telephone Canyon member rhyolite breccia (dated sample), 4080' fork of Gold Creek, 4440' elevation (on Payson 15' quadrangle).

Plot of normative plagioclase (Ab+An), orthoclase (Or), and quartz (Q) of the central Mazatzal Mts.

The area enclosed in dashed lines is the field of young obsidians as compiled by Anderson (1968).

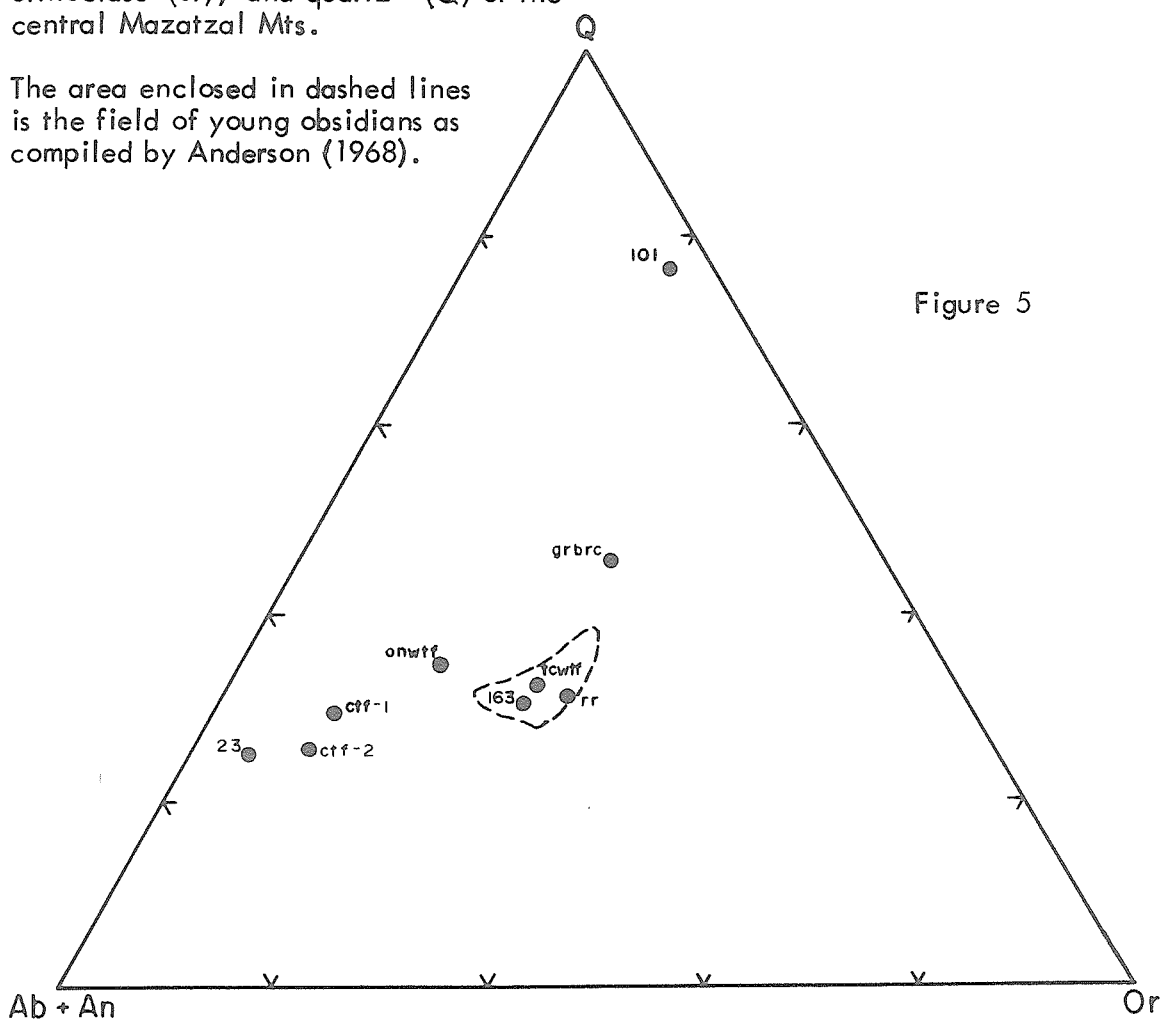


Figure 5

- 101: Red Rock rhyolite (Mt. Peeley mass), vitric tuff
 rr: Red Rock Rhyolite, welded tuff
 rr: Red Rock rhyolite, welded tuff
 163: Gold Creek intrusive (feeder to Red Rock rhyolite)
 tcwtf: Alder series, Telephone Canyon member welded tuff
 grbrc: Alder series, Telephone Canyon member rhyolite breccia
 onwtf: Alder series, Oneida member flattened pumice tuff
 23: Alder series, Cornucopia member volcanic breccia
 ctf-1: Alder series, Cornucopia member subaqueous lithic-crystal tuff
 ctf-2: Alder series, Cornucopia member subaqueous lithic-crystal tuff

AFM plot of Precambrian rocks
of the central Mazatzal Mts.
All Fe calculated as FeO

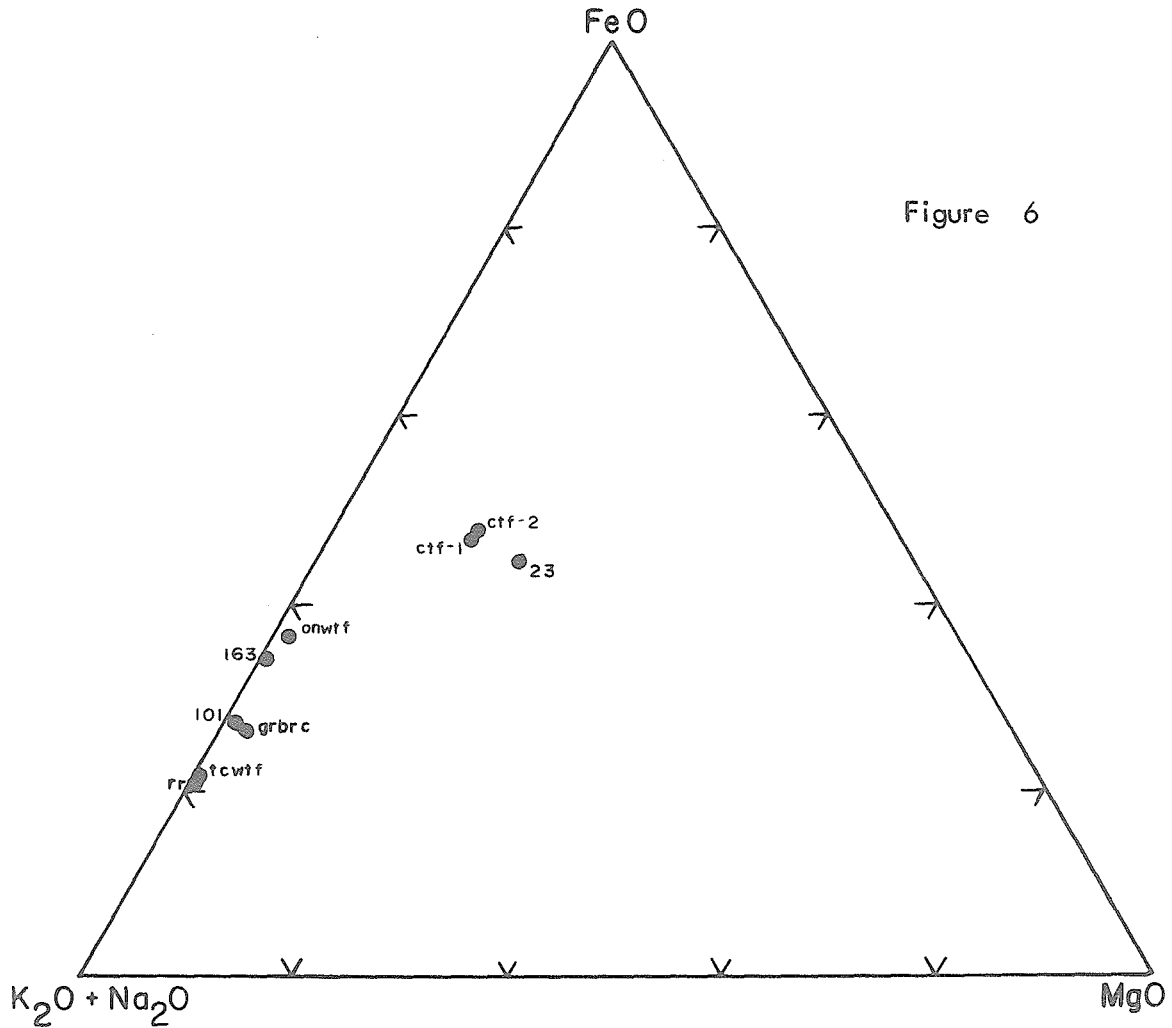


Figure 6

- 101: Red Rock rhyolite (Mt. Peeley mass), vitric tuff
 rr: Red Rock rhyolite, welded tuff
 163: Gold Creek intrusive (feeder to Red Rock rhyolite)
 tcwtf: Alder series, Telephone Canyon member welded tuff
 grbrc: Alder series, Telephone Canyon member rhyolite breccia
 onwtf: Alder series, Oneida member flattened pumice tuff
 23: Alder series, Cornucopia member volcanic breccia
 ctf-1: Alder series, Cornucopia member subaqueous lithic-crystal tuff
 ctf-2: Alder series, Cornucopia member subaqueous lithic-crystal tuff

APPENDIX II

Thin-Section Descriptions of Selected Rocks

Thin-Section Descriptions of Selected Rocks:

<u>Mapped Unit</u>	<u>Lithologic Type</u>
Alder Series: Horse Camp Member	Lithic Wacke

<u>Sample Location</u>	<u>Sample Number</u>
South of Horse Camp Seep	KL7A

<u>Mode (est.)</u>	
<u>Clasts:</u>	(80% of rock)
Lithic fragments	70%
Plagioclase	25%
Carbonate	5%
Quartz	trace
<u>Matrix</u>	(20% of rock)
Quartz + Feldspar	predominant
White Mica	
Opaques	minor
Chlorite	minor
Carbonate	minor

Textures:

Clasts: mostly $\frac{1}{2}$ mm-2 mm, angular, moderately elongate, with major axes subparallel to bedding. The bedding is poorly defined. The plagioclase is mostly only slightly altered, but some of the grains have been extensively altered to carbonate or white mica. The lithic clasts are of three types:

- a) clasts composed almost entirely of amorphous opaque minerals, in some cases displaying .1 mm \times .005 mm plagioclase indicating a volcanic origin. These make up about 30% of the lithic clasts.
- b) clasts composed predominantly of chlorite, or chlorite + carbonate.
- c) clasts composed of fine-grained (<.01 mm) leucocratic minerals - white mica, quartz, feldspar, and minor opaques.

All of these types are thought to be volcanic.

The matrix is fine-grained (less than .05 mm), and difficult to distinguish from the leucocratic lithic clasts.

Thin-Section Descriptions of Selected Rocks:

<u>Mapped Unit</u>	<u>Lithologic Type</u>
Resistant quartzite within Horse Camp Member of Alder Series	Quartzite
<u>Sample Location</u>	<u>Sample Number</u>
Mt. Ord	KL126

Mode (est.)

Quartz (>.1 mm)	80%
Quartz + Feldspar (<.1 mm)	8%
White Mica	8%
Opaque Minerals	4%

Textures

The rock is composed 80% of 2-4 mm quartz clasts, mostly sub-angular, elongate (length:width about 2), and with long axes aligned. All of the grains are highly strained, and show an irregular domained structure, evidently caused by accommodation to the stresses of the shearing. The quartz grains are typically ragged-edged due to recrystallization to fine-grained sericite (and fine-grained quartz?). The clasts are moderately to poorly sorted.

The matrix material is fine-grained (.01-.05 mm) and recrystallized. The quartz and feldspar in the matrix occurs as anhedral, interlocking grains, the white mica both as disseminated flakes and crudely oriented elongate aggregates. The opaque minerals are present as veinlets and irregular, anhedral patches. Most of the opaques are evidently hematite.

Thin-Section Descriptions of Selected Rocks:

<u>Mapped Unit</u>	<u>Lithologic Type</u>
Cornucopia Member of Alder Series	Greenstone (Meta-andesite or dacite)
<u>Sample Location</u>	<u>Sample Number</u>
West Fork Sycamore Creek	KL20

Mode (est.)

Chlorite	35%
Hornblende	5%
Tremolite	trace-1%
Zoisite	5%
Quartz	2%
Carbonate	1%
Apatite	trace
Epidote (>.01 mm)	20%
" (<.01 mm)	20%
Opaque minerals	10%

Textures

Chlorite - occurs as fine-grained aggregates and as 1-3 mm plates, mostly after hornblende.

Hornblende - occurs as small (0.2 mm-0.5 mm) anhedral to subhedral grains, altered partially to chlorite. The mineral is pleochroic in pale brown and green, $2V=90^\circ$.

Tremolite - occurs as clear needles, especially with quartz, about .01 mm \times 2 mm.

Quartz - occurs as veinlet-fillings with carbonate, and as anhedral, interstitial 0.2 mm-0.5 mm grains.

Carbonate - occurs as veinlet fillings with quartz, and as rare subhedral grains of about 1 mm.

Epidote - occurs as .1-.5 mm anhedral grains, and as larger (to 2 mm) skeletal grains and aggregates with chlorite, after hornblende(?). Also, as very fine-grained aggregates, in lath-shaped forms, about .2 mm \times 1 mm, after plagioclase(?).

Zoisite - occurs as 0.1 mm-0.5 mm anhedral grains.

Opaque minerals - occur as discrete, anhedral $\frac{1}{2}$ mm grains, and as fine-grained aggregates, pseudomorphous after clinopyroxene(?) or hornblende(?).

The rock is unfoliated.

Thin-Section Descriptions of Selected Rocks:

<u>Mapped Unit</u>	<u>Lithologic Type</u>
Cornucopia Member of Alder Series	Meta-basalt
<u>Sample Location</u>	<u>Sample Number</u>
East Fork, Sycamore Creek	KL90

Mode (est.)

Carbonate	35%
White Mica	30%
Epidote	20%
Chlorite	15%
Opaque Minerals	2%
Quartz	trace

Textures

The rock is unfoliated, however there is a crude alignment of the long axes of some of the relict phenocrysts and vesicles.

The relict vesicles (or amygdules) are about 1 mm in size, irregularly shaped, and filled with carbonate and chlorite. They make up about 2-5% of the rock. Relict phenocrysts are quite abundant (about 25% mode) and are pseudomorphous after eu-subhedral olivine and pyroxene of 1-2 mm size. None of the primary minerals remain, having been replaced by chlorite and carbonate.

The groundmass consists largely of pseudomorphs of white mica after randomly oriented 0.1 mm × 1 mm to 0.05 mm × ½ mm plagioclase lathes. Epidote is disseminated throughout the groundmass as .05 mm grains, as are opaques. Quartz is present as very rare, small interstitial grains in the groundmass, and is probably secondary.

Thin-Section Descriptions of Selected Rocks:

<u>Mapped Unit</u>	<u>Lithologic Type</u>
Cornucopia Member, Alder Series	Subaqueous Crystal-Lithic Tuff

<u>Sample Location</u>	<u>Sample Number</u>
4540' fork of West Fork, Sycamore Creek	KL21

Mode (est.)

Lithic fragments	50%
Plagioclase (>.2 mm)	25%
Quartz (>.2 mm)	1%
Quartz + Feldspar (<.2 mm)	5%
Carbonate	1%
Opagues	3%
Chlorite (not in lithic clasts)	3%
Epidote (not in lithic clasts)	0-5%
White Mica (not in lithic clasts)	10%

Textures

The lithic fragments are mostly very fine-grained (.01 mm), and consist predominantly of quartz + feldspar and white mica with accessory epidote(?) and opaque minerals. These clasts are generally elongate, and show a strong preferred orientation. Some of them are deformed or penetrated by other lithic clasts or crystals in the rock, while others are extremely flattened (length:width greater than 20), implying deformation of these clasts contemporaneous or penecontemporaneous with accumulation. It is difficult to distinguish the boundaries of many of the lithic clasts.

Plagioclase phenocrysts are anhedral to subhedral, 0.2 mm-2 mm, albitic, unzoned, and partially to extensively sericitized.

Quartz phenocrysts are $\frac{1}{2}$ -1 mm, an-subhedral, many broken, most rounded and embayed.

Carbonate occurs as colorless, subhedral to anhedral $\frac{1}{2}$ mm grains, and also as anhedral, 1-4 mm grains with pleochroism in light tan and brown, evidently caused by abundant, very fine-grained, oriented inclusions.

Opaque minerals are brownish, amorphous clots and stringers, and also as .05 mm-.15 mm rhombs (after carbonate?). The distribution of the opagues crosscuts primary textural elements.

Chlorite occurs as fine-grained aggregates in matrix material, as stringers and anhedral plates throughout the thin-section, and as .1 mm blebs in shard-rich (?) areas.

Cornucopia Member, Alder Series (continued)

Textures

White mica (sericite) is present as fine-grained, disseminated and aggregated material throughout the thin-section, but especially in lithic clasts and plagioclase grains.

The matrix material is very fine to fine-grained, and in many areas contains abundant, .05 mm-.1 mm arcuate and forked textures which appear to be relict shards. These relict shards are composed of interlocking quartz + feldspar in a chlorite-rich matrix.

The actual proportion of clasts and phenocrysts to matrix is difficult to estimate, as the boundaries of the lithic-clasts are poorly definable, but appears to be greater than ten.

Thin-Section Descriptions of Selected Rocks:

<u>Mapped Unit</u>	<u>Lithologic Type</u>
Alder Series: Cornucopia	Subaqueous Lithic-Crystal Tuff
<u>Sample Location</u> Member	<u>Sample Number</u>
Gold Creek	KL243A
<u>Mode (est.)</u>	
Quartz (>.05 mm)	3%
Plagioclase (>.05 mm)	1%
Quartz + Feldspar (<.05 mm)	20%
White Mica	50%
Opaque Minerals	10%
Chlorite	15%
Spinel	1%
Carbonate	tr.
Apatite	tr.

Textures

Most of the rock is composed of volcanic lithic fragments. These clasts are angular, many elongate, and 1-4 mm in size. They consist of a fine-grained (.01-.05 mm) assemblage of white mica flakes, opaque minerals, and quartz + feldspar. The long axes of the lithic clasts are aligned, and together with the orientation of chlorite aggregates give the rock a definite fabric.

Between 10% and 25% of the rock is complete sericitized, sub-euhedral feldspar of 1-3 mm size (counted as white mica in the modal abundances). A few unaltered plagioclase grains -- euhedral to sub-hedral, $\frac{1}{2}$ -3 mm remain, possibly due to a relatively sodic composition compared to the sericitized plagioclase.

Quartz phenocrysts occur as $\frac{1}{2}$ -3 mm subhedral, rounded or embayed grains. Both the plagioclase and quartz phenocrysts occur as separate grains or clasts, not within larger lithic fragments. Opaques occur both as very fine (less than .05 mm) disseminated grains and as anhedral grains up to 3 mm in size. Brown spinel occurs as anhedral, irregular-shaped grains of $\frac{1}{2}$ -2 mm size.

The size-sorting of the phenocrysts and the lithic clasts is good. No clearly identifiable matrix material is discernible.

Thin-Section Descriptions of Selected Rocks:

<u>Mapped Unit</u>	<u>Lithologic Type</u>
Cornucopia Member of Alder Series	Dacitic Breccia
<u>Sample Location</u>	<u>Sample Number</u>
Midway between the East and West Forks of Sycamore Creek	23
<u>Mode (est.)</u>	
Plagioclase (1 mm)	25%
Plagioclase (<1 mm, >.1 mm)	10%
Epidote	15%
Opaque Minerals	5%
Chlorite	5%
Quartz + Feldspar (<.1 mm)	20%
White Mica	20%
Apatite	trace

Textures

The area of the thin-section is a microbreccia, consisting of 1-10 mm textural domains, each a plagioclase porphyry, but varying in phenocrysts size distribution, abundance, and in preservation of matrix texture. The clasts are subangular and roughly equant. The groundmass consists of interlocking quartz and feldspar (less than .05 mm grain-size), altered to a varying degree to chlorite, epidote, and white mica. The matrix of the clasts is of essentially the same mineralogy as the clasts, and is similar texturally. Therefore, it is difficult to distinguish between the breccia clasts and matrix; the ratio of clasts to matrix, however, appears to be on the order of one.

Plagioclase occurs as subhedral to euhedral, 0.1-5 mm, twinned grains, many of which are rounded or broken. Most of the plagioclase grains are fresh-looking.

Epidote occurs in .05 mm-.1 mm anhedral aggregated and disseminated grains replacing groundmass material. More rarely, epidote is present in pseudomorphous aggregates after pyroxene(?) or hornblende(?).

Chlorite occurs in fine-grained aggregates replacing groundmass material, and also as pseudomorphs after subhedral hornblende(?).

White mica occurs as fine-grained, disseminated flakes replacing groundmass.

Thin-Section Descriptions of Selected Rocks:

<u>Mapped Unit</u>	<u>Lithologic Type</u>
Cornucopia Member of Alder Series	Volcanic Breccia Clast
<u>Sample Location</u>	<u>Sample Number</u>
Thicket Springs-McFarland Canyon Trail	KL-77
<u>Mode (est.)</u>	
Plagioclase (>.1 mm)	15%
Quartz (>.1 mm)	5%
Carbonate	10%
Epidote	3%
Quartz + Feldspar (<.1 mm)	35%
Chlorite	trace
Apatite	trace
White Mica	30%
Opaque Minerals	2%

Textures

The rock is a plagioclase-quartz porphyry with no stratification or foliation, and is probably a clast derived from an intrusive rock. The groundmass is very fine-grained, interlocking quartz + feldspar, partially altered to sericite flakes, opaques, chlorite and epidote.

Plagioclase phenocrysts are $\frac{1}{2}$ -4 mm, unoriented subhedral, sub-equant grains. They are mostly twinned, unzoned albite; some grains show possible relict zoning, however (zoned alteration to epidote, chlorite and carbonate). The plagioclase phenocrysts are slightly to moderately altered to very fine-grained material, and to epidote, sericite, and carbonate.

Quartz phenocrysts are $\frac{1}{2}$ -5 mm anhedral to subhedral, generally rounded and embayed, and in some cases (as also with the plagioclase) broken and brecciated with carbonate filling fractures.

Carbonate occurs also as irregularly-shaped aggregates replacing groundmass material.

Thin-Section Descriptions of Selected Rocks:

<u>Mapped Unit</u>	<u>Lithologic Type</u>
East Fork Member of Alder Series	Tuffaceous Siltstone

<u>Sample Location</u>	<u>Sample Number</u>
East Fork, Sycamore Creek	KL68

Mode (est.)

Opaque Minerals	60%
White Mica	30%
Quartz + Feldspar	10%

Textures

The rock is distinctly bedded, with .1-1 mm beds or laminations defined by grain size and by abundance of opaque minerals. The coarse laminae contain abundant (more than 50% by volume) relict shards, about $\frac{1}{2}$ mm in size, now composed of sericite. A well-defined crinkle structure is oblique to the bedding (nearly perpendicular), with spacings of crinkles of about $\frac{1}{2}$ mm.

The opaque minerals are amorphous black and brown patches, stringers, and disseminated .01-.05 mm grains.

White mica (sericite) is present as fine-grained aggregates and disseminated grains.

Quartz and feldspar occur as predominantly .01 mm grains, and also as sparse, angular .1 mm chips (mostly quartz).

Thin-Section Descriptions of Selected Rocks:

<u>Mapped Unit</u>	<u>Lithologic Type</u>
Alder Series; Thicket Springs Tuff Sub-member of East Fork Member	Vitric Tuff
<u>Sample Location</u>	<u>Sample Number</u>
Mt. Peeley, near Thicket Springs	KL32A
<u>Mode (est.)</u>	
Plagioclase (>0.1 mm)	2%
Quartz (>0.1 mm)	½%
Quartz + Feldspar (<0.1 mm)	30%
White Mica	50%
Opaque Minerals	15%

Textures

Most of the thin-section consists of fine-grained interlocking quartz + feldspar and white mica (sericite). Abundant relict shards of .05 mm-.2 mm size, now consisting of interlocking quartz + feldspar, are disseminated throughout the section. Elongation of opaque mineral patches, together with slight preferred orientation of the elongate feldspar grains defines a faint stratification. (In hand specimen, no bedding or foliation is discernible). The white mica distribution does not define a foliation.

Plagioclase occurs as anhedral, angular chips, 0.1-0.2 mm in size, fresh-looking.

Quartz occurs similar to the plagioclase.

White mica is present as fine-grained, disseminated flakes, replacing groundmass.

Opaque minerals are black and brown, anhedral, .01-.1 mm in size.

Thin-Section Descriptions of Selected Rocks:

<u>Mapped Unit</u>	<u>Lithologic Type</u>
Oneida Member	Vitric Tuff
<u>Sample Location</u>	<u>Sample Number</u>
Slate Creek	KL173
<u>Mode (est.)</u>	
Quartz + Feldspar	75%
Sericite	10%
Chlorite	5%
Opakes	10%

Textures

Fine-grained (.01-.05 mm), interlocking quartz + feldspar partially altered to oriented flakes and braids of sericite. In plain light, abundant, faintly discernible shards are distinguishable, and defined by a relative absence of sericite and a slightly coarser grain size of the quartz + feldspar. The size of the shards is .1-.3 mm. The chlorite is present as thin (.01-.2 mm), oriented stringers, and the opaque minerals as .1-1 mm, anhedral grains, red-brown on thin edges.

Thin-Section Descriptions of Selected Rocks:

<u>Mapped Unit</u>	<u>Lithologic Type</u>
Alder Series: Oneida Member	Welded Tuff

<u>Sample Location</u>	<u>Sample Number</u>
East Fork, Sycamore Creek	KL242

Mode (est.)

Quartz (>.05 mm)	20%
Quartz + Feldspar (<.05 mm)	40%
White Mica	20%
Opaques	15%
Carbonate	3%
Plagioclase (>.05 mm)	2%
Zircon	trace

Textures

Quartz phenocrysts are 1-2 mm (some up to 5 mm), subanhedral. They are rounded, strained, and many have been broken. The opaque minerals occur in disseminated grains (.01-1 mm, anhedral) and aggregates. Carbonate is present as euhedral rhombs, altering to a brownish amorphous material (Fe-oxides?). White mica (sericite) occurs as aligned braids and flakes, with optical continuity for as long as 1 cm. Plagioclase phenocrysts are present as (mostly) untwinned, some slightly antiperthitic, anhedral grains. They are slightly sericitized, and $\frac{1}{2}$ -1 mm in size.

The long axes of quartz phenocrysts tend to be aligned, and some show evidence of tensional fracturing concordant with the elongation.

Slight differences in relative mineral abundances in areal domains of the section suggest that the rock was originally composed of rhyolitic lithic clasts, with dimensions of from 1 × 5 mm to more than 3 × 12 mm.

Thin-Section Descriptions of Selected Rocks:

<u>Mapped Unit</u>	<u>Lithologic Type</u>
Telephone Canyon Member, Alder Series	Quartz-Lithic Wacke
<u>Sample Location</u>	<u>Sample Number</u>
Near Gold Creek, on road, 4160' elevation	KL183
<u>Mode (est.)</u>	
Quartz (>.1 mm)	20%
Quartz + Feldspar (<.1 mm)	5%
Plagioclase (>.1 mm)	trace
Opaques (>.1 mm)	10%
Opaques (<.1 mm)	10%
Carbonate	10%
Chlorite	20%
Epidote	5%
Sericite	15%
Apatite	trace

Textures

The larger quartz grains are $\frac{1}{2}$ -4 mm poorly sorted, angular to sub-rounded, and generally subequant in cross-section. Some of the quartz clasts are virtually unstrained, and others display multiple, interlocking domains of different optical orientation. Many appear to be whole or broken rounded, subhedral phenocrysts.

The single large plagioclase grain present in the section is 2 × 6 mm, twinned, subhedral, and partially altered to sericite + epidote. This grain may be part of a larger lithic fragment.

The larger opaque grains are generally equant, $\frac{1}{2}$ -1 mm, subhedral to anhedral. Carbonate is present as disseminated grains (up to 3 mm in size) and grain aggregates. Epidote and chlorite occur predominantly as small grains and flakes, both disseminated and aggregated. Sericite occurs as disseminated flakes and in aggregates, but not in braids or stringers.

Lithic fragments occur in the rock as $\frac{1}{2}$ -2 mm angular clasts, composed of fine-grained (<.05 mm), interlocking quartz + feldspar, and has a total abundance of about 3%.

The clast:matrix ratio of the rock is about 2:3 (fine-grained matrix).

Thin-Section Descriptions of Selected Rocks:

<u>Mapped Unit</u>	<u>Lithologic Type</u>
Alder Series; Telephone Canyon Member	Rhyolite Breccia
<u>Sample Location</u>	<u>Sample Number</u>
3760' fork, Gold Creek	KL233

Mode (est.)

Quartz (>.05 mm)	10%
K-Feldspar (>.05 mm)	5%
Quartz + Feldspar (<.05 mm)	65%
Opaque Minerals	2%
Zircon	trace
White Mica	15%

Textures

The thin-section shows that the rock is composed of identical-appearing, angular lithic fragments ranging in size from less than 1 mm to more than a centimeter. The clasts are rhyolitic, consisting of .01-.05 mm interlocking quartz + feldspar with quartz and feldspar phenocrysts. Some of the clasts display microspherulitic texture. The matrix material is similar in composition and texture to the clasts, but is generally more sericitized. The total abundance of matrix is difficult to determine, but apparently lies between 5% and 30%.

The quartz phenocrysts are mostly $\frac{1}{2}$ -2 mm, subhedral to anhedral, rounded and embayed. The K-feldspar phenocrysts are .1-5 mm, crudely twinned, some perthitic, sub-anhedral, and fairly fresh. The white mica (sericite) occurs as crudely oriented (aligned) flakes and aggregates. The opaque minerals (reddish and black) are subhedral to anhedral, .01-.5 mm.

Thin-Section Descriptions of Selected Rocks:

<u>Mapped Unit</u>	<u>Lithologic Type</u>
Telephone Canyon Member; Alder Series	Welded Vitric Tuff
<u>Sample Location</u>	<u>Sample Number</u>
4080' Fork of Gold Creek	KL231

Mode (est.)

Quartz ($>\frac{1}{2}$ mm)	2%
Plagioclase ($>\frac{1}{2}$ mm)	1%
Quartz + Feldspar ($<\frac{1}{2}$ mm)	45%
White Mica	50%
Opagues	3%
Zircon	trace

Textures

The quartz phenocrysts are subhedral (many intricately corroded and embayed), and range from $\frac{1}{2}$ mm to 5 mm. Plagioclase phenocrysts occur as sparse, twinned, anhedral sericitized grains, $\frac{1}{2}$ -2 mm. Opaque minerals occur as .05-5 mm, black to brownish amorphous aggregates or stringers, and anhedral $\frac{1}{2}$ mm grains.

Flattened relict shards are abundant, of .1 mm-1 mm size. The relict shards consist of interlocking, .01 mm quartz + feldspar, are relatively free from sericitization, and constitute about 40% of the rock.

The rock has a distinct foliation, defined by braids and stringers of white mica (sericite). The orientation of the deformed and flattened shards is concordant with the direction of foliation.

Thin-Section Descriptions of Selected Rocks:Mapped Unit

Red Rock Rhyolite

Lithologic Type

Welded Vitric Tuff

Sample Location

Mt. Peeley

Sample Number

KL65

Mode (est.)

Quartz (phenocrysts)	2%
K-Feldspar (phenocrysts)	trace
Plagioclase (phenocrysts)	trace
White Mica	20%
Opaque Minerals	1%
Quartz + Feldspar (<.1 mm)	75%

Textures

In plain light, abundant .2-2 mm compressed shards are readily discernible (now consisting of fine-grained, interlocking quartz-feldspar). The shards are locally oriented, but vary in orientation over a centimeter distance, possibly reflecting a turbulent flowage. These shards make up about 60% of the slide. No foliation is present.

Quartz phenocrysts are 1-2 mm, subhedral, rounded and embayed.

K-feldspar phenocrysts are mostly altered to sericite, and are about 1 mm, sub-anhedral.

Opaque minerals are amorphous, brownish patches of about .1 mm size.

White mica (sericite) is very fine-grained, and occurs as disseminated grains and as aggregates.

The groundmass material is predominantly .01 mm-.05 mm interlocking quartz + feldspar.

Plagioclase phenocrysts are highly altered to sericite or clays, and are subhedral to anhedral, about 1 mm in size.

Thin-Section Descriptions of Selected Rocks:

<u>Mapped Unit</u>	<u>Lithologic Type</u>
Red Rock Rhyolite	Rhyolitic Flow

<u>Sample Location</u>	<u>Sample Number</u>
Mercurio Creek	KL109

Mode (est.)

Quartz ($>\frac{1}{2}$ mm)	5%
Quartz + Feldspar ($<\frac{1}{2}$ mm)	70%
Opaque Minerals ($>.1$ mm)	3%
Opaque Minerals ($<.1$ mm)	2%
Plagioclase ($>\frac{1}{2}$ mm)	trace-1%
K-Feldspar ($>\frac{1}{2}$ mm)	trace
White Mica	20%
Zircon	trace

Textures

A turbulent, contorted structure is defined by vein-like coarser-grained textural elements in the rock, evidently the result of flow contemporaneous with accumulation. Large (10 mm) areas with patchy, very fine-grained, radial quartz and feldspar aggregates are present, and tend to be bounded by 1 mm wide 'walls' of fibrous quartz + feldspar, with the long axes of the fibers aligned perpendicular to the length of the 'wall'.

Quartz phenocrysts are sub-euhedral, and generally rounded and intricately corroded. Some grains have ragged edges to incipient recrystallization (to sericite).

Plagioclase phenocrysts (2V less than 80° , +) are generally untwinned, partially sericitized, corroded, subhedral to anhedral and $\frac{1}{2}$ -1 mm in size.

K-feldspar phenocrysts are $\frac{1}{2}$ -1 mm, untwinned or very crudely twinned, 2V about 50° , subhedral.

Opaque minerals are mostly about 1 mm, and are dominantly pyrite. Disseminated opaque dust is also present, especially in sericitized areas of fine radial aggregates of quartz and feldspar, giving these areas a reddish appearance.

Thin-Section Descriptions of Selected Rocks:

<u>Mapped Unit</u>	<u>Lithologic Type</u>
Foliated Rhyodacitic Intrusive (Red Rock Rhyolite Feeder)	Rhyolite Intrusive
<u>Sample Location</u>	<u>Sample Number</u>
Gold Creek	KL163
<u>Mode (est.)</u>	
Quartz (>.1 mm)	3%
Plagioclase (>.1 mm)	45%
Quartz + Feldspar (<.1 mm)	15%
Opaque Minerals	10%
White Mica	25%

Textures

Quartz occurs as anhedral, $\frac{1}{2}$ mm grains, as fine-grained aggregates with feldspar, and in micrographic and feathery intergrowths with feldspar.

The plagioclase occurs as subhedral to anhedral, 2-4 mm grains, some of which are zoned. The plagioclase grains are partially sericitized, albitic(?), and sparsely twinned.

Opaque minerals are black, about $\frac{1}{2}$ mm, euhedral to subhedral (rhombs common).

Fine-grained quartz + feldspar is abundant, with micrographic, mrymekitic, and feathery - radial aggregates common.

White mica occurs as disseminated flakes and aggregates, crudely aligned to give the rock a faint fabric.

Thin-Section Descriptions of Selected Rocks:

<u>Mapped Unit</u>	<u>Lithologic Type</u>
Mt. Ord Andesite	Dacitic(?) Intrusive

<u>Sample Location</u>	<u>Sample Number</u>
6150' on Mt. Ord Road	KL176

Mode (est.)

Quartz (>.1 mm)	10%
Epidote	30%
Chlorite	20%
Opaque Minerals	15%
Quartz + Feldspar (<.1 mm)	5%
White Mica	20%

Textures

Irregular-shaped quartz and chlorite-filled pods are abundant, with sizes from $\frac{1}{2}$ mm to 5 mm. These pods are evidently relict amygdules, and typically have a quartz lining and chlorite core, elongate and aligned.

The rock is not distinctly foliated, but does have a weak alignment of white mica (sericite), epidote, and chlorite, in directions both parallel and perpendicular to the preferred orientation of the relict amygdules. No phenocrysts are present.

Epidote occurs in small (.1 mm-.01 mm) grains and grain aggregates, the opaque minerals (brown and black in color) as subhedral to anhedral .01 mm-.5 mm discrete grains, and as braids and stringers intermixed with chlorite. White mica is present in grain aggregates and as disseminated flakes.

Thin-Section Descriptions of Selected Rocks:

<u>Mapped Unit</u>	<u>Lithologic Type</u>
Andesitic-Dacitic Intrusive Sheets	Dacitic Intrusive

<u>Sample Location</u>	<u>Sample Number</u>
Near Horse Camp Seep	KL61

Mode (est.)

Clinopyroxene (colorless, +2V=45°)	15%
Plagioclase	15%
Quartz	10%
Chlorite	30%
Epidote(?)	20%
Opaque Minerals	5%
White Mica	5%

Textures

Clinopyroxene occurs as 1-5 mm subhedral grains, some twinned, many partially chloritized. Some grains also show rounding or embayment.

Plagioclase is present as subhedral 2-5 mm lathes, distinctly zoned (oligoclase), largely altered to sericite and a very fine-grained, high-relief mineral (epidote?). The grains of plagioclase are randomly oriented. Some skeletal crystals, now almost entirely chlorite, sericite, and epidote(?), are present with sizes to 10 mm.

Quartz occurs as anhedral, 1-4 mm ragged-edged grains with pronounced strained extinction.

Chlorite (very pale green) occurs as fine-grained aggregates throughout the thin-section.

White mica (sericite) is present in fine-grained aggregates, especially in plagioclase.

Opaque minerals occur also as fine-grained aggregates, especially with plagioclase.

The rock is unfoliated.

Thin-Section Descriptions of Selected Rocks:

<u>Mapped Unit</u>	<u>Lithologic Type</u>
Mt. Ord Andesite	Meta-dacite or andesite

<u>Sample Location</u>	<u>Sample Number</u>
Mt. Ord Road, 6600' elevation	Ord Mt. Pyrox. #2

<u>Mode (est.)</u>		
Plagioclase (albite) (>½ mm)		10%
	(<½ mm)	20%
Clinopyroxene		1%
Opaque Minerals		10%
Chlorite		10%
Epidote (>.05 mm)		10%
Quartz (secondary)		5%
Very fine-grained groundmass (mostly epidote?)		30%
Olivine		2%
Hornblende		2%

Textures

Plagioclase - occurs as 1-3 mm subhedral to euhedral twinned phenocrysts, and as .01 mm × 1 mm randomly oriented laths. The phenocrysts are unzoned albite (about An₅₋₁₂), and contain a variable amount of fine epidote aggregates and needles of rutile(?) or actinolite(?) as inclusions.

Olivine - as 2-3 mm subhedral to anhedral phenocrysts, apparently partially altered, in patches, to pale green amphibole, and either intergrown with or reacted to clinopyroxene. 2V of the olivine is about (-) 80°. The olivine also occurs (with opaques) as anhedral aggregates of ovoid shape.

Epidote - occurs as inclusions in plagioclase, as vesicle fillings, and probably as the matrix material for the plagioclase laths.

Quartz - occurs both as fine and coarse radiating aggregates in vesicles, and as grains, in vesicles, of up to 1 mm.

Opaque minerals - occur as .01 mm disseminated grains, and as high-reflectivity, brownish amorphous aggregates in vesicles.

Rock Textures: The rock is unfoliated, and contains abundant (about 15% of the volume) 'vesicles', which are both ovoid and irregular and elongate in shape, about 2-8 mm, and contain opaques, chlorite, olivine, quartz, and epidote as fillings.

BIBLIOGRAPHY

Part I

- Anderson, C. A. (1951) Older Precambrian Structure in Arizona, Geol. Soc. Amer. Bull. 62, 1331-1346.
- Anderson, C. A. (1968) Metamorphosed Precambrian Silicic Volcanic Rocks in Central Arizona, Geol. Soc. Amer. Mem. 116, 9-44.
- Anderson, C. A., Blacet, P. M., Silver, L. T., and Stern, T. W. (1971) Revision of Precambrian Stratigraphy in the Prescott-Jerome Area, Yavapai County, Arizona, U.S. Geol. Surv. Bull. 1324-C.
- Bailey, E. H., Irwin, W. P. and Jones, A. L (1964) Franciscan and Related Rocks, and Their Significance in the Geology of Western California , Calif. Div. Mines & Geol. Bull., 183.
- Blacet, P. M., Silver, L. T., Stern, T. W., Anderson, C. A. (1971) Precambrian Evolution of the Big Bug Group (Yavapai Series) and Associated Rocks in the Western Bradshaw Mountains, Central Arizona, Geol. Soc. Amer., Cordilleran Section Meeting, Abstracts with Programs, 84.
- Carlisle, D. (1961) Pillow Breccias and Their Aquagene Tuffs, Quadra Island, British Columbia, Jour. Geol. 71, 48-71.
- Conway, C. M. (1973) Structure and Evolution of a Precambrian Rhyolite Volcanic Complex, Gila County, Arizona, Geol. Soc. Amer., Cordilleran Section Meeting, Abstracts with Programs, 75.
- Cooper, J. R. and Silver, L. T. (1954) Older Precambrian Rocks of the Dagoon Quadrangle, Cochise County, Arizona, Geol. Soc. Amer. Bull. 65, 1242.

- Cooper, J. R. and Silver, L. T. (1964) Geology and Ore Deposits of the Dragoon Quadrangle, Cochise County, Arizona, U.S. Geol. Surv. Prof. Pap. 416, 146 pp.
- Darton, N. H. (1925) A Resume of Arizona Geology, Bull. Ariz. Bur. Mines 119.
- Fiske, R. S. and Matsuda, T. (1964) Submarine Equivalentents of Ash-Flows in the Tokiwa Formation, Japan, Amer. Jour. Sci. 262, 76-106.
- Fiske, R. S. (1969) Recognition and Significance of Pumice in Marine Pyroclastic Rocks, Geol. Soc. Amer. Bull. 80, 1-8.
- Gastil, G. (1958) Older Precambrian Rocks of the Diamond Butte Quadrangle, Gila County, Arizona, Geol. Soc. Amer. Bull. 69, 1495-1514.
- Gastil, G. (1962) A Working Hypothesis for Arizona's Older Precambrian History, New Mexico Geol. Soc. 13th Field Conference; Guidebook of the Mogollon Rim Region, 52-54.
- Hinds, N. E. A. (1936) Ep-Archaeon and Ep-Algonkian Intervals in Western North America, Carnegie Inst. Wash. Publ. 463, 1-52.
- Hinds, N. E. A. (1938) Precambrian Arizonan Revolution in Western North America, Amer. Jour. Sci. 35, 445-449.
- Jaggar, T. A. and Palache, C. (1905) Description of Bradshaw Mountains Quadrangle, Arizona Jour. Geol. 38, 174-183.
- Kay, M. (1951) North American Geosynclines, Geol. Soc. Amer. Mem. 48.
- Lausen, C. (1926) Tourmaline-Bearing Cinnabar Veins of the Mazatzal Mountains, Arizona, Econ. Geol. 21, 782-791.
- Lausen, C. and Gardner, E. D. (1927) Quicksilver Deposits of Arizona, Ariz. Bur. Mines Bull. 122, 60-105.

- Lindgren, Waldemar (1926) Ore Deposits of the Jerome and Bradshaw Quadrangles, Arizona, U.S. Geol. Surv. Bull. 782, 192 pp.
- Livingston, D. E. (1962) Older Precambrian Rocks near The Salt River, Central Gila County, Arizona, New Mex. Geol. Soc., 13th Field Conference; Guidebook of the Mogollon Rim Region, 55.
- Livingston, D. E. and Damon, P. E. (1967) The Ages of Stratified Precambrian Rock Sequences in Arizona, Geochronology of Precambrian Stratified Rocks, University of Alberta, 67.
- Livingston, D. E. and Damon, P. E. (1968), The Ages of Stratified Precambrian Rock Sequences in Central Arizona and Northern Sonora, Can. Jour. Earth Sci. 5, 763-772.
- Nockholds, S. R. (1954) Average Chemical Compositions of Some Igneous Rocks, Geol. Soc. Amer. Bull. 65, 1007-1032.
- Pettijohn, F. J. (1957) Sedimentary Rocks, second edition, Harper & Bros., New York, 718 pp.
- Rankin, D. W. (1960) Paleogeographic Implications of Hot Ash-Flows, Internat. Geol. Cong., Rpt. of 21st Session, Norden, pt. XII, 19-34.
- Ransome, F. L. (1903) Geology of the Globe Copper District, Arizona, U.S. Geol. Survey Prof. Paper 21, 168 pp.
- Ransome, F. L. (1915) Quicksilver Deposits of the Mazatzal Range, Arizona, U.S. Geol. Surv. Bull. 620-f, 111-128.
- Ransome, F. L. (1916) Some Paleozoic Sections in Arizona and their Correlations, U.S. Geol. Surv. Prof. Paper 98K, 157-158.

- Ross, C. S. and Smith, R. L. (1961) Ash-Flow Tuffs; Their Origin, Geologic Relations and Identification, U.S. Geol. Surv. Prof. Paper 366, 81 pp.
- Schminke, H. U. and Swanson, D. A. (1967) Laminar Viscous Flowage Structures in Ash-Flow Tuffs from Gran Canaria, Canary Islands, Jour. Geol. 75, 641-664.
- Silver, L. T. (1955) The Structure and Petrology of the Johnny Lyon Hills Area, Cochise County, Arizona, Ph.D. Thesis, Calif. Inst. of Tech., 407 pp.
- Silver, L. T., McKinney, C. R., Deutsch, S., and Bolinger, J. (1963) Precambrian Age Determinations in the Western San Gabriel Mountains, California, Jour. Geol. 71, 196-214.
- Silver, L. T. (1964) Mazatzal Orogeny and Tectonic Episodicity, Geol. Soc. Amer. Spec. Pap. 82, 185-186.
- Silver, L. T. (1967) Apparent Age Relations in the Older Precambrian Stratigraphy of Arizona, Geochronology of Precambrian Stratified Rocks, University of Alberta, 87.
- Smith, R. L. (1960) Ash Flows, Geol. Soc. Amer. Bull. 71, 795-842.
- Turner, F. J. and Verhoogen, J. (1960) Igneous and Metamorphic Petrology, Second ed., McGraw-Hill, 694 pp.
- Walker, G. W. and Swanson, D. A. (1968) Laminar Flowage in a Pliocene Soda Rhyolite Ash-Flow Tuff, Lake and Harney Counties, Oregon, U.S. Geol. Surv. Prof. Pap. 600-B, B37-B47.
- Wilson, E. D. (1922) Proterozoic Mazatzal Quartzite of Arizona, Pan-Amer. Geol. 38, 299-312.

Wilson, E. D. (1939) Pre-cambrian Mazatzal Revolution in Central Arizona,

Geol. Soc. Amer. Bull. 50, 1113-1164.

Wilson, E. D. (1939A) Pre-cambrian of Arizona Basin Ranges, Proc. Sixth

Pac. Sci. Cong., 321-330.

Part II

LEAD ISOTOPE HETEROGENEITY IN PRECAMBRIAN IGNEOUS FELDSPARS

INTRODUCTION

PURPOSE AND SCOPE OF WORK

This investigation was undertaken initially with the general purpose of studying the systematics of original lead isotope composition of a number of plutons with closely similar ages of emplacement, tectonic setting, and post-crystallization history, but varying in geographic location. Initial feasibility studies of the volatilization method of lead removal applied to Precambrian feldspars, however, showed that techniques for isolating original rock leads of these old granites did not in fact exist, and that the feldspar lead isotopes were not homogeneously distributed within the feldspar concentrates. Therefore, a study was initiated to investigate the mechanisms and implications of this lead isotope heterogeneity.

The work concerns five case studies of the feldspar leads of Precambrian plutonic igneous rocks with diverse post-crystallization histories, ages, and locations. The systematics of the feldspar lead isotope distribution of the samples suggest a widespread failure of the closed U-Pb system assumption as applied to Precambrian plutonic feldspars, and require evaluation of possible open-system effects in interpreting any total-feldspar lead isotope analyses.

ROCK AND MINERAL LEADS: BACKGROUND

The lead atoms in the earth may be divided into two basic classes according to their origin. The first is that of lead atoms which were

introduced into the earth at the time of its formation. Because there are, and were, no significant abundances of radioactive isotopes of lead, and because there is no apparent escape mechanism for isotopes of lead, the number of these original atoms has remained constant. The isotopic composition of this primal lead can be reasonably estimated from that of leads present in uranium-free minerals of meteorites which are thought to be cogenetic with the earth. The reported isotopic composition of such leads varies little, with $206/204 = 9.30$ to 9.74 , $207/204 = 10.22$ to 10.70 , and $208/204 = 28.96$ to 30.28 (Patterson, 1955; Chow and Patterson, 1961; Starik et al, 1961; Murthy and Patterson, 1962; Oversby, 1970; Tatsumoto et al, 1973).

The second class is that of lead atoms created since the formation of the earth, by radioactive decay of U^{238} , U^{235} , and Th^{232} . The half-lives of these parent isotopes are such that significant amounts of their daughters (Pb^{206} , Pb^{207} , and Pb^{208}) have been produced throughout geologic time. Thus, of the four stable lead isotopes, only Pb^{204} (having no radioactive parent) has remained unchanged in abundance in the earth.

Therefore, the average lead isotopic composition of the earth has been changing according to the relative abundance of U, Th, and Pb, and the simple mathematical laws of radioactive decay (Appendix I). The differentiated individual crustal rocks and minerals which are available for analysis, however, are clearly not representative of the bulk terrestrial material, so that their leads will not have evolved in such a simple manner.

Consideration of the systematics of radioactive parent to stable daughter decay in natural systems shows that the lead isotope composition of any rock or mineral is a function of the U-Pb and Th-Pb ratios throughout the time spent in the various geochemical environments which are part of its elemental history. Indeed, naturally occurring leads vary widely in their isotopic compositions. Analyses of lead in galenas from ore deposits thought to be genetically related and contemporaneous with major igneous rock-forming events have revealed systematic variations in their lead isotopic compositions which appear to reflect the age and geochemical history of the source of the deposits (Stanton and Russell, 1959; Burger et al., 1962). In practical terms, then, the lead isotopic composition of any rock or mineral may give very significant information as to both the geochemistry and the time-parameters of its origin. Those mineral leads which have not evolved since their incorporation into minerals -- in other words, the leads in minerals which have been closed to lead gain, and which have negligible U and Th content -- are particularly useful as indicators of U-Th-Pb isotope relations in the reservoirs from which their host-rock systems were derived.

Following the earliest modern measurements of the isotopic composition of common (i.e., not predominantly U or Th-derived in situ) leads (Nier, 1938), simple models were proposed (Gerling, 1942; Holmes, 1946; Houtermans, 1947) to explain the observed variations. To a first approximation (in most cases), these simple lead evolution models are still consistent with the observed data. In essence, these models

require that,

1) At the time of its formation, the earth's lead was isotopically homogeneous,

2) The earth is closed to Pb, U, and Th gain or loss,

3) The abundance of Pb^{204} is constant, and that of Pb^{206} , Pb^{207} , and Pb^{208} has been changed only by addition of the U and Th daughters, and

4) There is no isotopic fractionation of lead,

and describe a physical system wherein source material (usually identified with the lower crust or upper mantle) had evolved in a simple manner until a definite time when material was chemically differentiated and emplaced into the upper crust. The mathematics and details of such a single-stage lead evolution model are given in Appendix I.

Most analyses of common leads have been done on the leads in galenas, because the large amount of lead available for analysis simplifies analytical problems. However, there is usually no direct way of determining the age of the galenas. This must generally be done by relating the ore deposit to an igneous body of geologically or isotopically determinable age, or to stratigraphic and structural relationships of some complexity. The data obtained from such conformable ore deposits are, for certain types, generally consistent with a single-stage evolution; however, there are ore deposits whose leads do deviate significantly from such a model. Both the deviations and the consistencies have strong bearings on the fundamental processes of crustal evolution.

FELDSPAR LEADS: PREVIOUS WORKS

The early studies of feldspar lead isotopic composition (Tilton *et al.*, 1955; Catanzaro and Gast, 1960; Doe, 1962b) showed that the feldspar leads also seemed to be close in isotopic composition to that predicted by a single-stage lead evolution model for the initial lead of the rock (of known age) from which they were separated. This was expected, because feldspars have a characteristically low U-Pb and Th-Pb ratio so that little change in feldspar lead isotopic composition should occur from time of crystallization of the mineral to the present. The above works also established that the U and Th content and the radiogenic lead content of the feldspars can be significantly reduced by pretreatment of the feldspar in hot mineral acids, implying that some of the U, Th, and radiogenic lead is loosely bound in the feldspar concentrates.

However, even after hot acid washing, the isotopic composition of Precambrian feldspar leads investigated by Catanzaro and Gast (1960) and Doe (1962b) still tended to have somewhat anomalously young model ages compared to the radiometric age of the rock or the model ages of related sulfide ores. Later work (Doe, Tilton, and Hopson, 1965; Stacey, Zartman, and Nkomo, 1968; Tilton and Steiger, 1969; Sinha, 1969) confirmed this trend, showing that leads from feldspars of Precambrian rocks approach any associated ore leads in their $^{206}/^{204}$, $^{207}/^{204}$, and $^{208}/^{204}$, but are generally slightly to moderately more radiogenic in character (higher $^{206}/^{204}$, $^{207}/^{204}$, and $^{208}/^{204}$).

Doe, Tilton and Hopson (1965), and Doe and Hart (1963) have suggested that gain or exchange of feldspar leads from other rock or mineral leads, addition of lead from other rock units, or admixing of lead from fluids, are possible mechanisms responsible for the generally anomalously radiogenic character of Precambrian feldspar leads.

Zartman (1965) studied the microcline leads of some 1000 m.y. - 1100 m.y. igneous and metamorphic rocks of Texas, and obtained isotopic compositions which generally agreed with that predicted by the single-stage evolution model, although a few of the microcline leads were anomalously radiogenic. Zartman and Wasserburg (1969), in their study of K-feldspar leads of some 1.0 b.y. North American igneous rocks, recognized the difficulty of proving the original character of feldspar leads, but concluded that the apparent efficacy of feldspar acid washing in removing U, Th, and radiogenic lead, and the lack of apparent effect on (in situ decay-corrected) lead isotopic compositions of widely varying U and Th contents of the feldspars, argued for the original character of the leads of their study.

Work by Sinha (1969) done concurrently with the author's, indicates that radiogenic leads may be preferentially removed in the most volatile fractions of the feldspar lead. He suggested that these radiogenic leads are concentrated along grain boundaries or in distorted lattice sites.

SAMPLES: INTRODUCTION

LAWLER PEAK GRANITE

The Lawler Peak granite is an unsheared, porphyritic, coarse-grained granite which crops out in central Arizona in the Bagdad area of Yavapai County. The body from which the analyzed sample was collected has a roughly equant areal exposure of about nine square miles (22 km²). The body was mapped and described by Anderson et al (1955), who describe the main facies of the Lawler Peak granite as a porphyritic biotite-muscovite granite with orthoclase phenocrysts to 3"-size (8 cm) in a medium to coarse-grained groundmass of orthoclase, plagioclase, quartz, biotite, and muscovite. They describe the orthoclase phenocrysts as oriented, and interpreted this as evidence of flowage orientation. There was no recognizable evidence of localized hydrothermal alteration at and near the sample location (Silver, personal communication) The radiometric age of the rock, as determined by Silver, is 1440 ± 10 million years.

Microscopic examination of the sampled rock shows that the K-feldspar is a fresh, zoned, perthitic microcline, and that the cores of the plagioclase (a sodic oligoclase) are partially altered to a fine-grained mineral assemblage (white mica, clays, and ?) (Plates 1 and 2).

The K-feldspar mineral concentrate from the Lawler Peak granite contains 98.6% K-feldspar, 1.4% quartz, and a trace (one grain in 500) of chlorite. About one quarter of the grains have good microcline twinning, and about 5%-10% of the feldspar is exsolved plagioclase.

Most of the grains show slight turbidity, due to the obscuring effects of a fine-grained alteration. Some of the grains, however, are quite clear, and still others completely obscured (Plates 17, 18).

A mineral concentrate enriched in plagioclase and quartz was also obtained from the Lawler Peak granite. This quartz-plagioclase concentrate contained approximately 25% plagioclase and 75% quartz (further plagioclase enrichment was impractical, due to overlapping of densities of the plagioclase and quartz). The plagioclase grains ranged in freshness from those with only slight (less than 10%) amount of fine-grained inclusions and alterations, to those which appeared almost opaque, due to a high abundance of relatively high-index inclusions.

RUIN GRANITE

The Ruin granite crops out in central Arizona near Roosevelt Reservoir, with an areal exposure of hundreds of square miles. Like the Lawler Peak granite, the Ruin granite is a porphyritic two-mica granite, but with a somewhat lower K-feldspar/plagioclase ratio than the Lawler Peak granite. The K-feldspar phenocrysts of the Ruin granite occur as centimeter-sized phenocrysts of zoned microcline with abundant inclusions of plagioclase, mica, and ore (Plates 3 through 8). The K-feldspar is fresh-looking, except for a patchy, fine-grained alteration involving about 40% of the area of the larger grains, as seen in thin-section. The rock has been dated by Silver at 1460 ± 20 m.y. No evidence of alteration at or near the sample locality was observed (Silver, personal communication).

The K-feldspar concentrate from the Ruin granite contains 99.5% K-feldspar grains, 0.5% quartz grains. Most of the feldspar grains are partially turbid, due to the presence of very fine-grained alteration. More than half of the grains are twinned, but none are perthitic.

MARBLE MTS. GRANITE

The Marble Mountains granite is part of a pluton of about sixty square miles exposure in the Mojave Desert of southeast California. The body is in part granodioritic, and in some localities is sheared. Lanphere (1964) suggested, from Rb-Sr dating, a 1400 m.y. age for the rock. Silver and McKinney (1962) dated the rock by U-Pb of cogenetic zircon fractions and obtained an age of 1430 ± 10 m.y. The sample from which the feldspar concentrate (and the U-Pb age) was obtained is unsheared, but slightly weathered. Microscopic examination shows the rock to be a hornblende-biotite granodiorite, with about 15% modal crudely twinned, inch-sized, subhedral, fresh-looking K-feldspar megacrysts. Plagioclase occurs as $\frac{1}{2}$ cm, twinned, partially sericitized grains.

The K-feldspar mineral separate from the Marble Mountains granite was predominantly (80%) quite fresh (less than 10% turbidity* of grains), but some grains were partially altered to a fine-grained mineral assemblage which caused 10%-80% turbidity. None of the feldspar grains of the concentrate are twinned, and about 20% are perthitic. The concentrate contains 99.7% K-feldspar, 0.3% quartz.

*a turbid area is defined as an area which absorbs or scatters virtually all of the light as it passes through the grain or thin-section, due to abundant fine-grained inclusions or alteration.

PAYSON GRANITE

The Payson granite is a porphyritic hornblende-biotite granite with perthitic, zoned, $\frac{1}{2}$ -1 cm K-feldspar phenocrysts. The pluton outcrops in central Arizona, near the town of Payson, and has an areal exposure of hundreds of square miles (L. T. Silver and C. Conway, personal communication). The rock has been dated by Silver (personal communication) at 1740 ± 20 m.y. The collected sample is unsheared, and slightly weathered.

The K-feldspar concentrate from the Payson granite consists of about 99.8% K-feldspar, and 0.2% spinel (? , isotropic, red-purple color). About half of the feldspar grains are perthitic, and about one-tenth are twinned. More than half of the grains are very fresh-looking, while about 40% show more or less turbidity due to fine-grained alteration.

GIANTS' RANGE GRANITE

The Giants' Range granite crops out in northern Minnesota, with an areal exposure of about 1000 square miles (2500 km^2). The collected sample is a coarse-grained, unsheared, very fresh-looking hornblende granodiorite, with abundant accessory sphene and apatite (Plates 15, 16). The K-feldspar grains of the rock are anhedral, twinned, non-perthitic, and fresh-looking, although the plagioclase is partially sericitized. The sample was dated by Silver (personal communication) at 2690 ± 10 m.y. Early (Goldich et al., 1961) K-Ar dates on the Giants Range batholith gave ages of 2300 - 2600 m.y., while more recent (Hanson, 1968) K-Ar

dates give ages of 2500 - 2660 m.y. U-Pb dates of sphenes done by Anderson and Gast (1965) give an age of 2650 ± 50 m.y. U-Pb dates on sphenes of the Giants' Range granite done by Hanson, Catanzaro, and Anderson (1971)* give ages of 2700 m.y., with a lower intersection on the concordia plot chord of 1100 m.y.

The nearest intrusive rocks to the sample collection site is the 1100 m.y. Duluth gabbro, 7 km horizontally distant. The collection site was a blasted roadcut in a glaciated outcrop. The pluton may have been exposed at the surface several times in its history; however, the scouring action of Pleistocene glaciation did remove a significant amount of the surface-exposed material (Silver, personal communication), and the sample rock appears very fresh.

The K-feldspar concentrate from the Giants' Range granite sample contains about 99.8% K-feldspar, and 0.2% quartz. About one-third of the K-feldspar grains show microcline twinning, but none are perthitic. Fine-grained alteration of the feldspar has caused about half the grains to be very turbid (nearly opaque in grain mount), and the remaining half to be partially turbid.

*samples collected within a few km of the Duluth gabbro contact.

EXPERIMENTAL TECHNIQUES AND ANALYTICAL PROCEDURES

SAMPLE PREPARATION

All mineral concentrates, except for the Ruin granite K-feldspar concentrate, were obtained from the acetylene tetrabromide float fraction of a Wilfley table concentrate of a 50-300 lb. sample collected by L. T. Silver. The samples were chosen by Silver for their relative freshness and isolation from evidence of later disturbance. The Pb-U apparent ages reported in this work for the sample rocks were derived from co-genetic zircon suites as described in Silver and Deutsch (1963).

The acetylene tetrabromide floats were sieved into several size fractions with nylon bolting cloth, of which only the 100-200 mesh (75-150 microns) fraction was used. These sized concentrates were then separated by density in an acetylene tetrabromide-isopropyl alcohol mixture. Several sequential density separations of this kind were performed, with the liquid density adjusted in each separation to give suitable mineral purification. The resulting concentrates were repeatedly cycled through a Frantz magnetic separator at 20° foretilt and 1°-10° side tilt at 1.0 to 1.8 amperes. The most pure and least altered (generally, the least magnetic) fractions were chosen for use. The treatment for the Ruin granite K-feldspar concentrate differed only in that the sized material was produced from hand-picked, pea-sized fragments of the rock, chosen for predominant K-feldspar content.

All of the K-feldspar concentrates were better than 99.5% pure, except for the Lawler Peak granite K-feldspar concentrate (with 1.4%

quartz). In most cases, quartz was by far the dominant grain impurity. The resulting concentrates were boiled in concentrated HNO_3 for 30 minutes, followed by 30 minutes in boiling concentrated HCl , rinsed with quadruply distilled water, and heat-dried.

VOLATILIZATION PROCEDURE*

The acid-washed mineral concentrates, from 0.2 to 12 grams weight, were placed in a fused quartz tube of about 15 mm x 60 mm size, closed at one end. This sample-containing insert was then placed in a larger fused-quartz tube of about 25 mm diameter and 200 mm length. A fused-quartz, water-cooled cold finger was fitted, using a greased ground-glass joint, to the loaded furnace tube, and the apparatus mechanically evacuated for 30 minutes to a pressure of 100 - 500 microns. A preheated electrical furnace with a cylindrical orifice only slightly larger than the furnace tube then received the furnace tube. The sample remained in the furnace (with the vacuum pump connected) for about two hours. During this time, the hottest part of the furnace was measured for temperature with an optical pyrometer. The sample was then cooled in air, and any volatiles condensed on the cold finger dissolved by swirling in warm 2 normal HCl for two minutes. The cold finger was then rinsed in quadruply-distilled water, and returned to the sample-containing furnace tube. The evacuation and heating procedures were repeated on this tube, except that the furnace temperature was maintained at about

*modified from Masuda (1964)

30°C higher than the initial run (usually about 1050°C). The volatilization and condensate solution procedures were successively repeated on the sample until the softening point of the fused quartz (about 1350°C) was approached.

At this stage, the K-feldspar concentrates were generally fused to a translucent to clear glassy lump which was optically isotropic. The lead in the dissolved condensates was extracted according to the procedures described elsewhere in this work. Yields of lead from the cold-finger were estimated from the dithizone endpoint, and are accurate only to $\pm 30\%$.

The temperature monitoring procedure was reasonably precise, with reproducibility of about $\pm 5^\circ\text{C}$ and accuracy of about $\pm 20^\circ\text{C}$ (compared to measurements with a precision thermocouple thermometer): however, the experimental reality of the measured temperatures is less clear due to,

- 1) a possible lack of equivalence of the temperature of the hottest part of the furnace (measured) and the temperature of the actual sample, and,

- 2) variations in the observed temperatures of up to 15°C because of fluctuations in the furnace line voltage.

The fused quartz apparatus was subjected to the same washing procedure as the other laboratory glassware (two washings in hot. concentrated HNO_3), and the inserts and heated part of the furnace tube were discarded and replaced after each complete volatilization series.

STEPWISE HF-DISSOLUTION PROCEDURE

In order to determine whether the isotopic composition of the K-feldspar concentrate lead varied with leachability in HF as well as with volatility, two feldspar concentrates were subjected to a stepwise HF attack. For each partial attack, the K-feldspar concentrate was immersed in 60-90 grams of warm, 5% HF and 2 grams HNO_3 or HClO_4 in a teflon dish for about 25 minutes. The liquid was then decanted, evaporated to dryness, and its lead composition analyzed. The undissolved sample was then rinsed in 3% NH_4OH and quadruply distilled water, dried, and again attacked for a controlled period. The stepwise attack series continued until all of the sample was dissolved. No lead yield data for these experiments was obtained.

TOTAL FELDSPAR AND WHOLE ROCK ANALYSES

The lead from the total feldspar was obtained by 20-hour exposure of the samples to an excess of 50% HF and concentrated HClO_4 in a covered teflon dish. The residue was dissolved in 2NHCl or concentrated HNO_3 , and the lead extracted using either the double-dithizone technique of Silver et al (1963) or the barium nitrate coprecipitation procedure of Tatsumoto (1966). The feldspar lead samples were run as the sulfide on a single tantalum filament and the feldspar uranium as the nitrate on a single tantalum filament. The whole-rock lead samples were run using silica gel-phosphoric acid on a single rhenium filament (modified after Cameron et al, 1969) and the whole-rock uranium and thorium as the nitrate on a triple rhenium filament. The whole-rock samples were

dissolved using the high-pressure HF technique modified after Krogh (1970).

CONCENTRATION DETERMINATIONS

The concentrations of lead, uranium, and thorium in the samples were determined by isotope dilution. These determinations are accurate to $\pm 2\%$ for lead and $\pm 2\%$ or 0.01 ppm for uranium, whichever was higher. The uranium was extracted by coprecipitation with $\text{Al}(\text{OH})_3$ (Silver *et al.*, 1963) for the feldspar samples, or (along with thorium), with an ion-exchange column in the case of the whole-rock samples.

BLANKS

Lead blanks for the volatilization procedure averaged about .08 micrograms, and decreased with time so that the later runs had blanks of about .04 micrograms. A Pb^{208} -rich spike was used as a carrier for the blank determinations, and the 206/207 ratio of the blank lead monitored (table 1). In most cases, the blank correction of the most sensitive lead isotope ratio, 206/204, was less than 0.1%. Uranium blanks were about .004 micrograms.

MASS SPECTROMETRY

The mass spectrometric analyses were carried out on a single-focusing, 30-cm radius, step-scanning, digital data acquisition machine. An electron multiplier was used for almost all of the runs. Comparison of analyses of CIT standard shelf lead run on this machine with the NBS standard values for this lead (Catanzaro, 1968) show that, for the lead

Table 1

Concentration and Isotopic Composition of Blank Leads

<u>Date</u>	<u>Type</u>	<u>Yield (μg)</u>	<u>206/207</u>	<u>206/204</u>
12/9/69	Volatilization	.15	1.22	-
12/10/69	"	.12	1.29	20.5
2/16/70	"	.27	1.10	17.2
2/24/70	Feldspar Chemical Attack	.22	1.22	-
2/24/70	Volatilization	.16	1.14	17.6
3/16/70	Feldspar Chemical Attack	.13	1.12	17.4
5/6/70	Fused Quartz Chemical Attack	.16	1.20	19
5/9/70	Volatilization	.070	1.1	-
7/17/70	"	.066	1.04	-
9/17/70	"	<.05	-	-
9/19/70	"	.041	1.27	-
10/1/70	High-Pressure Bomb Run	.021	1.36	-
3/20/70	Uranium Extraction	<.07	Uranium Blank	
9/20/70	"	.0034	Uranium Blank	

run as the sulfide on tantalum filaments using the electron multiplier, deviations from the NBS values are less than 0.10% for all ratios except those involving Pb^{208} , which show less than 0.15% deviation (table 2). The lead run on rhenium filaments using the silica gel-phosphoric acid technique was corrected for 0.075% per a.m.u. discrimination. These runs therefore are not corrected for any discrimination.

Internal precision for the ratios from a single run were typically about 0.15% for the 206/207 ratio, 0.20% for the 206/208 ratio, and 0.20% for the 206/204 ratio. Some runs, however, gave much poorer precision.

Table 2

Caltech Shelf Lead Standard: Analyses

<u>Date</u>	<u>206/204</u>	<u>207/204</u>	<u>208/204</u>	<u>206/207</u>	<u>206/208</u>
3/7/70 (chart read)	16.61	15.46	36.09	1.0748	.4602
3/26/70	16.63	15.49	36.29	1.0735	.4584
4/2/70	16.61	15.47	36.22	1.0742	.4587
4/27/70	16.63	15.48	36.24	1.0740	.4587
7/7/70	16.64	15.50	36.28	1.0732	.4586
12/4/70	16.64	15.49	36.27	1.0741	.4586
<u>Average</u> (excluding 3/7/70 run)	16.630	15.486	36.260	1.0738	.45860
Std. Deviation	.074%	.007%	.080%	.040%	.027%
NBS Values*	16.625	15.475	36.301	1.0743	.45798
Deviation from NBS	+.030%	+.071%	-.113%	-.047%	+.135%

*Catanzaro et al, 1968

EXPERIMENTAL RESULTS - INTRODUCTION

WHOLE FELDSPARS, WHOLE ROCKS, AND ACID LEACHES

Lawler Peak Granite

WHOLE FELDSPAR

The total feldspar lead of the Lawler Peak granite K-feldspar concentrate has lead isotope ratios of $206/204 = 17.01$, $207/204 = 15.44$, and $208/204 = 35.96$ (table 3). The concentrations of lead and uranium are, respectively, .077 ppm and 76.70 ppm. With such a high Pb/U ratio, only a slight correction for in situ-generated radiogenic lead is necessary. This correction, using the 1440 m.y. age of the rock, lowers the $206/204$ value to 16.99 and the $207/204$ value to 15.44. The (single-stage evolution) model age for this lead is 860 m.y.⁽¹⁾, much younger than the radiometric age of the rock. Thus, either the simple model from which the model age is calculated is not applicable, or the total feldspar lead composition does not represent the original rock lead, or both.

FELDSPAR ACID LEACH

The lead leached from the K-feldspar concentrate in the acid-

(1) The constants used in this work for calculating the model ages of leads are: $(\text{Pb}^{206}/\text{Pb}^{204})_{\text{initial}} = 9.56$, $(\text{Pb}^{207}/\text{Pb}^{204})_{\text{initial}} = 10.42$, decay constant of $\text{U}^{238} = 0.1537 \times 10^{-9}/\text{y}$, of $\text{U}^{235} = 0.9722 \times 10^{-9}/\text{y}$; age of the earth = 4550 m.y.

Table 3

LAWLER PEAK GRANITE K-FELDSPAR

Whole Feldspar Lead and Feldspar Acid Leach

	Whole Feldspar Lead				
	<u>206/204</u>	<u>207/204</u>	<u>208/204</u>	<u>206/207</u>	<u>206/208</u>
est. accuracy	17.01	15.44	35.96	1.1018	.4730
(±)	.25%	.25%	.25%	.15%	.20%

76.70 ppm Pb,

.077 ppm U

corrected for
in situ U-decay
(1440 m.y.)

16.99

15.44

-

1.1009

-

K-Feldspar Acid Washings (1.5 hours boiling 50% HNO₃ followed by ½ hour
boiling 8N HCl)

46.91

18.25

-

2.5705

- (1)

1%

1%

.20%

Yield: ½ µg Pb/g K-Feldspar

(1) Pb²⁰⁸ spike used as carrier for isotopic analysis.

washing pre-treatment (30 minutes each in boiling HNO_3 and HCl) was analyzed (about 0.5 micrograms of lead per gram of feldspar was leached). This lead was radiogenic in character (table 3), with $206/204 = 46.9$ and $207/204 = 18.25$. The model age for this radiogenic lead (that is, assuming closed-system, cumulative behavior for the lead) calculated from the $207/206$ ratio and correcting for the initial common lead, is 1525_{-100}^{+90} m.y. ⁽²⁾. The initial lead values used for correction were $206/204 = 16.16$, $207/204 = 15.40$ (a calculated value using data to be presented - see page 317). If an initial lead with $206/204 = 16.39$, $207/204 = 15.40$ is used (an observed lead fraction from this feldspar concentrate), the apparent age is reduced by 5 m.y. The age of 1525 m.y. is, within its error limits, indistinguishable from the radiometric age of the rock. Therefore, the radiogenic lead component leached from the feldspar by hot acids is 'normal' for radiogenic lead accumulated over the age of the rock.

(2) the error limits reflect the uncertainty in Pb^{204} of the analysis.

WHOLE ROCK

The Lawler Peak granite whole rock lead isotopic composition and concentration and the uranium and thorium concentrations were determined (table 4). The rock lead is significantly radiogenic, reflecting the high uranium content of the rock (15.73 ppm). The radiometric ages of the rock are markedly discordant. In Fig. 1, the data are plotted on a 'concordia' diagram (Wetherill, 1956). As is characteristic of systems which have gained lead or lost uranium, the data fall above the concordia curve. The relatively large errors in estimating the radiogenic Pb^{207} content of the rock prohibit precise estimation of the time that the rock became open to lead or uranium mobilization on an episodic loss model, but the data do suggest that if a single episodic loss or gain of uranium or lead occurred, it must have taken place during the latter part of the rock's history. Silver (personal communication) found disturbance in the zircons of the rock suggesting an apparent lower intersection on concordia of 200 ± 20 m.y.

The Pb^{207}/Pb^{206} 'age' of the rock is 1350 ± 140 m.y. ⁽¹⁾, using initial lead values of $206/204 = 16.16$, $207/204 = 15.38$ ⁽²⁾. This 'age' is not distinguishable from the radiometric age of the rock (within its error limits), and shows that the composition of the radiogenic lead of the rock is essentially 'normal' for the age of the rock.

(1) The error limits reflect the uncertainty in the estimation of Pb^{204} abundance.

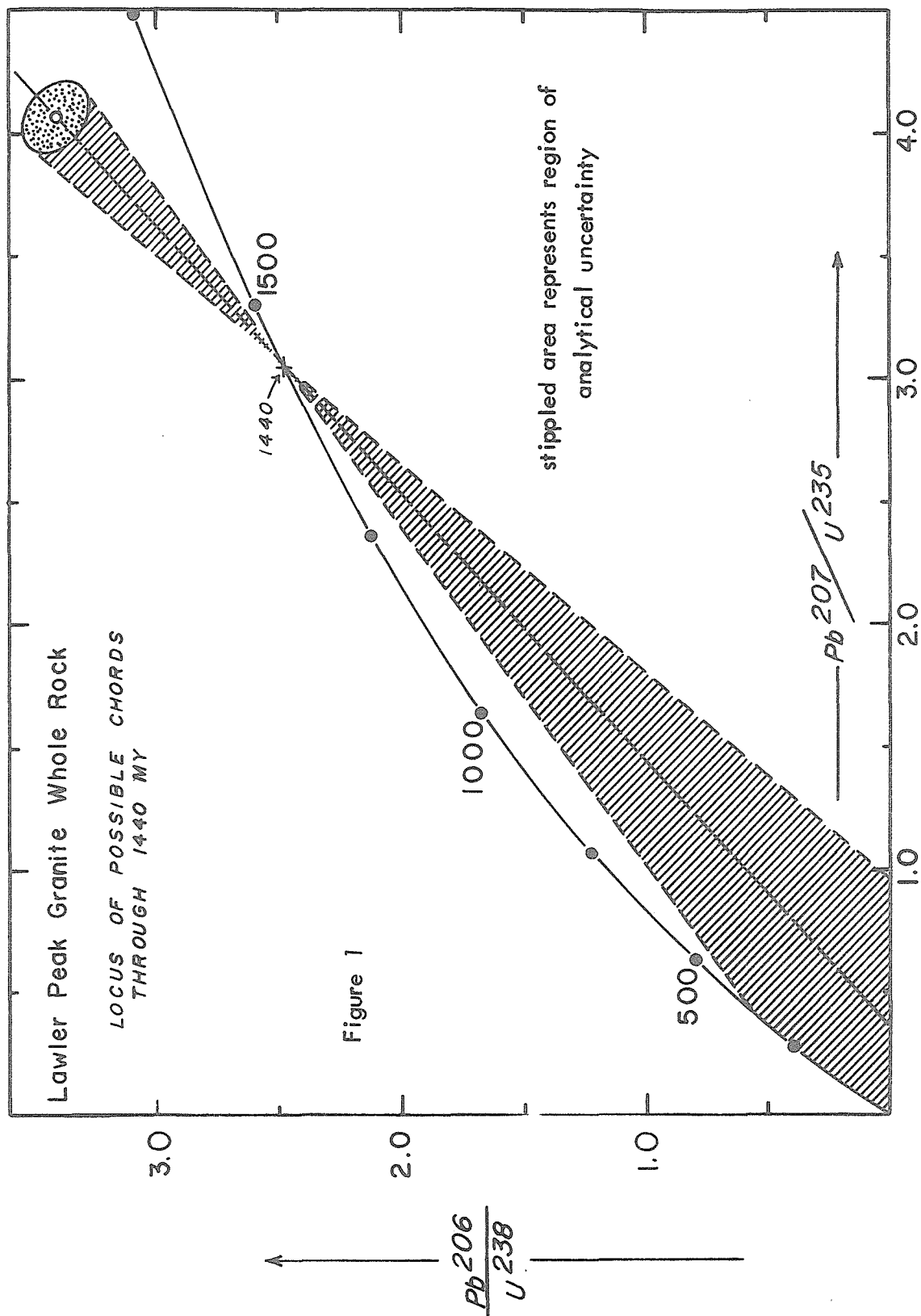
(2) Calculated initial lead values - see page 317.

Table 4

Whole-Rock Pb, U, and Th Isotopic Compositions and Concentrations

Rock	Pb (ppm)	U (ppm)	Th (ppm)	$\frac{\text{Th}^{232}}{\text{U}^{238}}$	$\frac{\text{U}^{238}}{\text{Pb}^{204}}$	$\frac{\text{Pb}^{207}}{\text{Pb}^{206}}$	$\frac{\text{Pb}^{207}}{\text{U}^{235}}$	$\frac{\text{Pb}^{206}}{\text{U}^{238}}$	$\frac{\text{Pb}^{208}}{\text{Th}^{232}}$	$\frac{\text{Pb}^{206}}{\text{Pb}^{204}}$	$\frac{\text{Pb}^{207}}{\text{Pb}^{204}}$	$\frac{\text{Pb}^{208}}{\text{Pb}^{204}}$
Lawler Peak Granite "age" (my)	34.35	15.73	28.95	1.90	33.37	.08567 1350	4.072 1670	.3408 1910	.05705 1140	27.53 ±.4%	16.35 ±.4%	39.35 ±.4%
Ruin Granite "age" (my)	33.06	3.145	28.17	9.26	8.16	.09091 1470	3.592 1570	.2867 1640	.0600 1190	20.76 ±.4%	15.69 ±.4%	39.41 ±.4%
Marble Mts. Granite "age" (my)	52.18	8.82	142.0	16.63	13.42	.07613 1120	3.356 1510	.3199 1810	.07729 1525	20.52 ±.5%	15.72 ±.5%	53.73 ±.5%
Payson Granite	-	2.092	11.3	5.58	-	-	-	-	-	-	-	-
Giants' Range Granite "age" (my)	2.568	0.693	3.54	5.28	15.70	.1569 2410	3.338 1490	.1570 940	.02708 540	15.94 ±.5%	14.89 ±.5%	35.47 ±.5%

¹Radiogenic lead isotopes. Common lead for correction taken as the least radiogenic observed value of stepwise-removed lead fractions, except for Lawler Pk. granite, for which the values calculated on page 317 were used.



The important considerations of the above data are that,

1) The U-Th-Pb system of the Lawler Peak granite whole rock has been strongly disturbed, and definitely has not behaved as a closed system throughout the age of the rock, and,

2) The uranium daughters have not been significantly fractionated in the whole-rock system.

Point (1) may well bear on the marked deviation from closed-system behavior of the feldspars of the Lawler Peak granite. The importance of the second point will become apparent upon consideration of the detailed systematics of the Lawler Peak granite feldspar leads.

Ruin Granite

WHOLE FELDSPAR

The total feldspar lead of the Ruin granite K-feldspar concentrate has lead isotope ratios of $206/204 = 16.44$, $207/204 = 15.40$, and $208/204 = 35.94$ (table 7). The lead and uranium concentrations are, respectively, 68 ppm and .065 ppm. Corrected for in situ decay of uranium over the 1460 m.y. radiometric age of the rock, the total feldspar lead ratios reduce to $206/204 = 16.43$, $207/204 = 15.40$. The single-stage evolution model age (Appendix I) for such a lead is 1250 m.y. - about 210 m.y. younger than the apparent age of the rock.

WHOLE ROCK

The whole-rock uranium, thorium, and lead concentrations and the lead isotopic composition are given in table 4. The Ruin granite, compared to the Lawler Peak granite, has only a fifth of the uranium but

an equivalent amount of thorium. The radiogenic lead component in the Ruin granite whole rock is much less than that of the Lawler Peak granite, so that the calculated U-Pb, Th-Pb, and Pb-Pb isotopic 'ages' given in table 4 have large uncertainties associated with them -- not the least of which is the choice of the initial rock lead isotopic composition. Nevertheless, it is clear that the rock has not behaved as a closed U-Th-Pb system, and has evidently either lost uranium or gained (radiogenic) lead. The Pb^{207}/Pb^{206} 'age', however, is consistent with the age of the rock, which suggests loss of uranium late in the history of the rock. Note that the pattern of discordance of the Ruin granite whole rock is the same as the pattern of discordance of the Lawler Peak granite whole rock (reverse U-Pb discordance, normal Th-Pb discordance, concordant Pb-Pb values, compared to the radiometric age from zircons).

Marble Mts. Granite

WHOLE FELDSPAR

The K-feldspar concentrate sample was consumed in the stepwise volatilization experiments and repeated attempts to obtain a usable total feldspar lead analysis. The analysis of the total lead from a different feldspar concentrate from the Marble Mts. granite would have much less value, since the (to be demonstrated) marked lead isotope heterogeneity of such feldspars implies that different degrees and patterns of lead isotope heterogeneity (and thus abundance) probably characterize different mineral separates.

The data from the stepwise volatilization experiment on the

K-feldspar concentrate of the Marble Mts. granite, however, were used to calculate a total feldspar lead isotopic composition from material balance considerations⁽¹⁾. This calculated total feldspar lead composition is $206/204 = 16.35$, $207/204 = 15.43$ ($208/204$ value not calculable because $208/204$ for all lead fractions was not determined). The feldspar has 97 ppm Pb, 0.2 ppm U, and 0.3 ppm Th. The calculated total feldspar lead composition, corrected for in situ decay of uranium, becomes $206/204 = 16.32$, $207/204 = 15.43$. The single-stage evolution model age (Appendix I) of this lead is 1360 m.y., only 70 m.y. younger than the radiometric age from zircons.

WHOLE ROCK

The whole rock of the Marble Mts. granite (table 4) has only a slight radiogenic lead component, so that uncertainties in the calculation of radiometric whole-rock 'ages' are very large. The uranium-lead isotopic 'ages', like the Lawler Peak and Ruin granites, show reverse discordance -- apparent ages older than that of the age of the rock from zircons. The Pb^{207}/Pb^{206} 'age' of the whole rock is not distinguishable from the apparent age of the rock, because the large errors in the estimation of the actual radiogenic Pb^{207} component result in possible errors in the Pb^{207}/Pb^{206} 'age' of about 500 m.y. Because of the unusually high thorium content of the whole rock (142 ppm, compared to 1.9 ppm for the Lawler Peak granite and 9.3 ppm for the Ruin granite),

(1) For this calculation, the $207/204$ of the unvolatilized, residual lead of the stepwise volatilization experiment was taken as 15.40 (see page 299), and the $206/204$ of this fraction adjusted accordingly.

there is a large radiogenic Pb^{208} component in the rock. The $\text{Pb}^{208}/\text{Th}^{232}$ 'age' is 1525 ± 40 m.y. -- slightly but significantly older than the apparent age of the rock. Therefore, the rock has either lost thorium or gained Pb^{208} .

Payson Granite

WHOLE FELDSPAR

No useful analysis of the lead of the Payson granite K-feldspar concentrate was obtained (several mass spectrometric runs of the total lead were unsuccessful, and left only enough sample for the stepwise lead removal experiments). The lead concentration of the feldspar concentrate was 32.80 ppm, the uranium and thorium concentrations .075 ppm and .17 ppm, respectively.

WHOLE ROCK

The Payson granite whole rock (table 4) contains 2.092 ppm uranium and 11.3 ppm thorium. The concentration and composition of the lead of the whole rock was not determined.

Giants' Range Granite

WHOLE FELDSPAR

The total feldspar lead of the Giants' Range granite K-feldspar concentrate has lead isotope ratios of $206/204 = 13.551$, $207/204 = 14.537$, and $208/204 = 33.320$. The lead and uranium concentrations are, respectively, 11.15 ppm and $.00^{+.02}_{-.00}$ ppm. The single-stage evolution model age for this lead is 2770 m.y. This model age is close to the

apparent age of 2690 m.y., as determined by Silver. Anderson and Gast (1965) reported model ages from feldspar leads of the Giants' Range granite which are essentially equivalent, 2750 ± 50 m.y.

WHOLE ROCK

The whole rock uranium and thorium concentrations are both quite low (.693 ppm U, 3.54 ppm Th), compared to the other granites analyzed for this study. Although the lead concentration (2.57 ppm) is also rather low, the radiogenic enrichment of the whole rock lead is slight (table 4), so that the whole-rock radiometric 'ages' given in table 4 have large uncertainties. The data do indicate that the whole rock system has either lost lead or gained uranium and thorium ('normal' discordance), and suggest that if this disturbance were episodic, that it occurred late in the history of the rock. The discordance suggests loss of about three-quarters of the radiogenic lead, or gain of uranium and thorium (which seems unlikely, in view of the present-day low concentrations of these elements) by a factor of about three.

VOLATILIZATION EXPERIMENTS

LAWLER PEAK GRANITE

K-Feldspar Concentrate

Eight stepwise-volatilized lead fractions and the unvolatilized lead in the residue were obtained and analyzed from the Lawler Peak granite K-feldspar concentrate (table 5). The isotopic composition of these lead fractions is variable, which strongly argues that the total feldspar lead (which has a negligible in situ-generated radiogenic lead component) is not representative of the original feldspar lead.

As figure 2 shows, there is a large variation in the 206/204 values of the volatilized lead fractions. The general trend is for the 206/204 to decrease as the volatilization sequence proceeds, so that there is a total variation in 206/204 of 11%. This difference is much greater than possible effects of analytical error or contamination. The detailed trend of the 206/204 values is not monotonic, but has two analytically real reversals in slope. The first reversal maximum occurs at the fraction volatilized at 1170°, and the second at the unvolatilized (residue) lead fraction.

The 207/204 values of the volatilized fractions and residue, however, do not vary demonstrably outside analytical errors. Furthermore, statistical analysis of the covariance of the 206/204 and 207/204 (appendix IV) shows no dependence of the 207/204 on the 206/204 within ± 0.02 (that is, the slope of the best fit line to these points has a 207/204:206/204 slope of $0.00 \pm .02$) (see fig. 3).

Table 5

Lawler Peak Granite K-Feldspar: Stepwise-Removed Lead Fractions

Volatilized Lead Fractions:

Fraction	$\frac{206}{204}$	$\frac{207}{204}$	$\frac{208}{204}$	$\frac{206}{207}$	$\frac{206}{208}$	yield (μg)	Temperature of Volatilization
A ⁽¹⁾	18.06	15.39	-	1.1748	-	3.4	1070°
est. acc.	.5%	.5%		.15%			
B	17.27 .15%	15.40 .15%	35.87 .20%	1.1216 .10%	.4815 .15%	12	1090°
C	17.14 .45%	15.45 .45%	36.13 .50%	1.1094 .35%	.4745 .35%	5	1120°
D	17.51 .15%	15.40 .15%	35.91 .20%	1.1368 .10%	.4876 .15%	15	1170°
E	17.19 .15%	15.40 .15%	35.77 .15%	1.1160 .10%	.4805 .10%	13	1200°
F	16.77 .15%	15.37 .15%	35.74 .15%	1.0910 .15%	.4692 .15%	10	1240°
G	16.54 .15%	15.37 .15%	35.78 .15%	1.0766 .10%	.4624 .15%	20	1290°
H	16.45 .15%	15.40 .15%	35.91 .15%	1.0683 .15%	.4582 .10%	11	1330°
Residue	16.74 .40%	15.45 .30%	36.22 .35%	1.0832 .25%	.4631 .25%	5	chemical attack

Stepwise Partial HF Attacks: 2.83 g K-spar in 5% HF

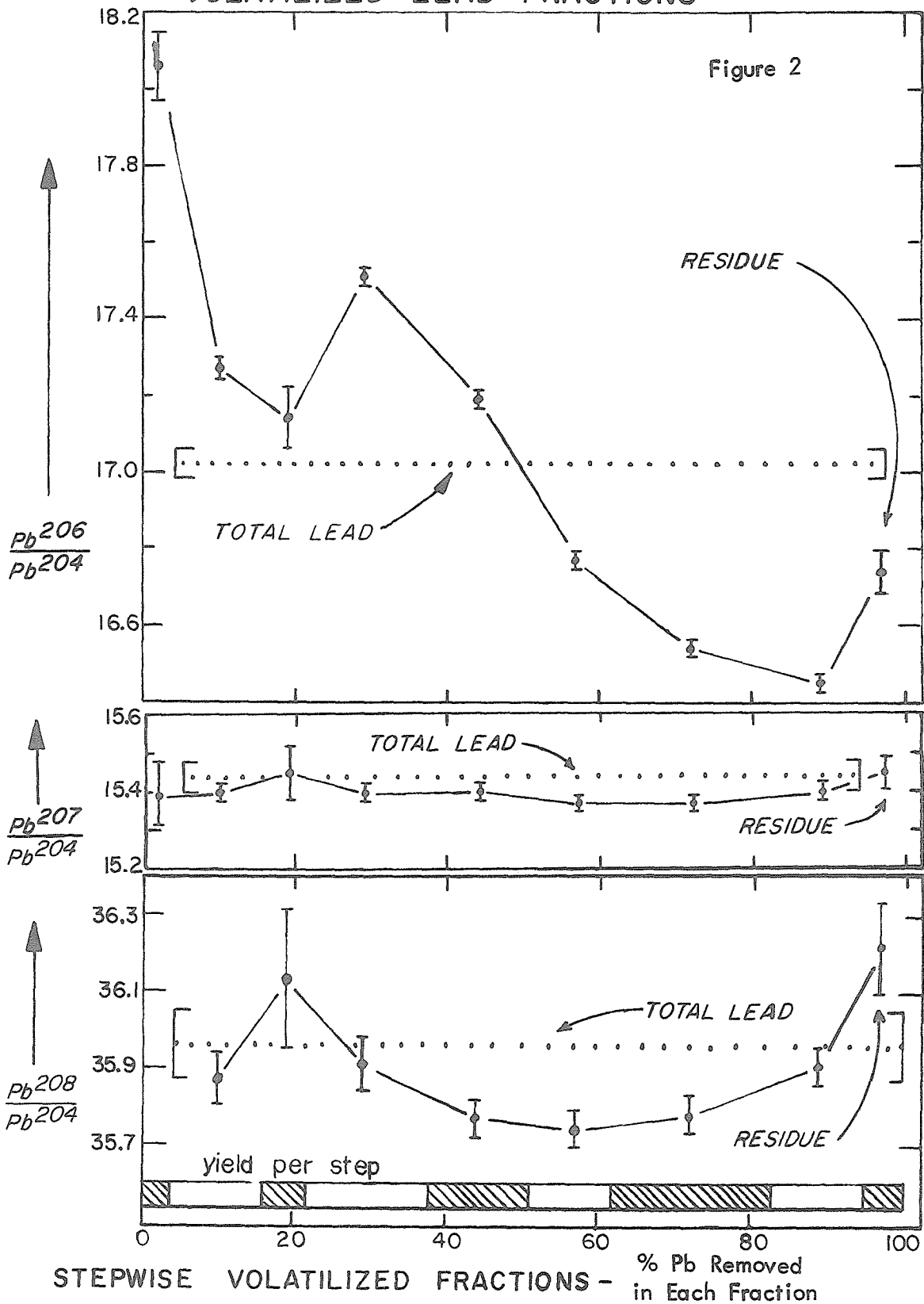
A ⁽²⁾	-	-	-	1.1630 .20%	.4983 .40%		no yield data
B	n o d a t a - - - - -						
C	16.39 .15%	15.40 .10%	35.86 .15%	1.0644 .10%	.4570 .15%		"

(1)Pb²⁰⁸ spike used as carrier for analysis.

(2)No Pb²⁰⁴ data.

LAWLER PEAK ²⁵²GRANITE K-FELDSPAR
VOLATILIZED LEAD FRACTIONS

Figure 2

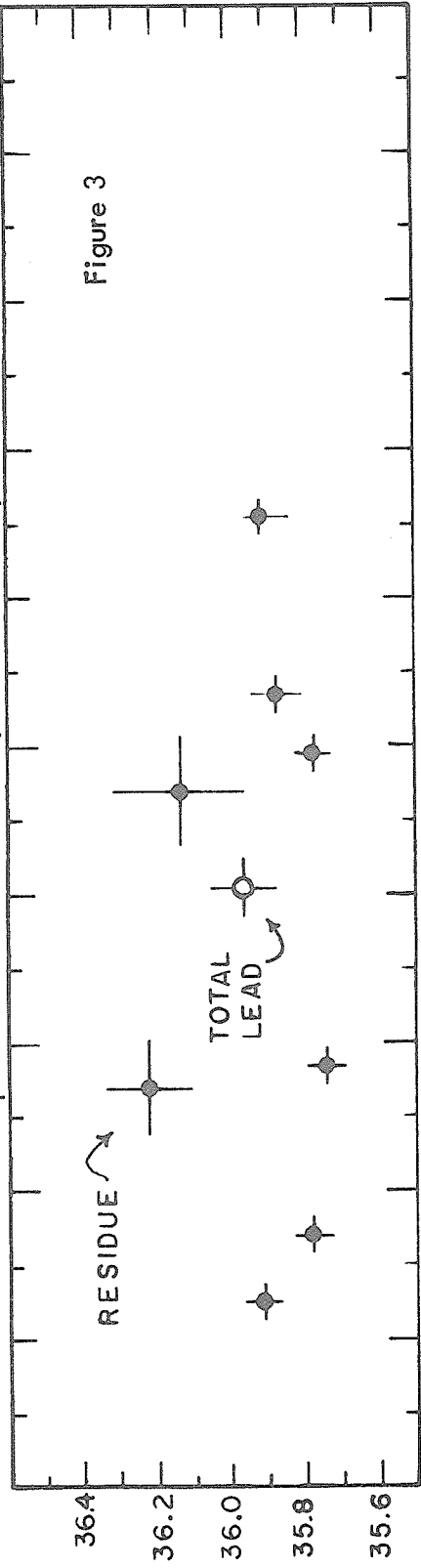


LAWLER PEAK GR. K-FELDSPAR VOLATILIZED LEAD FRACTIONS

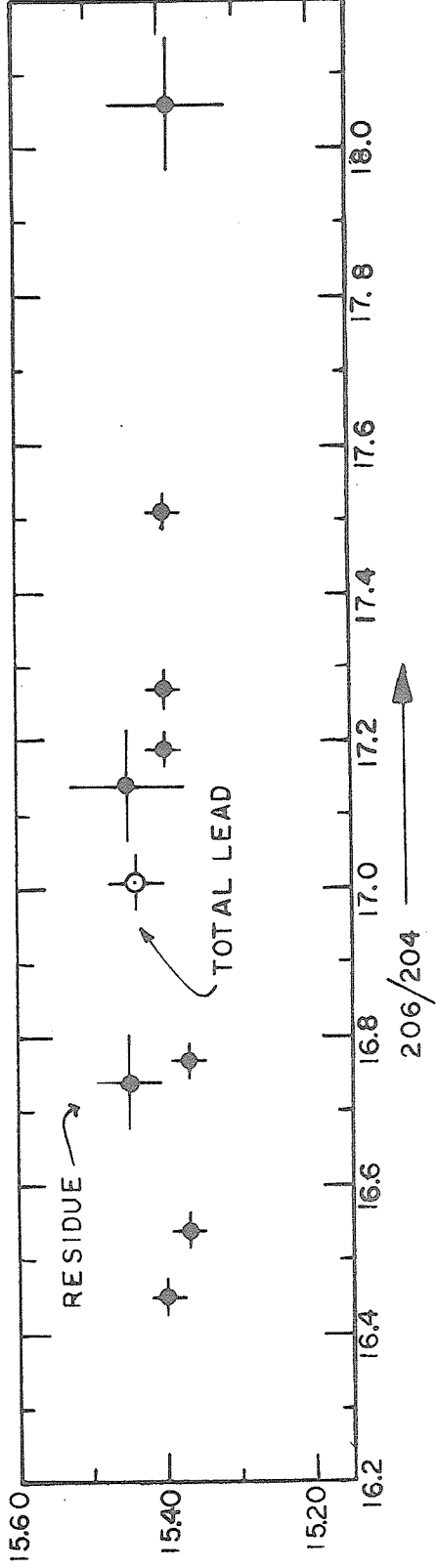
Crosses Represent Dimensions of Analytical Uncertainty

Figure 3

$\frac{208}{204}$



$\frac{207}{204}$



The 208/204 values of the volatilized fractions and residue do vary outside analytical error, so that the maximum observed variation is about 1.3% (between the residue lead and volatilized fraction F). This variation does not correlate simply with the variations in 206/204 of the fractions -- for instance, from the first until the fifth volatilized fractions, these ratios vary in an opposing sense.

The 207/204 variations, even though not outside analytical error, are generally similar in trend to those of the 208/204 of the fractions. A variable error in the measurement of the relative intensity of the (least intense and most subject to error) Pb^{204} peak would lead to such a covariance of 207/204 with 208/204. Examination of the data, however, precludes this, as a best-fit line through the 207/204 - 208/204 points of the volatilized fractions, residue, and total lead has a slope of 0.17 ± 0.03 (fig. 4). If the covariance were due to a variable error in 204 measurement, this slope would be about the average 207/208 value (0.43), clearly distinguishable from the observed slope. Therefore, the variation in 207/204 is not independent of 208/204 variation.

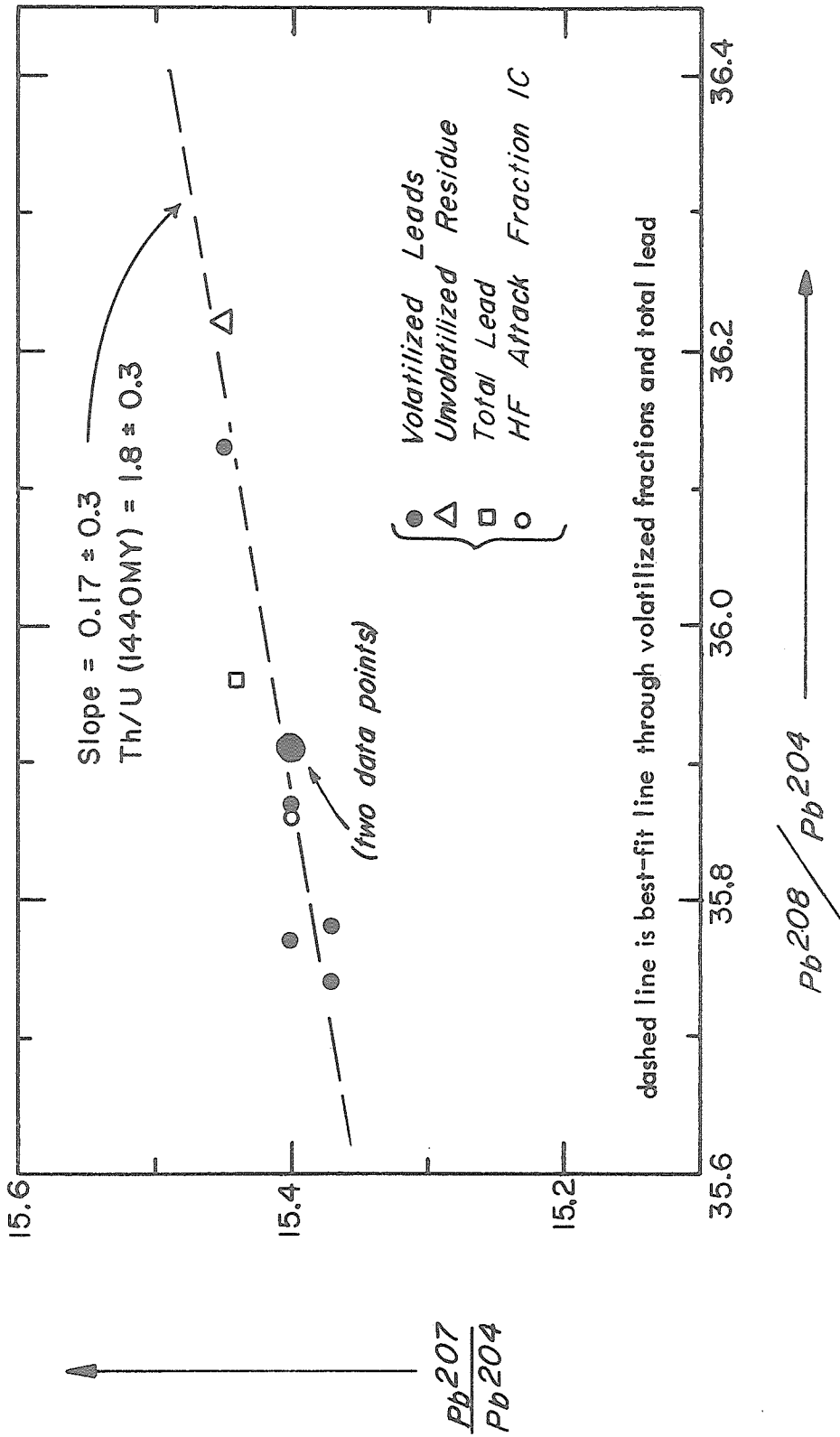
The general trend of the stepwise volatilized leads is for the less volatile fractions (except for the least volatile fraction) to be generally more primitive (lower 206/204, 207/204, and 208/204) in character than the more volatile fractions.

Quartz-Plagioclase Concentrate

The lead from the quartz-plagioclase concentrate (25% plagioclase, 75% quartz) was volatilized in four steps, and the volatilized lead

Figure 4

LAWLER PEAK GRANITE K-FELDSPAR LEADS



fractions analyzed. The lead analysis of the unvolatilized residue was not successful. The results are given in table 6 and figure 5.

The isotopic compositions of the volatilized lead fractions are variable, with the initially volatilized fractions higher in 206/204, 207/204, and 208/204 than any of the K-feldspar lead volatilized fractions. The most primitive fraction has a 206/204 (17.38) higher than the total feldspar lead 206/204 (17.01).

Although there was not enough of the concentrate to permit a total concentrate lead composition and uranium and lead concentrations, a lead concentration of 4.5 ppm may be roughly calculated from the observed dithizone yields of the volatilized fractions. The uranium concentration of the residue was analyzed, and determined to be 0.23 ppm. With this uranium/lead ratio, the in situ-generated radiogenic lead correction for 1440 m.y. is not negligible, and must be considered in estimating the original quartz-plagioclase concentrate lead isotopic composition. The necessary correction is about 0.4% in the 207/204 and 4% in the 206/204.

RUIN GRANITE K-FELDSPAR

Two stepwise volatilization series were performed on the Ruin granite K-feldspar concentrate; however, in neither series were successful mass spectrometric analyses of every lead fraction obtained.

The data (tables 7 and 8, figures 6, 7, and 8), although not as high in precision as the Lawler Peak granite K-feldspar lead analyses, show that the Ruin granite K-feldspar lead is not homogeneous in isotopic composition. Therefore, the K-feldspar has not been closed to

Table 6

Lawler Peak Granite Quartz-Plagioclase Concentrate Lead Analyses

(12.53 g sample: 75% quartz - 25% plagioclase)

Stepwise Volatilization Series Fractions:

	$\frac{206}{204}$	$\frac{207}{204}$	$\frac{208}{204}$	$\frac{206}{207}$	$\frac{206}{208}$	yield (μg)	Temperature of Volatilization
A ⁽¹⁾	24.7	16.4	-	1.5096	-	0.9	1090°C
est. acc.	± 1.5	± 0.4		$\pm 0.25\%$			
B	18.50	15.56	36.33	1.1890	.5092	25	1200°
	$\pm .15\%$	$\pm .15\%$	$\pm .15\%$	$\pm .10\%$	$\pm .10\%$		
C	17.41	15.40	35.98	1.1302	.4837	12	1240°
	$\pm .20\%$	$\pm .20\%$	$\pm .40\%$	$\pm .15\%$	$\pm .15\%$		
D	17.38	15.41	35.84	1.1280	.4851	15	1280°
	$\pm .15\%$	$\pm .15\%$	$\pm .15\%$	$\pm .10\%$	$\pm .10\%$		
Residue	n o	d a t a	- - - - -	- - - - -	- - - - -	≥ 4	
Total sample:	n o	d a t a					

Calculated Lead Concentration = 4.5 ppm

Uranium concentration of residue = 0.23 ppm

(1) Pb^{208} spike used as carrier for mass spectrometric analysis.

258
LAWLER PK. GRANITE QUARTZ-PLAGIOCLASE CONCENTRATE
VOLATILIZED LEAD FRACTIONS

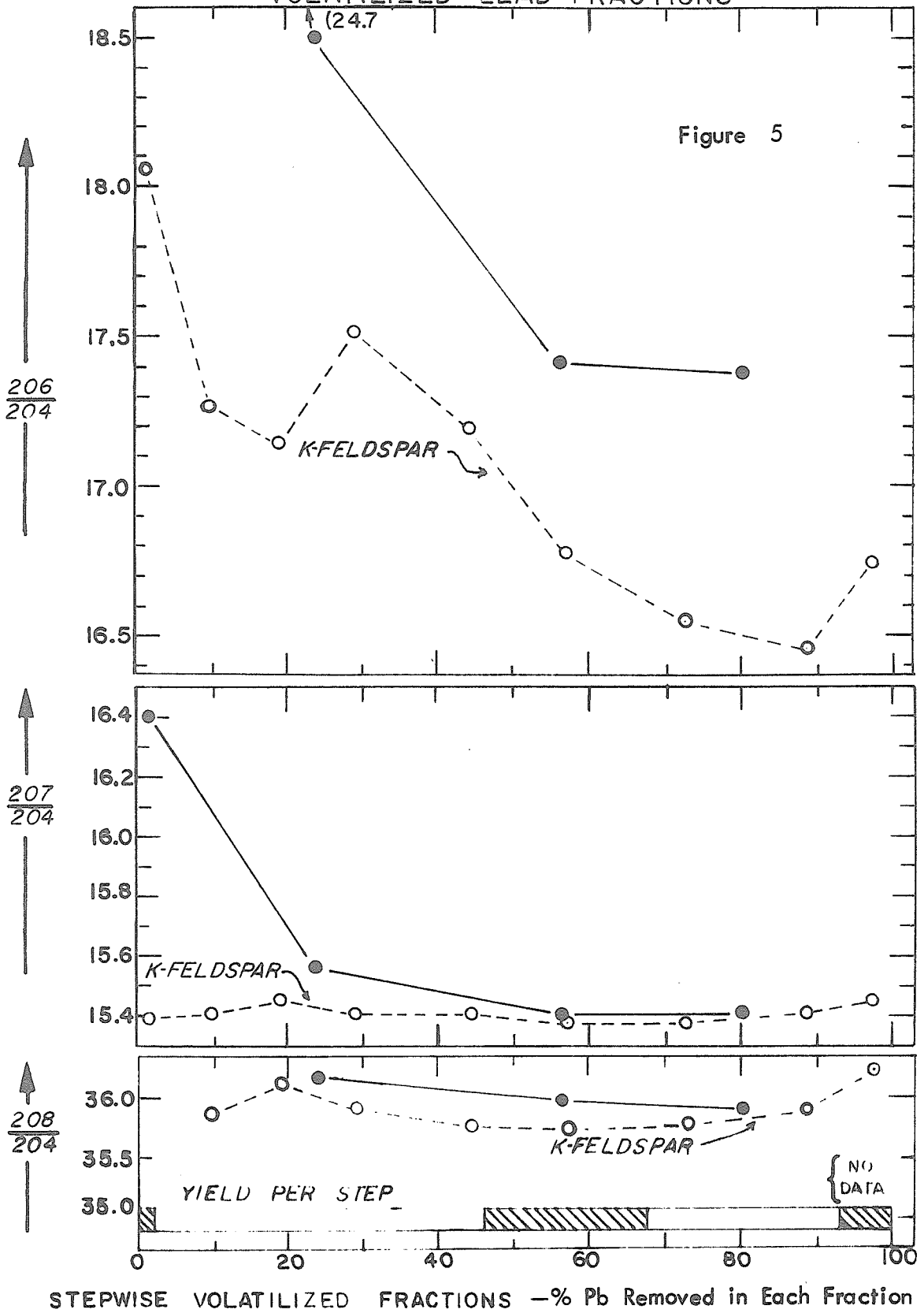


Table 7

Ruin Granite K-feldspar Lead Analyses

	<u>206/204</u>	<u>207/204</u>	<u>208/204</u>	<u>206/207</u>	<u>206/208</u>	Yield (μg)	Temperature of Volatilization
Total K-spar Lead	16.44	15.40	35.94	1.0694	.4575	68ppm Pb	
Est. accuracy	$\pm 1.5\%$	$\pm 1.5\%$	$\pm 1.5\%$	$\pm 0.5\%$	$\pm 1.0\%$.065ppm U	
Corrected for <u>in situ</u> U-decay (1.46 b.y.)	16.43	15.40		1.0665			

Stepwise Volatilization Series 1 Fractions: 1.45 g K-feldspar

1A (1)	-	-	-	1.0875	.4665	4	1070°C
				.10%	.15%		
1B	16.59	15.41	36.51	1.0772	.4545	5	1090°C
	.20%	.20%	.20%	.10%	.15%		
1C	16.53	15.40	36.06	1.0738	.4584	8	1120°C
	.15%	.15%	.15%	.10%	.12%		
1D	17.37	15.44	36.10	1.1251	.4811	8	1150°
	.30%	.30%	.30%	.16%	.20%		
1E	16.55	15.37	35.99	1.0768	.4598	7	1180°
	.20%	.20%	.20%	.15%	.15%		
1F	n o	d a t a	- - - - -	- - - - -	- - - - -	13	1200°
1G	16.32	15.38	35.86	1.0613	.4552	16	1230°
	.20%	.20%	.20%	.17%	.18%		
1H	16.32	15.42	35.94	1.0584	.4540	12	1250°
	.15%	.15%	.15%	.05%	.10%		
1 Residue (2)	16.27	15.34\$	-	1.0606	-	3	chemical attack
	.35%	.35%		.20%			

(1) Signal:background ratio not sufficiently high to permit accurate estimation of Pb²⁰⁴ abundance.(2) Pb²⁰⁸ spike used as carrier for mass spectrometric analysis.

Table 8

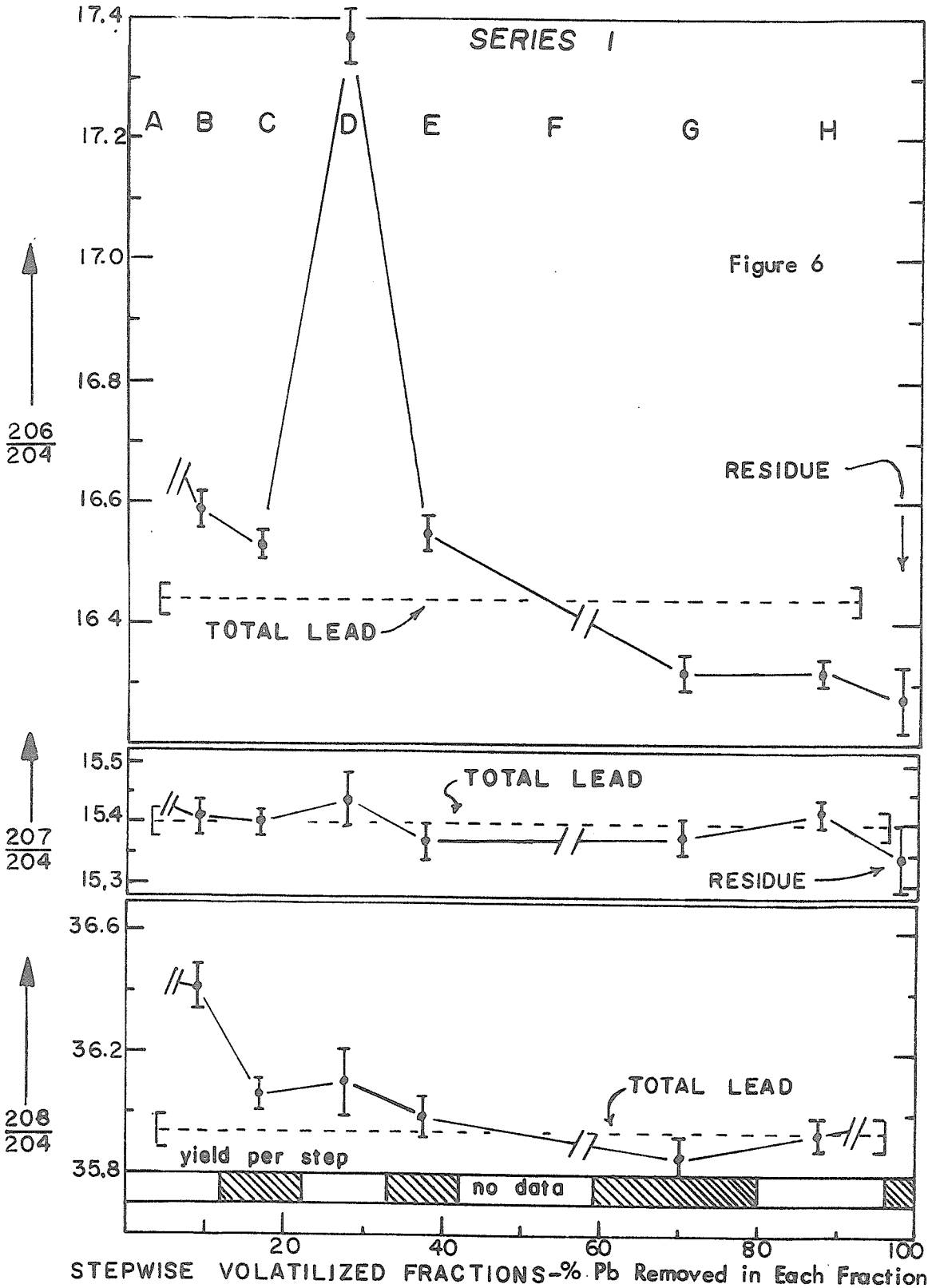
Ruin Granite K-feldspar Lead Analyses - Continued
Stepwise Volatilization Series 2 Lead Fractions: 1.33 g K-feldspar

<u>Fraction</u>	<u>206/204</u>	<u>207/204</u>	<u>208/204</u>	<u>206/207</u>	<u>206/208</u>	<u>Yield (μg)</u>	<u>Temperature of Volatilization</u>
Total K-spar Lead	16.44 .15%	15.40 .15%	35.94 .15%	1.0674 .05%	.4575 .10%		
2A (1)	-	-	-	1.0879 \pm .25%	.4650 \pm .40%	4	1060°C
Est. acc. (\pm)	-	-	-				
2B (1)	-	-	-	1.0745 .10%	.4595 .10%	10	1090°C
2C (1)	-	-	-	1.0732 .10%	.4585 .15%	7	1120°C
2D (2)	16.64 .25%	15.46 .25%	-	1.0762 .10%	-	8	1150°C
2E (1)	-	-	-	1.0781 .30%	.4602 .15%	3	1180°C
2F	16.43 .20%	15.41 .20%	35.96 .15%	1.0662 .10%	.4569 .10%	10	1220°
2G (1)	-	-	-	1.0621 .50%	.4560 .50%	20	1250°
2 Residue (1,2)	-	-	-	1.1886 .75%	-	2	Chemical attack

(1) Signal:background ratio of mass spectrometer run not high enough to permit accurate estimation of Pb²⁰⁴ abundance.

(2) Pb²⁰⁸ spike used as carrier for mass spectrometric analysis.

RUIIN GRANITE
K-FELDSPAR VOLATILIZED LEAD FRACTIONS



RUIN GRANITE K-FELDSPAR VOLATILIZED LEAD FRACTIONS

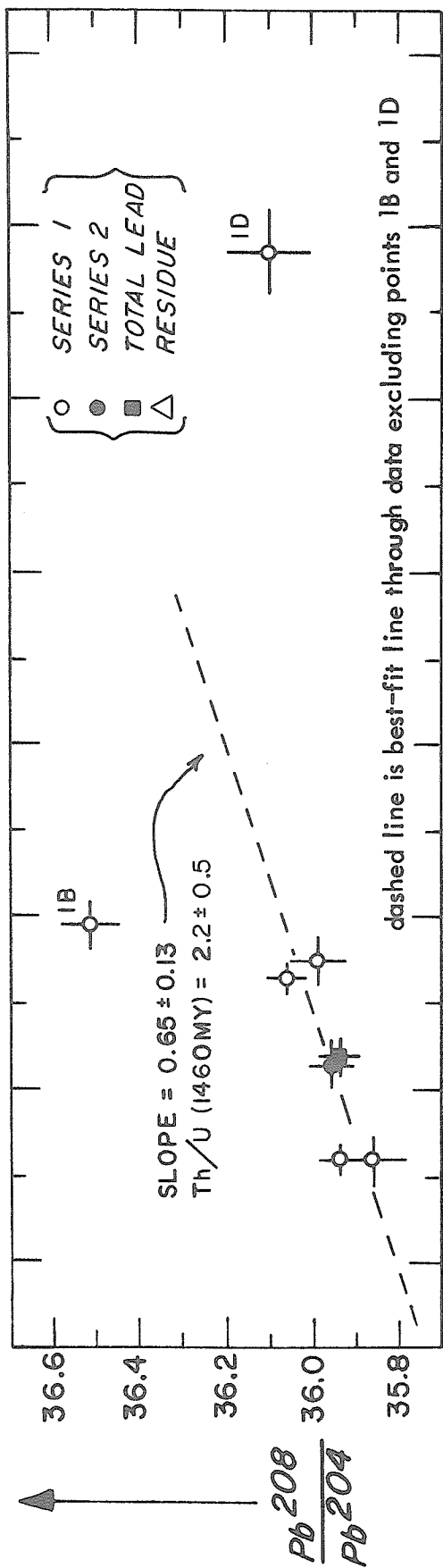
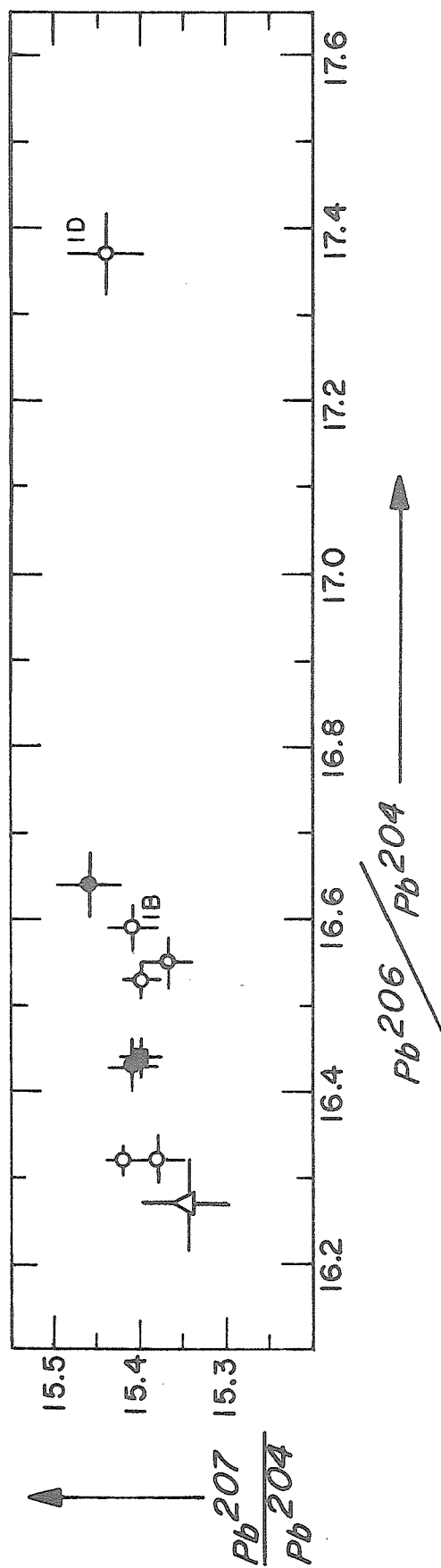
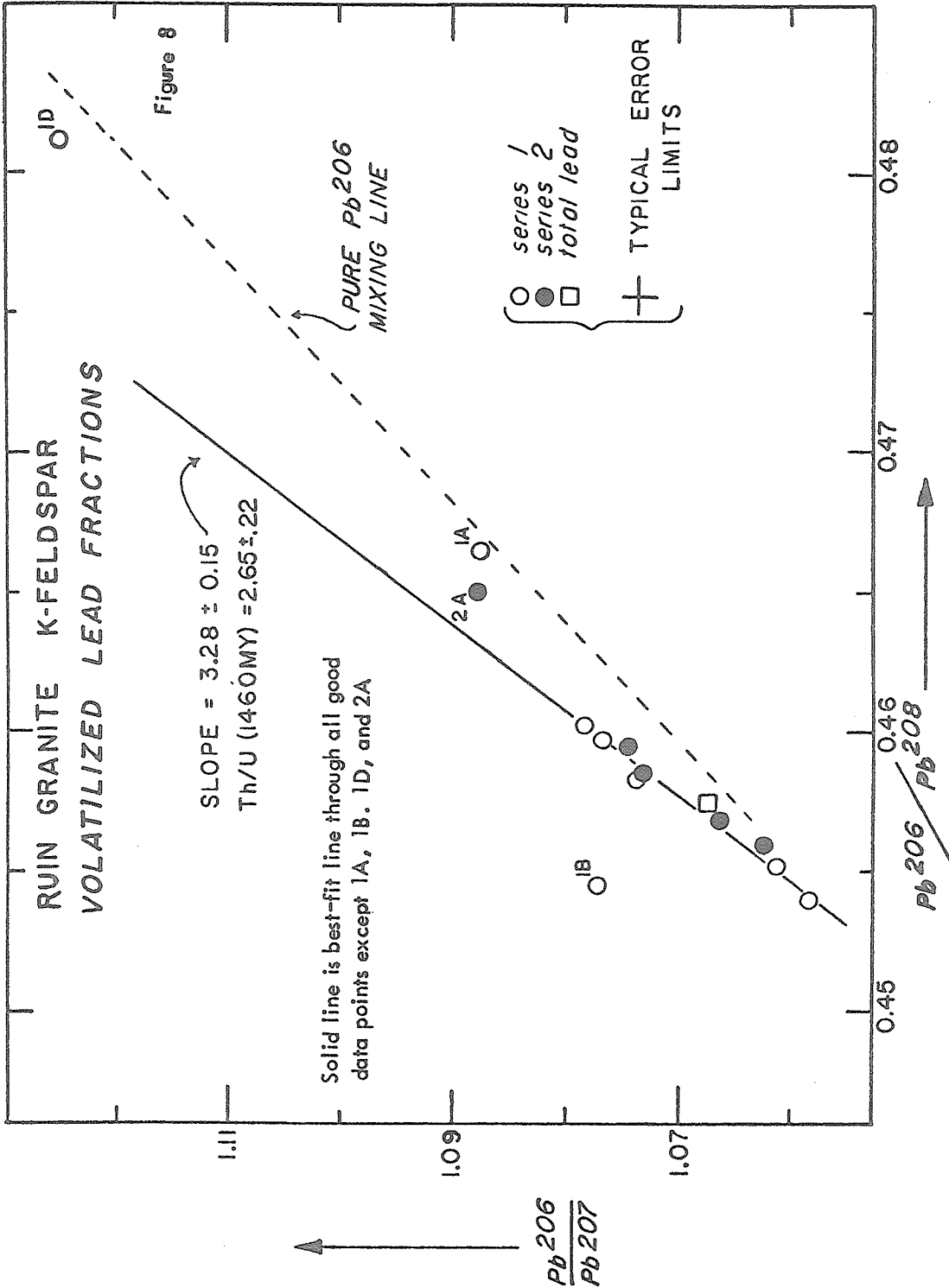


Figure 7





Pb gain or possibly to U loss, and does not represent the original rock lead. The 206/204 of the volatilized leads is the most variable ratio, ranging from 17.37 (fraction 1D) to 16.27 (unvolatilized lead, series 2). The 207/204 is somewhat scattered (ranging from 15.35 to 15.46), but, with the exception of fraction 2D, a value of 15.40 falls within the error limits of all of the lead fractions. The general trend of the volatilized leads is for the more volatile fractions to be higher in 206/204, 206/207, and 208/204 than the less volatile fractions; the trend is not simple, however, as reversals of the trend for 206/204 and 206/207 are present in the 1150°-1180° volatilized fractions.

Interpretation of the existence of a covariance of 207/204 with 206/204 is difficult, as the precision of the 207/204 determinations is only about 0.25%. From inspection, it appears that the scatter of the 207/204 data could be masking a (linear) dependence of 207/204 on 206/204 with possible slopes of from 0.00 to 0.09 (range of slopes of lines passing through error limits of most of the points).

The 208/204 variation appears to be dependent on the 206/204 variation (fig. 7). The best-fit line through the data, excluding fractions 1B and 1D, has a slope of 0.65 ± 0.13 . The 206/207 - 206/208 also appear covariant, with the best-fit line through most of the data (exceptions are discussed later) having a slope of 3.28 ± 0.15 (fig. 8). Volatilized fractions 1A, 1B, 1D, and 2A appear anomalous on these plots.

MARBLE MOUNTAINS GRANITE K-FELDSPAR

The lead from five stepwise volatilized fractions and the unvolatilized residual lead were analyzed for the Marble Mountains granite K-feldspar concentrate (table 9, figs. 9, 10, 11). The 206/204 and 208/204 of the volatilized leads and unvolatilized residue vary distinctly beyond analytical uncertainty, as do the 206/207 and 206/208. Except for the unvolatilized residual lead, which is believed to be biased by a 204 mass spectrometric measurement error (see p. 299), the 207/204 ratios do not vary outside of analytical error. The relatively large uncertainties in 204 measurement for most of the analyses of these fractions, however, could be obscuring a variation in 207/204 as high as about 0.6%. Compared to the variations of the Lawler Peak and Ruin granite K-feldspar leads, the Marble Mountain granite K-feldspar leads show much greater variation in 208/204.

The trend of variation of the 206/204 of the fractions is a monotonic decrease with decreasing volatility, so that the least volatile fractions have the lowest 206/204. The 206/207 has a similar trend of variation, while the trend in 208/204 is somewhat irregular.

GIANTS RANGE GRANITE K-FELDSPAR

The leads from three out of five volatilized lead fractions (two analyses were unsuccessful) and the unvolatilized residual lead fraction were analyzed for the Giants Range granite K-feldspar concentrate (table 10, figures 12, 13, 14). The 206/204 and 208/204 values of the volatilized fractions vary outside of analytical error, and are

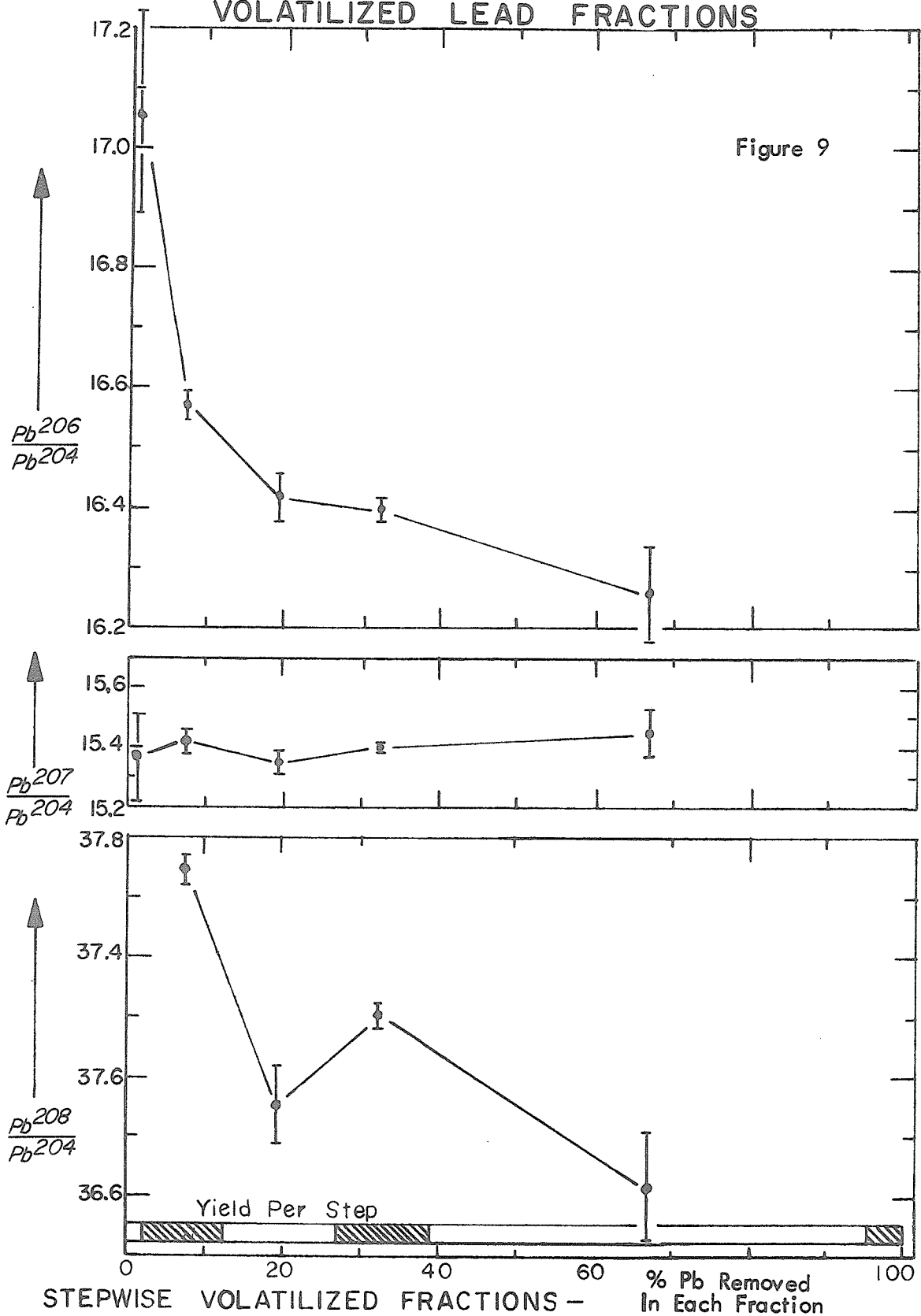
Table 9

Marble Mts. Granite K-feldspar Lead Analyses: Stepwise Volatilized Fractions (0.80 g K-feldspar)

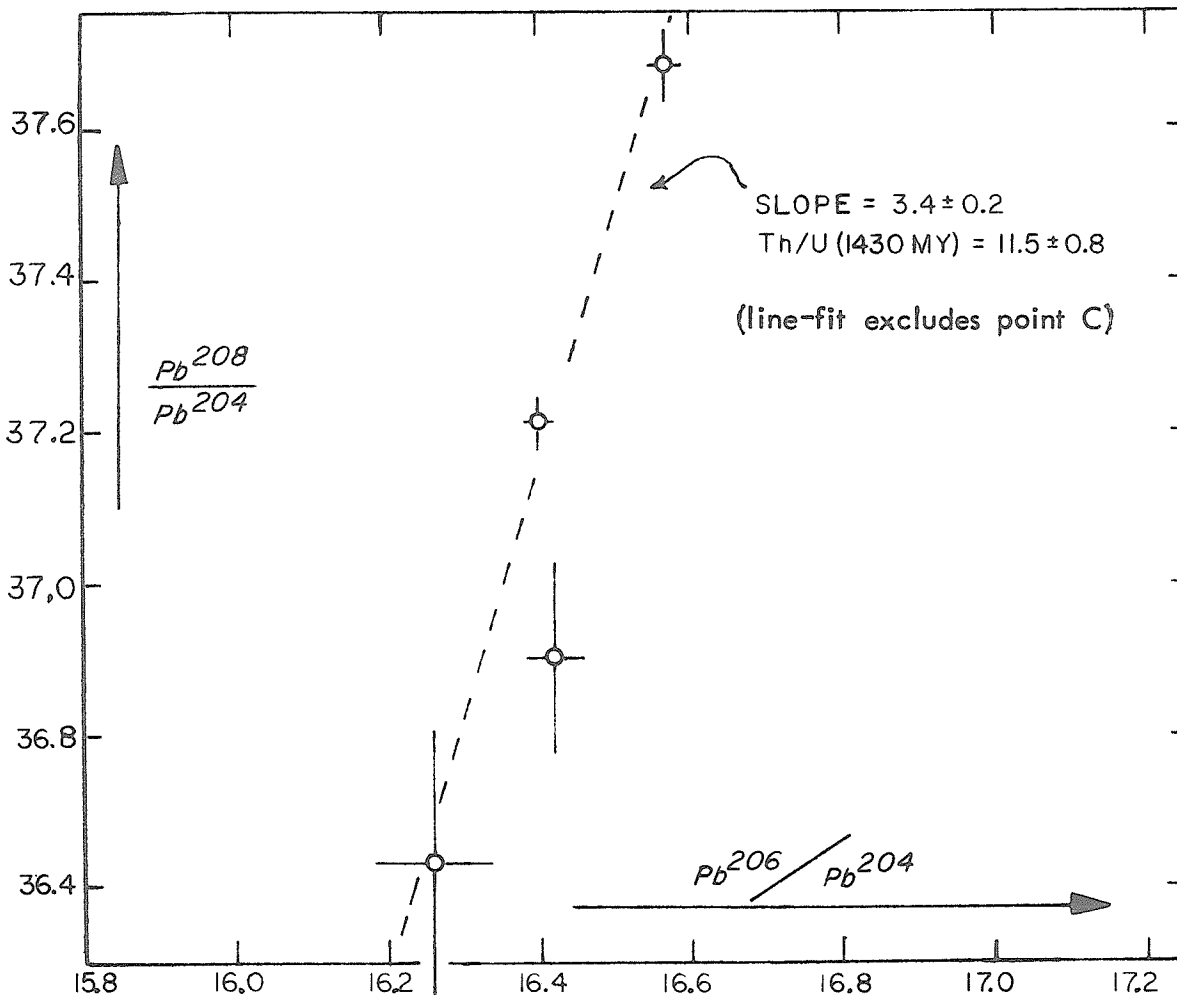
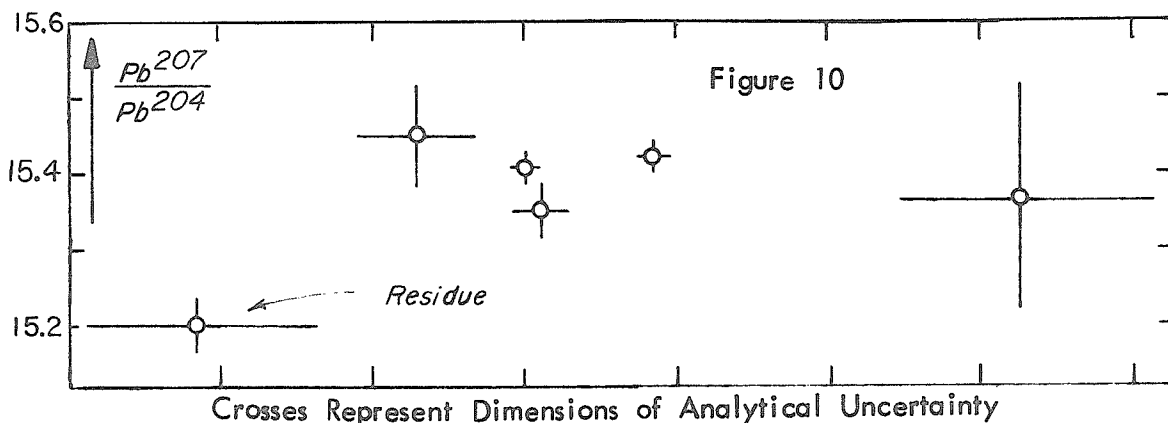
<u>Fraction</u>	<u>206/204</u>	<u>207/204</u>	<u>208/204</u>	<u>206/207</u>	<u>206/208</u>	<u>Yield (μg)</u>	<u>Temperature of Volatilization</u>
A (1)	17.06	15.365	-	1.1100	-	1.1	1090°C
Est. accuracy	$\pm 1\%$	$\pm 1\%$.25%			
B	16.57	15.42	37.68	1.0743	.4397	4.5	1135°
	.15%	.15%	.15%	.10%	.10%		
C	16.42	15.35	36.90	1.0700	.4451	6.5	1180°
	.25%	.25%	.35%	.20%	.35%		
D	16.40	15.405	37.21	1.0644	.4407	6	1220°
	.10%	.10%	.10%	.05%	.05%		
E	16.26	15.45	36.63	1.0521	.4438	26	1270°
	.50%	.50%	.50%	.35%	.35%		
Residue (1)	15.97	15.20	-	1.0509	-	2	Chemical Attack
(2)	1%	1%		1%			
Calculated Composite Feldspar Leads (2)							
	16.35	15.43	-	1.0597			
Corrected for <u>in situ</u> U-decay (1.43 b.y.)							
	16.32	15.43	-	1.0577			
K-feldspar Lead content	= 97.0 ppm						
K-feldspar Uranium content	= 0.23 ppm						
K-feldspar Thorium content	= 0.47 ppm						

(1) Pb²⁰⁸ spike used as carrier for mass spectrometric analysis.(2) Pb²⁰⁴ estimation of the residue lead evidently affected by non-lead mass 204 interference during analysis (see text). If 207/204 is actually 15.40, then 206/204 = 16.18. This figure used in weighted average calculation.

MARBLE MTS. GRANITE K-FELDSPAR
VOLATILIZED LEAD FRACTIONS



MARBLE MTS. GRANITE K-FELDSPAR
VOLATILIZED LEAD FRACTIONS



MARBLE MTS. GRANITE K-FELDSPAR
VOLATILIZED LEAD FRACTIONS

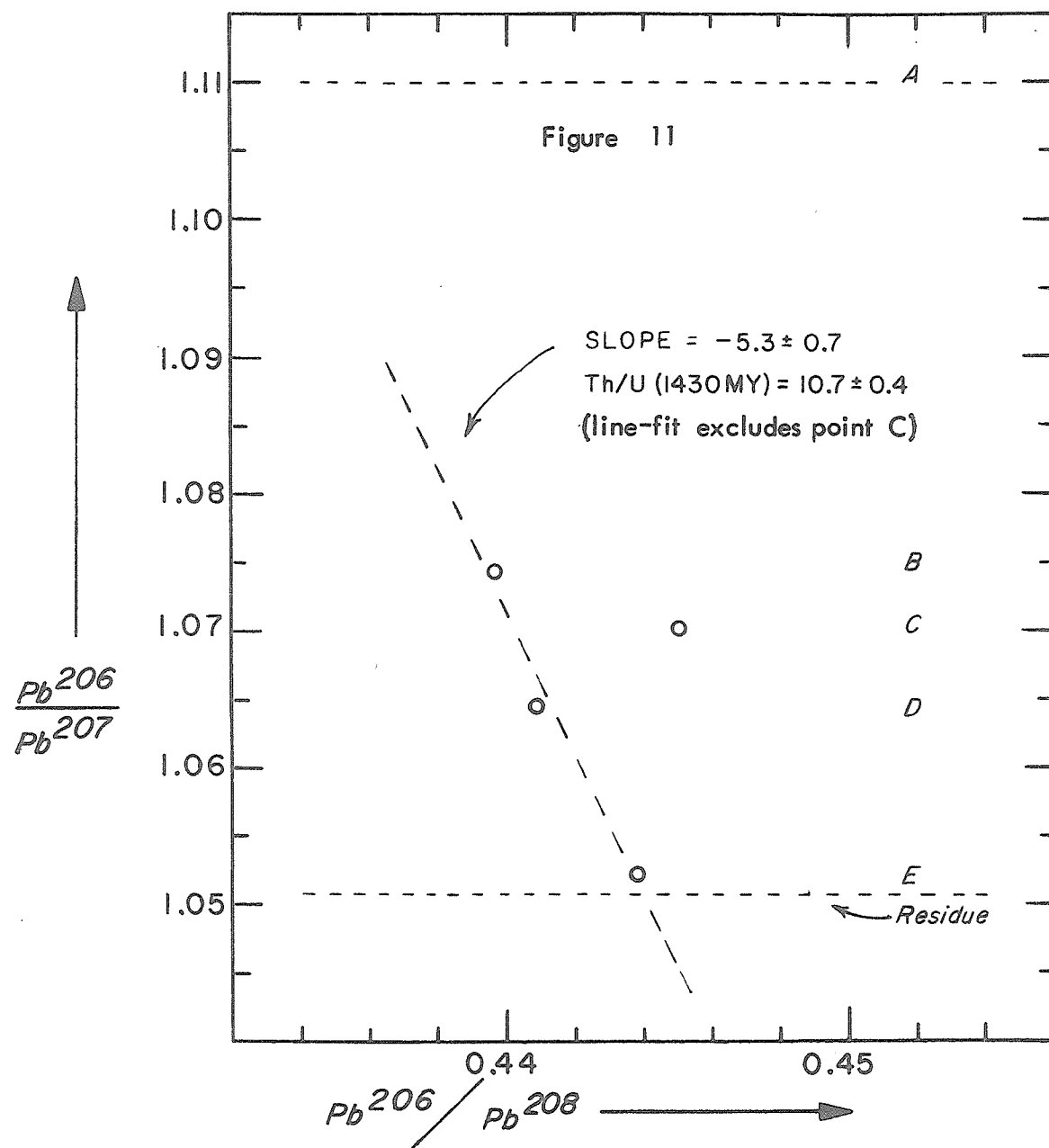


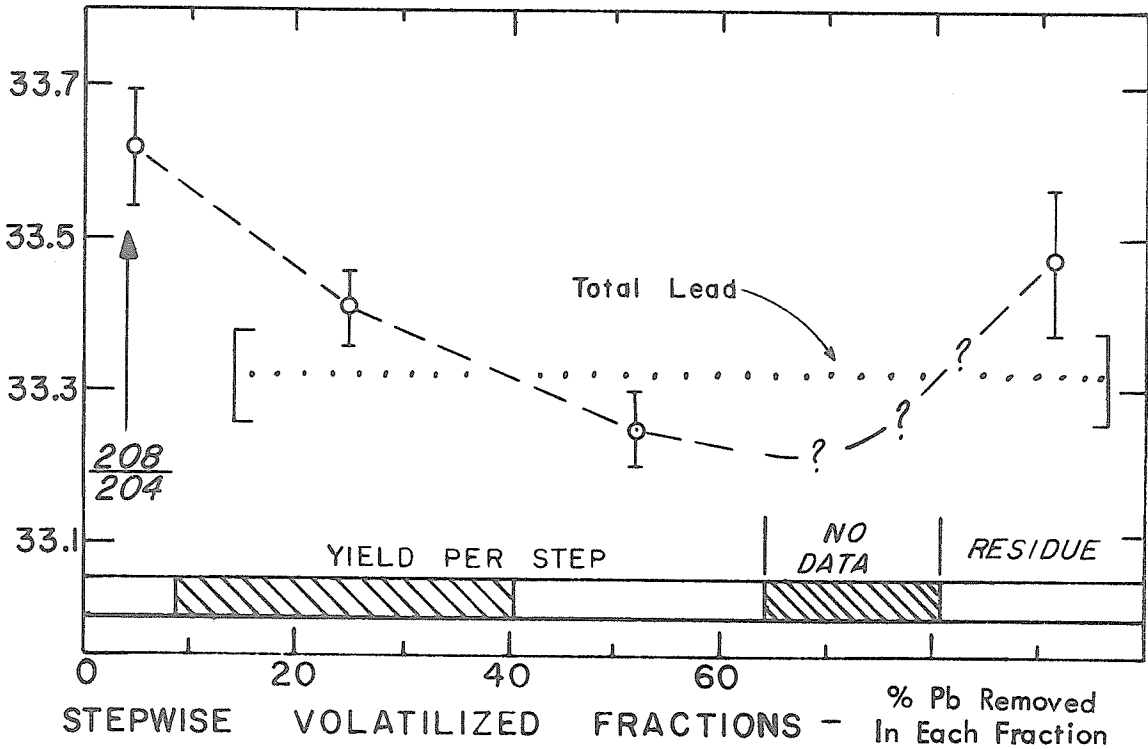
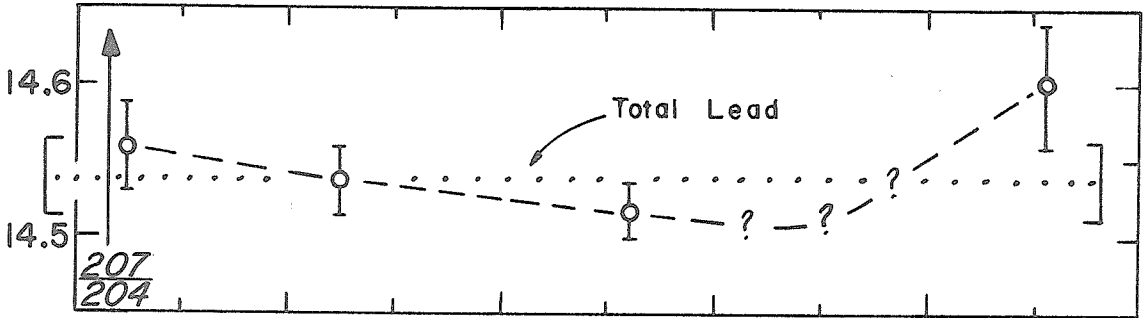
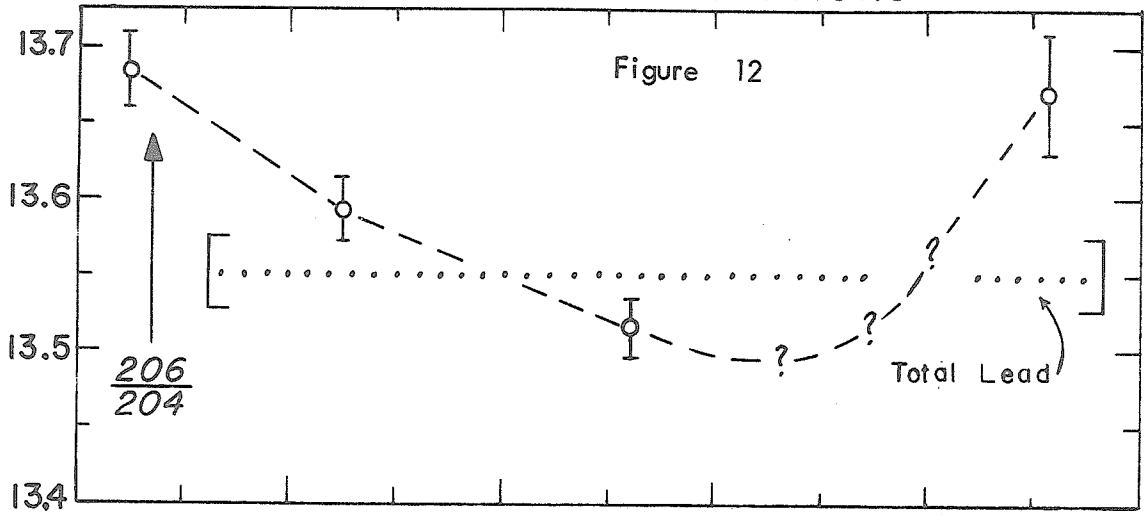
Table 10

Giant's Range Granite K-feldspar Lead Analyses

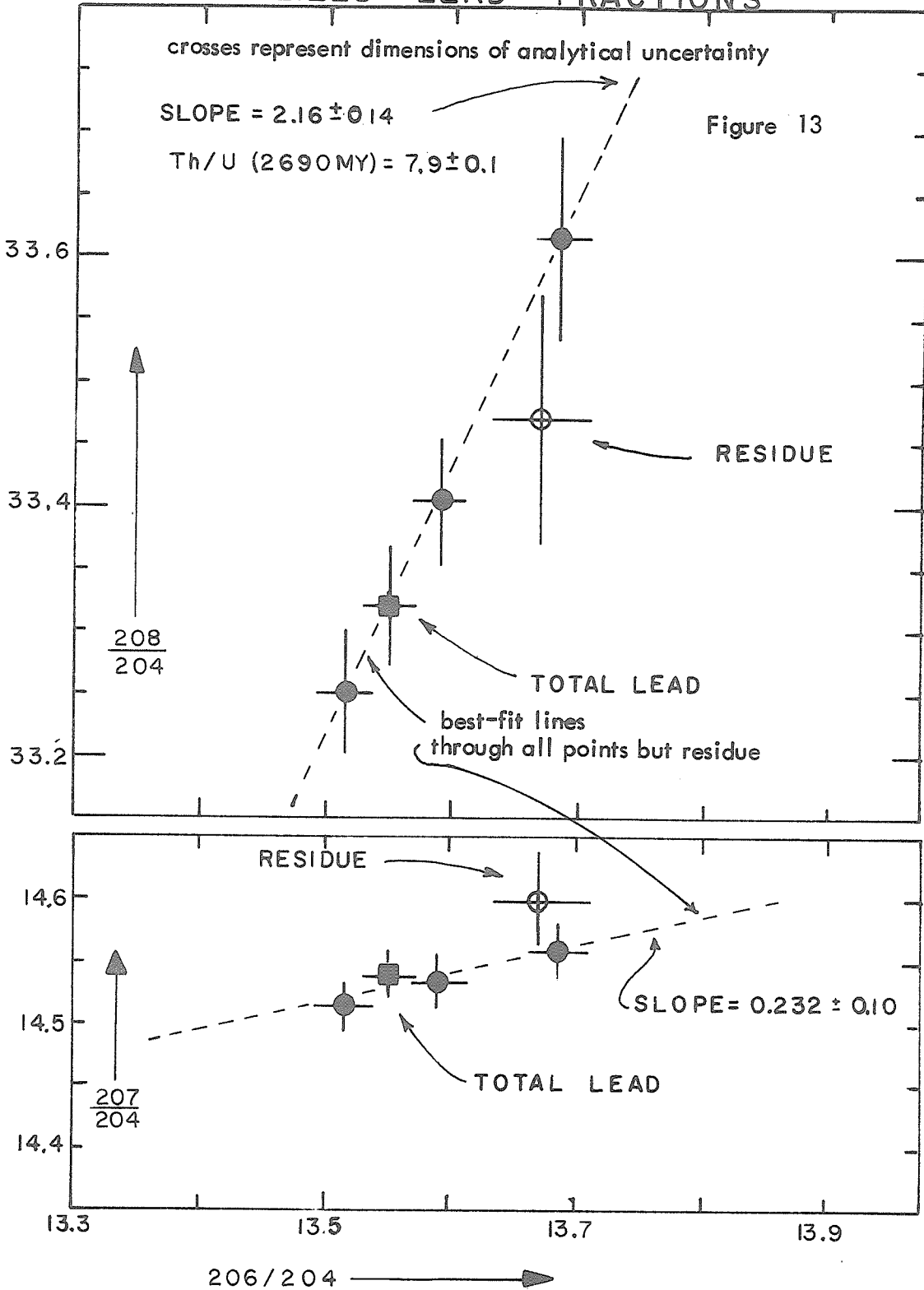
<u>Fraction</u>	<u>206/204</u>	<u>207/204</u>	<u>208/204</u>	<u>206/207</u>	<u>206/208</u>	<u>Yield (μg)</u>	<u>Temperature of Volatilization</u>
Total K-spar	13.551 \pm .15%	14.537 \pm .15%	33.320 \pm .15%	.9322 \pm .10%	.40669 \pm .15%	11.15 ppm Lead .00 ⁺ .02 ppm U -.00	
Lead Est. Accuracy							
Stepwise Volatilized Fractions: - 12.96 g K-feldspar							
A	-	-	-	-	-	0	1070°C
B	13.685 .20%	14.559 .20%	33.615 .25%	.9400 .10%	.40711 .20%	6	1120°
C	13.593 .15%	14.535 .15%	33.406 .15%	.9352 .10%	.40690 .10%	20	1150°
D	13.515 .15%	14.515 .15%	33.251 .15%	.9311 .05%	.40645 .10%	15	1170°
E	n o d a t a	n o d a t a	n o d a t a	n o d a t a	n o d a t a	8	1200°
F	n o d a t a	n o d a t a	n o d a t a	n o d a t a	n o d a t a	3	1230°
Residue	13.670 .30%	14.598 .30%	33.471 .30%	.9364 .15%	.40841 .15%	>12	Chemical Attack

GIANTS' RANGE GRANITE K-FELDSPAR VOLATILIZED LEAD FRACTIONS

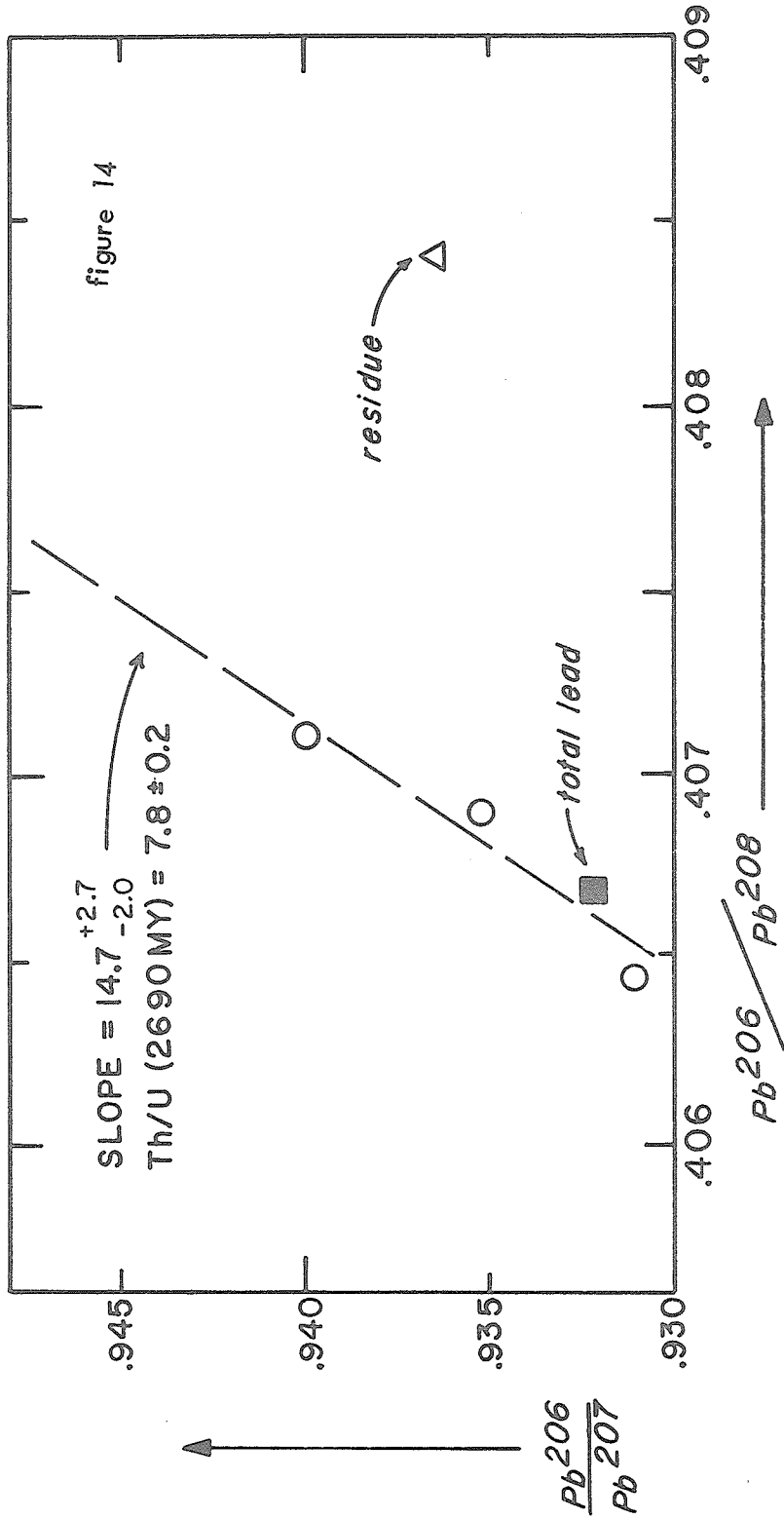
Figure 12



GIANTS' RANGE GRANITE K-FELDSPAR
VOLATILIZED LEAD FRACTIONS



GIANTS' RANGE GRANITE K-FELDSPAR
VOLATILIZED LEAD FRACTIONS



colinear within analytical error. The 207/204 of the volatilized lead fractions does not vary demonstrably outside of analytical error, but does vary approximately colinearly with the 206/204 and 208/204. The residual lead does not fall on the trend of the volatilized and total lead fractions*.

The trend of the three analyzed volatilized fractions is for the 207/204, 208/204, and 206/204 to be lower for less volatile lead fractions. The isotopic composition of the residual lead does not follow this trend.

*It is possible that the extended handling that the residue received during dissolution in HF increased the actual contamination beyond the estimated (blank) contamination. However, the necessary amount of contamination, 0.4 micrograms Pb, is greater than any observed blank value.

STEPWISE HF ATTACK EXPERIMENTS

PAYSON GRANITE K-FELDSPAR

The Payson granite K-feldspar concentrate was twice subjected to a series of partial stepwise HF attacks, and the leads from most of the partial attacks were analyzed (the last two attacks for the first series did not give successful mass spectrometric runs). The results from these experiments are given in table 11 and figure 15.

These data show variations in 206/204 and 208/204 of the stepwise dissolved lead fractions outside of analytical error, but only slight (within estimated analytical error) 207/204 variations*. The slight variation in the 207/204, however, is approximately colinear with the 206/204 and 208/204 variation. A best-fit line through the 207/204 - 206/204 points has a slope of $0.089 \pm .021$, so the 207/204 variation is evidently real.

In both stepwise attack series, the trend of lead isotopic variation is for the 206/204, 207/204, and 208/204 to be lower for the fractions dissolved later in the attack series.

The most noticeable physical effect of the partial HF attacks was a sharp reduction in the apparent degree of alteration (turbidity) of the feldspar grains. As plates 24, 25, and 26 show, there is a progressive decrease in the opacity of the grains, until virtually all

*(Total 206/204 variation = 3.9%, 208/204 variation = 1.1%, 207/204 variation = 0.39%).

Table 11

Payson Granite K-feldspar Lead Analyses

Total Feldspar: [Pb] = 32.80 ppm [U] = .075 ppm [Th] = 0.165 ppm

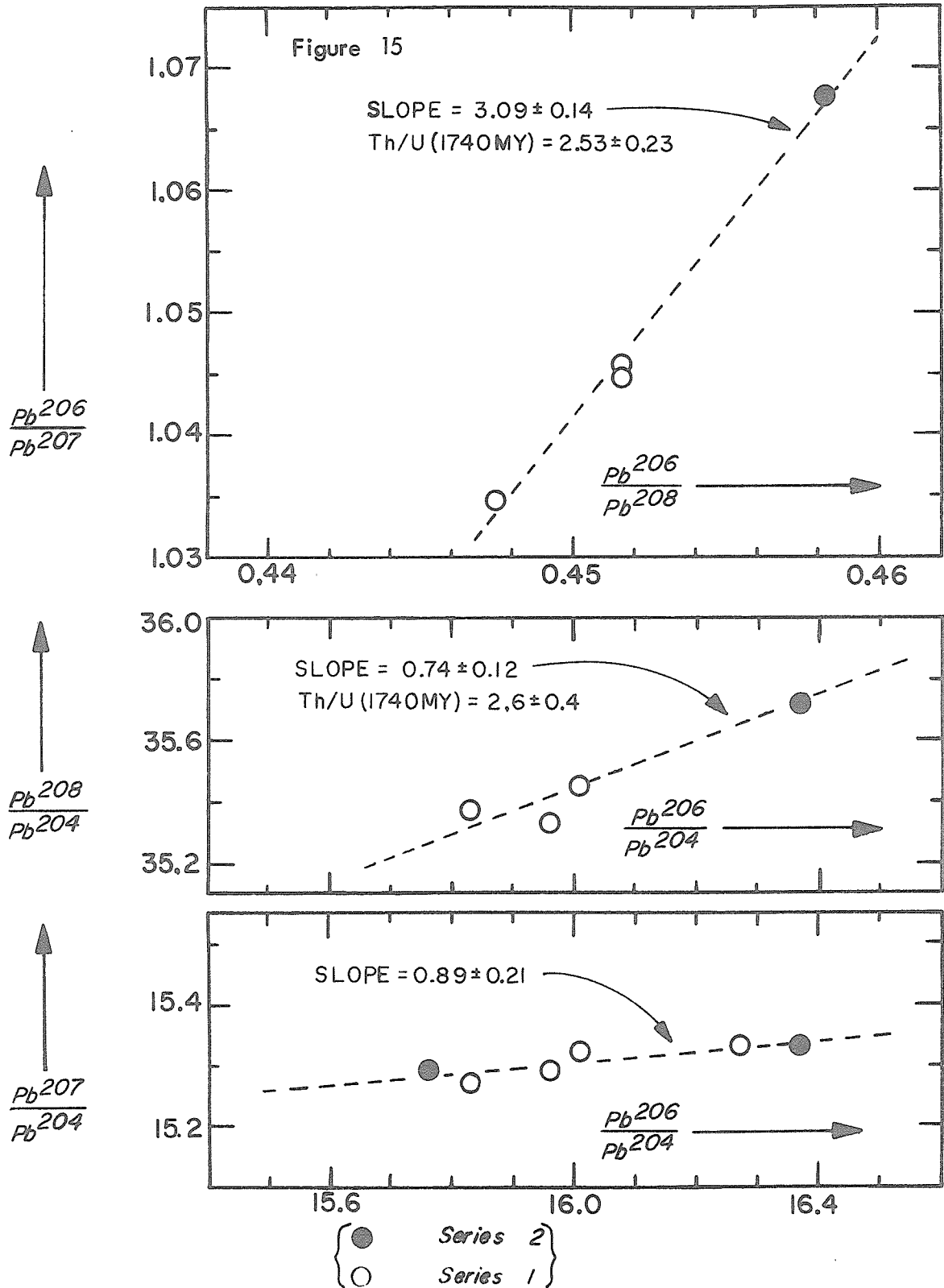
Stepwise Partial HF Attack Lead Fractions: (5% HF, 20 min. attacks)

<u>Fraction</u>	<u>206/204</u>	<u>207/204</u>	<u>208/204</u>	<u>206/207</u>	<u>206/208</u>
<u>Series 1:</u>					
1A ⁽¹⁾	16.27	15.33	-	1.0617	-
Est. accuracy	±.25%	±.25%		±.10%	
1B	15.96 .10%	15.29 .10%	35.33 .10%	1.0448 .10%	.4516 .10%
1C	16.01 .20%	15.32 .20%	35.45 .35%	1.0459 .10%	.4517 .35%
1D	15.83 +.30% -.10%	15.27 +.30% -.10%	35.37 +.30% -.10%	1.0348 ±.30%	.4475 ±.30%
1E	n o d a t a				
1 Residue	n o d a t a				
<u>Series 2:</u>					
2A	16.37 .20%	15.33 .20%	35.72 .20%	1.0676 .10%	.4583 .10%
2 Residue ⁽¹⁾	15.76 .30%	15.29 .20%	-	1.0308 .20%	-

(1) Pb²⁰⁸ spike used as carrier for mass spectrometric analysis.

PAYSON GR. K-FELDSPAR

STEPWISE HF ATTACK LEAD FRACTIONS



apparent alteration material is gone. A more subtle effect was the decrease in the abundance of perthitic grains with increasing HF attack. This, and the very ragged edges displayed by perthitic grains surviving extended attack, suggests that the exsolved plagioclase is preferentially dissolved in the HF.

LAWLER PEAK GRANITE K-FELDSPAR

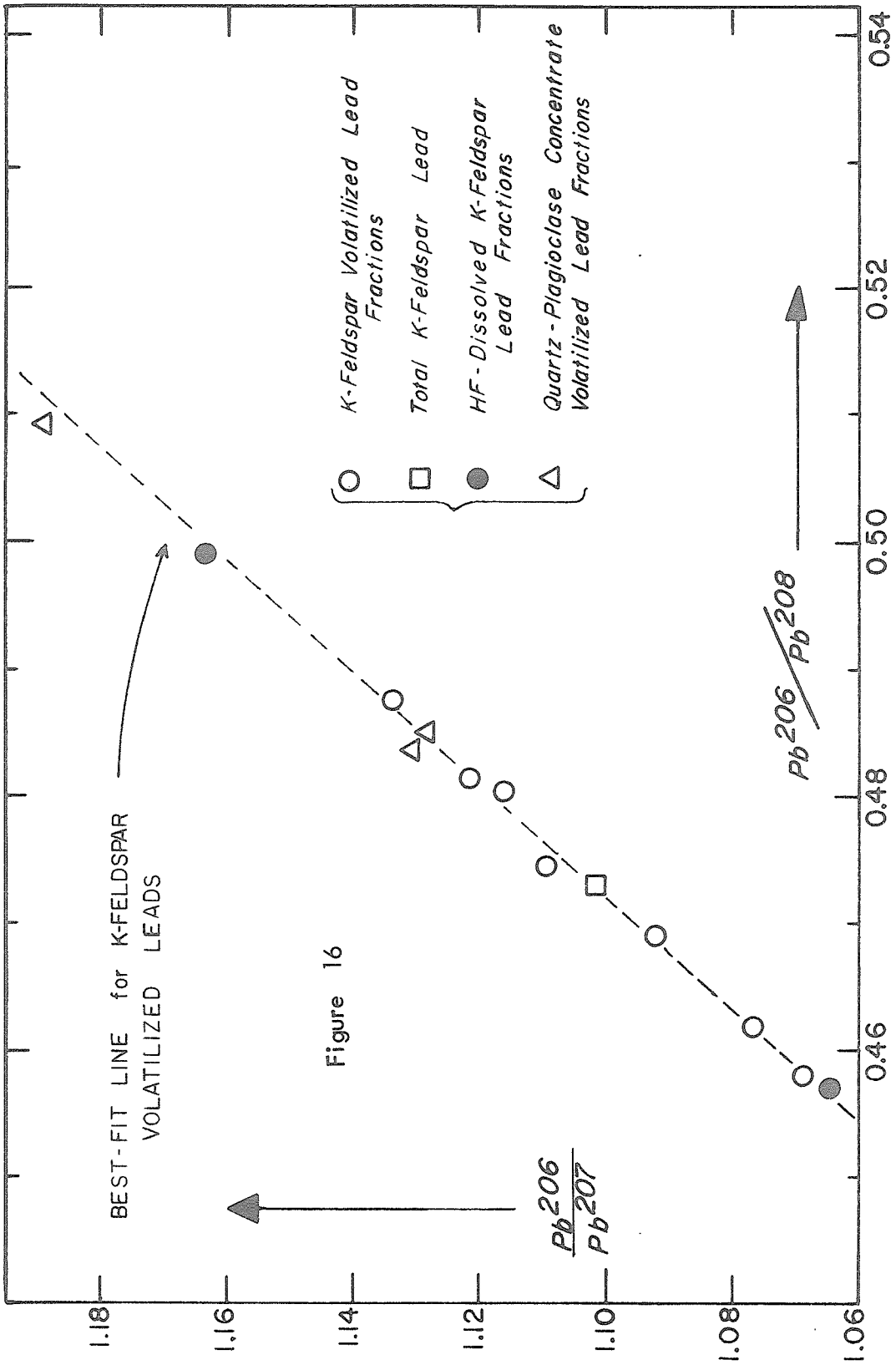
The Lawler Peak granite K-feldspar concentrate was subjected to a three-step HF attack. Analyses from the lead of the first and last dissolved fractions were obtained (table 5), but not for the intermediate fraction.

These data show a similar lead isotope heterogeneity as was observed for the volatilized K-feldspar concentrate lead fractions. The first-dissolved fraction (Pb^{204} data not obtained) falls, within analytical error, on the best-fit line through the volatilized lead fraction data on a 206/207 - 206/208 plot (fig. 16). This fraction is not as high in 206/207 and 206/208 as the first-volatilized fraction, but is distinctly higher in these isotope ratios than the total feldspar lead. The last-dissolved lead fraction is lower in 206/204 (206/204 = 16.39) than the volatilized lead fraction with the lowest 206/204 (step H, with 206/204 = 16.45), but slightly higher in 207/204 (15.40) and 208/204 (35.86) than several of the volatilized lead fractions.

The observable effects of the partial HF attack on the K-feldspar concentrate were (after the second partial attack),

a) increase in the quartz:K-feldspar ratio from about 0.14 in the

LAWLER PEAK GRANITE - LEADS



starting material to .15 - .20 in the second attack residue,

b) presence of fluorite in the second attack residue (plate 20), evidently a reaction product of the HF and exsolved plagioclase in the K-feldspar concentrate,

c) ragged edges and sharp embayments, together with an apparent 50% decrease in average K-feldspar grain volume, and

d) disappearance of perthitic grains and turbid K-feldspar grains.

These effects are similar to those observed in the Payson granite

K-feldspar concentrate stepwise HF attack experiment.

DISCUSSION OF EXPERIMENTAL RESULTS

LAWLER PEAK GRANITE - MAJOR PATTERNS

Volatilized Leads

K-FELDSPAR

The most striking facet of the variation in the lead isotopic composition of the Lawler Peak granite K-feldspar concentrate volatilized leads is the large (11%) 206/204 variation contrasted with a variation in 207/204 so slight (less than ½%) as to be negligible within analytical error. As mentioned previously, the covariance of 207/204 with 206/204 of the volatilized lead fractions is $0.00 \pm .02$ (one standard deviation error to best-fit line). The implications of this lack of covariance are important.

In view of the demonstrable isotopic heterogeneity of the feldspar concentrate lead, one must view the total feldspar lead as being a mixture of lead incorporated at the time of crystallization of the feldspar and of one or more lead components incorporated since the time of crystallization of the feldspar (in the absence of plausible mechanisms for a heterogeneity in lead isotopes in the feldspar at the time of crystallization). Natural physical fractionation of the lead isotopes cannot be invoked to explain the observed heterogeneity, because it is both theoretically implausible (Russell and Farquhar,

1960, p. 2) and inconsistent with the observed pattern of variation*.

The heterogeneously distributed Pb^{206} of the feldspar concentrate must therefore be partially radiogenic (i.e., ultimately derived from the decay of U^{238}). U^{238} is always associated with U^{235} , the parent isotope of Pb^{207} . No significant variation in the present-day abundance of U^{235} relative to U^{238} has been observed. Therefore, over any given time-interval some Pb^{207} must accompany Pb^{206} generated by equilibrium decay of uranium. Over the 1440 m.y. history of the Lawler Peak granite, the 207/206 of radiogenic lead has ranged from a maximum of 0.149 (instantaneously generated 1440 m.y. ago) to 0.046 (now being generated). The integrated radiogenic lead 207/206 over the last 1440 m.y. is 0.090. Therefore, if the radiogenic lead is not somehow isotopically fractionated, the minimum 207/206 of any radiogenic lead incorporated by the feldspar should be 0.046 -- corresponding to about $\frac{1}{2}\%$ higher 207/204 of the most volatile feldspar lead fraction compared to the least volatile. Because, however, negligible rock lead is generated by uranium over short (less than tens of millions of years) time intervals, the 207/206 of any incorporated radiogenic lead would probably be significantly higher than .046 (for instance, a ratio of .07 corresponds to radiogenic lead accumulated over the last 500 m.y.). No such covariance of 207/204 with 206/204 is observed, which suggests that uranium-derived intermediate daughter isotopes have been fractionated in such a way as to make available a radiogenic component enriched

*If mass-dependent fractionation were the mechanism for the observed variation, the 207/204 should vary about 3/2 the 206/204, and the 208/204 twice the 206/204.

in Pb^{206} relative to equilibrium radiogenic 207/206.

Processes leading to the enrichment of Pb^{206} by intermediate daughter fractionation have been proposed by Holmes (1948), and Kulp, Bate, and Broecker (1954). That Pb^{206} enrichment (or depletion) is a reasonable possibility is evident upon inspection and comparison of the two uranium isotope decay chains. The intermediate daughter element with the highest expected rate of diffusion is the noble gas, radon. This element is present in both the U^{238} and U^{235} decay chains; however, the half-life of the U^{238} radon intermediate daughter, Rn^{222} (3.8 days), is several orders of magnitude longer-lived than the U^{235} intermediate daughter, Rn^{219} . To the extent that diffusion alone contributes to intermediate daughter loss, then, Pb^{206} loss would be expected to predominate over Pb^{207} loss. Measurements of the radon leakage rate of minerals have been made by Giletti and Kulp (1955), Cherdyntsev (1961), and Starik et al (1955). The Rn^{222} leakage observed by Giletti and Kulp ranged from 0.3% to 17%, and the work of Cherdyntsev and of Starik et al showed that both Rn^{222} and Rn^{219} were lost by uranium-bearing minerals. The empirical possibility of Rn^{222} (and therefore Pb^{206}) mobility is thus well established.

The pattern of variation of the 208/204 and 207/204 (i.e., independent of 206/204 variation, apparently colinear with slope of $0.17 \pm .03$) requires, for the same reasons as stated for the Pb^{206} variation, that the feldspar have incorporated Th^{232} and U^{235} -derived radiogenic lead, as well as U^{238} -derived radiogenic lead, and that it have incorporated the radiogenic 207 and 208 in sites chemically distinguishable

from the sites of radiogenic Pb²⁰⁶ incorporation.

Since the 207/204 - 208/204 variations are not independent, one may use the colinearity of variation to calculate a model Th/U ratio for the source of the proposed admixed radiogenic lead component. Thus if the radiogenic lead component responsible for the 208/204 - 207/204 variation were generated and accumulated over a time, t, and the source Th/U remained constant for this time,

$$\eta = \left(\frac{\text{Th}^{232}}{\text{U}^{238}} \right)_{\text{source, present day}} = \frac{e^{\lambda_{235}t} - 1}{R_o \left(\frac{207}{208} \right)_{\text{observed radiogenic lead}} (e^{\lambda_{232}} - 1)}$$

where $R_o = \frac{\text{U}^{238}}{\text{U}^{235}}$ present day, λ_{235} , λ_{232} = decay constants of U²³⁵ and Th²³², and t = time before present.

Using $0.17 \pm .03$ as the 207/208 of the radiogenic lead component and 1440 m.y. as the time, the calculated η is 1.8 ± 0.3 . Except for zircon, which generally has η less than 0.5 (Silver, personal communication), such a value is reasonable for many of the common U and Th-bearing accessory minerals found in granites, such as sphene, allanite, monazite, and apatite¹.

At least two types of radiogenic lead, then, must have been incorporated by the feldspar. The first, predominantly pure Pb²⁰⁶

¹If variable errors in Pb²⁰⁴ measurement were contributing a small amount to the observed covariance, then the true 207/208 of the admixed lead is less than 0.17, and the η more than calculated.

possibly derived by long-term concentration of Rn²²², and the second a lead consisting of all of the radiogenic uranium and thorium daughter isotopes. The much larger and variable contribution of the (predominantly) pure Pb²⁰⁶ component prevents identification of small quantities of Pb²⁰⁶ associated with the 207 and 208-bearing component. The distinction (in volatilization experiments) between the two admixed radiogenic lead components is consistent with the different genetic interpretations proposed for them.

QUARTZ-PLAGIOCLASE CONCENTRATE

The quartz-plagioclase concentrate from the Lawler Peak granite, like the K-feldspar, evidently also incorporated radiogenic lead from outside of its mineral grains. Using an assumed lead isotopic composition for the (unanalyzed) residual unvolatilized lead slightly more primitive² ($206/204 = 16.4$, $207/204 = 15.4$) than the most primitive observed K-feldspar volatilized lead fraction ($206/204 = 16.45$, $207/204 = 15.40$)³, and using a total quartz-plagioclase concentrate lead calculated from the observed fractional yields and isotopic compositions, the in situ-decay corrected total concentrate lead had $206/204 = 17.23$, $207/204 = 15.43$. This $206/204$ is about 5% higher than that of the most primitive K-feldspar volatilized fraction.

²To put a conservative lower limit on estimating the amount of radiogenic lead in the quartz-plagioclase concentrate.

³In the absence of a total quartz-plagioclase concentrate lead analysis.

Calculating a total concentrate $207/204$ in the same manner, a value of 15.43 is obtained -- slightly higher, but within analytical error comparable to the more primitive of the K-feldspar volatilized leads. It is probable, however, that the quartz-plagioclase concentrate does contain a radiogenic lead component enriched in Pb^{206} . This conclusion is reached by calculating the total concentrate lead $206/207$. Using any plausible assumption for the isotopic composition of the lead of the unanalyzed residual lead ($206/204 = 16.2$ to 18.5 , $207/204 = 15.38$ to 15.60), and any reasonable initial rock lead ($206/204 = 16.2$ to 16.4 , $207/204 = 15.38$ to 15.40), the calculated $207/206$ of the admixed radiogenic lead is about $0.06 \pm .05$. Radiogenic lead accumulated over the age of the rock, however, would have $207/206 = 0.090$. Thus, unless the admixed radiogenic lead were generated predominantly only after the first third of the rock's history, a radiogenic lead component enriched in Pb^{206} is present in the quartz-plagioclase concentrate. The near-coincidence of the volatilized lead fractions of the quartz-plagioclase concentrate on a $206/207 - 206/208$ plot (fig. 16) with the best-fit line to the volatilized leads of the K-feldspar concentrate also suggests that the radiogenic lead of the quartz-plagioclase concentrate is similar to that of the K-feldspar.

DETAILED ANALYSIS OF THE LAWLER PEAK GRANITE FELDSPAR LEAD SYSTEMATICS

Reversals in Trend of Volatilized Leads

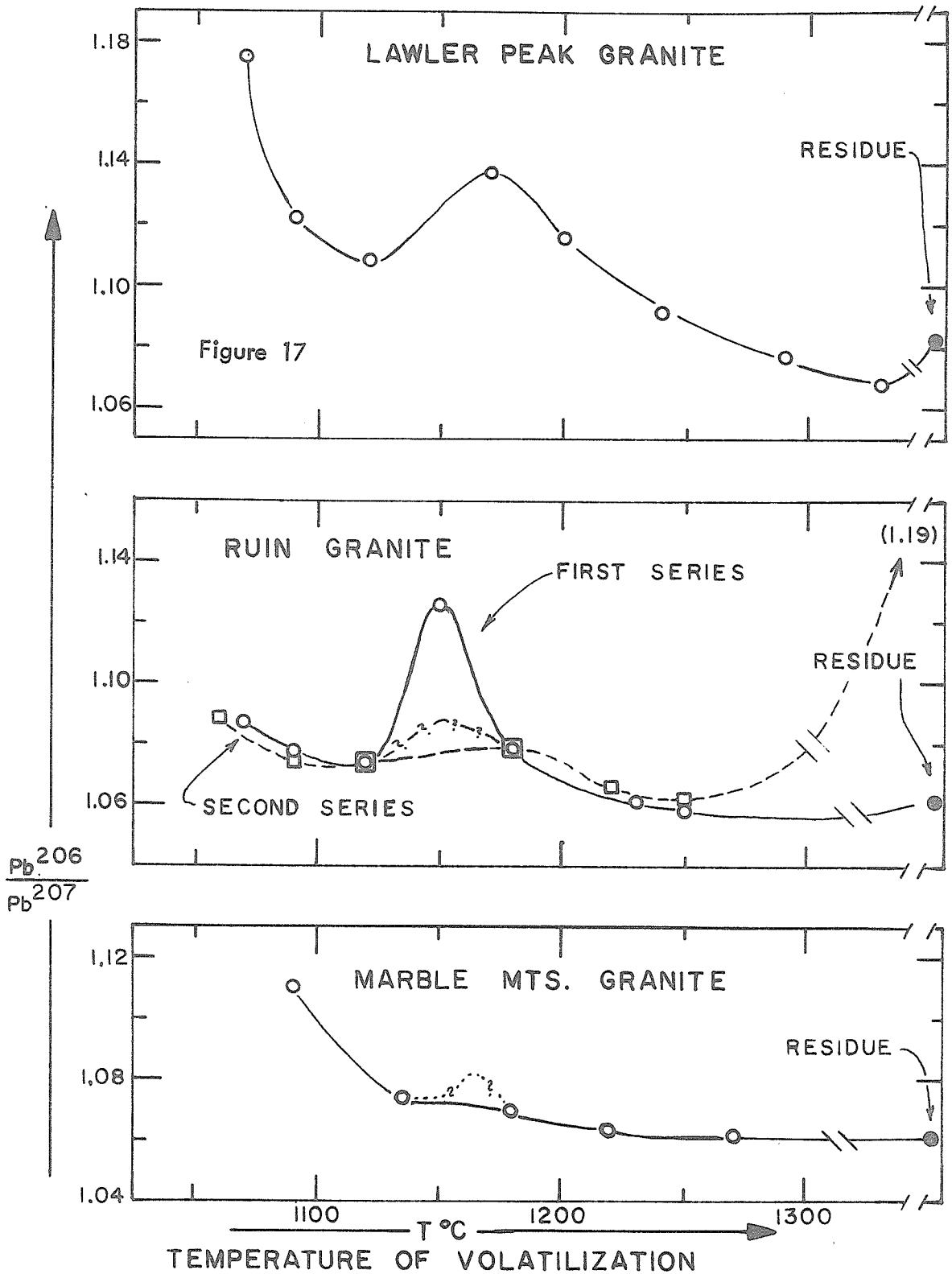
The two reversals in the trend of generally decreasing $206/204$ of the volatilized K-feldspar leads are worthy of comment. These reversals, with maxima at the fourth volatilization step and at the unvolatilized

residue, appear superimposed on the general trend (fig. 2). They cannot be spurious, and due to a Pb^{204} measurement error, as the very precisely measurable 206/207 value of the lead fractions demonstrates an identical pattern of variation (fig. 17). The 208/204 (and the more precisely measurable 208/207) shows a slight reversal at the third volatilization step, and at the unvolatilized residue.

The high 206/204 of the initially volatilized leads probably reflects the relatively loosely bound or thermally unstable nature of the radiogenic lead component responsible for the major 206/204 variation. The secondary maximum at the 1170° volatilization step suggests that radiogenic lead occupying a specific site or class of sites, whose stability vanishes at about 1170°, is present in the K-feldspar concentrate. Perhaps the radiogenic lead causing the high 206/204 of the initially volatilized fractions is present mainly in internal fractures, on grain boundaries, or perhaps in lattice defects within the K-feldspar. The lead causing the 1170° reversal in 206/204 trend, however, may correspond to radiogenic lead released from trace mineral impurities in the K-feldspar or mineral concentrate, or from specific structural sites in the K-feldspar or exsolved plagioclase.

The slight, but analytically real, reversal of 206/204 in the residual, unvolatilized K-feldspar lead cannot be due to the retention of admixed radiogenic lead in specific and very stable structural sites of the K-feldspar itself, however, because the mineral concentrate was fused and optically isotropic at this stage. But trace mineral impurities, such as zircon, xenotime, or monazite, may have withstood the

VARIATION OF K-FELDSPAR LEADS WITH TEMPERATURE OF VOLATILIZATION



high-temperature conditions, and released their radiogenic lead only under the conditions of hydrofluoric acid attack. An alternative explanation is that there may have been a partial equilibration of the admixed radiogenic lead and original feldspar lead, which took place during the high-temperature environment of the volatilization experiments. Thus, original and radiogenic lead components would have been mixed together, both occupying more stable and indistinguishable sites.

If such a lead mixing process were responsible for the reversal of trend of the lead isotopic compositions of the unvolatilized fraction, serious doubts would be raised as to the potential of the stepwise volatilization procedure for isolation of original feldspar lead. The opposing tendencies of the preferential volatilization of the radiogenic lead and a thermal homogenization of original and radiogenic leads might preclude more than an approach to the original values of lead isotopic composition.

Implications of the Lead Obtained by Stepwise HF Attack of the Lawler Peak Granite K-Feldspar Concentrate

The last-dissolved lead fraction of the HF-attack series had a $^{206}/^{204}$ lower than any of the volatilized lead fractions, while its $^{207}/^{204}$ and $^{208}/^{204}$ were higher than several of the volatilized lead fractions. Therefore, the Pb^{206} -rich radiogenic lead component was more depleted (perhaps even entirely removed) from the K-feldspar than by the stepwise volatilization procedure. The slightly elevated values of $^{207}/^{204}$ and $^{208}/^{204}$ of this last-dissolved lead (over volatilized fractions E, F, and G) must then be due to the presence of the 'normal'

(see pp. 284-285) radiogenic lead component, with all of the U and Th daughter leads. Thus, the least mobile lead fractions of both the HF attack series and the stepwise volatilization procedure are slightly enriched in the 'normal' radiogenic lead component.

A possible explanation for such behavior is that a refractory uranium and thorium-bearing mineral is present in trace amounts in the K-feldspar mineral concentrate, which mineral is resistant to attack by HF. The modal concentration of this mineral is calculated at one part in three-thousand, assuming,

- 1) a uranium content of the mineral of 3000 ppm (L. T. Silver - personal communication - found that the zircons of the rock range up to and above 4000 ppm),

- 2) a density of the mineral of about twice that of the K-feldspar,

- 3) an age of 1440 m.y.,

- 4) that the Th/U of this mineral is 1.8, as indicated by the covariance of $^{207}/^{204}$ with $^{208}/^{204}$ for the volatilized lead fractions (see page 284), and

- 5) that the amount of radiogenic lead contained by this trace mineral is calculated from the difference in lead $^{208}/^{204}$ values of the total feldspar lead and the lowest $^{208}/^{204}$ value of the volatilized lead fractions.

However, these calculations require that the total feldspar concentrate should have contained much more uranium (2.7 ppm) than was actually observed (.077 ppm). Therefore, the hypothetical mineral impurity can only exist if it did not release its uranium under the

the conditions of the HF attack used to determine the total feldspar lead and uranium concentration and composition. Such minerals as zircon, monazite, and xenotime are suitably resistant to HF.

If, on the other hand, no such resistant, radioactive trace mineral is present in the feldspar concentrate, then it is difficult to understand how a mineral phase or set of sites can exist which has preferentially incorporated radiogenic lead generated from without the K-feldspar, yet which is resistant to HF attack.

In terms of the analytical errors, it is perhaps possible for the difference in the lead 208/204 and 207/204 values of volatilized fraction F and the last-dissolved fraction of the HF attack series to represent merely analytical scatter, and that the coincidence of the 207/204 and 208/204 of the last-dissolved fraction of the HF attack series with the best-fit 207/204 - 208/204 line of the volatilized fractions (fig. 4) is fortuitous. A high-pressure HF attack of the K-feldspar concentrate, which would tend to dissolve most or all of most resistant uranium-bearing minerals, might resolve the question.

RUIN GRANITE K-FELDSPAR VOLATILIZED LEADS - MAJOR PATTERNS

The best-fit line to the 208/204 - 206/204 of the volatilized lead fractions (fig. 7), except for 1B and 1D which clearly do not fall on the main trend, has a slope of 0.65 ± 0.13 . As with the 207/204 - 208/204 covariance of the Lawler Peak granite K-feldspar volatilized leads (page 284), this covariance may be used to calculate a model Th/U for the source of the admixed radiogenic lead component(s). The

assumptions, again, are that the radiogenic lead was generated over the age of the rock - 1460 m.y. -- from a homogeneous source closed to loss or gain of Th and U. The calculated $\text{Th}^{232}/\text{U}^{238}$ for the observed slope is 2.2 ± 0.5 -- rather similar, but slightly higher, than that obtained from the Lawler Peak granite data (1.8 ± 0.3). Of course, this result is sensitive to errors in the 204 measurement of the lead fractions (page 284, ff.). This can be avoided by using a 206/207 - 206/208 plot (fig. 10). This plot shows a striking colinearity for ten of the data points, while fractions 1A, 1B, 1D, and 2A fall off the main trend. The best-fit line to the main trend¹ has a slope of 3.28 ± 0.15 . To calculate the model source Th/U, one must know the initial 206/207 and 206/208 of the rock or feldspar; however, the calculation is not sensitive to the (reasonable) choice of initial composition. In the event, I have used a slight extrapolation of the observed trend² ($[\text{206/207}]_{\text{initial}}$ of 1.055, $[\text{206/208}]_{\text{initial}}$ of .45315), but whether the initial 206/207 is 1.06 or 1.05 has only a slight effect on the result. The pertinent equations are derived in appendix II. The Th/U of the source(s) calculated from the slope of 3.28 ± 0.15 , and a time of 1460 m.y., is 2.65 ± 0.22 -- in agreement with the number (2.2 ± 0.5) calculated using the apparent 208/204 - 206/204 covariance.

¹not including the two lowest-precision analyses 2G and 2A, which in any case fall essentially on the line.

²because even the least radiogenic observed lead fractions probably still contain a slight radiogenic component.

Anomalous Lead Fractions

Fraction 1D of the volatilization experiments is anomalously enriched in Pb^{206} compared to the other volatilized lead fractions of the Ruin granite K-feldspar. This is reflected in its high 206/204, 206/207, and 206/208 ratios. There are two general mechanisms for obtaining the isotopic composition of the lead of fraction 1D by mixing a radiogenic lead with the original feldspar lead.

The first requires that the radiogenic lead component be 'normal' -- that is, containing all of the uranium and thorium lead daughters in their equilibrium abundances and accumulated over the age of the rock -- but for its source to have a lower Th/U than the source responsible for the main mixing line. The required Th/U can be calculated in just the same way as was calculated for the straight-line, main-trend points on the 206/207 - 206/208 plot. This calculation results in a model $\text{Th}^{232}/\text{U}^{238}$ for the hypothetical source of the radiogenic component responsible for fraction 1D of about one. This value is indeed distinctly lower than that calculated for the main-trend points (2.65). However, a radiogenic lead which, when mixed with an original feldspar lead with 206/204 values ranging from 16.32 (the lowest precise value observed) to 17.37 (the 206/204 of volatilized fraction 1D) would have increased the 207/204 from 15.40 to 15.49¹. The value of 15.49 is at the margin of the estimated error limits of the measured 207/204

¹ assuming a 1460 m.y. time of generation, with no fractionation of the uranium daughters.

($15.44 \pm .05$) of fraction 1D, thus this explanation is possibly permitted by the data.

The second general mechanism is simply the concentration and incorporation of radiogenic Pb^{206} produced by intermediate daughter fractionation, as proposed to explain the Lawler Peak granite K-feldspar lead data. Again, the possible error in the 207/204 analysis of fraction 1D (± 0.05) permits the 207/204 of the fraction to be compatible (i.e., unchanged from the least radiogenic 207/204 values of the feldspar leads) with the model. But, notice that on the 206/207 - 206/208 plot (fig. 8), fraction 1D is almost coincident with the mixing line of pure Pb^{206} and the estimated (206/207 = 1.055, 206/208 = .4532) original feldspar lead. The plot cannot distinguish between this mixing line and the mixing line of 'normal' 1460 m.y.-generated radiogenic leads from a source with Th/U of about 1; nevertheless, the coincidence is very suggestive. Other information -- specifically, the trend of compositions of the volatilized fractions with temperature of volatilization -- in fact supports the pure Pb^{206} end-member hypothesis and will be discussed.

The first-volatilized fractions, 1A and 2A, are anomalous in the same manner as fraction 1D (fig. 8), and in fact fall, within their analytical error, on the mixing line of fraction 1D and the estimated original feldspar lead. Therefore, it is reasonable to conclude that these fractions are enriched in the same radiogenic lead component as fraction 1D.

DETAILED ANALYSIS OF RUIN GRANITE K-FELDSPAR LEAD DATA

The two reversals in the general trend of decreasing lead 206/207 and 206/204 with decreasing volatility of the fractions are especially significant in the light of the previously discussed Lawler Peak granite data.

Figure 17, on which the 206/207 of the volatilized fractions of both volatilization series is plotted against the temperature of volatilization, is strikingly like the similar plot for the Lawler Peak granite K-feldspar data. In both cases, the 206/207 of the volatilized lead fractions shows a maximum or secondary maximum between 1130° and 1180°, and also in the unvolatilized, residual lead fraction. The first Ruin granite K-feldspar volatilization series shows a pronounced peak at about 1150°, and a very slight reversal at the residue. The second volatilization series, however, resolved only a slight reversal in the 1130°-1180° region, but a pronounced reversal at the residue.

The near-coincidence in the temperature of the 'reversed' volatilized fractions of the Ruin granite and Lawler Peak K-feldspar leads indicates that the 1130°-1180° reversal may be due to a similar radiogenic lead component, present in similar sites, preferentially volatilized in both cases. Arguing by analogy from the Lawler Peak granite data, this radiogenic lead component in the Ruin feldspar is enriched in Pb^{206} over that of a normal radiogenic lead. The fact that fractions 1A, 1D, and 2A fall slightly (and within analytical error) but consistently to one side of the line of mixing of pure Pb^{206} and

an original feldspar lead on the 206/207 - 206/208 plot is probably due to a slight dilution of the pure Pb^{206} radiogenic component with the 'normal'* radiogenic lead component.

The difference in relative intensities of the two reversals in trend of the 206/207 ratios of the volatilized fractions from the Ruin granite K-feldspar must be at least partly due to kinetic effects. The first volatilization series involved about 20% more (five hours) exposure to the high-temperature conditions of volatilization than the second volatilization series, and therefore may reflect a greater degree of equilibration of the lead isotopes between more than one site in the feldspar. A simple explanation consistent with such a process is that the radiogenic lead component responsible for the high 206/207 values of the unvolatilized lead fractions was initially present in sites of greater thermal stability than the common lead of the K-feldspar. A refractory mineral with the property of retaining lead at high temperatures could provide such sites. During the volatilization experiments, this radiogenic lead may leave its host mineral and either be volatilized or mix with the common lead of the feldspar. To fit the observed systematics, this radiogenic lead should not be volatilized as rapidly as the common lead.

The relatively short duration of high-temperature conditions of the second volatilization series did not permit as much migration of

*in this case, from a model source with Th/U of about 2.7.

this radiogenic lead from the proposed refractory mineral or stable sites compared to the first volatilization series. The ratio of radiogenic lead to common lead in the proposed refractory trace mineral or stable sites if further increased by the lesser amount of common lead (1.3 ppm Pb) remaining in the residue of the second volatilization series (2.1 ppm Pb).

The difference in the magnitude of the 1130° - 1180° reversal in 206/207 values is most likely a combination of two effects. The first is simply that the second volatilization series data did not resolve the magnitude of the reversal as well as the first series. Good resolution depends on the near-coincidence of the temperature of a volatilization step with the release temperature of the radiogenic lead, and on having a relatively small yield of volatilized common lead in this fraction so that the common lead component does not mask the reversal. The second possible effect bearing on the difference in the magnitudes of the 206/207 reversals is a greater degree of prior thermal homogenization of the radiogenic lead with the original (common) feldspar lead during the more lengthy second volatilization series.

The second-volatilized fraction of the first volatilization series (fraction 1B) is anomalously rich in Pb^{208} , as shown on figs. 7 and 8. Taken at face value, this fraction must represent the mixing of a radiogenic lead enriched in the thorium daughter lead with the original feldspar lead. If this component was accumulated over the age of the rock, then, using the same type of calculation as was used to calculate model Th/U values for the source(s) of the other radiogenic components, its source must have had Th/U greater than 6.6. The site of this radiogenic

lead component must also be clearly distinguishable from other radiogenic lead components.

There is, however, a possibility that this anomaly is due not to an inherent property of the sample, but to contamination by Pb^{208} spike of the sample lead during extraction in the laboratory. In order to monitor the 206/207 of the blank lead, it was necessary to expose the glassware and teflon beakers to the Pb^{208} spike lead. The most likely equipment to retain traces of lead are the teflon beakers used for final oxidation of the lead dithizonate. Spot checks on the 'memory' of these beakers showed that from .001 to .004 micrograms of spike lead were released by these beakers during each use. Although these amounts are not enough to effect the data, it is possible that the beaker used for final oxidation of the lead of fraction 1B had adsorbed an unusually large amount of Pb^{208} spike, which was released during sample oxidation. That such a contamination might be responsible for the observed Pb^{208} content of fraction 1B is also suggested by the absence of any such lead in the second volatilized series (two of the fractions, however, were not analyzed for Pb^{208}).

MARBLE MTS. GRANITE K-FELDSPAR VOLATILIZED LEADS: MAJOR PATTERNS

The data from the stepwise volatilized leads from the Marble Mts. granite K-feldspar are plotted in figures 9, 10, and 11. Except for the unvolatilized residual lead, the 207/204 values of the lead fractions do not vary outside of analytical error. The residual lead analysis (table 9) is believed to be biased by a mass 204 measurement error (possibly caused by a non-lead peak at the mass 204 position).

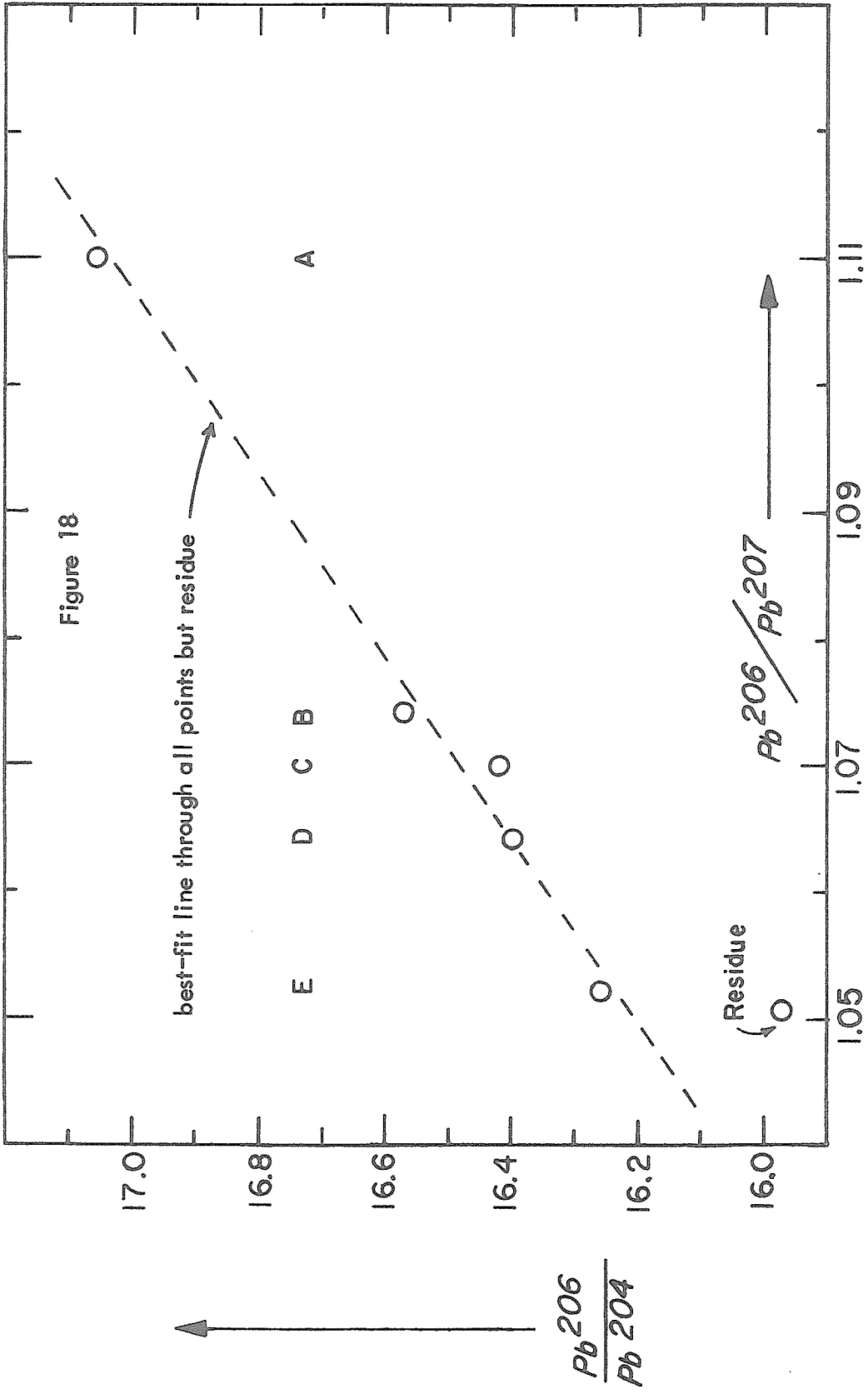
Although the 206/207 of the residue is quite consistent with the trend of 206/207 with step of volatilization (fig. 17), the 207/204 is distinctly anomalous (fig. 18)*. Disregarding the residual lead analysis, the data do not permit distinction between lead isotope heterogeneity in the K-feldspar caused by admixture with a 'normal' radiogenic lead generated over 1430 m.y. ($207/206 = .09$) and a Pb^{206} -enriched radiogenic lead.

The 208/204 of the volatilized leads shows a total variation of 2.9%. The range in 208/207 is similar (3.0%), indicating that the abundance of Pb^{208} did indeed vary. The Th/U of the source of the admixed radiogenic lead may be calculated, in the same manner as for the Lawler Peak granite and Ruin granite K-feldspar leads, from the 206/204 - 208/204 and 206/207 - 206/208 plots (figs. 11, 12). The lead from volatilized fraction C does not fit a simple mixing line on the plots of figs. 10 and 11 and was thus not included in the fitting of the best-fit line. An independent justification for excluding this fraction will be presented.

The best-fit line to the three data points on the 206/204 - 208/204 plot has a slope of 3.4 ± 0.2 , which corresponds to a source with a Th^{232}/U^{238} (present-day) value of 11.5 ± 0.8 , for an age of 1430 m.y. The best-fit line to the three points on the 206/207 -

*If the apparent residual lead 207/204 (15.20) were real, then the 207/206 ratio of the lead apparently added to the feldspar is not permissible for a lead generated in this rock, unless Pb^{206} has been lost from the rock (for instance, due to migration of Rn^{222}).

MARBLE MTS. GRANITE K-FELDSPAR - VOLATILIZED LEAD FRACTIONS



206/208 plot (fig. 11) has a slope of -5.3 ± 0.7 , which corresponds to a source with a $\text{Th}^{232}/\text{U}^{238}$ (present day) value* of 10.7 ± 0.4 . The agreement in source Th/U by the two methods is satisfactory, which again shows that the covariance of 206/204 with 208/204 is not due to error in Pb^{204} analysis.

If the source of the radiogenic lead component in the Marble Mts. granite K-feldspar concentrate is a trace mineral, it must then be one which has a relatively high thorium content and Th/U ratio. Minerals such as sphene, allanite, uranothorite, monazite, and apatite are common granitic accessory minerals which meet these conditions. The whole-rock (table 4) is quite thorium-rich (142 ppm Th) and has a high Th/U ratio (16.63), and thus is consistent with the thorium-rich nature of the radiogenic lead source. The measured Th/U value of the K-feldspar concentrate (2.0), however, shows no relation to the apparent Th/U of the radiogenic lead source, so that in situ-generated radiogenic lead cannot be called upon to have supplied the observed radiogenic lead component of the K-feldspar.

Volatilized fraction C is anomalous in that it contains too much Pb^{206} for its Pb^{208} content to fall on the 'main' isotopic mixing trends. This fraction was volatilized at 1180° . This is close to the temperature at which the Lawler Peak granite and Ruin granite K-feldspars

*The initial lead used for this calculation was $206/207 = 1.0500$, $206/208 = 0.4440$. This is a slight extrapolation of the observed trend in order to correct approximately for the probable radiogenic component remaining in the least radiogenic volatilized lead fraction.

released leads with a distinct maximum in radiogenic lead content. In both of these samples, the radiogenic component released near this temperature were demonstrated to contain a Pb^{206} -enriched component. Evidently, then, the lead of the Marble Mts. granite K-feldspar also contains a Pb^{206} -enriched radiogenic component, located in a similar site or sites as in the Lawler Peak granite and Ruin granite K-feldspars. The effect of this component, in the case of the Marble Mts. granite K-feldspar, is not pronounced (fig. 17), but rather causes only a change of slope in the trend of 206/207 values with temperature of volatilization. Therefore, the Pb^{206} -enriched radiogenic lead component in this sample is not the dominant radiogenic lead component.

GIANTS' RANGE K-FELDSPAR LEAD: MAJOR PATTERNS

The total range of variation of the 206/204 of the volatilized fractions is about 1.3% (fig. 12) -- a distinctly reduced variability compared to the K-feldspar leads from the southwestern granites studied. Although the 207/204 values of the K-feldspar lead fractions do not vary outside of analytical error, the best-fit line to the volatilized fractions and total lead on a 206/204 - 207/204 plot (fig. 13) is 0.232 ± 0.010 . The 207/204 therefore does vary (again, a variable error in 204 estimation would give a significantly higher slope than 0.232) and is dependent on the 206/204. If this line is considered a mixing line of the original feldspar lead and a radiogenic component, this radiogenic component has $207/206 = 0.232 \pm .010$. The radiogenic lead

$^{207}/^{206}$ 'age' (that is, the $^{207}/^{206}$ which corresponds to a radiogenic lead derived and accumulated continuously from equilibrium decay of uranium for a given time until the present) of this ratio is 3110 ± 70 m.y. This is distinctly older than the radiometric age of the rock. In other words, if the observed K-feldspar lead isotopic heterogeneity is indeed due to the mixing of an original lead and a single type of radiogenic lead, then the $^{207}/^{206}$ value of this lead indicates that there is not enough lead present which was generated during the latter part of the rock's history to give the correct $^{207}/^{206}$ value for the age of the rock.

The simplest model which can fit the observed data is that the radiogenic lead component was generated from the time of formation of the rock (2690 m.y.) but ceased at a time significantly before the present. The calculated* time of this 'event' (which caused the incorporation, by the feldspar, of radiogenic lead generated until the time of the event) is 1010 ± 150 m.y. before the present. A geological interpretation of this calculation would be the following: from the time of crystallization of the pluton (2690 m.y. ago) until about 1010 m.y. ago, radiogenic lead from the uranium and thorium of the rock accumulated either in the same minerals as the parent isotopes or elsewhere in the rock as easily remobilized material. At $1010 (\pm 150)$ m.y.,

*assuming a Pb^{207}/Pb^{206} value for the radiogenic lead of $0.232 \pm .010$ and an age of the rock of 2690 m.y.

a thermal event caused a slight redistribution of the more mobile radiogenic lead components, so that they were in part driven into sites in the K-feldspar. These sites were not identical with those of the original feldspar lead. This secondary event correlates most reasonably with the time of emplacement of the Duluth Gabbro complex (1120-1140 m.y. - Silver and Green, 1972), about 7 km distant¹.

The 206/204 and 208/204 of the volatilized and total feldspar lead appear also to vary colinearly (fig. 13). A model Th/U for the source of the radiogenic lead component may be calculated from the slope of the best-fit line to the data on this plot in the same manner as was done for the other rock feldspars. This best-fit line has a slope of 2.16 ± 0.04 . If the radiogenic lead were accumulated (from a source with constant Th/U) from 2690 m.y. to the present, the calculated present-day $\text{Th}^{232}/\text{U}^{238}$ of the source is 7.88 ± 0.14 . If one assumes the radiogenic lead accumulated from 2690 m.y. to 1010 m.y., the calculated $\text{Th}^{232}/\text{U}^{238}$ of the source is slightly greater, about 8.3.

Using the 206/207 - 206/208 plot (fig. 14), on which the data have a best-fit line with slope of $14.7^{+2.7}_{-2.0}$, the $\text{Th}^{232}/\text{U}^{238}$ for the source of leads generated from 2690 m.y. to the present is $7.88 \pm .18^2$ - in good agreement with the 206/204 - 208/204 -- calculated number.

¹Sphenes and zircons from 1/10 to 3 km from the Duluth gabbro contact were analyzed by Hanson, Catanzaro, and Anderson (1971), who concluded that these minerals had episodically lost radiogenic lead at the time of intrusion of the Duluth gabbro.

²using for an original feldspar lead a slight extrapolation of the observed trend, with $206/207 = .929$, $206/208 = .4064$.

This apparent Th/U of the source of the radiogenic lead component of the Giants' Range granite K-feldspar is relatively high, although the whole-rock Th/U value (5.28) is not particularly high. Both sphene and apatite -- minerals which generally have relatively high Th/U values (L. T. Silver, personal communication) -- are abundant in the rock, and one of these minerals might have supplied radiogenic lead of the appropriate isotopic composition.

PAYSON GRANITE K-FELDSPAR LEAD DATA: MAJOR PATTERNS

A best-fit line to the 207/204 and 206/204 of the stepwise-dissolved lead fractions of the Payson granite K-feldspar has a slope of $.089 \pm .021$ (fig. 15). The dependence of the 207/204 with 206/204 implies a heterogeneity of 207/204, even though the variations in 207/204 observed are within analytical precision. Therefore, both radiogenic Pb^{207} and Pb^{206} were incorporated by the K-feldspar, and a component of 'normal' radiogenic lead is present.

The available lead isotopic data from the Payson granite K-feldspar suggests that the observed lead isotope heterogeneity is the result of the incomplete mixing of a two-component system (the high degree of colinearity of the available data on the 206/207 - 206/208 plot especially supports this interpretation), which components are the original feldspar lead and a radiogenic lead. The 207/206 of the radiogenic component must be $.089 \pm .021$. The radiogenic lead-lead 'age' which corresponds to this ratio is 1425_{-560}^{+400} m.y. The radiometric age

of the rock (1740 m.y.) is included by this figure, so that the admixed radiogenic lead component could have been derived from the (integrated) production of radiogenic lead from uranium and thorium in the rock over the entire history of the rock, and no uranium intermediate-daughter fractionation need have occurred.

If, however, the true slope of the 207/204 - 206/204 mixing line is indeed less than that expected for mixing with 1740 m.y. radiogenic lead ($207/206 = 0.105$), two explanations are available. The presence of a Pb^{206} -enriched radiogenic lead component, as proposed for the Lawler Peak granite and Ruin granite K-feldspar leads, could decrease the 207/206 of the admixed radiogenic lead. This component cannot be as dominant as for the Lawler Peak granite K-feldspar radiogenic lead component, but it may be present to a subordinate degree.

Or, the lower slope of the mixing line may reflect a geological effect. The well-documented 1420-1470 m.y. plutonic event (Silver, 1968) of the southwest could have induced a loss of some of the more mobile early-generated radiogenic leads of the Payson granite at about 1425 m.y. Such an event might have been mild enough (in terms of heat and fluid input) so as not to leave a metamorphic imprint on the rock. With the loss of the easily mobilized fraction of the radiogenic leads formed between 1740 m.y. and 1425 m.y., only leads generated from 1425 m.y. to the present would be available for later incorporation by the feldspar. This hypothesis is quite speculative since the possible error in the best-fit 207/204 - 206/204 slope is large, but geologically very reasonable.

The best-fit line to the Payson granite K-feldspar lead data on a 208/204 - 206/204 plot has a slope of 0.74 ± 0.12 (fig. 15). Using the usual assumptions, the calculated present-day $\text{Th}^{232}/\text{U}^{238}$ for the source of the radiogenic lead component with $208/206 = 0.74$ is 2.6 ± 0.4 . If the last 1425 m.y. is used as the time of generation, the result is lower by 0.1. If the data are plotted on a 206/207 - 206/208 diagram (fig. 15), and the slope (3.09 ± 0.14) is used to calculate the Th/U of the source, the resulting value is $2.53 \pm 0.23^*$ -- in good agreement with the 206/204 - 208/204 calculation. The excellent fit of the 206/207 - 206/208 data to a straight line suggests that a Pb^{206} -enriched radiogenic lead component is not present, because when present it does not occupy the same sites as the 'normal' radiogenic lead (see the discussion of the Lawler Peak granite and Ruin granite data), and would have a different rate of solution in HF.

The most primitive lead fraction obtained from the Payson granite K-feldspar (the last-dissolved lead fraction of the second attack series) corresponds to a single-stage evolution lead with an age of 1650 m.y., about 5% lower than the radiometric age of the rock. Since the data do not show that a reproducibly least radiogenic composition was obtained in the course of the stepwise HF attack series, this most primitive lead fraction represents only a maximum limit for the original feldspar lead 206/204, 207/204 and 208/204.

*An initial lead with $206/207 = 1.03$, $206/208 = .4464$ was used -- again, a slight extrapolation of the observed trend to correct approximately for a residual radiogenic lead component.

CONCLUSIONS AND IMPLICATIONS

ISOLATION OF ORIGINAL FELDSPAR LEADS

The experiments performed on the feldspar concentrates from the five Precambrian granites have demonstrated the presence of a significant radiogenic lead component in each. The data show that, in general, the less mobile leads are the less radiogenic; in two of the volatilization experiments (Lawler Peak granite K-feldspar and Ruin granite K-feldspar), however, the least mobile lead fractions were not the least radiogenic. Therefore, the stepwise volatilization technique cannot by itself be relied on as a technique to selectively remove radiogenic lead component(s) from Precambrian K-feldspar concentrates.

Although each experiment of stepwise fractional lead removal succeeded in significantly reducing the proportion of radiogenic to original lead in one or more of the lead fractions, none of the data indicate that original feldspar lead was ever isolated -- e.g., no least radiogenic fractions were repeatedly isolated from any of the feldspar concentrates. The technique of stepwise partial HF attack appears to be more promising in this regard. This technique was responsible for a closer approach to the original lead of the Lawler Peak granite K-feldspar with a two-step attack than the nine-step volatilization experiment.

The observed changes in the appearance and composition of the K-feldspar concentrates exposed to partial HF attack suggest that the removal of the radiogenic lead component(s) may result from the dissolution of plagioclase feldspar and fine-grained alteration minerals, so

that the grains remaining after the first few partial attacks are mineralogically purer than the initial concentrate. The disadvantage of the technique is that it requires relatively large amounts of sample, compared to a total feldspar lead analysis, since as little as one-tenth of the original sample weight may remain after the initial HF attacks.

Two possible refinements of the stepwise partial HF attack technique are,

a) precise control of the temperature and time of reaction of each step, so that as few partial attacks as possible could be used to best remove the radiogenic lead component(s).

- The data from the two Payson granite K-feldspar stepwise partial HF attack series indicate that an initial attack which dissolves most of the sample is more effective than a series of less vigorous attacks in removing radiogenic lead from the concentrate -
and,

b) the use of relatively mild attack conditions (in terms of strength of the acid, its temperature, and duration of attack) on a relatively fine-grained (say, to pass 400 mesh) sample.

- Thus more of the reactive phases would be directly exposed (rather than in the interior of a K-feldspar grain) to attack, thereby allowing a 'clean' K-feldspar concentrate to be achieved without excessive loss of original K-feldspar lead.

ORIGIN OF THE RADIOGENIC FELDSPAR LEAD COMPONENTS

Of the five K-feldspar samples studied, the three from the 1450 \pm 20 m.y. age southwest U.S. granites are interpreted as containing two distinguishable radiogenic lead components. The component unique to these samples is evidently concentrated in sites which become unstable in the 1120°-1180° range, so that lead fractions volatilized in this temperature range have distinctly higher Pb^{206} concentrations than fractions volatilized either just above or below these temperatures. The data for all three of these samples suggest that this radiogenic lead component is richer in Pb^{206} than the 'normal' radiogenic lead component which is present in all of the samples studied, and the superior quality data for the Lawler Peak granite K-feldspar leads further indicate that it is composed of essentially pure Pb^{206} .

The proposed explanation for this pure Pb^{206} radiogenic lead component (page 283) is the continuing separation and concentration of the U^{238} intermediate daughter Rn^{222} . The facts that this radiogenic lead component is distinguishable (in terms of volatility) from the 'normal' radiogenic lead component, and that it is volatilized in a sharply restricted temperature range, suggest that this component is located in specific sites in the K-feldspar concentrates -- possibly a specific mineral phase present in trace amounts. This trace phase must have one of two properties: either it could incorporate elemental radon in a specific site, or it could incorporate loosely bound lead (as Pb) preferentially to the K-feldspar. The ability to incorporate

an atom as large as radon must be restricted to a very few minerals -- conceivably, some zeolites and clays might be able to accommodate the atom.

If the Pb^{206} -enriched radiogenic lead component were incorporated in its final site as lead rather than radon, then the (hypothesized) trace mineral discussed above would need only the capacity to incorporate loosely bound lead preferentially to the K-feldspar. However, since the Pb^{206} -enriched and 'normal' radiogenic lead components occupy distinguishable sites, a mechanism must have existed to separate the two radiogenic lead components before the incorporation of each type of radiogenic lead in the trace minerals or sites. Such a mechanism is readily provided by the differential mobility of radon compared to lead, so this two-stage process of radiogenic lead incorporation is an attractive model. The process of final radiogenic lead distribution might well correspond to the Mesozoic and Tertiary hydrothermal and plutonic events common to the southwest.

The Lawler Peak granite K-feldspar acid leach and quartz-plagioclase concentrate volatilization experiments shed some light on the nature of the site of the Pb^{206} -enriched radiogenic lead component. The lead dissolved by exposure of the K-feldspar concentrate to hot, concentrated nitric and hydrochloric acids contained no significant Pb^{206} -enriched radiogenic lead component; rather, the radiogenic lead dissolved was 'normal' in isotopic composition for the age of the rock. The Pb^{206} component, therefore, must either be in sites with no surface communication, or in sites specifically impervious to hot mineral acids.

Grain boundaries and surface-communicating fractures thus cannot be considered as possible sites.

The data of the stepwise volatilization of the quartz-plagioclase concentrate leads¹ indicate that the amount of exogenous radiogenic lead incorporated by the quartz-plagioclase concentrate was about $0.20\mu\text{g}/\text{cc}$ ². The similar calculation for the K-feldspar concentrate gives a radiogenic Pb^{206} concentration of $2.5\mu\text{g}/\text{cc}$. This large difference indicates that surface area of the mineral grains is probably not a significant factor in determining the amount of radiogenic Pb^{206} incorporation (the difference may be even more significant, because the K-feldspar grains tend to be larger than the plagioclase or quartz grains, and thus have less grain-boundary surface area/cc).

An interesting additional calculation is to determine the radiogenic Pb^{206} content of the plagioclase assuming that the quartz contains no lead. This calculation gives a ratio of incorporated radiogenic Pb^{206} per unit volume of the plagioclase compared to the K-feldspar of about 1:/4.1. This number is not strikingly different from the average distribution factor of lead between plagioclase and K-feldspar of 1/2.4 reported by Doe and Tilling (1967). It is remarkably similar to the common lead distribution factor which can be calculated from the yield data of the quartz-plagioclase concentrate volatilization experiment

¹ using the total concentrate lead concentration and composition calculated on pages 256, 285.

² assuming an initial lead 206/204 of 16.16 (see p. 317).

by assuming that the quartz contains no lead - 1/4.3. Such calculations, therefore, suggest that the ability of a mineral to incorporate exogenous radiogenic Pb^{206} may be related to its ability to accommodate lead, as a trace element, during crystallization, and that the lead is actually in the feldspar structure rather than a trace mineral.

The nature of the site(s) of the 'normal' radiogenic lead component, present in all of the feldspar concentrates studied, is unclear. Some of this lead must arise from the in situ decay of the uranium and thorium known to be present in the mineral concentrates. In no case, however, could the uranium and thorium concentrations (where determined) account for the major part of the 'normal' radiogenic lead component; further, for one of the two samples with both uranium and thorium determinations available (the Marble Mts. granite K-feldspar), the U/Th of the K-feldspar concentrate is strikingly different than the calculated U/Th of the source of the 'normal' radiogenic lead component.

At least part of the 'normal' radiogenic lead component must be in relatively refractory trace minerals or highly stable sites, since the unvolatilized lead fractions of the Lawler Peak granite, Ruin granite and Giants' Range granite K-feldspars contained a greater proportion of 'normal' radiogenic lead component than some of the more volatile fractions. The implications of the existence of a trace amount of a refractory, radioactive mineral are discussed on page 296, in connection with the Lawler Peak granite K-feldspar data. It should be noted that there is no independent evidence for the presence of such a mineral in the K-feldspar concentrates, and that the calculated Th/U for

the 'normal' radiogenic lead source in the case of the Lawler Peak, Ruin, and Payson granite K-feldspars (1.8, 2.6, and 2.5, respectively) is greater than the Th/U of the zircons from those rocks, but less than typical Th/U values for the common radioactive accessory minerals in granitic rocks (L. T. Silver, personal communication).

The K-feldspars which contain the 'normal' radiogenic lead components with the highest and the lowest calculated source Th/U values (The Lawler Peak granite K-feldspar, with a value of 1.8, and the Marble Mts. granite K-feldspar, with 11) correspond to those whole rocks with the highest and the lowest observed Th/U values (1.90 for the Lawler Peak granite, and 16.63 for the Marble Mts. granite). Also, the rocks with the highest uranium (Lawler Peak granite) and the highest thorium (Marble Mts. granite) contents correspond to those feldspar samples which show the greatest absolute degree of incorporation of the uranium-daughter and thorium-daughter radiogenic leads, respectively.

The data, therefore, suggest that at least a large part of the radiogenic leads incorporated by the feldspars of this study were generated within the rock, and were not derived from systems exogenous to the rock and with significantly different Th/U ratios.

The data also suggest that the geologic history of the rocks can have a very significant effect on the composition and concentration of the K-feldspar radiogenic lead components. The Payson granite and Giants' Range granite were both either near to, or actually intruded by Precambrian intrusives of younger age. In both cases, the isotopic composition of the K-feldspar radiogenic lead component is apparently

simply related to the known time of these intrusive events. In the case of the three 1450 ± 30 m.y. old granites (Lawler Peak, Ruin, and Marble Mts.) and the Payson granite, it may have been the Mesozoic or Tertiary plutonic, volcanic, and hydrothermal events which were responsible for the 'opening' of the K-feldspar lead system.

ORIGINAL LEAD OF THE 1450 ± 20 M.Y.-OLD GRANITES

The Lawler Peak, Ruin, and Marble Mts. granites have important similarities in age, composition, and tectonic setting. They appear to be three of many such plutons, all with (zircon U-Pb) radiometric ages of 1450 ± 30 m.y., granitic (predominantly) to granodioritic in composition, with large (2-10 cm) K-feldspar megacrysts, emplaced without related tectonic or metamorphic activity (Silver, 1968; Anderson and Silver, 1971). Granitic plutons with these characteristics and zircon U-Pb ages have been found by Silver in California, Nevada, Arizona, Utah, Colorado, Wyoming, New Mexico, and Sonora, and may be even more widespread.

The leads from the K-feldspar concentrates of the three 1450 ± 30 m.y. granites studied contain a variable amount of radiogenic lead (this work). Stepwise volatilization and partial HF attack of the K-feldspars has yielded lead fractions which are enriched in the original (common) lead component, and has also allowed estimates of the Th/U of the source of one of the radiogenic lead components. The actual original feldspar lead (= original rock lead) isotopic composition can be of great use in understanding the significance of the similarities of these granites,

and in gleaning information about the pre-emplacment, magmatic history of the rocks.

Estimates of Original Leads

The lead fraction of the Lawler Peak granite K-feldspar which was least soluble in HF (partial HF attack fraction C) had the lowest in $^{206}\text{Pb}/^{204}\text{Pb}$ value (16.39) of any of the ten fractions for which this data was available. The $^{207}\text{Pb}/^{204}\text{Pb}$ (15.40) and $^{208}\text{Pb}/^{204}\text{Pb}$ (35.86) values of this fraction, however, exceed those of three of the volatilized fractions. Both a ^{206}Pb -enriched and a 'normal' radiogenic lead component were identified in the Lawler Peak K-feldspar lead. The plot of $^{207}\text{Pb}/^{204}\text{Pb}$ versus $^{208}\text{Pb}/^{204}\text{Pb}$ (fig. 4) demonstrated that the slight variations in $^{207}\text{Pb}/^{204}\text{Pb}$ and $^{208}\text{Pb}/^{204}\text{Pb}$ were in fact real, were not the result of variable error in ^{204}Pb estimation, and indicated a radiogenic lead from a model (derived over total age of the rock) source with Th/U of about 1.8.

The lowest $^{206}\text{Pb}/^{204}\text{Pb}$ but slightly elevated $^{207}\text{Pb}/^{204}\text{Pb}$ and $^{208}\text{Pb}/^{204}\text{Pb}$ of the least (HF)-soluble lead fraction of this feldspar can be simply interpreted as the result of a greater degree of removal of the ^{206}Pb -enriched radiogenic component, compared to the volatilized fractions, but a lesser degree of removal of the 'normal' radiogenic lead component. With this interpretation, a maximum value for the original lead $^{206}\text{Pb}/^{204}\text{Pb}$ can be calculated. To the extent that the lead fraction (F) with the lowest $^{208}\text{Pb}/^{204}\text{Pb}$ is the result of complete removal of the 'normal' radiogenic lead component, the following calculation yields the true original lead of the Lawler Peak granite.

The 208/204 of volatilized fraction F (35.74) is taken as the maximum possible value for the original lead 208/204. Assuming that only the 'normal' radiogenic lead component, from a source with Th/U = 1.8, is contributing to the least (HF)-soluble fraction, then the amount of Pb^{206} which must be present due to this component may be calculated* from the difference between its 208/204 (35.86) and 35.74. Correcting, in this manner, for the Pb^{206} of the 'normal' radiogenic lead component, the value of 16.39 for the least (HF)-soluble lead becomes 16.16 -- the maximum possible value for the Lawler Peak granite original lead. The 207/204 of this fraction is similarly corrected, from 15.40 to 15.38. The (single-stage evolution) model-lead age for a lead with this isotopic composition (using the constants and assumptions given in appendix I) is 1440 m.y. (calculated $\mu = 8.63$). This is in agreement with the radiometric age of the rock from zircons. Because the lowest 208/204 value (from which this original feldspar lead isotopic composition was calculated) probably still reflects a radiogenic component which was not volatilized from the K-feldspar, the actual original feldspar (and rock) lead probably would give a model-lead age which is somewhat older. In any case, the improvement in agreement of the lead isotope model age from both the most primitive observed lead fraction (206/204 = 16.39, 207/204 = 15.40, model age = 1280 m.y.) and the calculated

*from equations similar to the one on page 284 - for a given Th/U and time of generation, a specific amount of Pb^{206} and Pb^{207} must accompany each radiogenic Pb^{208} atom.

original lead composition model age (1440 m.y. - above) is great compared to the model-lead age of the observed total feldspar lead model-age (860 m.y.).

While the best estimate of the original Lawler Peak granite lead 207/204 value is 15.38, the data from the less volatile lead fractions of the Ruin and Marble Mts. granite K-feldspars are slightly scattered around a value of close to 15.40. These values must be very close to the true original lead 207/204 values, because both theoretical calculations and the small observed variations in 207/204 show that the effect of the admixed radiogenic lead on this ratio cannot be large. Therefore, the original rock lead 207/204 values of these three plutons were remarkably similar.

This similarity in itself is a strong argument for a related origin of these rocks. The (original) rock lead 207/204 value is sensitive to both long-term variations in the U^{238}/Pb^{204} of the source material, and to relatively ancient changes in the U^{238}/Pb^{204} of the source material*. Therefore, unless the sources of these rocks evolved in unrelated paths which happened to converge to a similar lead 207/204 about 1450 m.y. ago (which seems unlikely), the sources for these rocks have shared similar U^{238}/Pb^{204} for the greatest part of their history.

But the 207/204 of the (original) rock lead is not sensitive to changes in source U/Pb for relatively short time intervals late in the

* because, with a half-life of only about 713 m.y., the rate of production of radiogenic Pb^{207} was very high early in the earth's history.

history of the source. For example, a change in the U^{238}/Pb^{204} (present values) at a time 1650 m.y. ago from 8.5 to 10 would result, 200 m.y. later in a change in 207/204, compared to the lead from a rock whose source did not undergo such a change in U/Pb, of 0.01. That is, instead of, say, 15.39, the 207/204 of the original rock lead would have evolved to 15.40 -- a very slight effect.

The lead 206/204 and 208/204 ratios, however, are more sensitive to late-occurring changes in U/Pb and Th/Pb. If the 206/204 and 208/204 as well as the 207/204 of different plutons (at the time of emplacement) are similar, then it may be inferred that the sources of the plutons not only shared a parallel evolution for most of their history, but for virtually all of it. The question of possible similarity of the original rock lead 206/204 and 208/204 for the 1450 ± 30 m.y. plutons may be approached in the following manner.

Only the Lawler Peak granite K-feldspar lead appears to have contained a large Pb^{206} -enriched radiogenic component. Therefore, increments in Pb^{206} , Pb^{207} , and Pb^{208} of the other two samples over their initial lead composition must arise mainly or entirely from the 'normal' radiogenic lead component. Thus, if any one of the initial isotope ratios 206/204, 207/204, or 208/204 is known or can be assumed, the other two initial ratios can be calculated by the method discussed on page 317. The observed least-radiogenic lead fractions are tabulated in table 12, along with best estimates for least-radiogenic lead compositions from analyses with no Pb^{204} data, but with primitive-looking

Table 12

Least Radiogenic K-feldspar Lead Fractions of 1450 m.y. Granites

	$\frac{206}{204}$	$\frac{207}{204}$	$\frac{208}{204}$	$\frac{206}{207}$
<u>Lawler Pk. Granite K-Spar</u>				
	(1)	(2)	(2)	(1)
Observed fractions	16.39	15.37	35.74	1.0644
Est. accuracy (\pm)	.15%	.15%	.15%	.10%
(3) Calculated values -original lead-	16.16	15.38	35.74	1.0508
<u>Ruin Granite K-Spar</u>				
	(4)	(4)	(4)	(5)
Observed fractions	16.32	15.40	35.90	1.0584
Est. accuracy (\pm)	.15%	.15%	.15%	.05%
<u>Marble Mts. Granite K-Spar</u>				
	(6)	(7)	(6)	(8)
Observed fractions	16.26	15.40	36.63	1.0509
Est. accuracy (\pm)	.50%	.50%	.50%	1%
Estimated least radiogenic values	(9) 16.18	(7) 15.40	(10) 36.46	(8) 1.0509

(1) HF attack fraction C.

(2) Volatilized fraction F.

(3) From method described on page 317.

(4) Average, volatilized fractions 1G and 1H.

(5) Volatilized fraction 1H.

(6) Volatilized fraction E.

(7) Average, volatilized fractions C, D, and E.

(8) Residue of volatilization series run.

(9) Volatilized fraction E, but assumes that the true 207/204 of this fraction is 15.40, and uses the observed 206/207 value.

(10) The calculated value for volatilized fraction E, using the observed 206/207 value and the observed linear 206/207 - 206/208 covariance.

Table 13

Original Leads of 1450 m.y. Granites: Some Calculated Values ⁽¹⁾

	<u>206/204</u>	<u>207/204</u>	<u>208/204</u>	<u>206/207</u>	⁽²⁾ <u>Model Age; μ</u>
<u>Lawler Pk. Granite K-Feldspar:</u>					
From method described on p. 317	16.16	15.38	35.74	1.0508	1440 my; 8.63
<u>Ruin Granite K-Feldspar</u>					
Assume $\frac{206}{204}=16.16$	(16.16)	15.39	35.78	1.0500	1450 my; 8.65
Assume $\frac{208}{204}=35.74$	16.09	15.38	(25.74)	1.0462	1490 my; 8.65
<u>Marble Mts. Granite K-Spar</u>					
Assume $\frac{206}{204}=16.16$	(16.16)	15.40	36.39	1.0494	1460 my; 8.67
Assume $\frac{208}{204}=35.74$	15.97	15.38	(35.74)	1.0384	1580 my; 8.69

(1) Calculated assuming accumulation of 'normal' radiogenic lead over the inferred age of the rock from a source with Th/U as defined by the observed mixing lines of the stepwise-removed lead fractions. The radiogenic increment is assumed to be defined by one or the other of the most primitive values of 206/204 or 208/204 of the Lawler Peak granite K-feldspar lead fractions.

(2) The single-stage evolution model described in appendix I and using the constants given there.

Pb^{206}/Pb^{207} values. Calculated initial lead compositions are given in table 13. These calculations are performed in two ways, both of which assume that the calculated Lawler Peak granite original lead (page 317) is valid. The first calculation assumes that all of the rocks had the same initial lead 206/204 as the Lawler Peak granite, and gives initial 208/204 and 207/204 lead values for the Ruin and Marble Mts. granites. The second calculation assumes that all of the rocks had the same initial 208/204 as the Lawler Peak granite, and gives initial 206/204 and 207/204 values for the lead of the other two granites.

To calculate initial 207/204 and 208/204 from the initial 206/204, or the initial 206/204 and 207/204 from the initial 208/204, it is necessary only to assume that the radiogenic increment is from a 'normal' radiogenic lead, derived over the age of the rock from a source with the Th/U calculated from the observed original lead-radiogenic lead mixing lines from analyses of the stepwise-derived lead fractions (see discussion and figures of the lead fraction analyses for each K-feldspar).

Results of Calculations

If all of the rocks had the same initial 206/204 of 16.16, the calculated initial 208/204 for the Lawler Peak, Ruin, and Marble Mts. granites are, respectively, 35.74, 35.78, and 36.39. The Lawler Peak and Ruin granite values are quite similar, but the Marble Mts. granite calculated initial 208/204 is almost 2% higher -- a significant difference, implying that either the initial lead 208/204 of the three rocks were not identical, or that the initial 206/204 of the rocks was not

similar and equal to the calculated original value for the Lawler Peak granite.

If, on the other hand, all of the three rocks had the same initial 208/204 of 35.74, the calculated initial 206/204 of Lawler Peak, Ruin, and Marble Mts. granites are, respectively, 16.16, 16.09, and 15.97. This represents a poorer agreement than the 'raw' ratios (16.16, 16.30, 16.18).

The most plausible interpretation of these calculations is that the Lawler Peak and Ruin granites had similar initial lead 206/204, 207/204, and 208/204, but that the Marble Mts. granite had either a higher initial lead 208/204 or a lower 206/204 than either the Lawler Peak or Ruin granites. This in turn implies that the Marble Mts. granite was formed from a source which had undergone a chemical differentiation (in terms of Th/U) from a source common to all three rocks, shortly before emplacement. Because the thorium content of the Marble Mts. granite is much higher than that of the Lawler Peak or Ruin granites (142 ppm versus 29 ppm and 28 ppm), it is most likely that this differentiation was of the form of an increase in Th/Pb, and that the high initial 208/204 derived by assuming similar initial 206/204 for all of the rocks is qualitatively more correct. The time before emplacement that this penultimate differentiation can have occurred is limited by the similarity of original rock lead 207/204 values to a few hundreds of millions of years*.

* assuming that any change in U/Pb was accompanied by a change in Th/Pb.

The chain of inferences involved in the above discussion is too long for a high degree of confidence to be placed in the conclusion; nevertheless, such conclusions are clearly of great significance in regard to the systematics of crustal evolution, and illustrate the value of the ability to recover true original lead isotopic compositions for such (possibly) cogenetic plutons. A systematic study, present in embryo in the above discussion, which could trace the differentiation history of the sources of such plutons would be of great interest.

COMMENTS ON PRECAMBRIAN FELDSPAR LEAD ANALYSES

The foregoing demonstrations of the presence of radiogenic lead in high-purity Precambrian K-feldspar concentrates should be borne in mind when interpreting existing analyses of Precambrian feldspar leads, and in the analysis and interpretation of data yet to be collected. Unless the K-feldspar lead analyses agree with those of associated conformable ore leads, or unless analyses of the lead of several cogenetic K-feldspars from different parts of the rock body of different composition agree, isotopic analyses of Precambrian feldspar leads cannot be assumed to be free of the effects of an admixed radiogenic lead. The effect may be slight, as in the case of the Giants' Range granite, or it may be profound, as in the case of the Lawler Peak granite. For uses such as the correction (for common lead) of the radiogenic lead isotope ratios of a mineral to be used for dating, a slight radiogenic lead component is not important, especially if the component is similar in isotopic composition to the radiogenic lead of the mineral being used

for dating. However, even a slight effect becomes significant if complex lead evolution models are being fitted to a number of such data. Therefore, if existing Precambrian feldspar lead analyses are to be used for such a purpose, they should be critically examined for the possibility of bias due to the incorporation of radiogenic lead.

Although the five rocks studied are too few to make reliable generalizations, the following correlations should be kept in mind in predicting the magnitude of the radiogenic lead admixture in feldspars of rocks;

a) The K-feldspar which contained by far the most radiogenic lead component came from a rock (the Lawler Peak granite) which was unusually high in uranium; and,

b) The K-feldspar which contained the least amount of radiogenic lead component came from a rock (the Giants' Range granite) which had a relatively uneventful phanerozoic history, a low uranium content, and which was the freshest-appearing of any of the rocks studied.

Thus, it seems likely that relatively undisturbed K-feldspar leads can be found in rocks of average to low uranium and thorium content which cannot have been significantly disturbed by phanerozoic intrusive or hydrothermal events*. The younger (Precambrian) granites of Precambrian shields would presumably be the best candidates for having

*Precambrian events can clearly affect the K-feldspar lead composition, as suggested by the Payson and Giants' Range granites data, but short time intervals between crystallization and disturbance mean that the amounts of radiogenic lead which can have been generated in those intervals is relatively small.

undisturbed feldspar leads. On the other hand, K-feldspar leads from rocks which may have been affected by younger (Mesozoic or younger, for instance) intrusive or hydrothermal events (especially in regions of hydrothermal mineralization) should be viewed with extreme suspicion.

In cases where the samples are not expected to be significantly affected by an admixture of radiogenic lead, but where it is important that such an effect not be present, a simple check involving only one additional analysis, and without additional equipment such as is needed for the volatilization procedure, is available. This check is simply the comparison of a lead isotopic analysis of the most HF-soluble fraction of the K-feldspar lead with the least HF-soluble, or even remaining lead fraction. If the two analyses agree, the feldspar lead is probably undisturbed*.

GENERAL SUMMARY

The stepwise lead removal experiments described in this study have shown that, for all of the five rocks studied, the leads of Precambrian feldspars (or, more precisely, high-purity K-feldspar concentrates) are not now isotopically equivalent to the leads originally present in the feldspars. Although the original feldspar lead is the dominant

* However, because the experiments and data in this work are very limited, it might still be possible for a radiogenic lead component to be present which does not differ in HF-solubility from the original lead.

component, variable amounts of radiogenic leads are also present in the feldspars. The mechanisms of radiogenic lead incorporation, and the location of the radiogenic leads remains unclear; however, the experimental results suggest the following conclusions:

a) Part of the feldspar radiogenic lead of some of the rocks studied is derived from mobile Rn^{222} , an intermediate daughter of U^{238} , and is composed of essentially pure Pb^{206} ,

b) The Pb^{206} -enriched radiogenic lead component of the feldspars is concentrated in a specific site or class of sites, which becomes unstable and releases its lead at about $1150^\circ \pm 30^\circ\text{C}$.

c) In all cases, some or all of the feldspar radiogenic lead is evidently derived from the rock uranium and thorium, and its time of incorporation by the feldspar influenced by the geologic history (thermal and hydrothermal) of the rock,

d) The original feldspar lead is concentrated by treatment (thermal or chemical) which removes easily mobilized lead from the feldspar concentrate, and

e) Part of the radiogenic lead of some of the feldspar concentrates is less mobile under high-temperature conditions than the original feldspar lead; therefore, the highest proportion of original lead is not necessarily obtained in the least volatile lead fraction from a stepwise volatilization experiment.

The original lead of the three 1450 ± 20 m.y. old granites which were studied were evidently very similar in isotopic composition ($207/204 = 15.39 \pm .02$, $206/204 = 16.1 \pm 0.1$), even though these

granites are separated by hundreds of miles. The original lead 208/204 value of one of these rocks, however, was evidently significantly different from the original 208/204 values for the other two rocks. The lead isotope data from the feldspars suggests that the three 1450 ± 20 m.y. granites shared the same source material until only a few hundreds of millions of years before emplacement, at which time a change in composition reflected by a change in the U/Th and Th/Pb ratios occurred.

Appendix I

Radioactive Decay Systematics and Lead Evolution Equations

The basic law of radioactive decay is that

$$\frac{dN}{dt} = -\lambda N \quad \text{and} \quad N = N_0 e^{-\lambda t}$$

where N is the number of radioactive atoms existing at time t , N_0 is the number of these atoms at some initial time, and λ is the radioactive decay constant, in units of inverse time. For this work, the following constants have been used:

	Stable	daughter
$\lambda(\text{U}^{238}) = \lambda_{238} = 0.1537 \times 10^{-9} \text{ yr}^{-1*}$	Pb ²⁰⁶	
$\lambda(\text{U}^{235}) = \lambda_{235} = 0.9722 \times 10^{-9} \text{ yr}^{-1*}$	Pb ²⁰⁷	
$\lambda(\text{Th}^{232}) = \lambda_{232} = 0.0499 \times 10^{-9} \text{ yr}^{-1§}$	Pb ²⁰⁸	
$\text{U}^{238}/\text{U}^{235}$ (present day) = 137.8 [†]		

(If the recently determined U^{238} and U^{235} decay constants of Jaffe et al (1971) are used for model-lead age calculations, the effect is to decrease the model age from that calculated using the above constants. The effect is about 240 m.y. at 1450 m.y. (using the above constants) and 180 m.y. at 2700 m.y.)

The abundance of radiogenic lead isotopes in a closed U-Th-Pb system is given by the following equations:

$$\text{Pb}^{206} = \text{U}_0^{238}(1 - e^{-\lambda_{238}t})$$

$$\text{Pb}^{207} = \text{U}_0^{235}(1 - e^{-\lambda_{235}t})$$

$$\text{Pb}^{208} = \text{Th}_0^{232}(1 - e^{-\lambda_{232}t})$$

*Fleming et al, 1952.

§Kovarik and Adams, 1938; Picciotto and Wilgain, 1956.

†Inghram, 1946.

where U_o^{238} , U_o^{235} , and Th_o^{232} are abundances of these isotopes at the start of radiogenic lead accumulation, and the lead abundance is measured after t years of radiogenic lead accumulation. The Pb^{207}/Pb^{206} of this system is thus

$$\left(\frac{Pb^{207}}{Pb^{206}} \right)_{\text{radiogenic}} = \frac{e^{\lambda_{235}t} - 1}{137.8(e^{\lambda_{238}t} - 1)}$$

for systems measured at the present time.

Single-Stage Evolution of Lead:

If the closed U-Th-Pb system contains some initial Pb^{206} , Pb^{207} , and Pb^{208} , the variation of lead isotopic composition with time is given by

$$\left(\frac{Pb^{206}}{Pb^{204}} \right)_t = \left(\frac{Pb^{206}}{Pb^{204}} \right)_{t_0} + \mu(e^{\lambda_{238}t_0} - e^{\lambda_{238}t})$$

$$\left(\frac{Pb^{207}}{Pb^{204}} \right)_t = \left(\frac{Pb^{207}}{Pb^{204}} \right)_{t_0} + \frac{\mu}{137.8} (e^{\lambda_{235}t_0} - e^{\lambda_{235}t})$$

$$\left(\frac{Pb^{208}}{Pb^{204}} \right)_t = \left(\frac{Pb^{208}}{Pb^{204}} \right)_{t_0} + \eta\mu(e^{\lambda_{232}t_0} - e^{\lambda_{232}t})$$

where t_0 is the time of initial radiogenic lead accumulation, t is the time of interest, $\mu = (U^{238}/Pb^{204})_{\text{today}}$ in the system, and $\eta = (Th^{232}/U^{238})_{\text{today}}$ in the system.

t_0 is generally taken to be the time of formation of the earth. For this work, the value 4.55×10^9 years (Patterson, 1955; Murthy and Patterson, 1962) is used. The initial lead isotopic composition is taken to be the average primordial lead as determined by Murthy and Patterson (1962)

$$\text{with } \left[\frac{206}{204} \right]_{t_0} = 9.56 \quad \left[\frac{207}{204} \right]_{t_0} = 10.42 \quad \left[\frac{208}{204} \right]_{t_0} = 29.71$$

Physical interpretation of the single-stage lead evolution model is generally that the U-Pb-Th system is the earth's mantle, or a significant fraction of the mantle, and that emplacement into the crust of the lead defines the end of this single-stage evolution. Of course, if the lead, after emplacement into the crust, is still associated with U and Th, evolution of its isotopic composition continues.

Appendix II

Radiogenic-Common Lead Mixing Equations

If a common lead and a radiogenic lead are mixed in varying proportions, then the leads representing varying degrees of mixing will plot on a straight line on both a $(\text{Pb}^{208}/\text{Pb}^{204}) - (\text{Pb}^{206}/\text{Pb}^{204})$ and $(\text{Pb}^{207}/\text{Pb}^{204}) - (\text{Pb}^{208}/\text{Pb}^{204})$ plot, with slopes equal to the $(\text{Pb}^{208}/\text{Pb}^{206})$ and $(\text{Pb}^{207}/\text{Pb}^{208})$, respectively, of the radiogenic lead. If the radiogenic lead is derived from accumulation of Pb^{206} , Pb^{207} , and Pb^{208} from a system with a constant $\text{Th}^{232}/\text{U}^{238}$, η , (except for radioactive decay) over a time, t , until the present, then

$$\eta = \frac{e^{-\lambda_{235}t} - 1}{137.8(\text{Pb}^{207}/\text{Pb}^{208})_{\text{radio-genic}} (e^{\lambda_{232}t} - 1)} = \frac{e^{-\lambda_{238}t} - 1}{(e^{-\lambda_{232}t} - 1)(\text{Pb}^{206}/\text{Pb}^{208})_{\text{radio-genic}}}$$

On a $(\text{Pb}^{206}/\text{Pb}^{207}) - (\text{Pb}^{206}/\text{Pb}^{208})$ plot, the compositions of the variably mixed leads will not plot on a straight line. If the degree of radiogenic lead in the mixtures is given by $\rho = (\text{Pb}^{206})_{\text{radiogenic}} / (\text{Pb}^{206})_{\text{common}}$, then

$$\left[\frac{\text{Pb}^{206}}{\text{Pb}^{207}} \right]_{\text{mixture}} = \frac{1 + \rho}{\left[\frac{\text{Pb}^{207}}{\text{Pb}^{206}} \right]_{\text{common}} + \frac{\rho}{137.8} \left[\frac{e^{\lambda_{235}t} - 1}{e^{\lambda_{238}t} - 1} \right]}$$

$$\left[\frac{\text{Pb}^{206}}{\text{Pb}^{208}} \right]_{\text{mixture}} = \frac{1 + \rho}{\left[\frac{\text{Pb}^{208}}{\text{Pb}^{206}} \right]_{\text{common}}} + \rho \eta \left[\frac{e^{\lambda_{232}t} - 1}{e^{\lambda_{238}t} - 1} \right]$$

But for small amounts of admixed radiogenic lead, and thus small ρ , the equations reduce to linear form such that

$$\left[\frac{\text{Pb}^{206}}{\text{Pb}^{207}} \right]_{\text{mixture}} = \left[\frac{\text{Pb}^{206}}{\text{Pb}^{207}} \right]_{\text{common}} + \rho \left\{ \left[\frac{\text{Pb}^{206}}{\text{Pb}^{207}} \right]_{\text{common}} - \left[\frac{\text{Pb}^{206}}{\text{Pb}^{207}} \right]_{\text{common}}^2 \frac{(e^{\lambda_{235}t} - 1)}{137.8(e^{\lambda_{238}t} - 1)} \right\}$$

and

$$\left[\frac{\text{Pb}^{206}}{\text{Pb}^{208}} \right]_{\text{mixture}} = \left[\frac{\text{Pb}^{206}}{\text{Pb}^{208}} \right]_{\text{common}} + \rho \left\{ \left[\frac{\text{Pb}^{206}}{\text{Pb}^{208}} \right]_{\text{common}} - \left[\frac{\text{Pb}^{206}}{\text{Pb}^{208}} \right]_{\text{common}}^2 \frac{(e^{\lambda_{232}t} - 1)}{\eta(e^{\lambda_{238}t} - 1)} \right\}$$

so the slope of the mixing line,

$$\frac{(\text{Pb}^{206}/\text{Pb}^{207})_{\text{mixture}} - (\text{Pb}^{206}/\text{Pb}^{207})_{\text{common}}}{(\text{Pb}^{206}/\text{Pb}^{208})_{\text{mixture}} - (\text{Pb}^{206}/\text{Pb}^{208})_{\text{common}}} = S_0$$

becomes

$$S_o = \left[\frac{\text{Pb } 208}{\text{Pb } 207} \right]_{\text{common}} \frac{1 - \left[\frac{\text{Pb } 206}{\text{Pb } 207} \right]_{\text{common}} \frac{(e^{\lambda_{235}t} - 1)}{137.8(e^{\lambda_{238}t} - 1)}}{1 - \left[\frac{\text{Pb } 206}{\text{Pb } 208} \right]_{\text{common}} \frac{(e^{\lambda_{232}t} - 1)}{\eta(e^{\lambda_{238}t} - 1)}}$$

thus the $\text{Th}^{232}/\text{U}^{238}$ (η) of the radiogenic lead source today is given by

$$\eta = \frac{1 - \frac{1}{S_o} \left[\frac{\text{Pb } 208}{\text{Pb } 207} \right]_{\text{common}} \left\{ 1 - \left[\frac{\text{Pb } 206}{\text{Pb } 207} \right]_{\text{common}} \frac{(e^{\lambda_{235}t} - 1)}{137.8(e^{\lambda_{238}t} - 1)} \right\}}{\left[\frac{\text{Pb } 206}{\text{Pb } 208} \right]_{\text{common}} \left[\frac{e^{\lambda_{232}t} - 1}{e^{\lambda_{238}t} - 1} \right]}$$

Appendix III

Mass Spectrometric Data Collection Modes

The isotope ratios reported in this work were obtained by the averaging of the ratios from many individual sets which included peaks of all of the isotopes of the element. Thus, a single set of lead was obtained by step-scanning over Pb^{206} , Pb^{207} , Pb^{208} , and Pb^{204} . If the background intensity was constant, and the intensity of the isotopic peaks in question high, the backgrounds were monitored only every 10-15 sets. The total time necessary for one complete lead isotope set was about $1\frac{1}{2}$ minutes. Since the signal intensity was generally fairly stable (usually less than 10% intensity change in 10 minutes), the data were reduced by assuming a linear change in intensity with time. The fitting of an exponential or quadratic curve to the assumed intensity change would not have significantly improved the data of the runs.

Non-lead peaks were sometimes present during the lead runs, although generally with less than 0.1% intensity than the Pb^{204} peak. For those runs where the intensity of the non-lead peaks was greater than 0.1% of the Pb^{204} peak, a correction was made for the interpolated contribution of a non-lead mass 204 peak. As the non-lead peaks only varied, among themselves, in intensity by less than a factor of two, the correction (based on the average intensity of the non-lead peaks in the mass 204 region) did improve the precision and accuracy of the results. However, uncertainty as to the actual magnitude of the predicted non-lead mass 204 peak was assumed to be about $2/3$ the magnitude of the

correction, for purposes of estimating possible error in the lead isotope ratios.

The estimated error limits reported in this work for the lead isotope ratios are an intuitive synthesis of the following factors:

a) Error in the correction for non-lead mass 204 peaks - discussed above.

b) Uncertainty introduced by blank-correction; the concentration and composition of the blank lead was obtained by interpolation of blank determinations -- in cases where the ratio of blank lead to sample lead was high (such as when samples of less than about three micrograms were run), the uncertainty as to the actual composition and concentration of the attendant blank lead was significant.

c) The probable error based on the standard deviation of the ratios of the individual sets and the number of sets (95% confidence limit, as generally defined, was used).

A typical run involved 30-70 sets which were averaged.

Appendix IV

Fitting of Straight Lines to the Lead Isotope Data

A modification of the reduced major axis method (Kermack and Haldane, 1950; Imbrie, 1956) was used for the fitting of straight lines to the lead isotope data. With the reduced major axis method, the slope of the best-fit line is given by

$$M = \frac{S_y}{S_x}$$

where M - the best-fit slope, S_y and S_x are the variances of the y and x parameters of the data points. The intersection of the line is determined by forcing the line through the average of both parameters of the data points, \bar{X} and \bar{Y} . The standard slope error is given by

$$M_k = \frac{S_y}{S_x} \sqrt{\frac{1 - r^2}{n}}$$

where M_k is the standard slope error, r is the correlation coefficient determined by

$$r = \frac{\Sigma(x-\bar{x})(y-\bar{y})}{\sqrt{\Sigma(x-\bar{x})^2 \Sigma(y-\bar{y})^2}}$$

To compensate for the tendency of this method to give biased slopes when the points scatter around a line of low slope, the data points were first rotated so that they scattered about a line with a slope of about one before the final line was fit, then returned to their original position.

Appendix V

Rock Thin-Section Descriptions

Lawler Peak Granite Sample:

Mode:

Plagioclase - 25%	Opaque Minerals - 0.3%
Quartz - 24%	White Mica - 7%
K-feldspar - 42%	Chlorite - 1%
Biotite - 1%	Trace Minerals - epidote, apatite, zircon

Plagioclase - occurs as 2-6 mm anhedral to subhedral grains. Most grains show albite twinning, and are zoned. Pericline twins are present, but rare. The cores of the strongly zoned plagioclase grains are highly altered to a fine-grained assemblage of sericite + clays(?).

Quartz - occurs as 4-8 mm, anhedral, strained grains.

K-feldspar - occurs as 4-10 mm subhedral grains. They are perthitic, with an exsolved plagioclase content of about 10-15%. The exsolved plagioclase is present as elongate, untwinned patches, irregular-shaped, twinned patches, and fine elongate threads. The K-feldspar shows good gridiron twinning, and displays euhedral interior zones defined by concentrations of abundant, aligned plagioclase and mica inclusions. The K-feldspar shows almost no alteration.

Biotite - occurs as 1-2 mm, subhedral to anhedral grains, pleochroic in dark brown, light tan, and dark olive (basal plates). The biotite is partially altered to chlorite, epidote, and white mica(?), and commonly includes small grains of epidote, opaque minerals, and apatite.

Opaque Minerals - occur as $\frac{1}{2}$ -2 mm anhedral to euhedral grains. The well-formed grains are generally square or rhomb-shaped in cross section (magnetite?). Some opaque grains with a deep red color of thin edges is also present (hematite?).

White Mica - occurs as 0.1-2 mm anhedral to subhedral grains, generally intergrown with biotite. White mica is also common as an alteration product of the plagioclase.

Chlorite - occurs as 1-2 mm anhedral to subhedral grains, pleochroic in grass-green and light tan.

Ruin Granite Sample:

Mode:

Plagioclase - 25%	Opaque Minerals - 1%
Quartz - 33%	White Mica - 4%
K-feldspar - 28%	Chlorite - 3%
Biotite - 7%	Trace Minerals - apatite, epidote, zircon

Plagioclase - occurs as strongly zoned, 2-10 mm, subhedral grains. The plagioclase is highly sericitized, especially in the cores of the grains. The zoning is somewhat complex, with evidently later, untwinned overgrowths on more calcic, twinned cores, and also in a patchy pattern in some grains.

Quartz - occurs as 1-4 mm, anhedral grains. The quartz grains are in many cases interlocked with other quartz grains, and may show strain.

K-feldspar - occurs as 1-20 mm anhedral to subhedral grains, most of which show gridiron twinning. The larger grains may be distinctly zoned, both optically and in the distribution of inclusions. The inclusions are abundant in the larger grains, and are plagioclase (zoned and altered), biotite, white mica, opaque minerals, and blebs of quartz. The K-feldspar is fresh except for a patchy alteration which covers about 40% of the surface of the large grains. The smaller K-feldspar grains (under 3 mm) are anhedral and generally interstitial with other mineral grains (except quartz).

Biotite - occurs as 1-10 mm subhedral to anhedral grains, pleochroic from very light tan to dark and light olive. Most grains are fresh, but many are intergrown with chlorite. Most have inclusions of apatite, opaques, zircon or other minerals.

Opaque Minerals - occur as anhedral to euhedral 1-2 mm grains.

White Mica - occurs as 1-3 mm, anhedral to subhedral grains, mostly with biotite. (Also as alteration product of feldspar).

Chlorite - occurs as an alteration mineral of biotite. Pleochroic from emerald green to pale tan.

Marble Mts. Granite Sample:

Mode:

Plagioclase - 35%	Opaque Minerals - 0.1%
Quartz - 40%	Chlorite + Epidote - 1%
K-feldspar - 14%	Trace Minerals - apatite, zircon, uranothorite
Hornblende + Biotite - 10%	

Plagioclase - occurs as 2-8 mm subhedral to anhedral grains. Most of the plagioclase grains are untwinned, and many contain exsolved K-feldspar. Inclusions are common in the larger grains, which are largely sericitized.

Quartz - occurs as 2-5 mm, anhedral, strained grains.

K-feldspar - occurs as subhedral, 2-10 mm perthitic grains. Twinning is either absent, or very rudimentary. The grains are fresh, zoned, and generally include small grains of plagioclase, biotite, and hornblende. The exsolved plagioclase occurs as very fine threads. A few grains show carlsbad twinning.

Hornblende - occurs as 1-3 mm subhedral grains, pleochroic from tan to reddish brown. The hornblende shows incipient alteration to biotite and chlorite. The relative abundance of the hornblende is much less than that of the biotite.

Biotite - occurs as 1-5 mm, anhedral grains, strongly pleochroic in light tan and dark reddish-brown. Inclusions of opaque minerals and apatite are common. The biotite is frequently partially altered to chlorite.

Opaque Minerals - occur as $\frac{1}{2}$ -2 mm, anhedral grains, generally associated with biotite and chlorite.

Chlorite - occurs as 1-3 mm anhedral grains, pleochroic from grass-green to light tan. The chlorite is generally associated with biotite.

Payson Granite Sample:

Mode:

Plagioclase - 11%	Biotite - 3%
Quartz - 21%	Opaque Minerals - 1%
K-feldspar - 58%	Trace Minerals - zircon, apatite, rutile
Hornblende - 6%	

Plagioclase - occurs as 2-5 mm, subhedral to anhedral partially sericitized grains. The plagioclase is zoned and twinned, with the rims of the grains much less altered than the cores.

Quartz - occurs as 2-5 mm anhedral, strained grains.

K-feldspar - occurs as 5-10 mm, sub-anhedral, perthitic grains. Some show carlsbad twinning, but gridiron twinning is rare. Irregular extinction of the K-feldspar grains suggests that they are zoned. The exsolved plagioclase varies from 10% to 40% in volume of the K-feldspar grains, and is partially altered. The K-feldspar is fresh-looking.

Hornblende - occurs as 2-6 mm anhedral to subhedral grains, pleochroic from light tan to brown to olive. The hornblende grains are fresh, and commonly contain inclusions of biotite, opaque minerals, and zircon.

Biotite - occurs as $\frac{1}{2}$ -5 mm anhedral to subhedral grains, pleochroic from tan to dark red-brown. The biotite in some cases is intimately associated with hornblende as inclusions or intergrowths, and contains abundant opaque mineral and zircon inclusions.

Opaque Minerals - occur as $\frac{1}{2}$ -1 mm anhedral to subhedral grains.

Giants' Range Granite Sample:

Mode:

Plagioclase* - 54%	Hornblende - 14%
Quartz - 11%	Chlorite - 1%
K-feldspar - 17%	Trace Minerals - apatite - $\frac{1}{2}\%$ sphene - $\frac{1}{2}\%$ opaques - tr.

Hornblende - occurs as 2-5 mm, anhedral grains, pleochroic from almost colorless to blue-green. The hornblende generally shows some alteration to chlorite, and sphene and apatite inclusions are abundant.

Plagioclase - occurs as 2-10 mm, anhedral grains. The larger grains are largely altered to sericite + clays(?). Both zoned and unzoned grains are present.

Quartz - occurs as 2-4 mm, anhedral, strained (slightly) grains.

K-feldspar - occurs as 1-3 mm, anhedral, grains with gridiron twinning. The K-feldspar is non-perthitic, and very fresh looking. About 5-10% of the surface of the grains, in thin-section, does show alteration to the usual fine-grained sericite + clays(?).

Chlorite - occurs as 1-4 mm anhedral grains, pleochroic from pale tan to grass-green. The chlorite is generally associated with hornblende, and commonly includes small grains of sphene and apatite.

Sphene - occurs as $\frac{1}{2}$ -2 mm, subhedral to euhedral grains, commonly showing some degree of alteration to a fine-grained, opaque mineral (leucoxene?). Inclusions of quartz or apatite are not uncommon. The sphene grains are in many cases corroded and embayed by feldspar grains.

*including alteration minerals.

PHOTOMICROGRAPHS OF ROCKS AND FELDSPAR CONCENTRATES

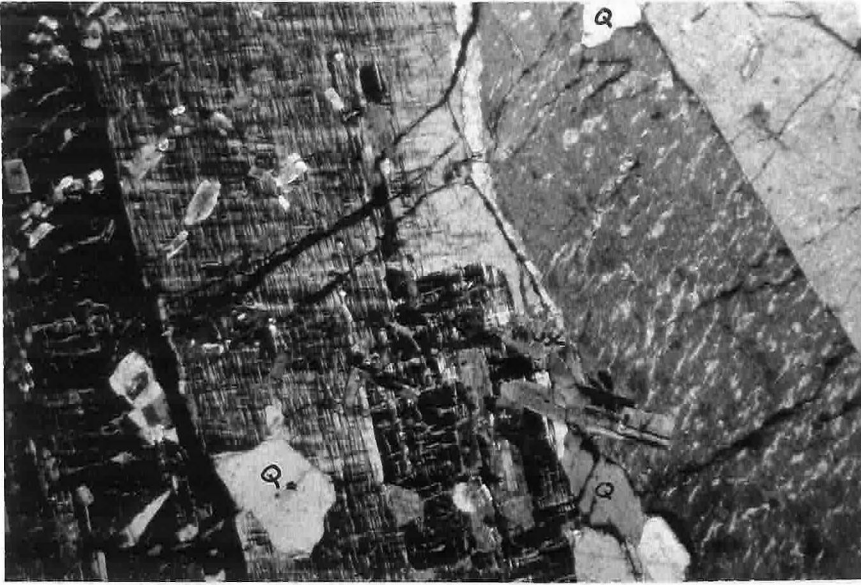


Plate 1. Thin-section of Lawler Peak Granite; 7 x 10 mm field, crossed nicols. K-feldspar phenocrysts with exsolved albite and abundant inclusions. All inclusions, except those otherwise marked, are plagioclase. (Q = quartz, musc = muscovite, bio = biotite, chlor = chlorite).

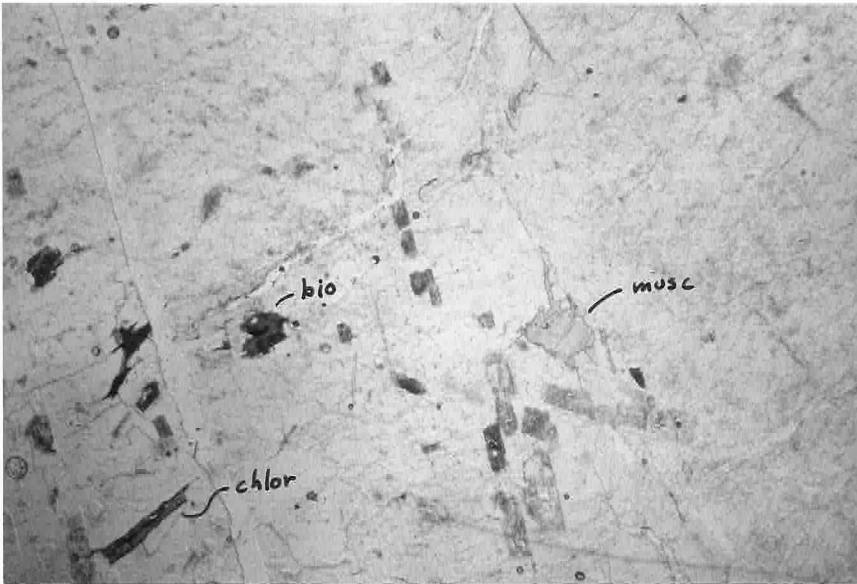


Plate 2. Same as Plate 1, but plane-polarized light. The plagioclase inclusions are typically more altered than the K-feldspar.

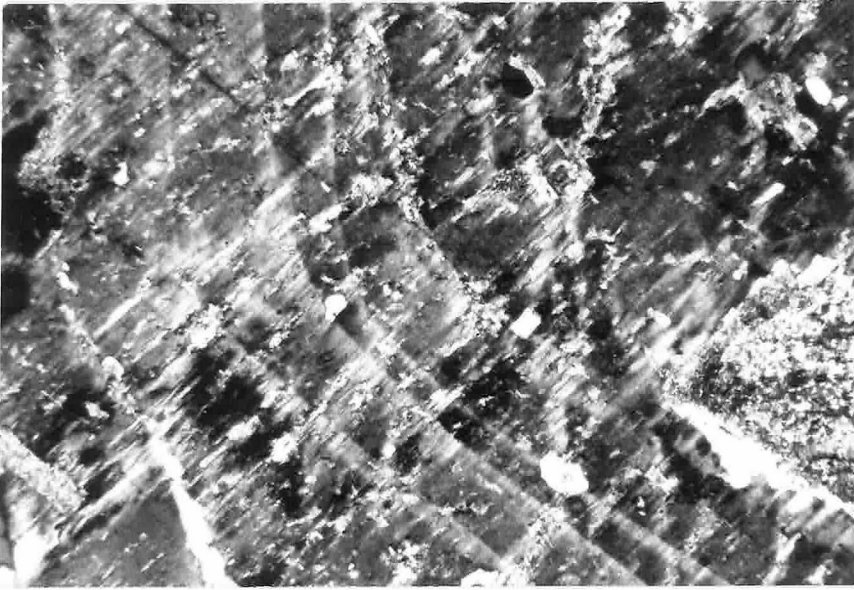


Plate 3. Zoned K-feldspar phenocryst in Ruin Granite. At upper left is altered plagioclase inclusion. Exsolved plagioclase is present as oriented, elongate patches. Crossed nicols, 2.2 mm x 3.4 mm field.

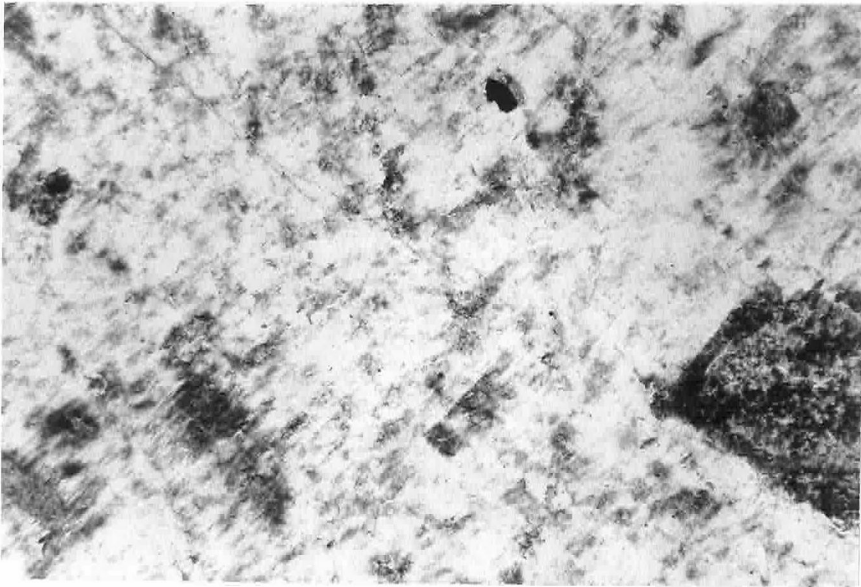


Plate 4. Same as Plate 3, but plane-polarized light. Areas of abundant, fine-grained, high-index inclusions are generally associated with exsolved plagioclase, but also occur within the K-feldspar.

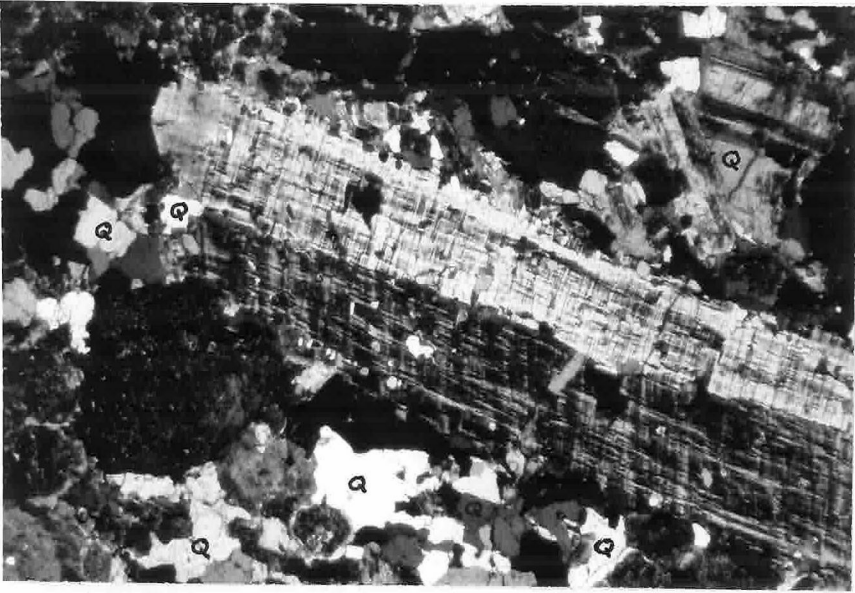


Plate 5. Ruin Granite; twinned K-feldspar phenocryst. The inclusions are mostly plagioclase and quartz. Crossed nicols, 7 x 10 mm field.

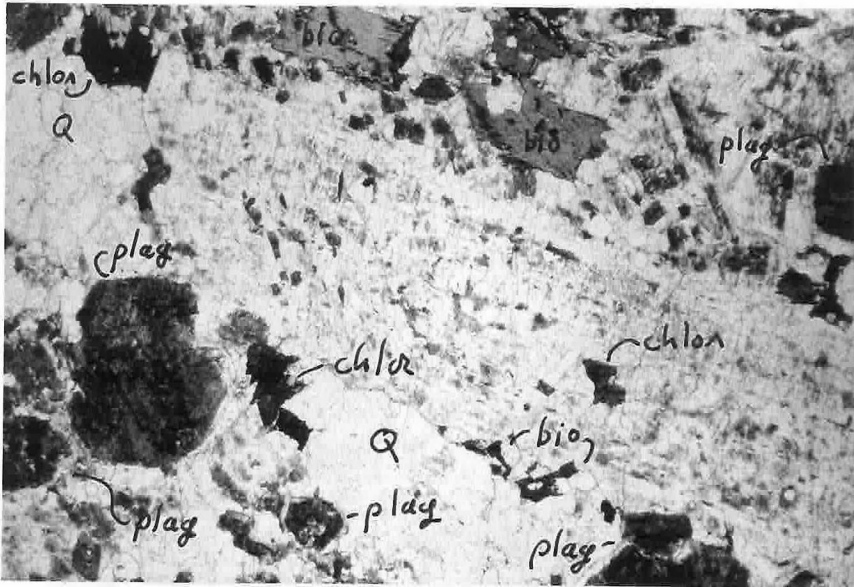


Plate 6. Same as Plate 5, plane-polarized light. Q = quartz, Plag = plagioclase, Chlor = chlorite, Bio = biotite, Musc = white mica.

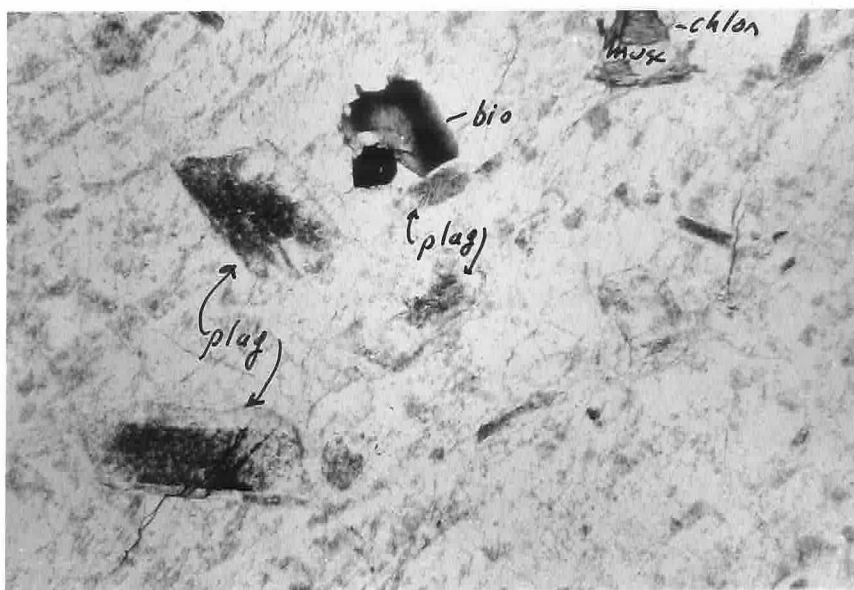


Plate 7. Ruin Granite; inclusions in K-feldspar phenocryst. Plane-polarized light, 2.2 x 3.4 mm field. Q = quartz, chlor = chlorite, bio = biotite, musc = white mica.

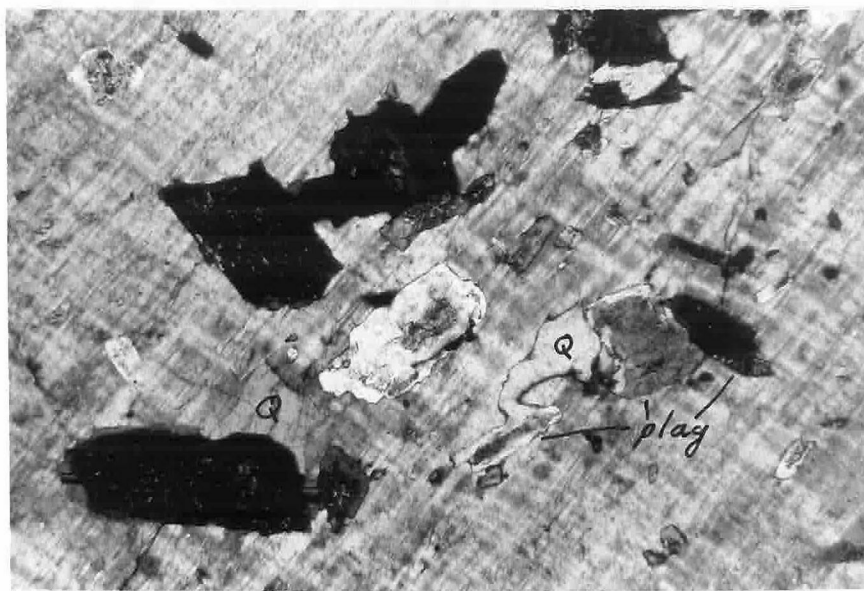


Plate 8. Same as Plate 7, crossed nicols.

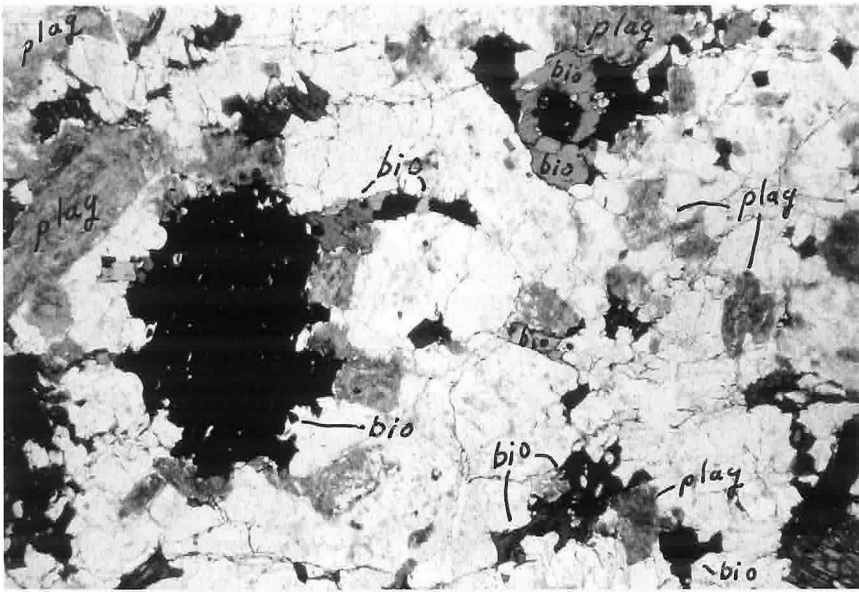


Plate 9. Marble Mts. Granite; the plagioclase is typically altered to sericite, but the K-feldspar is relatively fresh (see Plate 10). Plane-polarized light, 7 x 10 mm field.

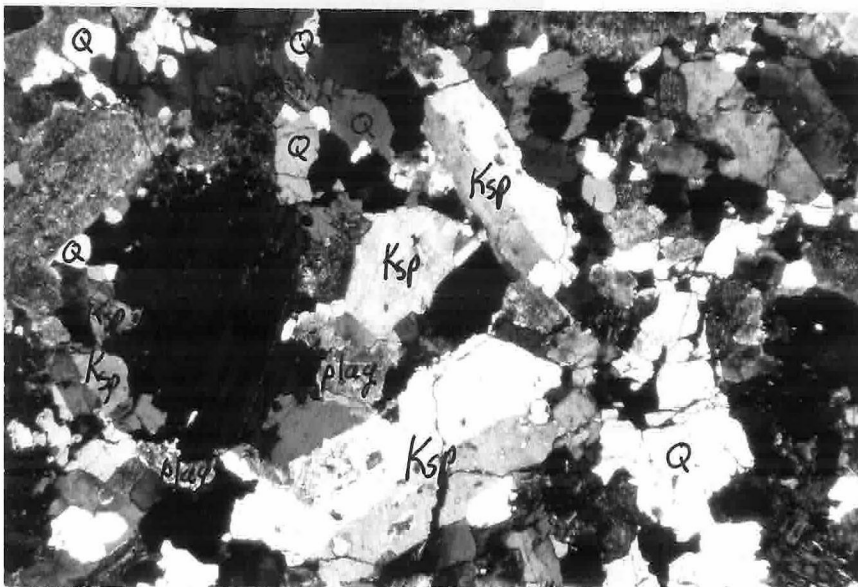


Plate 10. Same as Plate 9, crossed nicols. Plag = plagioclase, Q = quartz, bio = biotite, Ksp = K-feldspar.

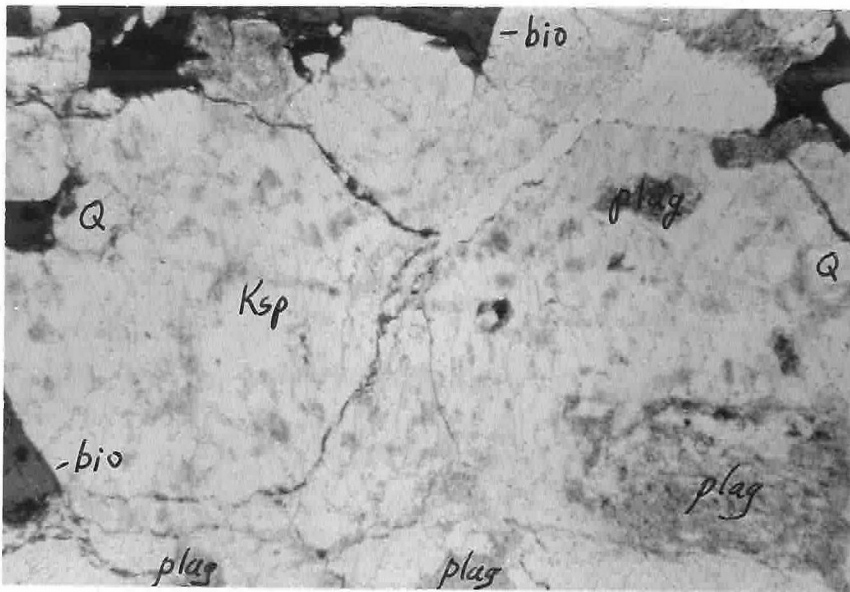


Plate 11. Marble Mts. Granite; zoned K-feldspar phenocryst. Plane-polarized light, 2.2 x 3.4 mm field.

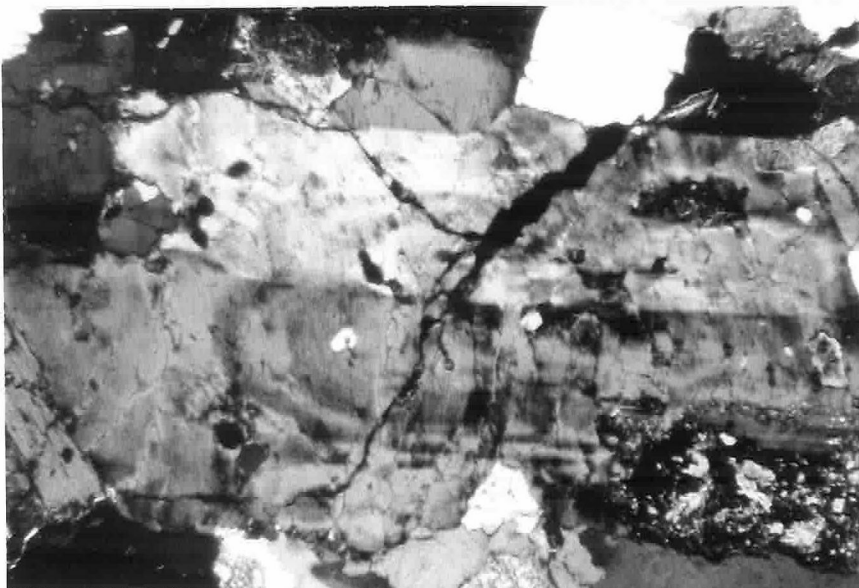


Plate 12. Same as Plate 11, crossed nicols. Q = quartz, plag = plagioclase, Ksp = K-feldspar, bio = biotite.

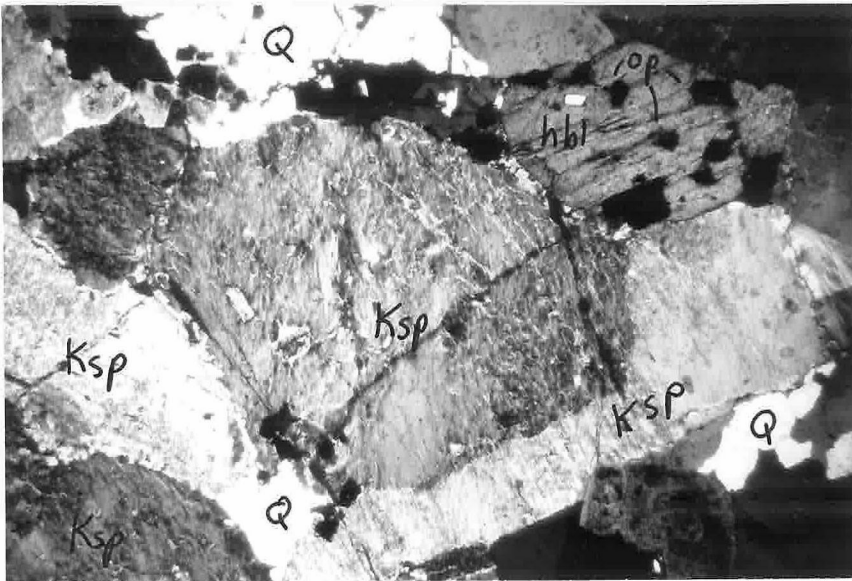


Plate 13. Payson Granite; large perthite phenocryst in center of field. Crossed nicols, 6 x 9 mm field. Q = quartz, pl = plagioclase, op = opaque minerals, Ksp = K-feldspar, Hbl = hornblende.

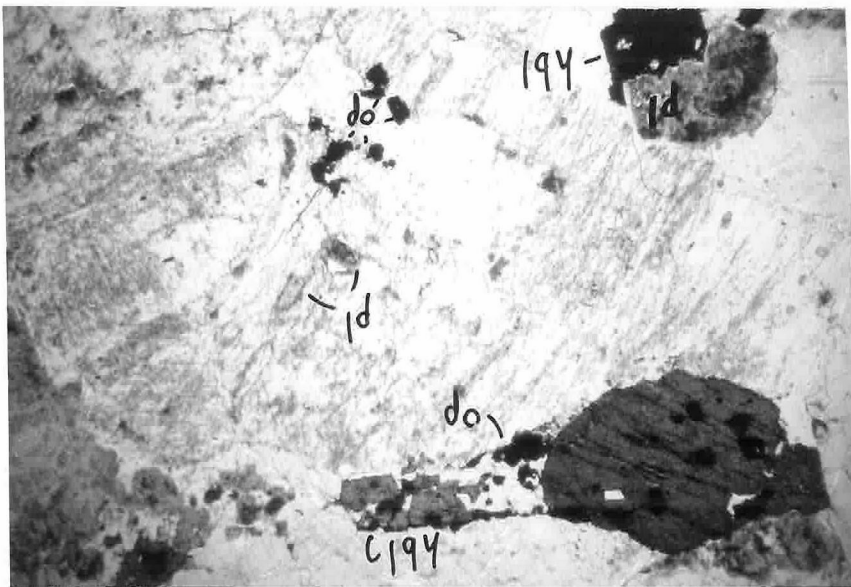


Plate 14. Same as Plate 13, plane-polarized light.



Plate 15. Giants Range Granite; crossed nicols,
2 x 3 mm field.

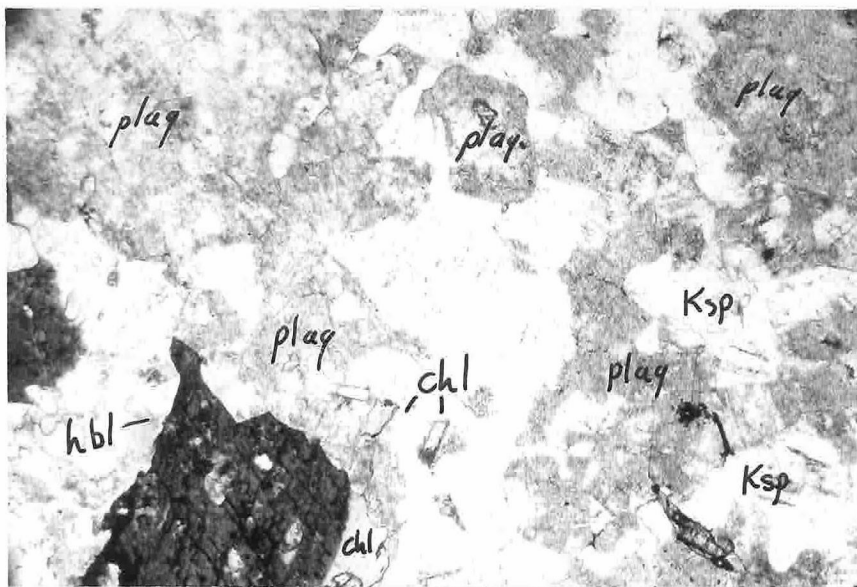


Plate 16. Same as Plate 15, plane-polarized light.
The plagioclase includes abundant fine-grained alteration(?) minerals, but the K-feldspar appears fresh.
Ksp = K-feldspar, plag = plagioclase, chl = chlorite,
hbl = hornblende.

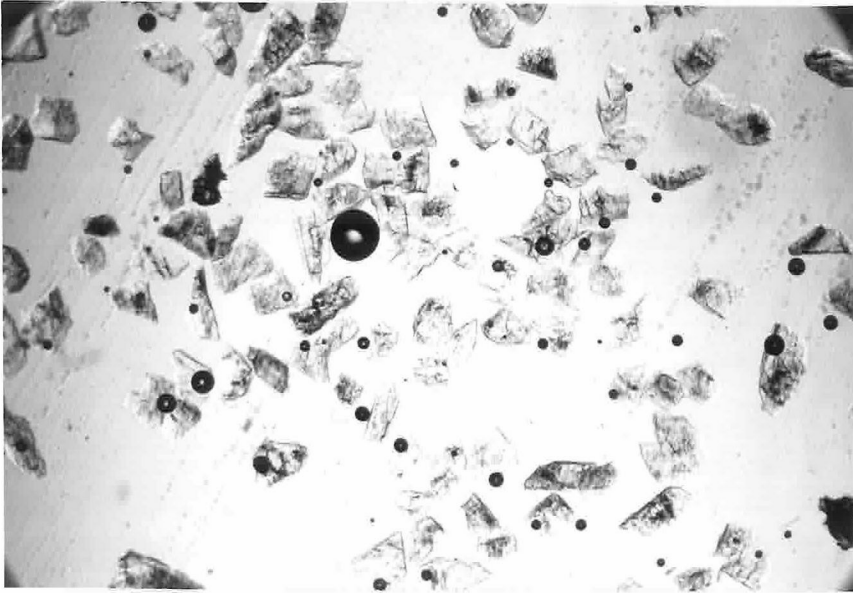


Plate 17. Lawler Peak Granite K-feldspar concentrate. 2 x 3 mm field, plane-polarized light (relief enhanced by small substage diaphragm aperture).

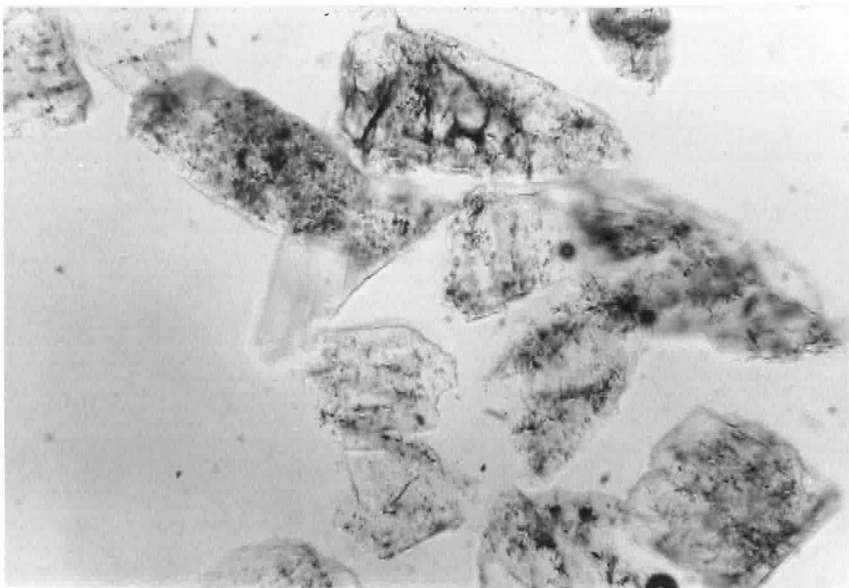


Plate 18. Lawler Peak Granite K-feldspar concentrate; plane-polarized light, 0.5 x 0.8 mm field.

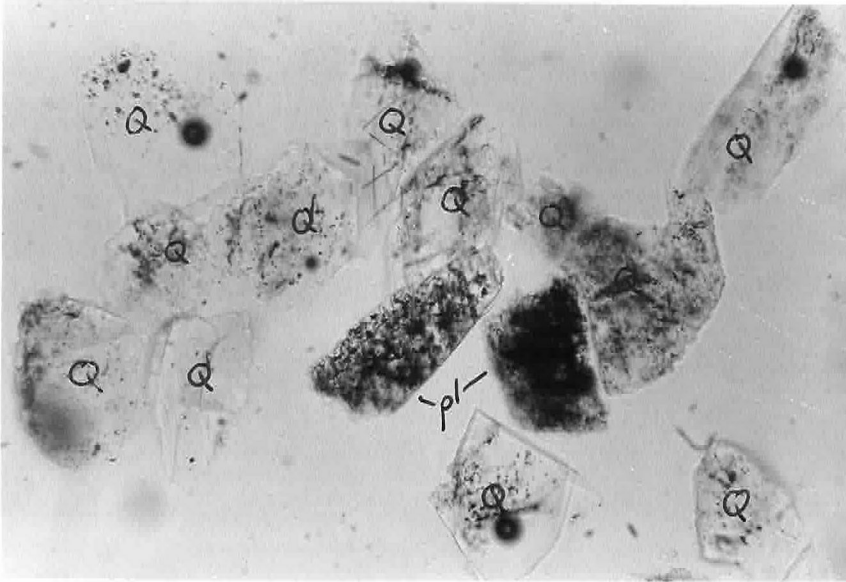


Plate 19. Lawler Peak granite quartz-plagioclase concentrate. Plane-polarized light, 0.5 x 0.8 mm field. Q = quartz, pl = plagioclase.

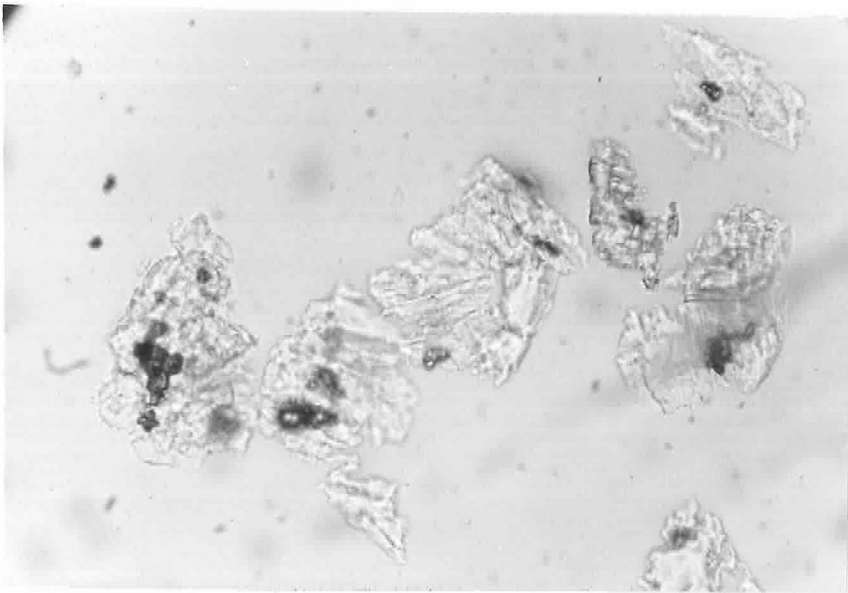


Plate 20. Lawler Peak granite K-feldspar concentrate, residue after second partial HF attack. Compare with Plate 18. The high-index grains are fluorite. Plane-polarized light, 0.5 x 0.8 mm field.

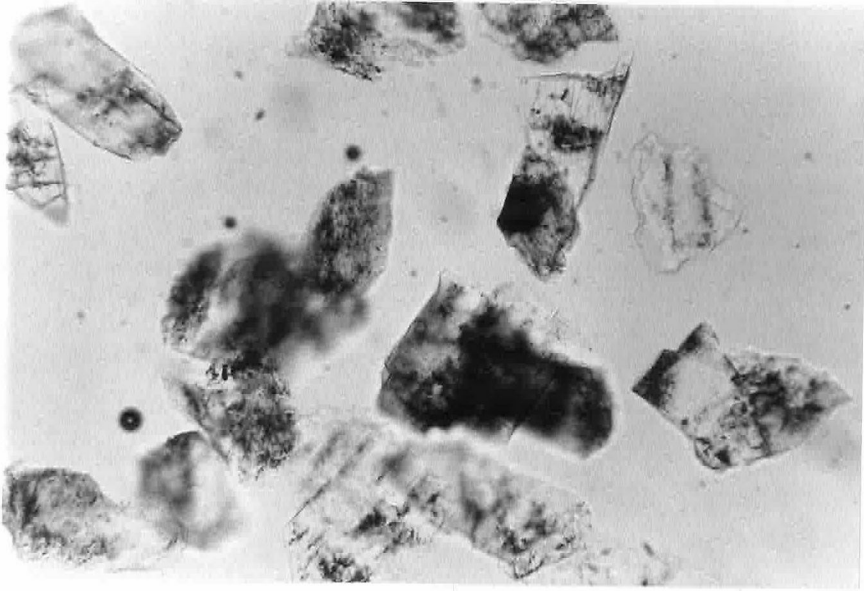


Plate 21. Ruin granite K-feldspar concentrate.
Plane-polarized light, 0.5 x 0.8 mm field.

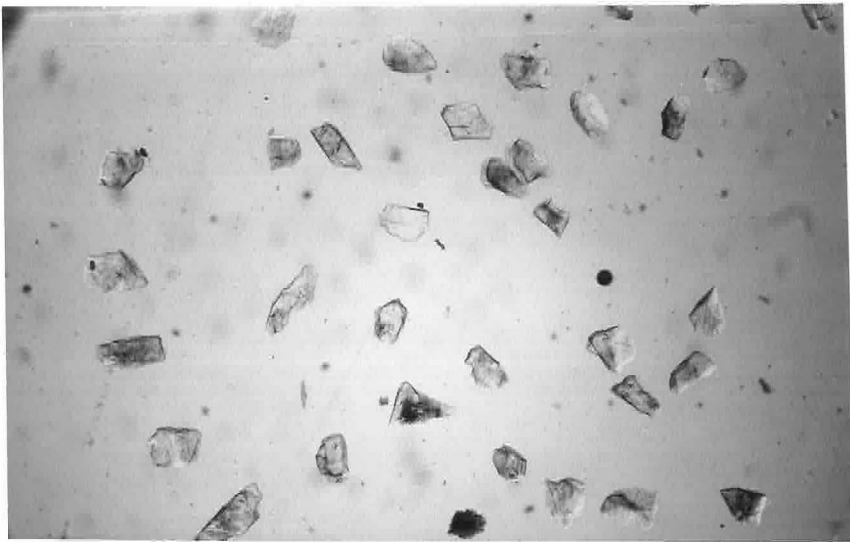


Plate 22. Ruin granite K-feldspar concentrate.
Plane-polarized light, 2 x 3 mm field.

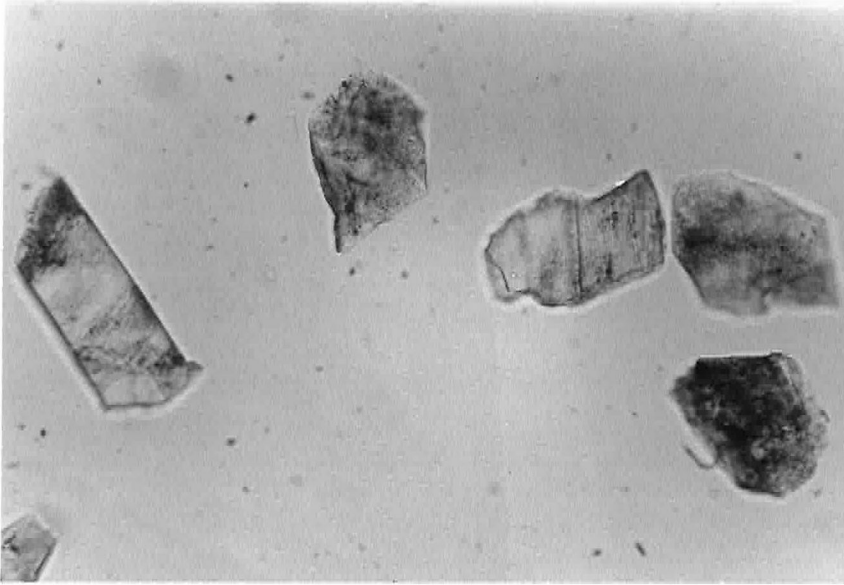


Plate 23. Marble Mts. granite K-feldspar concentrate.
Plane-polarized light, 0.5 x 0.8 mm field.

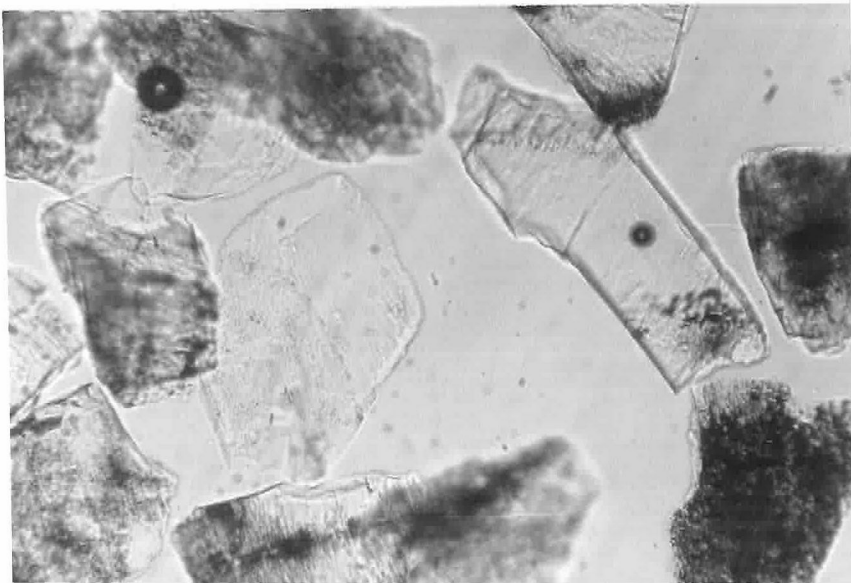


Plate 24. Payson Granite K-feldspar concentrate.
Plane-polarized light, 0.6 x 0.9 mm field.

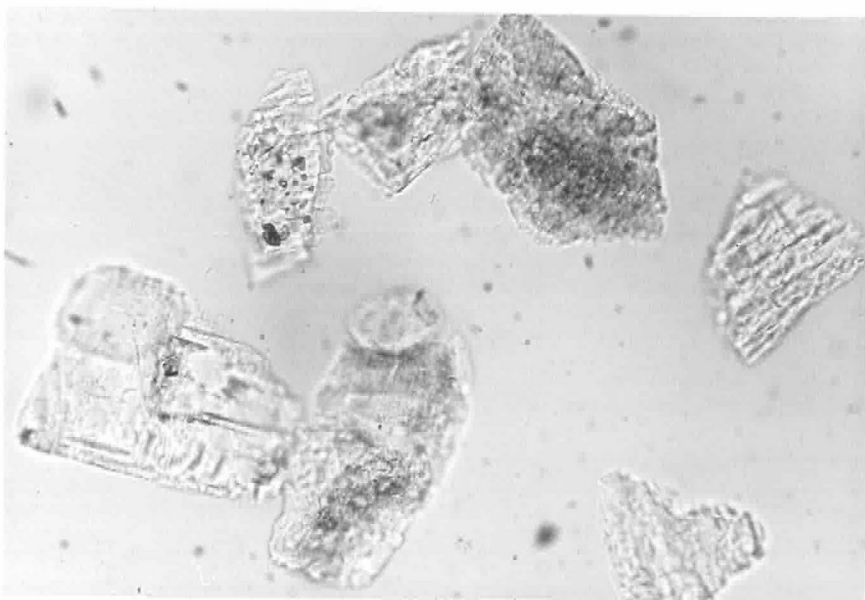


Plate 25. Payson granite K-feldspar concentrate, after third partial HF attack. Plane-polarized light, 0.6 x 0.9 mm field.

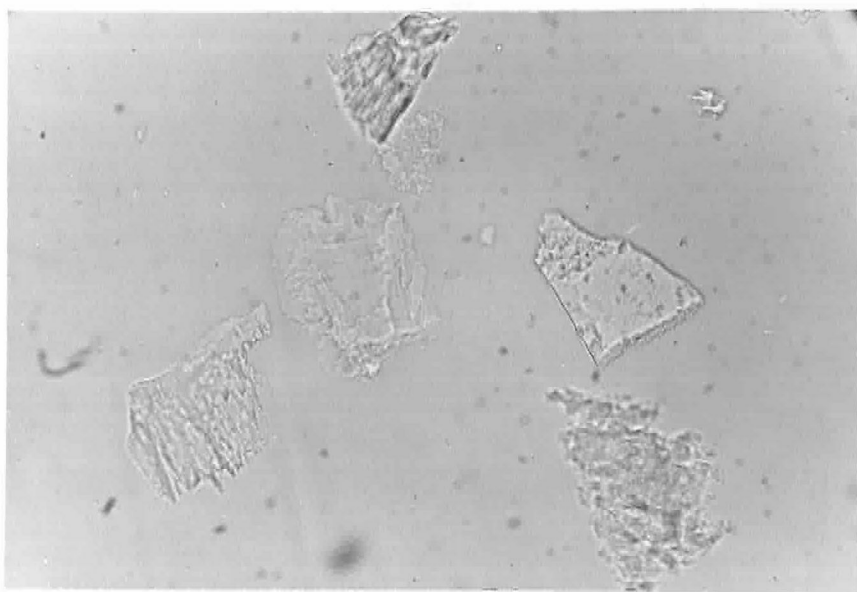


Plate 26. Payson granite K-feldspar concentrate, after fifth partial HF attack. Plane-polarized light, 0.6 x 0.9 mm field.

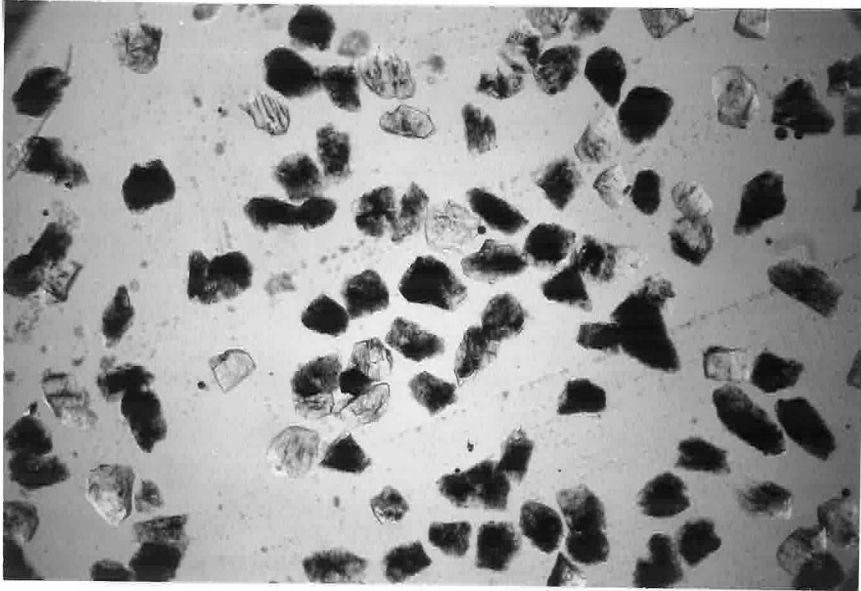


Plate 27. Giants Range granite K-feldspar concentrate.
Plane-polarized light, 2 x 3 mm field.

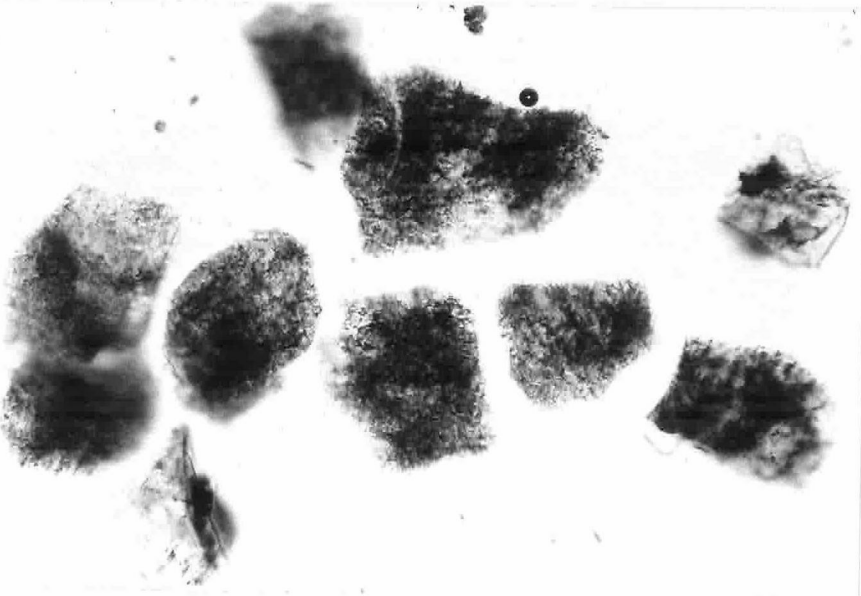


Plate 28. Giants Range granite K-feldspar concentrate.
Plane-polarized light, 0.5 x 0.8 mm field.

BIBLIOGRAPHY

Part II

- Aldrich, L.T., Davis, G.L., Tilton, G.R., and Wetherill, G.W. (1956) Radioactive Ages of Minerals from the Brown Derby Mine and the Quartz Creek Granite near Gunnison, Colorado, Jour. Geophys. Res. 61, 215-232.
- Anderson, C.A., Scholz, E.A., and Strobell, J.D. (1955) Geology and Ore Deposits of the Bagdad Area, Yavapai County, Arizona, U.S. Geol. Survey Prof. Paper 278.
- Anderson, D.H., and Gast, P.W. (1965) Uranium-Lead Zircon Ages and Lead Isotope Compositions in Two Algomian Granites of Northern Minnesota, Geol. Soc. Amer. Spec. Papers, 82, 3-4.
- Anderson, T.H., and Silver, L.T. (1971) Preliminary History for Precambrian Rocks, Bamori Region, Sonora, Mexico, Geol. Soc. Amer. Abstr. with Progr. 3, p. 72.
- Anderson, T.H., Silver, L.T., Cordoba, D., Pearson, M., and Baenteli, G. (1972) Geochronologic Observations concerning the Crystalline Complexes of Sonora and Oaxaca, Mexico, Geol. Soc. Mexico Meeting, Mazatlan (in press).
- Burger, A.J., Nicolaysen, L.O., and De Villiers, J.W.H. (1962) Lead Isotopic Compositions of Galenas from the Witwatersrand and Orange Free State, and their Relation to the Witwatersrand and Dominion Reef Uraninites, Geochim. et Cosmochim. Acta 26, 25-29.
- Cameron, A.E., Smith, D.A., and Walker, R.L. (1969) Mass Spectrometry of Nanogram-Size Samples of Lead, Anal. Chem. 41, 525-526.
- Catanzaro, E.J., and Gast, P.W. (1960) Isotopic Composition of Lead in Pegmatitic Feldspars, Geochim. et Cosmochim. Acta 19, 113-126.
- Catanzaro, E.J., Murphy, T.J., Shields, W.R., and Garner, E.L. (1968) Absolute Isotopic Abundance Ratios of Common, Equal-Atom, and Radiogenic Lead Isotope Standards, Jour. Res. Natl. Bur. Std. A. Phys. Chem. 72A, 261-267.
- Cherdynstev, V.V. (1961) Abundance of Chemical Elements, trans. by W. Nichiporuk, U. of Chicago Press.
- Chow, T.J., and Patterson, C.C. (1961) On the Primordial Lead of the Canyon Diablo Meteorite, Geokhimiya, no. 12, 1124-1125.

- Doe, B.R. (1962a) Distribution and Composition of Sulfide Minerals at Balmat, New York, Geol. Soc. Amer. Bull. 73, 833-854.
- Doe, B.R. (1962b) Relationships of Lead Isotopes among Granites, Pegmatites, and Sulfide Ores near Balmat, New York, Jour. Geophys. Res. 67, 2895-2906.
- Doe, B.R. (1970) Lead Isotopes, Springer-Verlag, New York, 137 pp.
- Doe, B.R., and Hart, S.R. (1963) Effect of Contact Metamorphism on Lead in Potassium Feldspars near the Eldora Stock, Jour. Geophys. Res. 68, 3521.
- Doe, B.R., and Tilling, R.I. (1967) Distribution of Lead between Coexisting K-feldspar and Plagioclase, Amer. Mineralogist 52, 805-816.
- Doe, B.R., Tilton, G.R., and Hopson, C.A. (1965) Lead Isotopes in Feldspars from Selected Granitic Rocks Associated with Regional Metamorphism, Jour. Geophys. Res. 70, 1947-1968.
- Fleming, E.H. Jr., Ghiorso, A., and Cunningham, B.B. (1952) The Specific Alpha Activities and Half-Lives of U^{234} , U^{235} , and U^{236} , Phys. Rev. 88, 642-652.
- Gerling, E.K. (1942) Age of the Earth According to Radioactivity Data, C.R. Acad. Sci. U.S.S.R., 34, 259.
- Giletti, B.J., and Kulp, J.L. (1955) Radon Leakage from Radioactive Minerals, Amer. Mineralogist 40, 481-496.
- Goldich, S.S., Nier, A.O., Baadsgaard, H., Hoffman, J.A., and Krueger, H.W. (1961) The Precambrian Geology and Geochronology of Minnesota, Univ. Minn. Geol. Surv. Bull. 41, 62-65.
- Green, J.C. (1970) Lower Precambrian Rocks of the Gabbro Lake Quadrangle, Northeastern Minnesota, Minn. Geol. Surv. Spec. Publ. Series 13, 52-61.
- Hanson, G.N. (1968) K-Ar Ages from Granites and Gneisses and for Basaltic Intrusives in Minnesota, Minn. Geol. Surv. Rept. Inv., 8, 4.
- Hanson, G.N., Catanzaro, E.J., and Anderson, D.H. (1971) U-Pb Ages for Sphene in a Contact Metamorphic Zone, Earth and Planet. Sci. Letters 12, 231-237.
- Holmes, A. (1948) An Estimate of the Age of the Earth, Nature 157, 680.

- Houtermans, F.G. (1947) Time of the Formation of Uranium, Naturwissenschaften 33, 185-186.
- Imbrie, J. (1956) Biometrical Methods in the Study of Invertebrate Fossils, Bull. Amer. Mus. Nat. Hist. 108, 211-252.
- Jaffey, A.H., Flynn, K.F., Glendenin, L.E., Bentley, W.C., and Essling, A.M. (1971) Precision Measurement of Half-Lives and Specific Activities of ^{235}U and ^{238}U , Phys. Rev. C, 4, 1889-1906.
- Kermack, K.A., and Haldane, J.B.S. (1950) Organic Correlation and Allometry, Biometrika 37, 30-41.
- Kouvo, O. (1958) Radioactive Age of Some Finnish Precambrian Minerals, Finlande Comm. Geol. Bull. 182, 70 pp.
- Kovarik, A.F., and Adams, N.I. Jr. (1938) The Disintegration Constant of Thorium and the Branching Ratio of Thorium C, Phys. Rev. 54, 413-421.
- Krogh, T.E. (1970) A Low Contamination Method for Decomposition of Zircon and Extraction of U and Pb for Isotopic Age Determinations, Carnegie Inst. Wash. Yearbook, 1970-71, 258-266.
- Kulp, J.L., Bate, G.L., and Broecker, W.S. (1954) Present Status of the Lead Method of Age Determination, Amer. Jour. Sci. 243A, Daly Volume, 369-416.
- Lanphere, M.A. (1964) Geochronologic Studies in the Eastern Mojave Desert, California, Jour. Geol 72, 381-399.
- Livingston, D.E. (1962) Older Precambrian Rocks near the Salt River Canyon, Central Gila County, Arizona, New Mexico Geol. Soc. Thirteenth Field Conf. Guidebook, 55-56.
- Masuda, M. (1964) Lead Isotopic Composition in Volcanic Rocks of Japan, Geochim. et Cosmochim. Acta 28, 292.
- Murthy, V.M., and Patterson, C.C. (1962) Primary Isochron of Zero Age for Meteorites and the Earth, Jour. Geophys. Res. 67, 1161-1167.
- Nier, A.O. (1938) Variations in the Relative Abundances of Isotopes of Common Lead from Various Sources, Amer. Chem. Soc. Jour. 60, 1571-1576.
- Oversby, V.M. (1970) The Isotopic Composition of Lead in Meteorites, Geochim. et Cosmochim. Acta 34, 77-88.

- Patterson, C.C. (1955) The Pb^{206}/Pb^{207} Ages of Some Stone Meteorites, Geochim. et Cosmochim. Acta 7, 151-163.
- Patterson, C.C. (1956) Age of Meteorites and the Earth, Geochim. et Cosmochim. Acta 10, 230-237.
- Picciotto, E.E., and Wilgain, S. (1956) Confirmation of the Half-Life of Thorium-232, Nuovo Cimento 4, 1525-1528.
- Russell, R.D., and Farquhar, R.M. (1960) Lead Isotopes in Geology, Interscience, New York, 243 pp.
- Silver, L.T. (1964) Relation between Radioactivity and Discordance in Zircons, Nucl. Geoph., Natl. Acad. Sci. Pub., 1075.
- Silver, L.T. (1968) Precambrian Batholiths of Arizona, Geol. Soc. Amer. Spec. Papers, 121, 558-559.
- Silver, L.T., and McKinney, C.R. (1962) U-Pb Isotopic Age Studies of a Precambrian Granite, Marble Mountains, San Bernardino County, California, Geol. Soc. Amer. Spec Papers, 73, 65.
- Silver, L.T., and Deutsch, S. (1963) Uranium-Lead Isotopic Variations in Zircons - A Case Study, Jour. Geol. 71, 721-758.
- Silver, L.T., McKinney, C.R., Deutsch, S., and Bolinger, J. (1963) Precambrian Age Determinations in the Western San Gabriel Mountains, California, Jour. Geol. 71, 196-214.
- Silver, L.T., and Green, J.L. (1972) Time Constants for Keeweenawan Igneous Activity, Geol. Soc. Amer. Abstr. with Progr. 4, 665-666.
- Sinha, A.K. (1969) Removal of Radiogenic Lead from Potassium Feldspars by Volatilization, Earth and Planet. Sci. Letters 7, 109-115.
- Stacey, J.S., Zartman, R.E., and Nkomo, I.T. (1968) A Lead Isotope Study of Galenas and Selected Feldspars from Mining Districts in Utah, Econ. Geol. 63, 796-814.
- Stanton, R.L., and Russell, R.D. (1959) Anomalous Leads and the Emplacement of Lead Sulfide Ores, Econ. Geol. 54, 588-607.
- Starik, I.E., Melikova, O.S., Kurbatov, V.V., and Aleksandrochuk, V.M. (1955) Byulleten' Komissi Po Opredeleniyu Absolutnogo Vozrasta Geologicheskikh Formatsii 1, No. 22, Acad. Sci., U.S.S.R.

- Starik, I.E., Shats, M.M., and Lovtsyus, A.V. (1961) On the Problem of the Isotopic Composition of Lead in Iron Meteorites, Akad. Nauk. SSSR Meteoritika, no. 20, 103-113.
- Tatsumoto, M. (1966) Genetic Relations of Ocean Basalts as Indicated by Lead Isotopes, Science 153, 1094.
- Tatsumoto, M., Knight, R.J., and Allegre, C.J. (1973) Time Differences in the Formation of Meteorites as Determined from the Ratio of Lead-207 to Lead-206, Science 180, 1279-1283.
- Tilton, G.R., Patterson, C.C., Brown, H., Inghram, M., Hayden, R., Hess, D., and Larsen, E. Jr. (1955) Isotopic Composition and Distribution of Lead, Uranium, and Thorium in a Precambrian Granite (Ontario), Geol. Soc. Amer. Bull. 66, 1131-1148.
- Tilton, G.R., and Steiger, R.H. (1969) Mineral Ages and Isotopic Composition of Primary Lead at Manitouwadge, Ontario, Jour. Geoph. Res. 74, 2118-2132.
- Wetherill, G.W. (1956) Discordant Uranium-Lead Ages, Amer. Geophys. Union Trans. 36, 320-326.
- Zartman, R.E. (1965) The Isotopic Composition of Lead in Microclines from the Llano Uplift, Texas, Jour. Geoph. Res. 70, 965-975.
- Zartman, R.E., and Wasserburg, G.J. (1969) The Isotopic Composition of Lead in Potassium Feldspars from Some 1.0 b.y. Old North American Igneous Rocks, Geochim. et Cosmochim. Acta 33, 901-942.